April 2010

Geological and Geographical Attributes of the South Texas Uranium Province

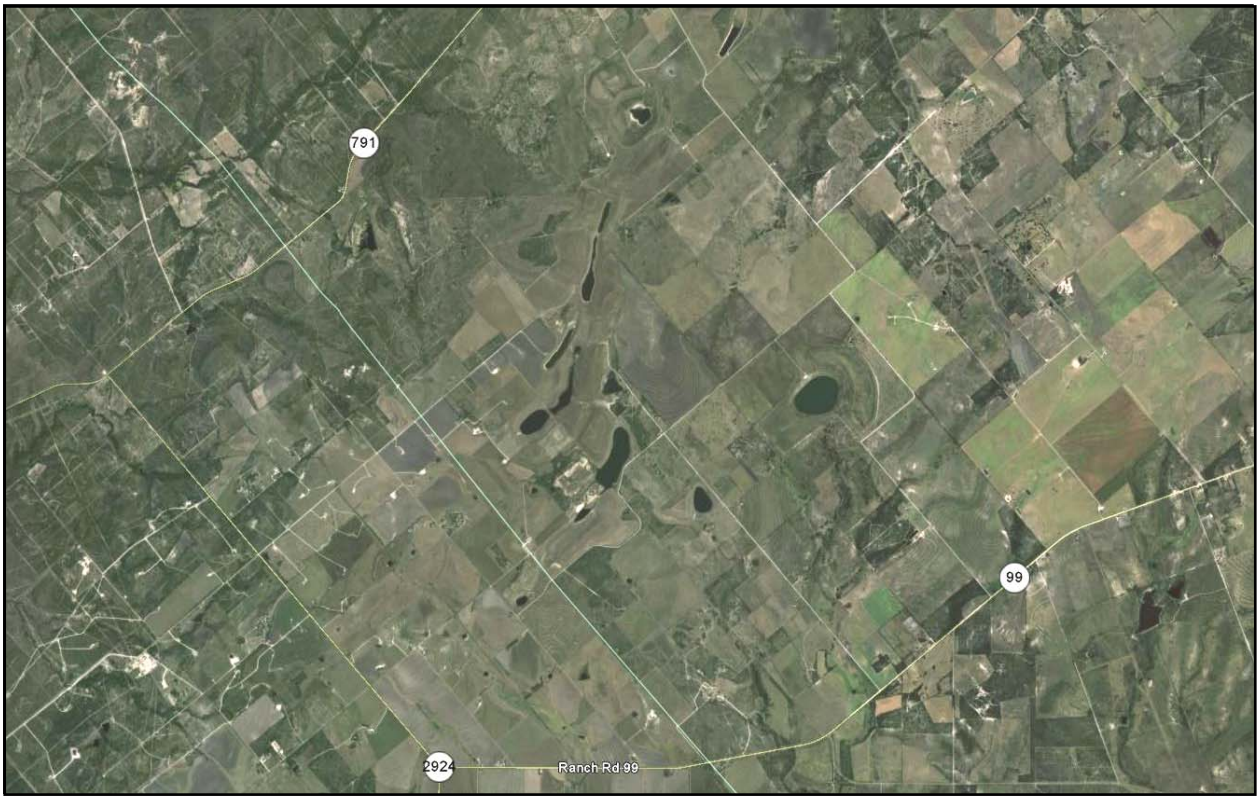

Prepared for:
Texas Commission on Environmental Quality
by

Jean-Philippe Nicot, Bridget R. Scanlon, Changbing Yang, and John B. Gates

Assisted by Caroline L. Breton, Kuldeep Chaudhary, and Nathan A. Sheffer

Bureau of Economic Geology
Scott W. Tinker Director
John A. and Katherine G. Jackson School of Geosciences
The University of Texas at Austin
Austin, Texas 78713-8924

Cover photo: Aerial view of abandoned/reclaimed open pits following surface uranium mining a few miles west of Karnes City, Karnes County, Texas. Courtesy of Google Earth.

Initial Release

Geological and Geographical Attributes of the South Texas Uranium Province

Prepared for:
Texas Commission on Environmental Quality

under
Umbrella Contract No. 582-4-69718

Jean-Philippe Nicot, Bridget R. Scanlon, Changbing Yang, and John B. Gates
Assisted by Caroline L. Breton, Kuldeep Chaudhary, and Nathan A. Sheffer

April 2010

Bureau of Economic Geology
Scott W. Tinker Director
John A. and Katherine G. Jackson School of Geosciences
The University of Texas at Austin
Austin, Texas 78713-8924

Abstract

The South Texas Uranium Province, which includes about 20 counties, mostly wraps around a formation known as the Catahoula Formation, from the Mexican border to south of San Antonio. Approximately 100 open-pit mines operated in the second half of the 20th century, but, after a hiatus of several decades, the industry is now investing in in situ recovery operations of additional uranium deposits.

Important volcanic episodes, centered around Catahoula deposition times more than 20 million years ago, are credited, through ash-fall and related sediments, as being the source of uranium deposits, as well as associated elements such as arsenic and selenium. These trace elements, enriched in local sediments, were quickly mobilized in their soluble form by infiltrating waters. Then, after flowing deeper into the subsurface along stratigraphic dip within high-transmissivity, sand-rich formations deposited by rivers, uranium encountered more reducing conditions and precipitated out of solution in a pattern known as *roll front*. Selenium and molybdenum are also redox sensitive and accumulated in the solid phase at the redox front along with uranium. Other trace elements, such as arsenic, vanadium, boron, and fluorine, behave differently and remained mostly in solution.

Mechanisms resulting in commercial deposits are

- Source: Leaching of uranium and other elements (As, Mo, V, Se, B, F) from volcanic rocks (~fresh ash fall and reworked ash sediments) by oxidized, slightly alkaline waters and migration downdip. Volcanic rocks are more prone to alteration because of their glassy nature and because crystals are often small and easily weathered, especially in derived sediments.
- Migration: Controlled primarily by transmissive depositional axes (high-permeability channels) while uranium is being mobilized by oxidizing alkaline waters. In environmental conditions of Eh and pH, uranium forms mobile uranyl-carbonate complexes.
- Trapping Mechanism: Reducing conditions due to periodic intermittent oil/gas/H_2S migrating along faults (and subsequent sulfide precipitation) or, less commonly, organic-rich sediments forcing uranium to change redox state from a soluble oxidized form U(VI) to an insoluble reduced form U(IV). Uranium drops out of solution as water passes the redox flow as uraninite (UO_2, uranium oxide) or coffinite ($USiO_4$, uranium silicate). Chromatographic precipitation of other trace elements mobilized along with uranium according to redox behavior and geochemical gradients.
- Concentrating Mechanism: Multiple occurrences of dissolution/precipitation as the redox front moves downdip and downgradient owing to a continuous stream of oxidizing recharging waters, bringing more uranium and dissolving previously precipitated uranium to be deposited together.
- Host Rock: High-permeability sand channels allowing continuous flow unaffected by slight changes in sand porosity.

Surface alteration of some deposits when exposed to oxidizing waters can remobilize uranium and other trace elements. However, the extent of poor-quality water from ore bodies, including unmined subeconomic ore bodies, remains an open question.

Table of Contents

List of Figures

List of Tables

Acknowledgments

This report benefited from the input of numerous people not included in the author list, either through constructive discussions or through use of their printed material. Bill Galloway, at the UT Institute of Geophysics, generously shared his experience of the South Texas Uranium Province with us. He, Al Cherepon (TCEQ), and Jon Brandt (RRC) are some of the many people with a continuing interest (professional and otherwise) in the South Texas Uranium Province. Bill Ambrose (BEG) allowed us to make use of his recently published material as well. We also thank Gary Smith and Susan Jablonsky, Director of the Radioactive Materials Division, in charge of this project at TCEQ. Lana Dieterich (BEG) edited a near-final version of this document.

Acronyms

AML	Abandoned Mine Land (program)
BEG	Bureau of Economic Geology
bgs	Below ground surface
FeOx	Ferric hydroxides and oxides
GAM	Groundwater availability model
GCAS	Gulf Coast Aquifer System
GCD	Groundwater conservation district
GMA	Groundwater management area
gpm	Gallons per minute
gpd	Gallons per day
ISL	In situ leach (mining)
ISR	In situ recovery
MCL	Maximum contaminant level
m.y.	million years
NCDC	National climatic data center, operated by NOAA
NOAA	National Oceanic and Atmospheric Administration
NURE	National Uranium Resource Evaluation
OM	Organic material, organic matter
ppb	parts per billion
ppm	parts per million
RASA	Regional aquifer–system analysis
RRC	Railroad Commission of Texas
RWPG	Regional Water Planning Group
SECO	State Energy Conservation Office
STU	South Texas Uranium
TCEQ	Texas Commission on Environmental Quality
TDS	Total dissolved solids
TWDB	Texas Water Development Board
UIC	Underground injection control
UMTRA	Uranium Mill Tailings Recovery Act
USDOE	U.S. Department of Energy
USGS	U.S. Geological Survey

Executive Summary

The South Texas Uranium (STU) Province contains about 100 known uranium deposits that were developed in the second half of the 20th century. Abundant literature captures the knowledge acquired during this production phase, particularly reports and papers written by BEG and USGS staff, as well as data from the U.S. Department of Energy NURE program.

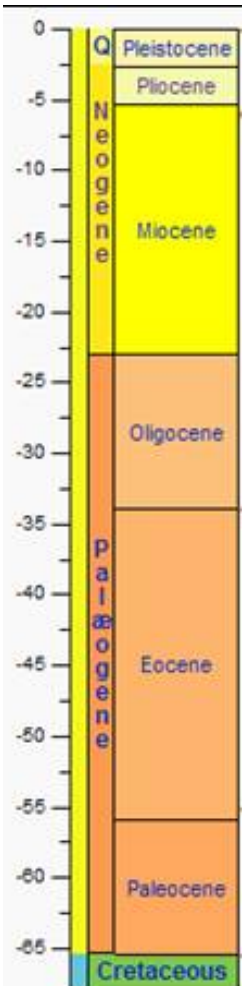

Figure ES1. Geochronologic column

Deposits are hosted by four formations (Figure ES1), whose sedimentary and hydrostratigraphic characteristics are:

(1) Eocene Jackson Group, consisting of nearshore and shore sediments: barrier islands, lagoons, etc. The group contains small, mostly brackish aquifers.

(2) Oligocene/Miocene Catahoula Formation, consisting of fluvial deposits, mostly sands, clay, and volcaniclastics. The formation, although very permeable at the time of deposition, is now considered an aquitard with some brackish water lenses. Locally the top of the formation, when sandy, is part of the Jasper aquifer.

(3) Miocene Oakville Formation, consisting of fluvial deposits (sands, some clay). The formation composes most of the Jasper aquifer. The aquifer is mostly brackish except in a narrow band along the outcrop. It is separated from the Evangeline aquifer by a leaky aquitard known as the Burkeville Confining Unit.

(4) Miocene/Pliocene Goliad Formation, consisting of fluvial deposits, mostly unconsolidated sands. The formation is mostly equivalent to the Evangeline aquifer. This aquifer is the most heavily used in the STU Province.

The Jackson Group consists of a strandplain depositional system, an important characteristic of which is the strike-trending, relatively clean sand bodies (limiting flow downdip) and abundant organic matter sometimes accumulating in lignite beds. The Jackson Group has some limited volcanic influence and was deposited under a climate more humid than the current climate. The Catahoula Formation was deposited under a bedload fluvial system (resulting in possibly good permeability in fluvial channels) and organized into several complex dip-oriented sand belts. The formation contains many paleosols demonstrating frequent exposure to the atmosphere. The system was periodically choked by ash falls that degraded to montmorillonite and kaolinite clays during diagenesis. Sands are “dirty” and dominated by plagioclase feldspars and rock fragments with minor quartz. The climate was similar to current climate

The Oakville Sandstone deposition also occurred as a bedload fluvial system. In the STU, it consists of three broad, dip-oriented fluvial axes merging farther downdip into strike-oriented deltaic and strandline sand systems. Sandstones are dominated by feldspars and rock fragments with ubiquitous minor metal oxides and calcite cement. Paleosols are common, and climate was also similar to current climate. During deposition of the Goliad Sands, volcanic influence was

waning, but abundant feldspars and rock fragments of volcanic origin still exist south of the Nueces River. Overall the Goliad Sands contain abundant caliche layers and carbonates. Structurally the STU Province is impacted by the Wilcox and Fashing Fault Zones.

All uranium deposits are genetically associated with sand bodies in a type of accumulation known as “roll-front” deposits. Understanding of ore deposits requires description of at least four attributes: (1) a source of the uranium (and other elements)—leached from fresh volcanic ash; (2) a migration / transport mechanism—uranium is mobilized by oxidizing alkaline waters and travels along high-permeability channels; (3) a concentrating / trapping mechanism—multiple encounters with reducing material, either organic matter (Jackson Group) or sulfides dispersed in the rock; and (4) a host rock with sufficient volume to reach economic levels—porosity of sand is sufficiently high to allow stable flow while uranium minerals are deposited as grain coatings or globules.

Mechanisms of uranium mobilization and accumulation are well known and have been described in the STU Province and elsewhere in the U.S. Uranium and oxyanions (As, Mo, Se, V) generally traveling with it are leached under oxidizing conditions from fast-degrading volcanic glass by recharging waters. Uranium-bearing uranyl ions are stabilized in solution by carbonate ligands and travel downdip along high-transmissivity sand zones corresponding to stacked fluvial channels until they encounter reducing material. Two types of reducing material exist in the STU Province: organic material, abundant mostly in the Jackson Group, and sulfides, particularly abundant in the Oakville Sandstone. Iron sulfides result from interaction of primary metal oxides abundant in the formation, with very reducing fluids coming up faults and most likely linking to sour hydrocarbon accumulations present in older formations. Invasion of H_2S-rich fluids was intermittent, but they created permanent reducing material through sulfide accumulation. As more uranium-laden oxidizing fluids pass through the aquifer, they oxidize and mobilize the reduced uranium previously precipitated in a continuous process that results in enrichment of uranium at the redox front, as well as in its migration downdip (Figure ES2). Note that flow is not impeded. If flow is blocked, accumulation stops growing. Other postdeposition events that would alter the position of the redox front relative to uranium accumulation also fossilize the accumulation. These events include a sulfidization event of the uranium accumulation or the accumulation being brought up into the oxidizing zone because of partial erosion of overlying formations (Figure ES3).

Uranium is also associated with companion elements that may or may not precipitate along with it, depending on their behavior when redox conditions become more reducing. Arsenic and vanadium are typically soluble at the prevalent, mildly reducing conditions and typically do not precipitate when passing through the redox front (they remain in the aqueous phase, where they can reach concentrations above the MCL). Other elements, such as boron and fluorine, also commonly associated with volcanic deposits, are insensitive to mildly reducing conditions as well. Selenium generally precipitates ahead of uranium, whereas molybdenum precipitates behind the redox front. This polarity with the downdip sequence of selenium, uranium, and molybdenum provides the observer with an easy way to pinpoint the flow as minerals accumulate. It also follows that there is a regional correlation between these trace elements that may not translate into a correlation at the well level because of these chromatographic-like separation effects owing to the redox gradients.

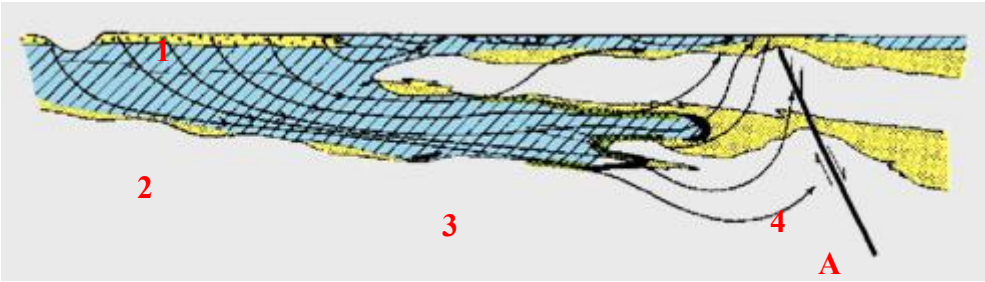

Source: Galloway (1977)

Figure ES2. Diagrammatic cross section of roll-front active accretion: 1 = uranium leached from surficial ash; 2 = uranium moves into groundwater system; 3 = uranium transported down hydrodynamic gradient in semiconfined aquifer; 4 = uranium concentrated near margins of oxidation tongue. Feature A represents the fault that brought reductant to the system (ultimately stored as iron sulfides)

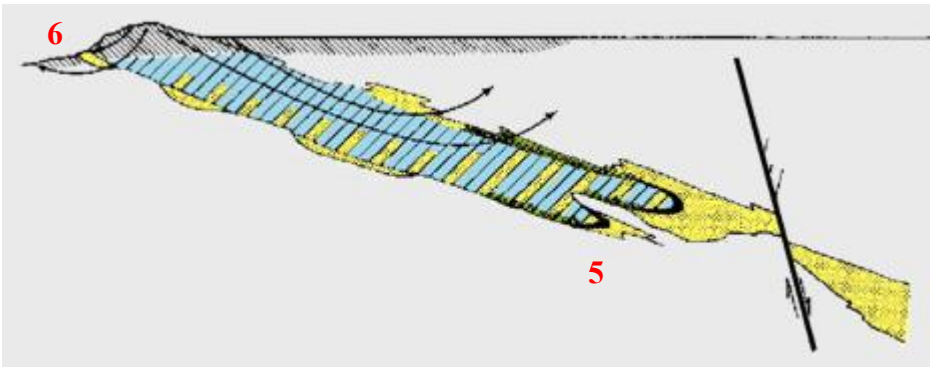

Source: Galloway (1977)

Figure ES3. Diagrammatic cross section of possible postore processes in a mature flow system: 5 = resulfidization of deposits through additional input of reducing fluids or return to reducing conditions because of a reduction in groundwater flux; 6 = surface oxidation

Examining the impact of the uranium deposits on the water quality of the local aquifers, redox conditions (Eh) are only one environmental factor governing behavior of trace elements in the aqueous phase; pH is also very important. In particular, pH drives the ability of iron and other metal oxides to sorb oxyanions under oxidizing conditions. However, sorption of oxyanions, such as As, Se, and Mo, is not efficient at the alkaline pH possibly generated by abundant carbonate minerals currently present in the shallow subsurface of the STU Province (semiarid climate).

I. Introduction

The Texas Commission on Environmental Quality (TCEQ) contracted the Bureau of Economic Geology (BEG), The University of Texas at Austin, to summarize physical and geological attributes of the South Texas Uranium (STU) Province. The STU Province is an arbitrary subset of the Gulf Coast Uranium Province as defined by Finch (1996) and extends into Mexico (Figure 1). This report synthesizes and discusses general information about regional geographic and geological characteristics, such as topography, precipitation, soil distribution, stratigraphy, hydrostratigraphy and aquifers, and geological structure, as well as geochemical characteristics of formations containing uranium deposits. Additional references are provided so that readers can quickly locate more detailed information on any topic covered in this report. Areas of interest include Goliad and Karnes Counties and surrounding Atascosa, Bee, Brooks, Duval, Jim Hogg, Kleberg, Live Oak, McMullen, and Webb Counties (2+9 total). Ten tier-2 counties, such as Aransas, Dewitt, Gonzales, Jim Wells, Kenedy, La Salle, Nueces, Refugio, San Patricio, and Wilson, were also added (Table 1) because of their historical importance or potential future importance and because of insights they can provide to improve understanding of the geochemical behavior of the entire region (Figure 2).

From a practical standpoint, figures in this report fall into two categories: those specifically developed for this report and those gleaned from outside sources—a judicious choice of maps and figures scanned (and referenced) from several public-domain and published reports and then adapted to suit this document. A future revision of or addition to this report will include digitized and georeferenced shape files of the most useful of these scanned figures. Similarly, this report provides a discussion of geochemistry at a relatively high level; however, more detailed information on this topic will be provided in a future report focusing on geochemistry of uranium deposits.

I-1. The Uranium Province

The STU Province largely overlaps the surface extent of the southern or central parts of the Gulf Coast Aquifer System (GCAS), especially its sections with older formations. GCAS forms a broad band along the coast of the Gulf of Mexico, spanning approximately 5º of longitude. It is approximately 90 mi wide in the uranium mining region and 120 mi wide at its broadest section (central part). Defined by its surface extent, it has an area of approximately 23,000 mi^2. The GCAS consists of the Jasper and Evangeline aquifers, hosts to some commercial uranium mineralization, but the GCAS also includes the overlying Chicot aquifer.

A recent increase in the price of uranium has renewed interest in the STU Province. Mining in the province began shortly after discovery of radiometric anomalies in western Karnes County in December 1954 (Moxham, 1964; Handbook of Texas Online, 2008). Oxidized uranium ore deposits near Tordilla Hill in Karnes County were later discovered to be responsible for the anomalies. According to Cherepon et al. (2007), by the summer of 1956 about 15 prospects were located along a narrow strip 300 mi long, extending from Fayette County to Starr County and closely associated with the Catahoula Formation (Figure 2). The first mining operations took place next to Deweesville and near Tordilla Hill, 10 mi west of Falls City, both located in Karnes County. The first shipment of coastal plain ore was made in December 1958 to a processing plant in New Mexico (Moxham, 1964; p. 313). Between 1958 and the early 1990's, when uranium mining and processing essentially ceased, several companies operated more than 60

mines (mostly open-pit mines), several in situ leaching sites, and four mills in the STU Province. After depletion of the shallow oxidized ore, production moved to deeper, reduced uranium ores. The first such ore was mined in 1963 at a depth of 90 ft (RRC, 1994, p. 4.1), and open-pit mines eventually reached depths of more than 300 ft. Total production from the STU Province through 1994 was about 70,000,000 lb U_3O_8 (Finch, 1997, p. 8). However, the uranium grade of the STU Province is relatively lean by world and U.S. standards (resulting in more tailings relative to deposits, with better uranium grades). Uranium grade in sandstone-hosted deposits, that currently account for 1/3rd of the recent world production, typically ranges from 0.05 to 0.5% (Cuney and Kyser, 2009, p.8). Another third of the global production originates from unconformity- related deposits. They have an average uranium grade of 0.8% with the largest deposits up to 23% (Cuney and Kyser, 2009, p.6). In 2003, the Energy Information Administration (EIA, 2003) projected that 6,000,000 lb U_3O_8 at 0.077% U_3O_8 on average and 23,000,000 lb U_3O_8 at about 0.063% U_3O_8 on average remained in the ground in Texas, for a market price of $30 and $50/lb U_3O_8, respectively. As of February 2010, market price hovered at around $40-50/lb. These reserves are, however, dwarfed by reserves in the western states (Wyoming, New Mexico, Arizona, Colorado, Utah), with 259 (at 0.178 % U_3O_8) and 867 (at 0.105 % U_3O_8) million pounds U_3O_8, for the same price cutoff of $30 and $50/lb, respectively.

Mining companies have mostly moved away from open-pit mining and are now focusing on in situ recovery (ISR) (also called in situ leaching [ISL]) mining in several counties, including Brooks, Duval, Goliad, and Kleberg. According to B. Knape, TCEQ (presentation at San Antonio GWPC UIC meeting, January 2009), five locations hold an active permit: Kingsville Dome in Kleberg County; Rosita and Vasquez, both in Duval County; Alta Mesa in Brooks County; and Palangana Dome in Duval County. The first three are operated by Uranium Resources, Inc. (URI), whereas the latter two are operated by Mestena and South Texas Mining Venture (STMV), respectively. A sixth permit is pending in Goliad County (Uranium Energy Corp.—UEC) and has generated vigorous public participation. The Railroad Commission of Texas (RRC) website lists 17 exploration permits as of February 12, 2009, involving 7 companies in 13 counties (Atascosa, Bee, Brooks, Duval, Goliad, Jim Hogg, Jim Wells, Karnes, Kleberg, Live Oak, McMullen, Nueces, and Zavala) and an additional permit in Briscoe County in the Texas Panhandle.

Regulatory oversight of the uranium mining industry is complicated. RRC regulates surface mining of lignite and uranium, and current regulations require the RRC to permit exploratory wells and test holes. It requires the TCEQ UIC Permit team to permit ISR UIC Class III injection wells (in case of in situ treatment), however, and the TCEQ Radioactive Materials division to issue licenses for uranium processing facilities (B. Knape, TCEQ, personal communication, 2009). Estimation of the total number of mines is fraught with uncertainty. EPA (2006) compiled uranium-mine sites across the nation, including those in Texas (Figure 3 and Figure 4). Information was obtained from three sources: (1) (at the time) Texas Department of Health ("DB17") with 25 locations, (2) Adams and Smith (1981) paper ("DB21") with 26 locations, and (3) database at the RRC ("DB25") with 101 locations. The latter figure of 101 mines is higher than the usually cited number of mines in South Texas because some uranium deposits are located in West Texas, from overlaps and also from possible splitting at two locations of a mine under a single name (EPA, 2006, p. 10). The RRC (1994) suggested a total of 60+ mines, tentatively estimated to be 71 in EPA (2006) (actual number will most likely not ever be known). Other institutes have also launched independent tentative counts (e.g., Beaman and McGee, 2002). The State of Texas has required reclamation of surface uranium operations since 1975.

Mines abandoned prior to 1975 are eligible for the Abandoned Mine Land (AML) program operated by RRC (e.g., RRC, 1994). Approximately half of the mines of the STU Province had been abandoned prior to 1975 and fall into the AML program (Brandt in Cherepon et al., 2007), the so-called “pre-act” mines.

The STU Province is centered in the Catahoula Formation of Oligocene and Miocene age, although deposits are also present in older (Eocene Whitsett, Oligocene Frio) and younger (Miocene Oakville, Pliocene Goliad) formations (Figure 5). Whitsett, Catahoula, Oakville, and Goliad Formations all consist of a relatively narrow outcrop area with a much wider downdip section. Closer to the Gulf of Mexico, these formations are overlain by the Beaumont Clay and more recent formations (Figure 6). The stratigraphic column in Figure 7 displays additional intermediary formations, as well as units from which uranium has been extracted. In the STU Province, uranium mineralization is often coupled with water-bearing sandstones. The Karnes District contains most of the deposits of the Jackson Group. Bruni (Webb County), House-Seale (Live Oak), and Holiday-El Mesquite are examples of mines hosted by the Catahoula Formation. Ray Point and George West Districts in Live Oak County are contained in Oakville deposits. Deposits hosted by the Goliad Formation (Alta Mesa, Kingsville Dome, Palangana Dome) are genetically related to salt diapirism or dome motion and are spatially associated with hydrocarbon deposits. The Goliad and Oakville Sands make up most of the Evangeline and Jasper aquifers, respectively, whereas sand bodies of the Whitsett, Catahoula, and Fleming Formations, unless in direct contact with the above-mentioned aquifers, are not legally recognized by the state as aquifers and do not have a name provided by the Texas Water Development Board (TWDB).

This report draws from a wide range of earlier publications for data and interpretation. Because of the importance of the province to U.S uranium production in the 1970’s and 1980’s, a large body of information has been made available on mining exploration and production, as well as targeted studies on specific districts and mines, available either on the internet or as hardcopy. Reports include those produced by the USGS, the National Uranium Resource Evaluation (NURE) Federal Program, the Bureau of Economic Geology (BEG), and others. Most relevant are several reports on the geologic, geochemical, and hydrologic factors associated with uranium mining in the STU Province that were published in the BEG’s Reports of Investigation series in the late 1970’s and early 1980’s. Geologic depositional systems as related to uranium mineralization were discussed by Galloway (1977) for the Catahoula Formation and Galloway et al. (1982a) for the Oakville Sandstone Formation and were recently summarized by Ambrose (2007). The role of fluid flow in the spatial distribution of uranium deposits was the focus of Galloway (1982a). Henry and Kapadia (1980) and Henry et al. (1982a) both discussed various aspects of environmental chemistry (primarily regarding soils and groundwater, respectively). Smith et al. (1982a) provided details on the physical and chemical hydrogeology of the Oakville aquifer and, to a lesser extent, its neighboring hydrostratigraphic units. Henry et al. (1982b) discussed potential impacts of uranium mining on Oakville groundwater resources. The report of Galloway et al. (1982b) summarizes the findings of these eight investigations. South Texas was (is) also subject to intense oil and gas exploration and production and, although hydrocarbon deposits are located much deeper than uranium deposits, information collected from there has also contributed to the overall geological knowledge of the province.

More recently, Scanlon et al. (2005) described groundwater geochemistry of the GCAS, including concentrations and spatial distribution of uranium. GCAS and STU Province largely

overlap, but the Jackson Group is not formally part of the GCAS, and the youngest formations of the Gulf Coast system are not mineralized with uranium. Gates et al. (2008, 2009) provided additional information on trace-element distributions, particularly within the Oakville Sandstone/Jasper aquifer. The groundwater system was also discussed in detail by Mace et al. (2006) and Chowdhury et al. (2004). Non-uranium-specific general information is also relatively abundant because of widespread oil and gas exploration and production. These reports contain detailed information on the surface and subsurface environment, hydrology, and other factors that may be important to consider within the review process of uranium in situ leach mining applications. Many additional references pertaining to the study area are also included.

Table 1. Area and population of counties within the South Texas Uranium Province

	Area (mi^2)	**Pop. (2000)**	**Pop. Density (2000)**	**Pop. 2007 (Estimate)**
Aransas	251.86	22,497	89.3	24,721
Atascosa	1,232.12	38,628	31.4	43,589
Bee	880.14	32,359	36.8	32,689
Brooks	943.28	7,976	8.5	7,589
DeWitt	909.18	20,013	22	19,730
Duval	1,792.71	13,120	7.3	12,187
Goliad	853.52	6,928	8.1	7,154
Gonzales	1,067.75	18,628	17.4	19,210
Jim Hogg	1,136.11	5,281	4.6	4,973
Jim Wells	864.52	39,326	45.5	41,119
Karnes	750.32	15,446	20.6	15,067
Kenedy	1,456.77	414	0.3	394
Kleberg	870.97	31,549	36.2	30,390
La Salle	1,488.85	5,866	3.9	6,009
Live Oak	1,036.30	12,309	11.9	11,349
McMullen	1,113.00	851	0.8	874
Nueces	835.82	313,645	375.2	321,135
Refugio	770.21	7,828	10.2	7,358
San Patricio	691.65	67,138	97	68,520
Webb	3,356.83	193,117	57.5	233,152
Wilson	806.99	32,408	40.2	39,264
Total	23,108.90	885,327	38.3	946,473

Source: U.S. Census Bureau, http://quickfacts.census.gov/qfd/states/48000.html, last accessed February 2009

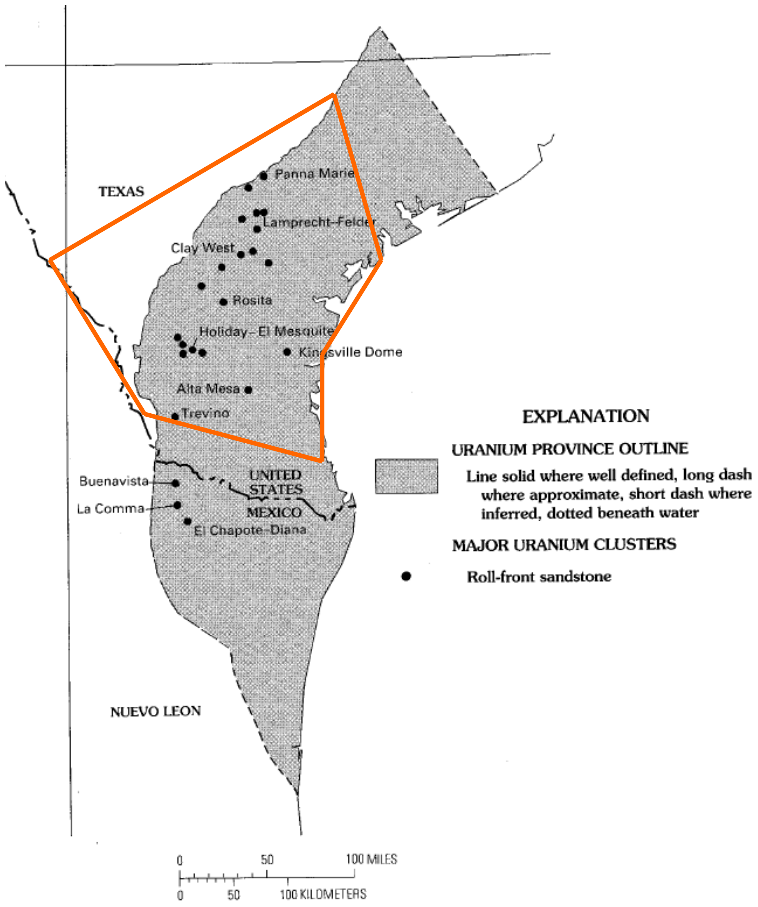

Note: The Gulf Coast Uranium Province is larger than and includes the STU Province.

Figure 1. Footprint of Gulf Coast Uranium Province (Finch, 1996) displaying outline of study area

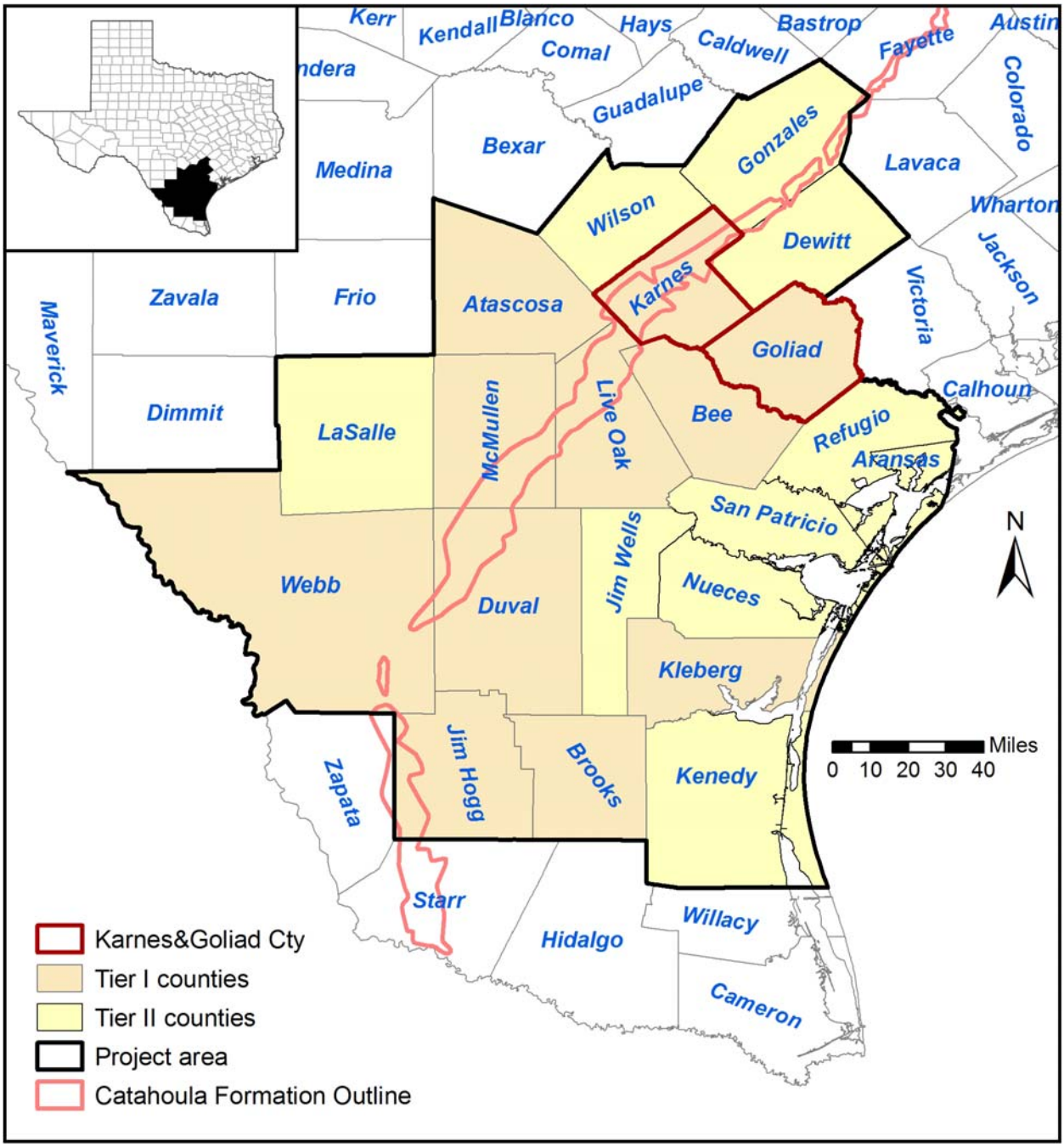

Figure 2. Location of study area showing county boundaries and outline of Catahoula Formation and related formations; Karnes and Goliad Counties and other tier 1 and tier 2 counties highlighted

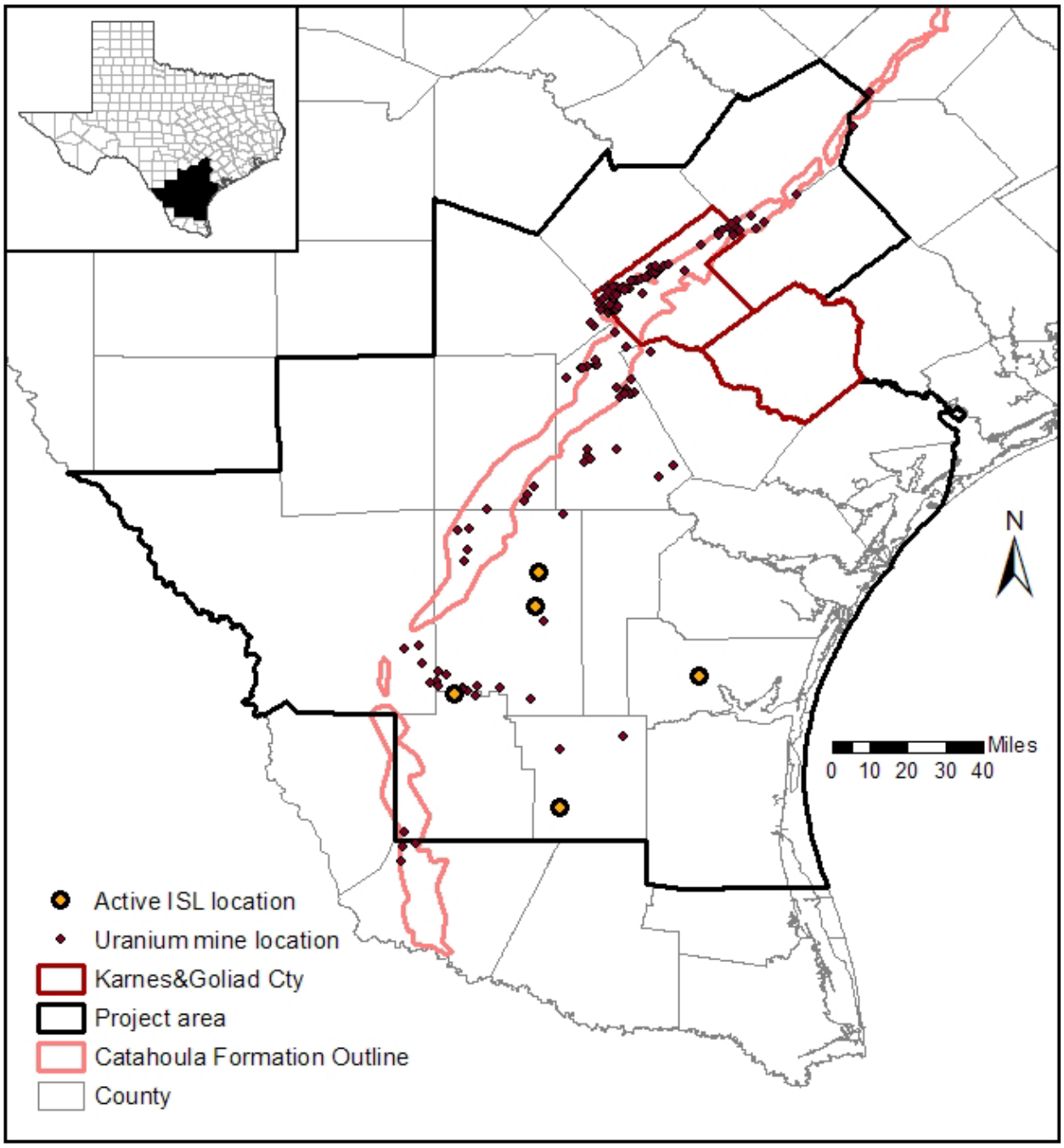

Source: EPA TENORM website (http://epa.gov/radiation/tenorm/pubs.html) and EPA (2006), active sites from TCEQ (Ben Knape, 2009 GWPC UIC meeting)
Note: map does not include recent in situ leaching (ISL) projects

Figure 3. Uranium mine locations in South Texas Uranium Province.

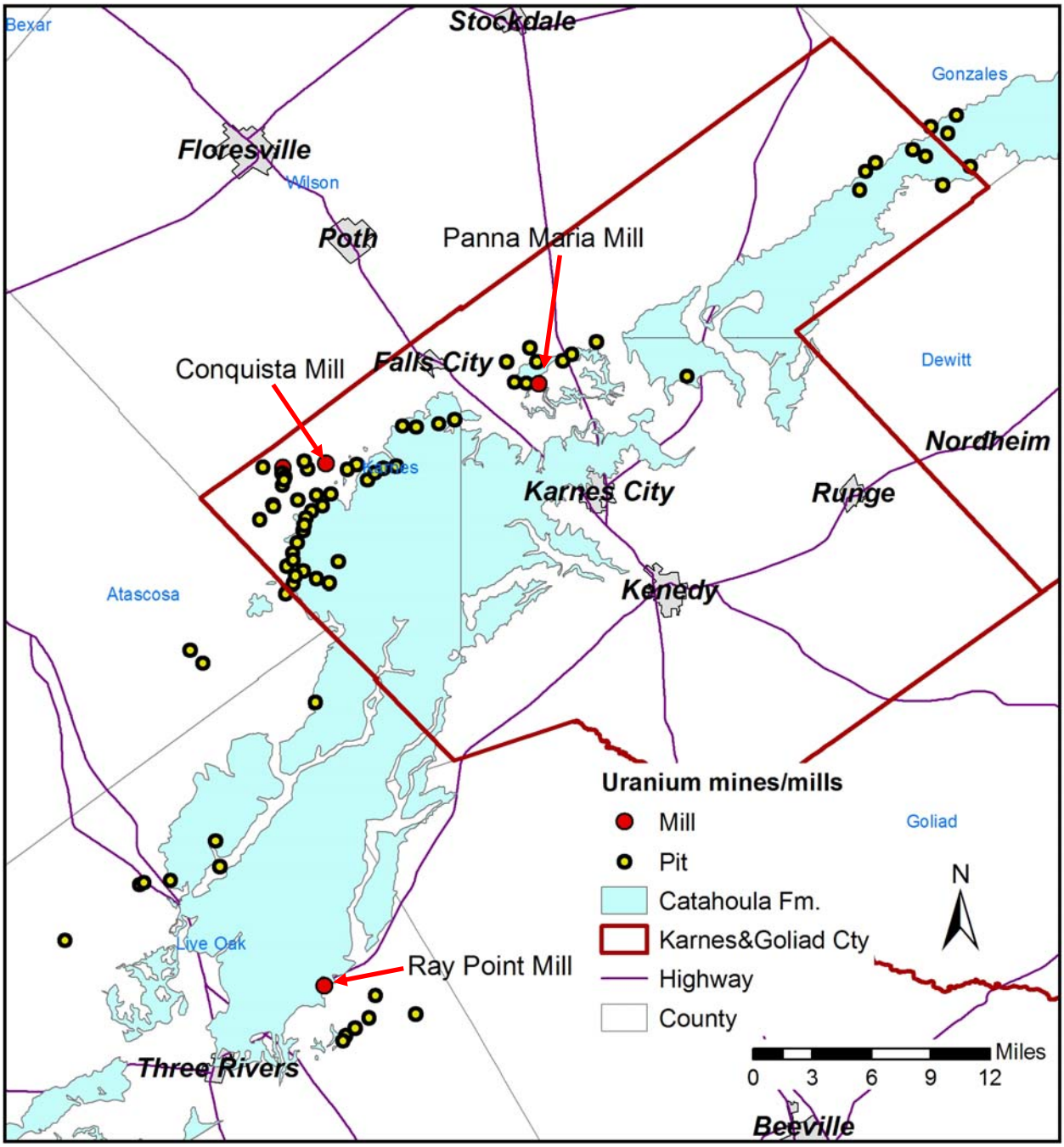

Source: Abandoned Mine Land Program, Surface Mining and Reclamation Division, Railroad Commission of Texas. Courtesy of Jon Brandt (RRC)

Figure 4. Uranium-mining-related locations within and near Karnes County; historical mills of interest to TCEQ also shown

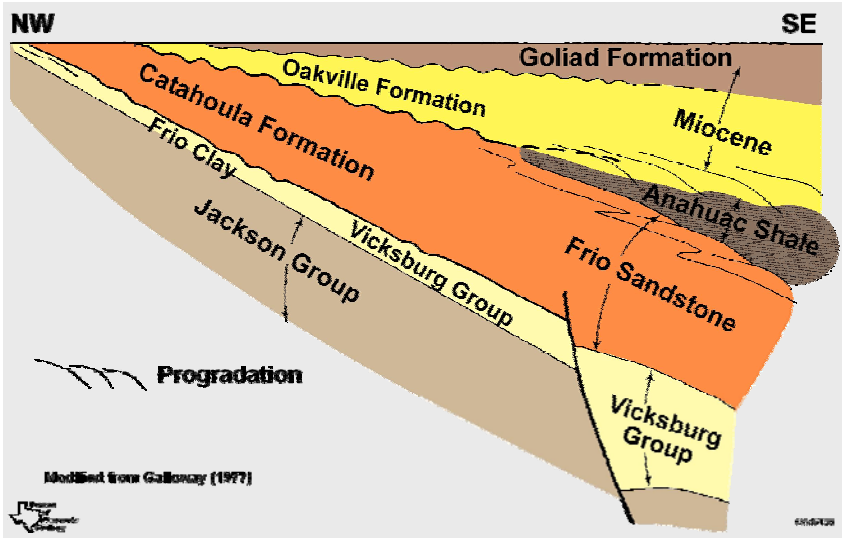

Source: Courtesy of William A. Ambrose (BEG); modified from Galloway (1977, p. 4)

Figure 5. Generalized cross section of Tertiary uranium-bearing units

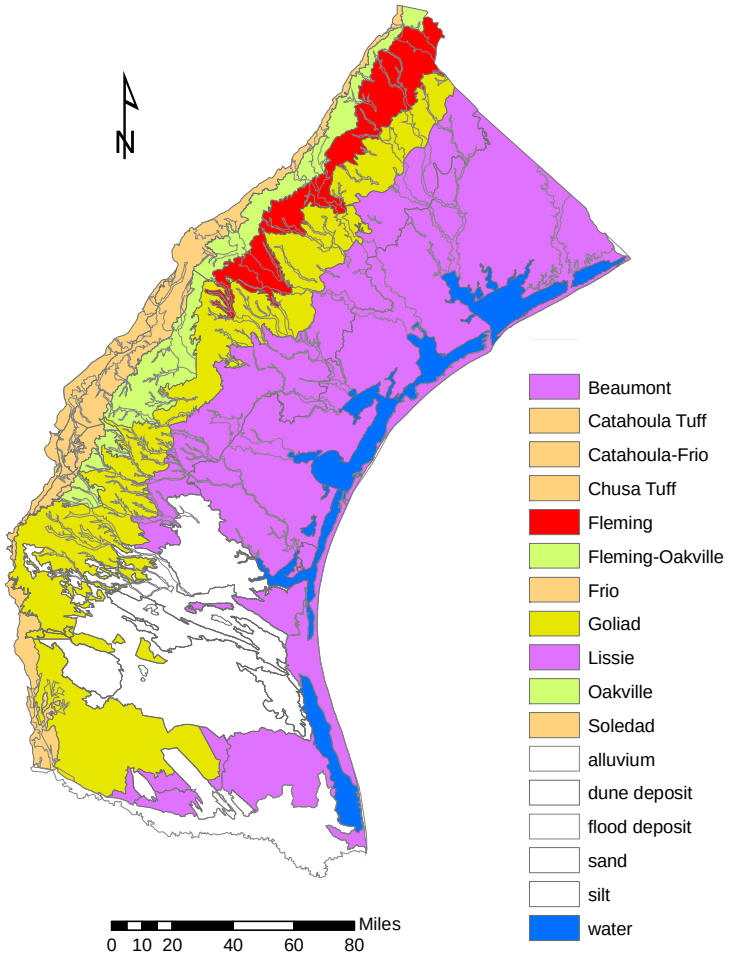

Source: Chowdhury et al. (2004)

Figure 6. Simplified geologic map of southwestern Gulf Coast region

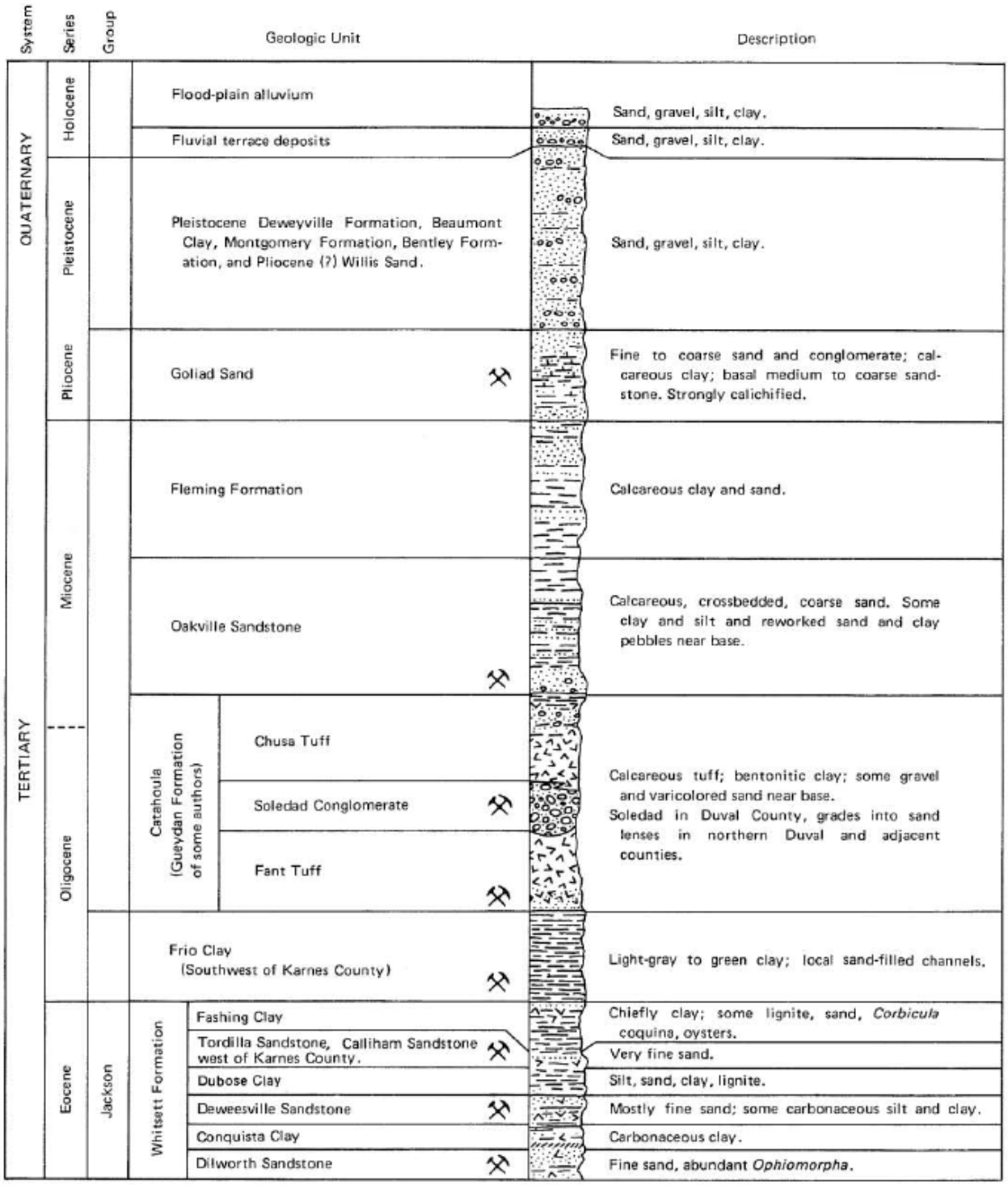

Source: Henry et al. (1982b)

Figure 7. Generalized stratigraphic section, STU Province; crossed picks indicate units from which uranium has been extracted; note contrast in organic content in Eocene and younger units

I-2. Cultural Attributes

The STU Province is located between several major cities and urbanized areas (San Antonio, Corpus Christi, Laredo, and the Rio Grande Valley), and, according to the 2000 U.S. census, the total population of the STU Province is approximately ½ million residents, not counting large cities. Population density ranges from very low (fewer than one inhabitant per square mile) in McMullen County (Figure 8) to that of large cities on the periphery of the study area. However, population density remains low along the Catahoula outcrop. The tier-1 study area contains many small towns but no large cities (Figure 9). Only the city of Corpus Christi is included in the larger study area, and the city of San Antonio is located a short distance to the north. Population density, along with land use, can be used as a proxy for domestic and industrial water use and for groundwater well density in rural and suburban areas (they generally tap the shallowest aquifer).

Administrative divisions of interest include groundwater conservation districts (GCD) (Figure 10), regional water planning groups (RWPG) (Figure 11), and groundwater management areas (GMA) (Figure 12).

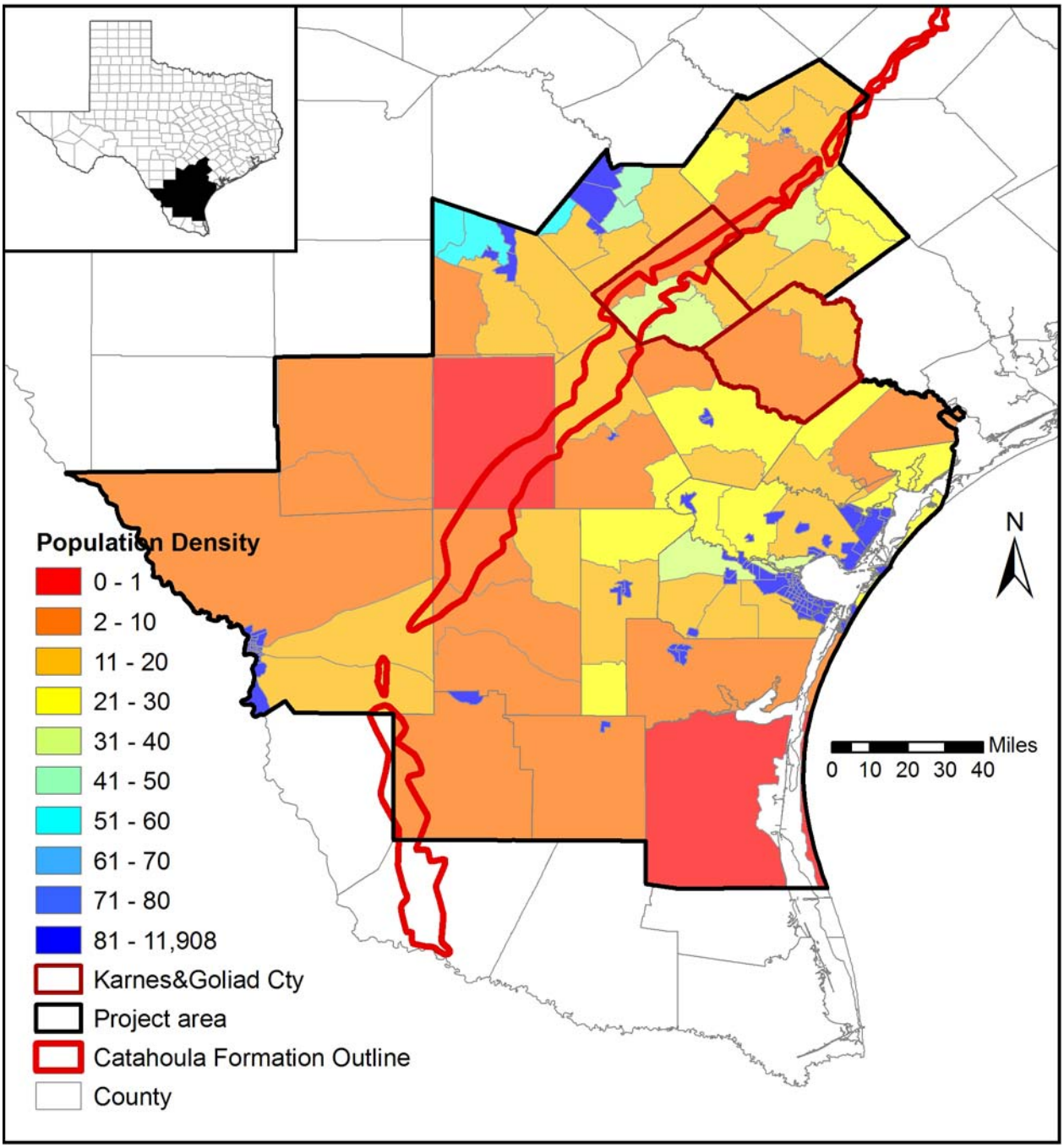

Source: U.S. Census Bureau (http://www.census.gov/)—data for 2000; http://www.census.gov/geo/www/cob/bdy_files.html for census tract definition and http://www.census.gov/geo/www/cenpop/cntpop2k.html for census track population

Figure 8. Population density (people per square mile) across the study area in 2000

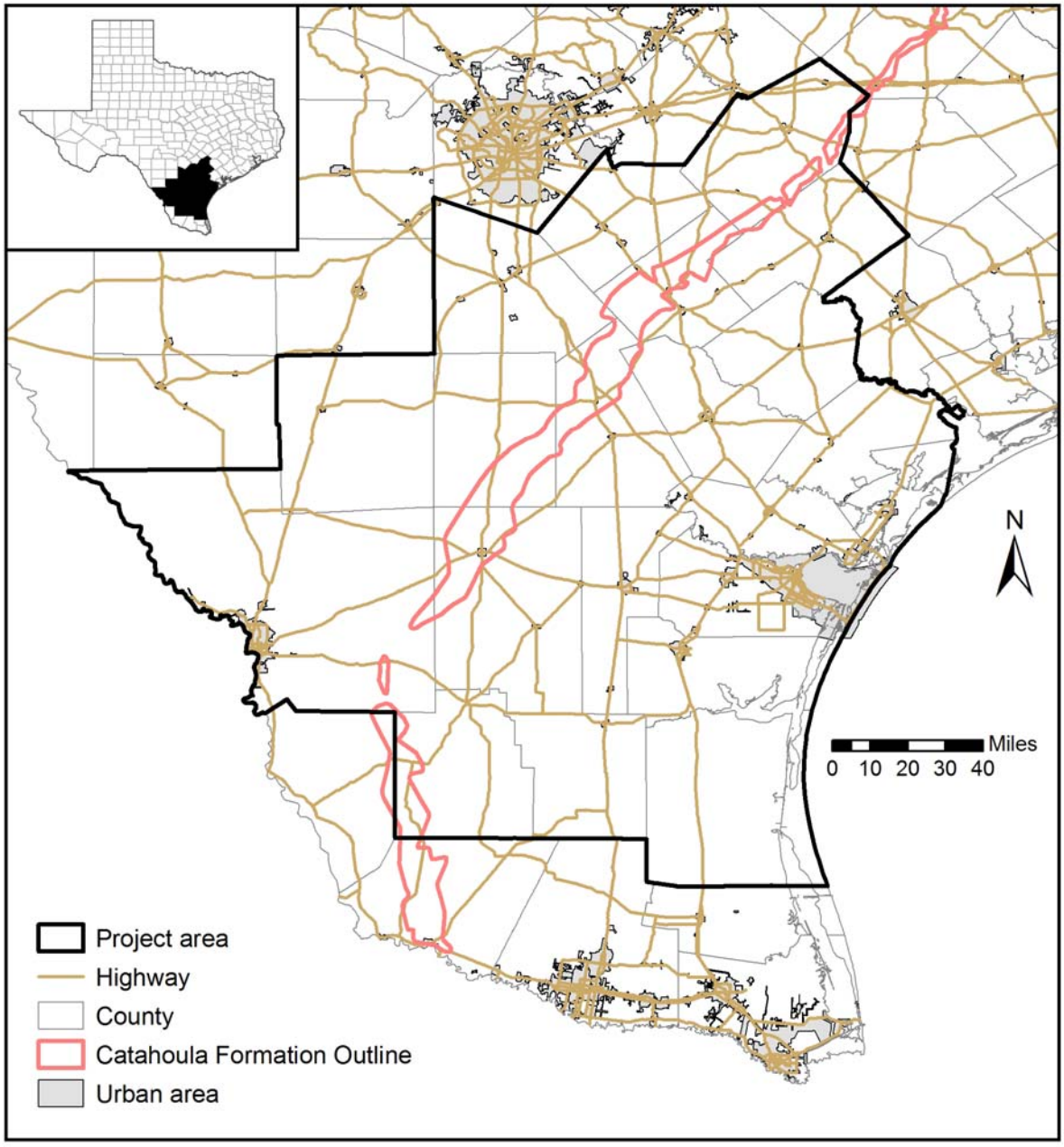

Source: TWDB, http://www.twdb.state.tx.us/mapping/gisdata.asp, January 2009

Figure 9. Cities, towns, and roadways in the study area

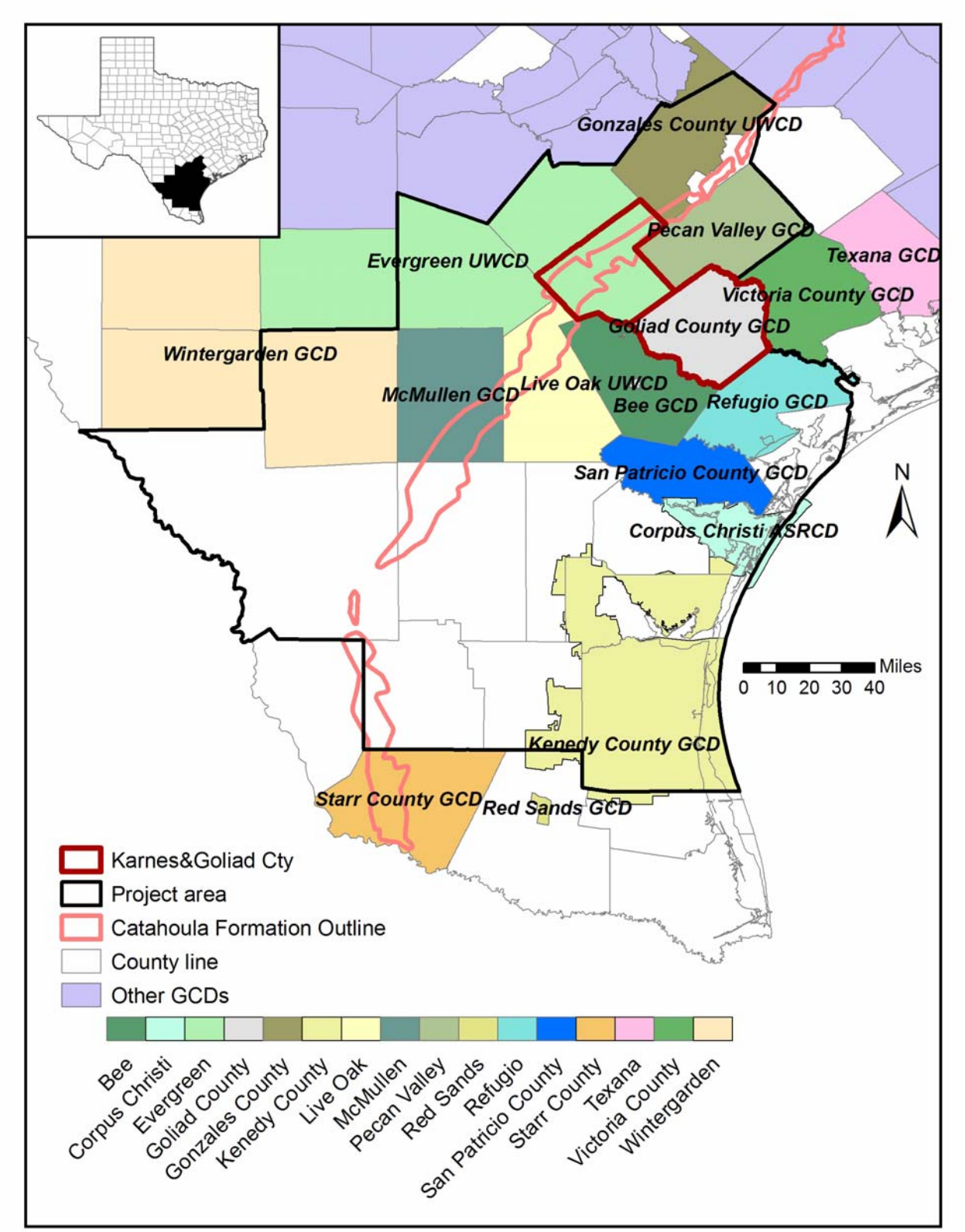

Source: TWDB, http://www.twdb.state.tx.us/mapping/gisdata.asp, January 2009

Figure 10. Location of Groundwater Conservation Districts in the study area as of October 2008.

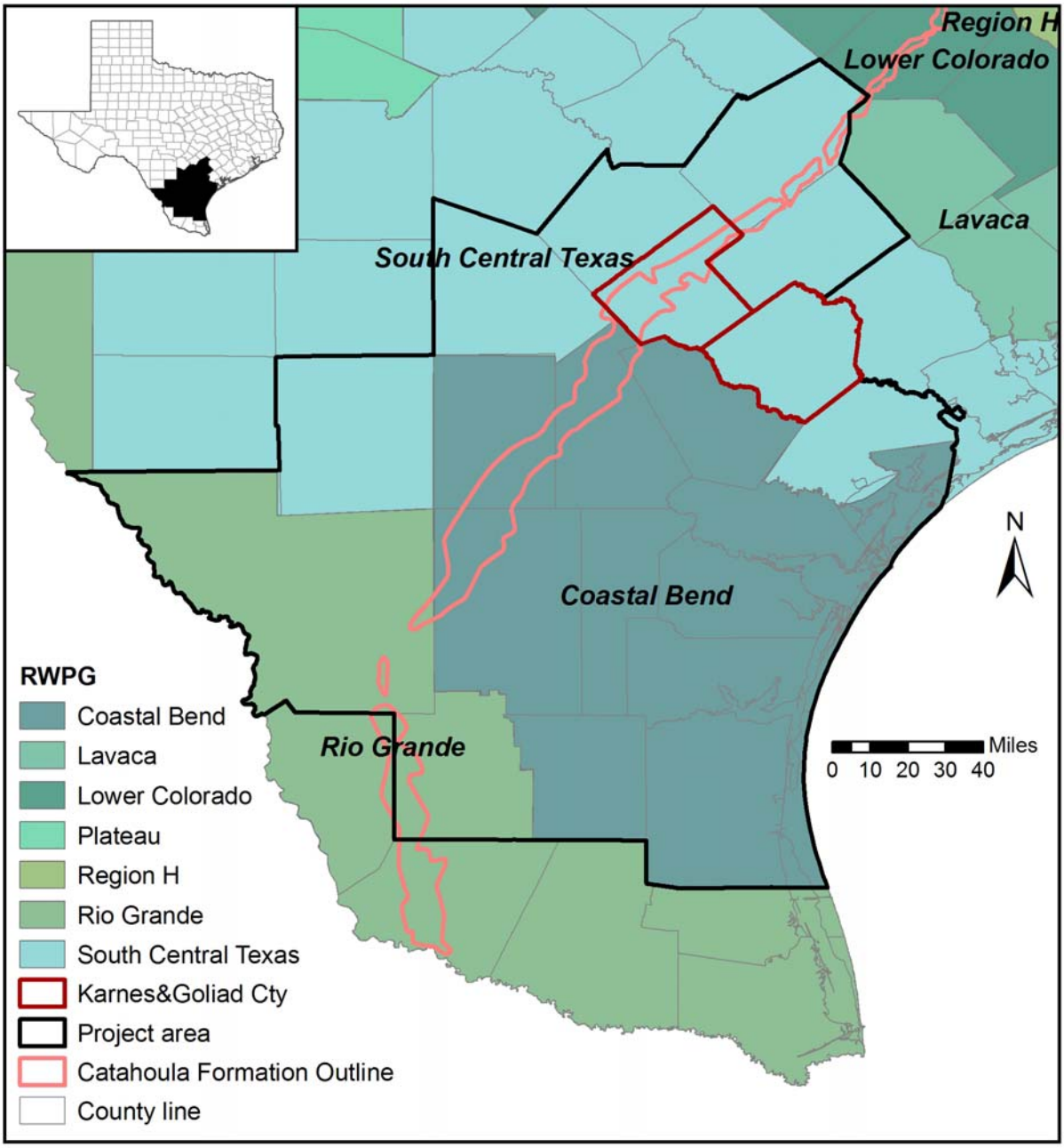

Source: TWDB, http://www.twdb.state.tx.us/mapping/gisdata.asp, January 2009

Figure 11. Location of Regional Water Planning Groups in the study area as of March 2008

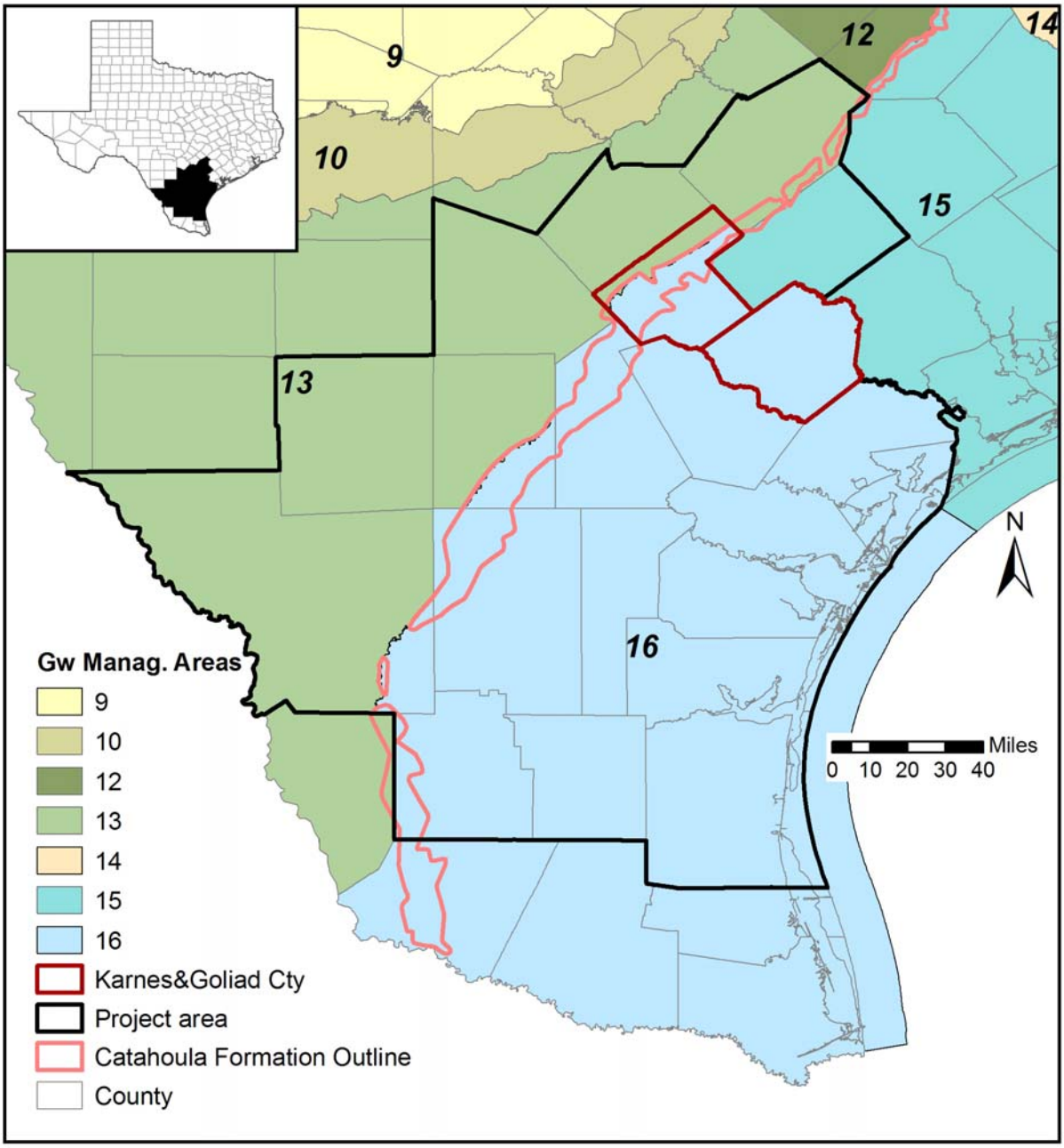

Source: TWDB, http://www.twdb.state.tx.us/mapping/gisdata.asp, January 2009

Figure 12. Location of Groundwater Management Areas in the study area as of August 2007

II. Physiography and Climate

Physiography and climate do more than just set the stage. For example, recharge to aquifers is impacted by precipitation and when it occurs during the year. Vegetation through evapotranspiration, in particular, and parameters such as rooting depth, perennial character, and leaf area index also make an important impact on recharge and shallow subsurface processes. Topography and river network are two factors controlling rejected recharge, i.e., groundwater that discharges to streams and does not move downdip into the confined parts of the aquifers. Knowledge of extreme precipitation events and their frequency helps explain controls on flushing of soil water in the vadose zone.

The coast of the Gulf of Mexico forms a flat, low-lying, wide arc from Florida to Mexico. Topography of the lower Gulf Coast is relatively flat, whereas the upper Gulf Coast, including most of the current and past mining operations of the STU Province, generally has low relief (rolling plains) except where it is locally dissected by rivers and streams (Figure 13). Elevations range from sea level to about 800 ft in the southwest. Three major rivers from south to north are: the Nueces River, which flows into Corpus Christi Bay, and the San Antonio and Guadalupe Rivers, which flow into San Antonio Bay southeast of the city of Victoria. The Rio Grande in the west and the Lavaca River in the northeast bound the study area. Rivers and river basins are shown in Figure 14. The river and stream network is important because of permanent interaction between surface water and groundwater and typically alternating losing and gaining sections. Several researchers have documented stream and lake contamination resulting from natural aquifer or mine-generated contamination (Brandenberger et al., 2004).

The STU region encompasses many climatic regions, and its climate ranges from semiarid in the southwest to semihumid in the northeast, with temperature and precipitation both varying significantly across this gradient. Overall the climate is warm and dry, with hot summers and relatively mild winters. However, the region is strongly influenced by its proximity to the Gulf of Mexico and, as a result, has a much more marine-type climate than the rest of Texas, which is more typically continental. A network of weather stations provides data to develop the interpolated maps that follow (Figure 15).

Mean annual precipitation across the region varies from less than 20 inches/yr at the U.S.-Mexico border to slightly more than 35 inches/yr toward the northeast of the study area (Figure 16). On average the wettest months are May and September, which tend to see more than 4 inches per month, and the driest months are January, February, and March, with approximately 2 inches per month. Most of the remainder of the study area follows the same relative trends (Figure 17). USGS has published data summaries on extreme events (e.g., Lanning-Rush et al., 1998). The NCDC publishes maps showing precipitation intensity during a given time period at a given recurrence interval (NCDC, 2009). A recurrence interval of 25 yr seems a good compromise for future activity on the legacy waste. Along the Catahoula outcrop, precipitation intensity with a return interval of about 25 yr is 8 to 9 inches during a 24-h period, 5.5 to 6.5 inches (6 h), 4.3 to 4.7 inches (2 h), 3.4 to 3.7 inches (1 h), and about 2.8 inches (30 min) (Figure 18). Similar maps have also been published by the USGS (Asquith and Roussel, 2004).

Monthly mean temperatures range from 55ºF (mean daily minimum temperature of 42ºF) in January to 84ºF (mean daily maximum temperature of 96ºF) in August. Mean annual temperatures are between those two extremes and vary from 68ºF to 74ºF (Figure 19). Pan

evaporation ranges from 85 inches/yr in the southwest to 45 inches/yr in the northeast (Larkin and Bomar, 1983; Williamson and Grubb, 2001), implying a general excess of evapotranspiration over precipitation over much of the south Gulf Coast region. Average gross lake evaporation varies from 40+ to 70+ inches/yr (Figure 20). Net lake annual evaporation (evaporation–precipitation) is always positive and varies from a small value in the northeast of the STU to 40+ inches/yr in Webb County (Figure 21).

Major natural regions (Figure 22) depend on topography, lithology, and climate. The Gulf Coast prairies of the lower Gulf Coast run along the Gulf of Mexico. Trees are uncommon except along streams and locally on coarser sediments. Most of the Catahoula outcrop and surrounding formations, including most historical open-pit mines, belong to the so-called South Texas brush country. The region is blanketed with low-growing, mostly thorny vegetation. Where conditions allow, a dense understory of small trees and shrubs develops (TPWD, 2010). The STU Province is mostly sparsely populated, and the land use / land cover map reflects mostly natural regions (Figure 23).

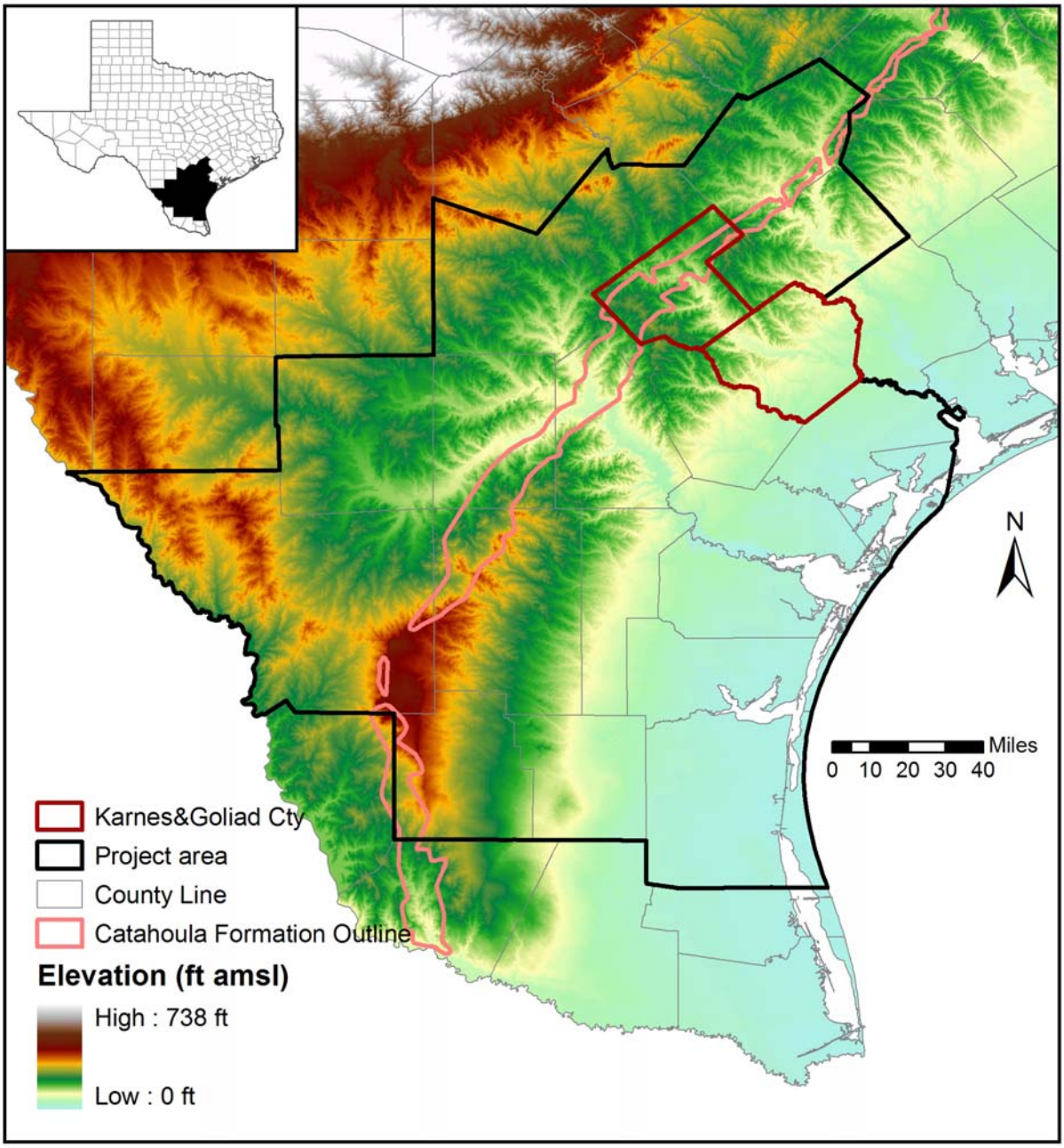

Source: USGS http://www.usgs.gov/pubprod/data.html#data

Figure 13. Topographic map of the South Texas area

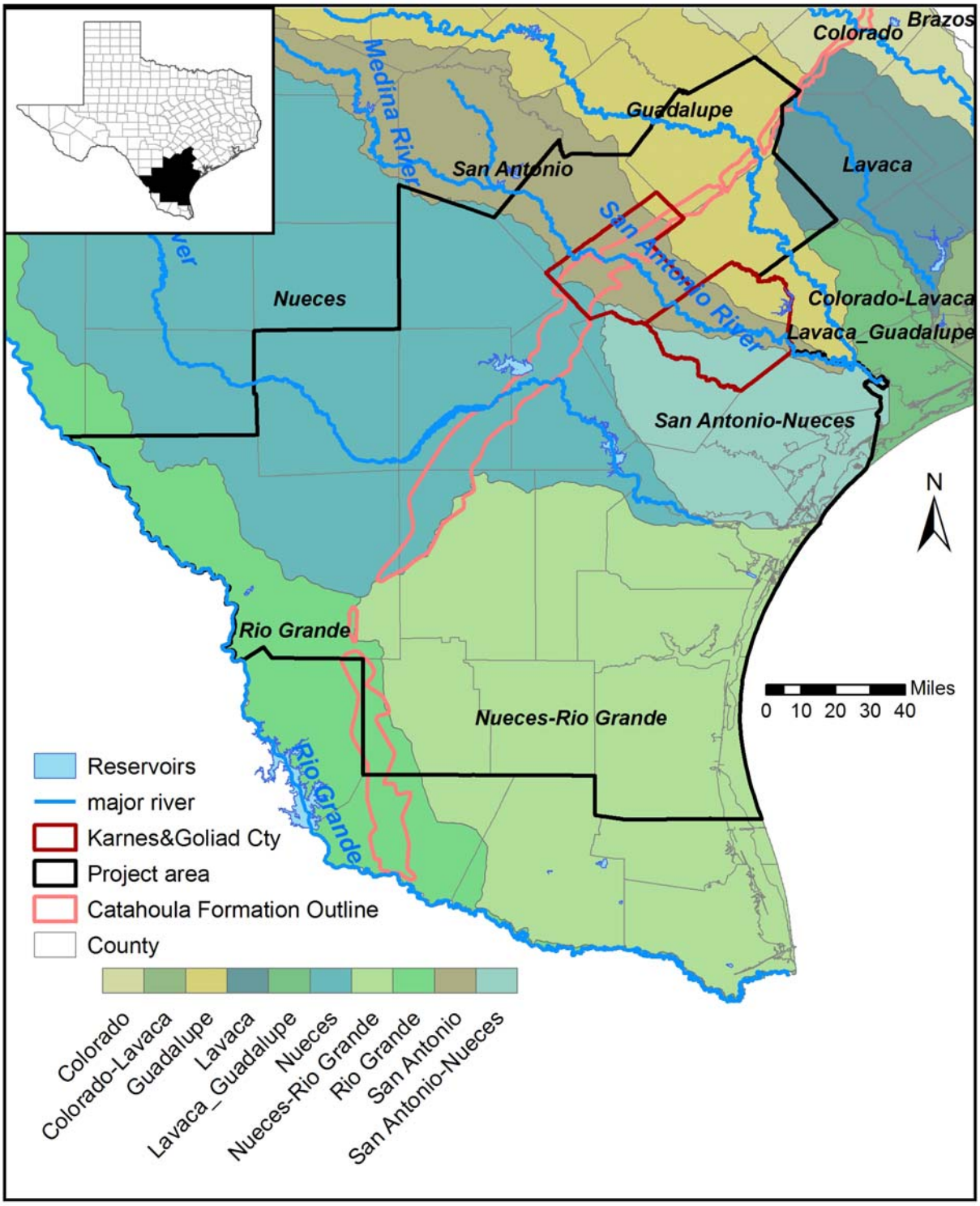

Source: TWDB, http://www.twdb.state.tx.us/mapping/gisdata.asp, January 2009

Figure 14. Rivers and river basins in the study area

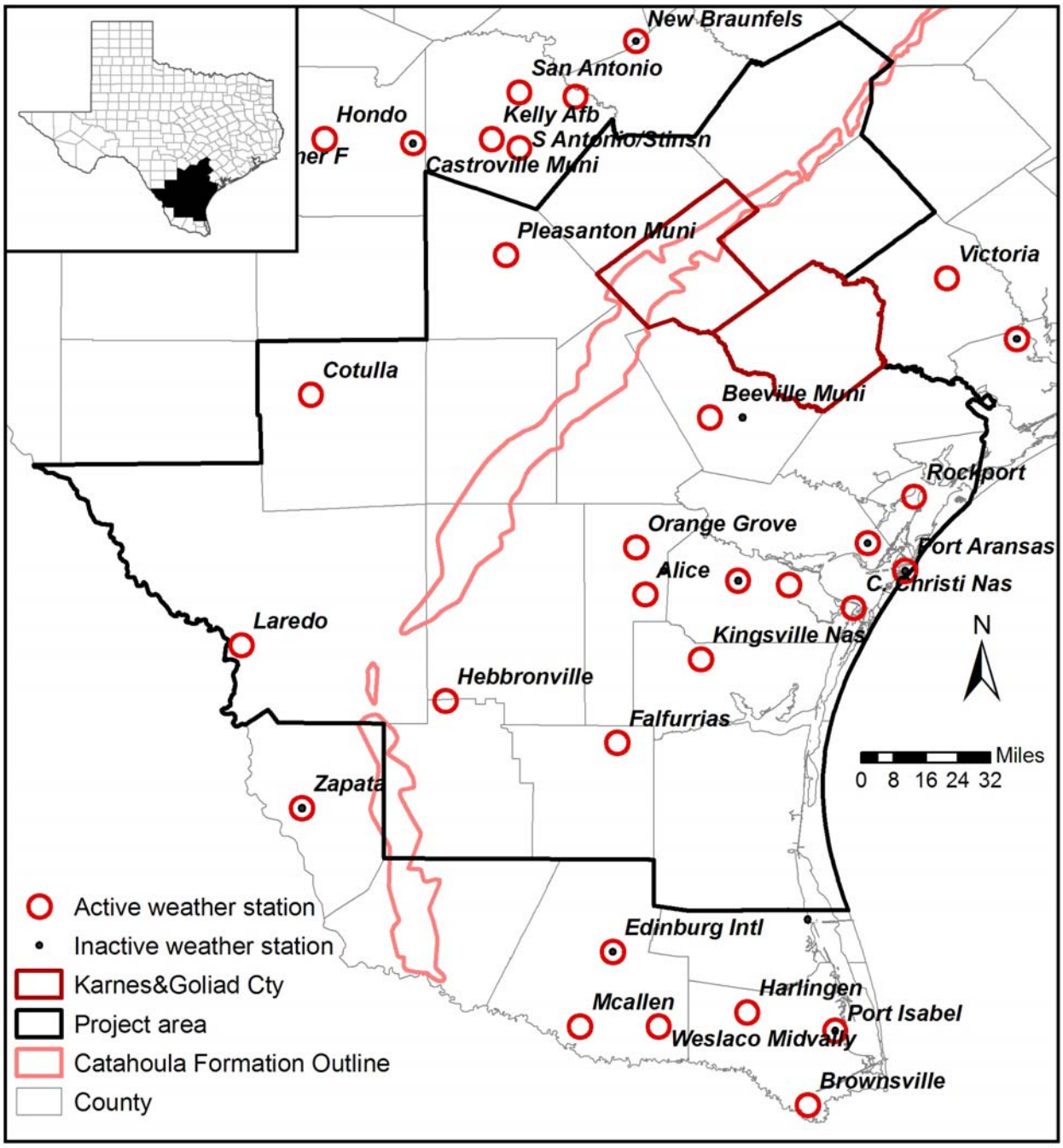

Source: National Center for Atmospheric Research http://www.rap.ucar.edu/weather/surface or http://www.rap.ucar.edu/weather/surface/stations.txt

Figure 15. Weather station locations

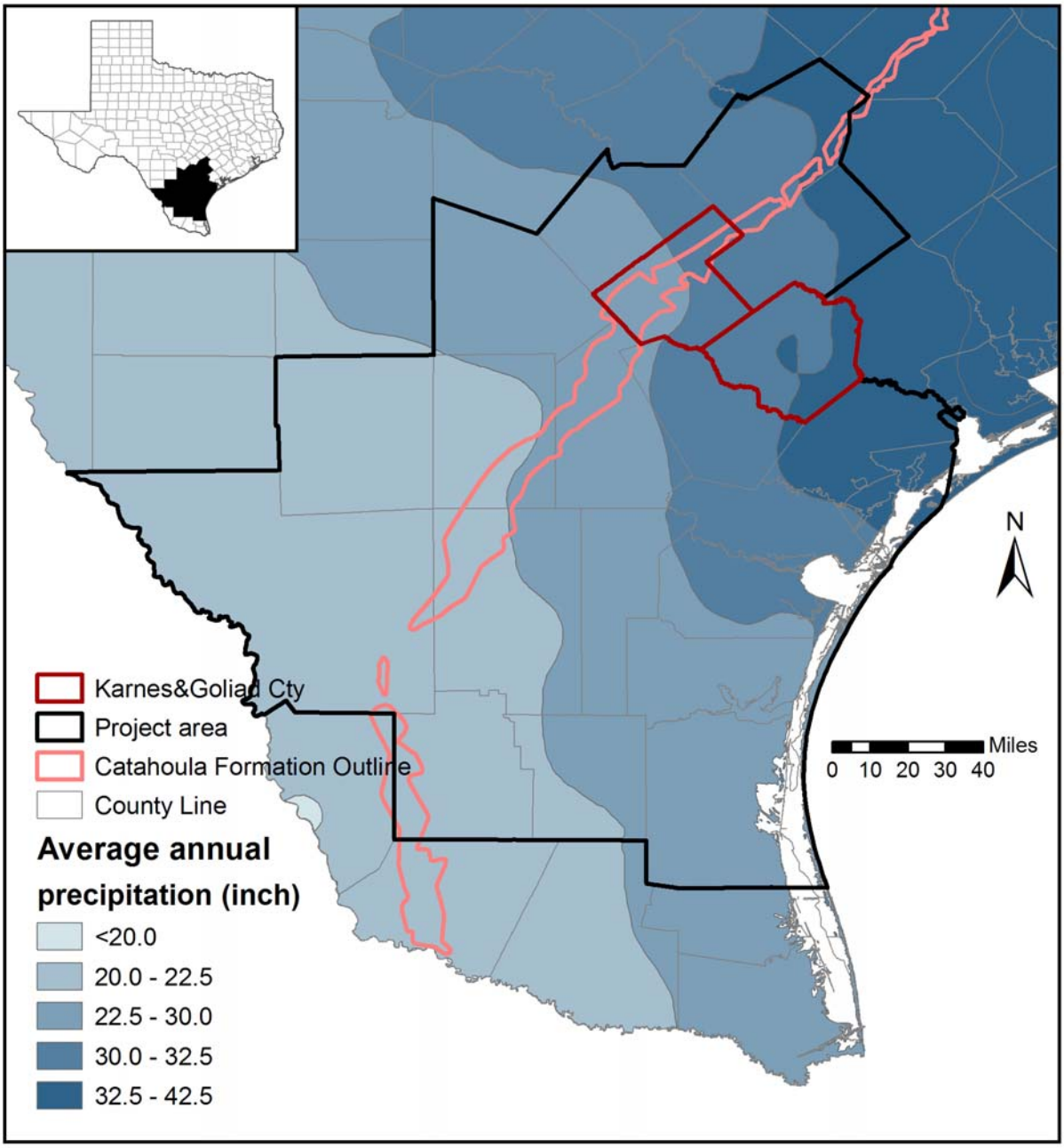

Source: National Center for Atmospheric Research

Figure 16. Mean annual precipitation

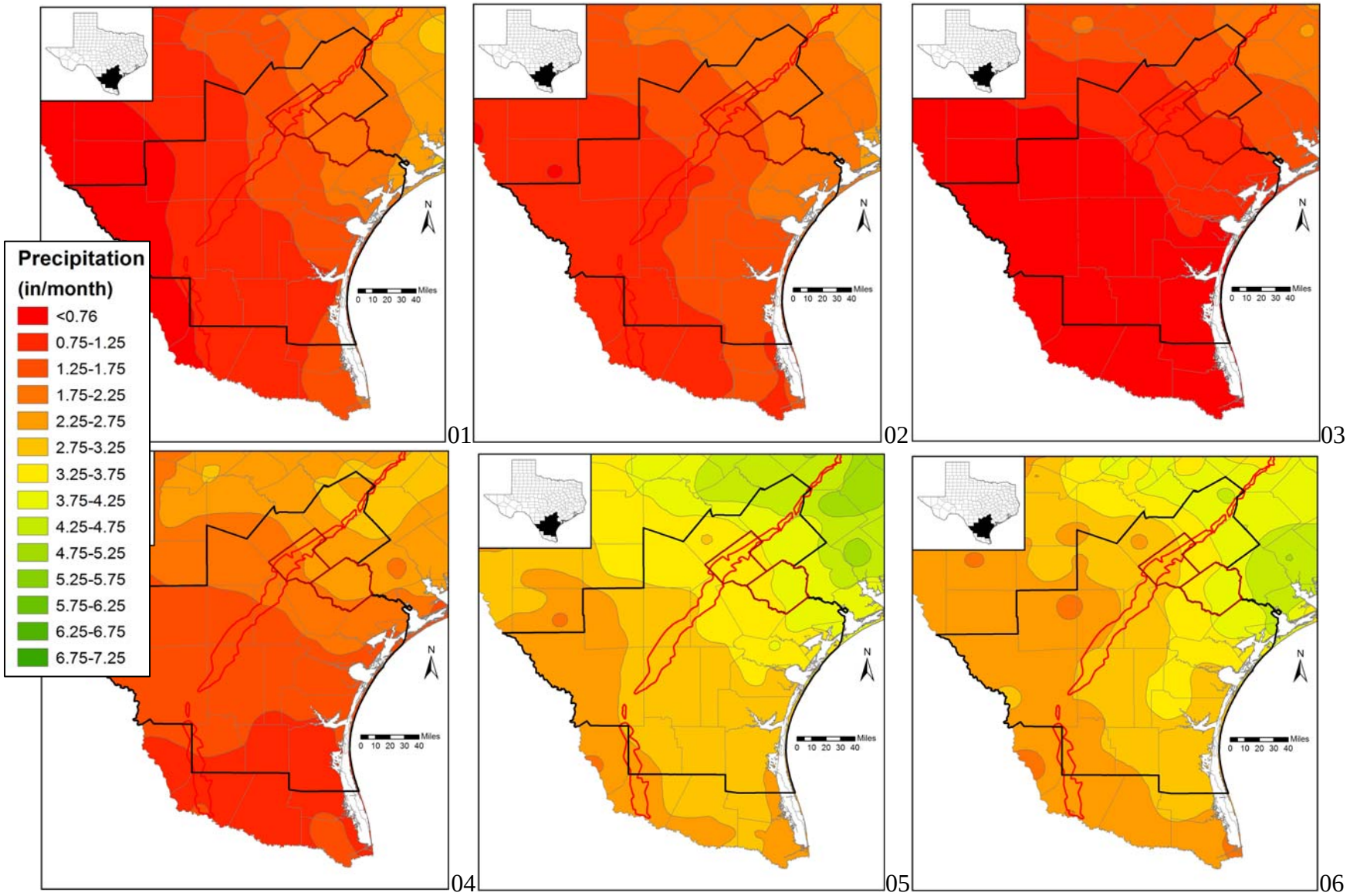

Figure 17. Average monthly precipitation

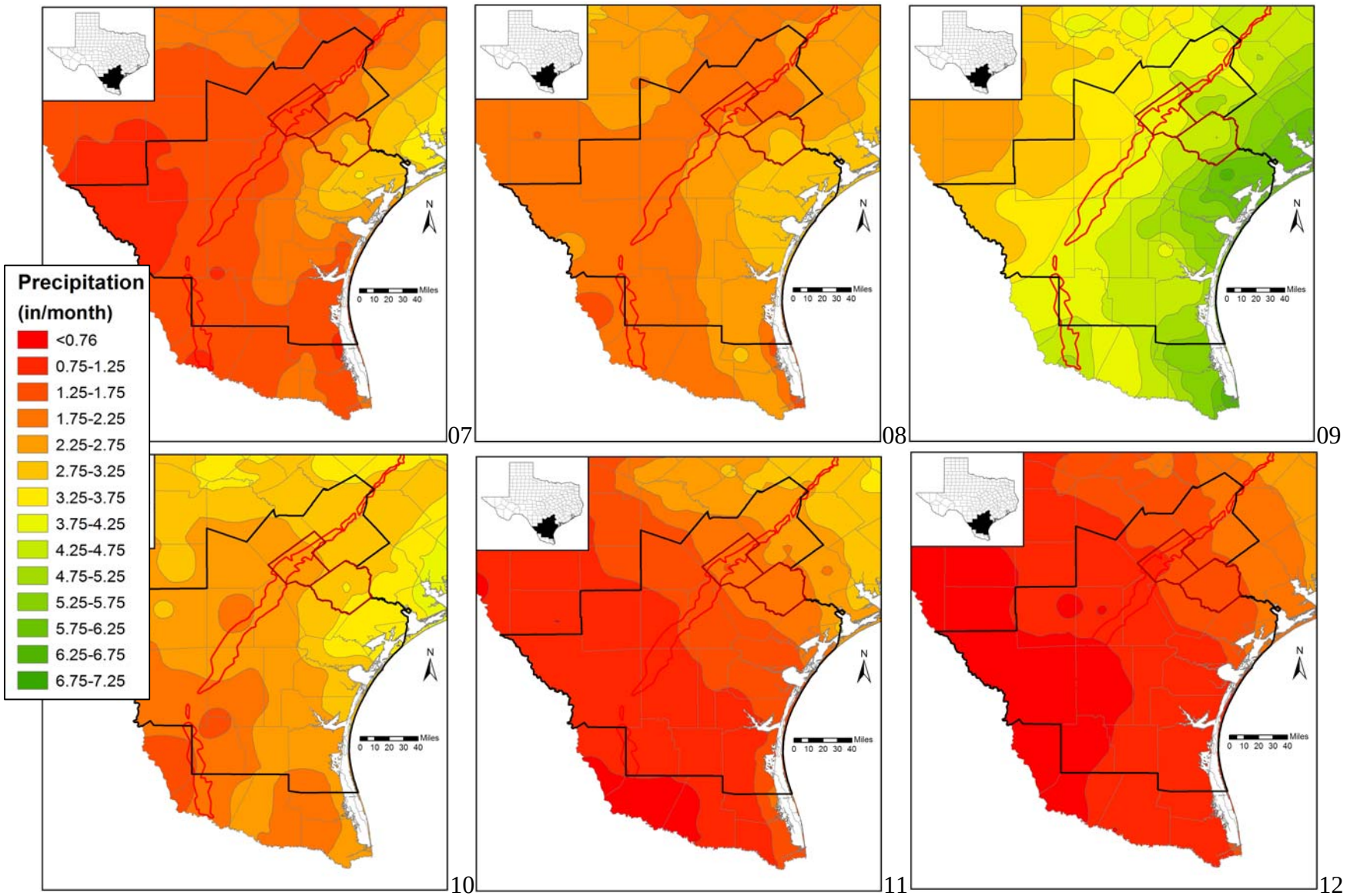

Figure 17. Average monthly precipitation (continued)

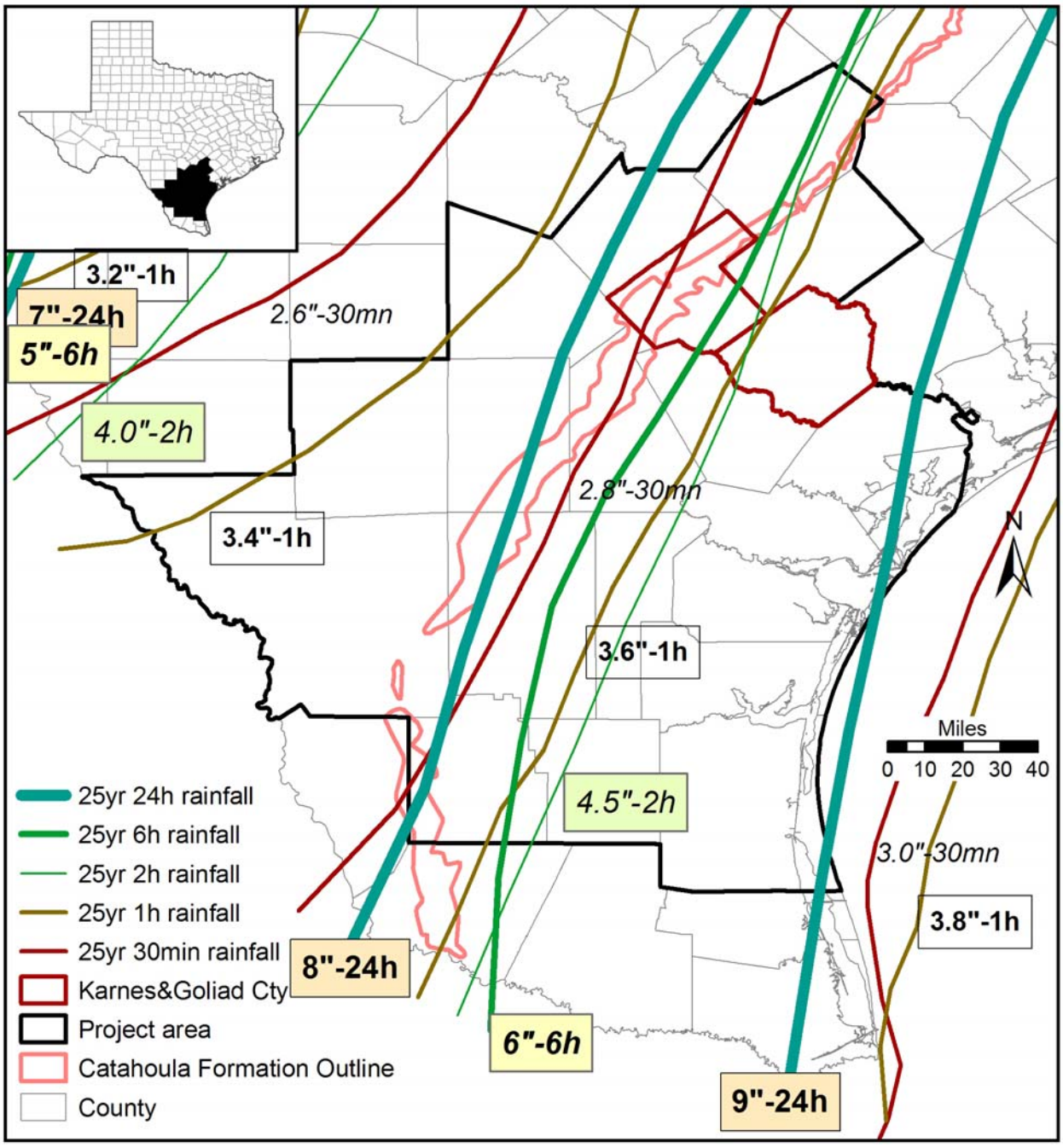

Source: http://www.ncdc.noaa.gov/oa/documentlibrary/rainfall.html and Hershfield (1961)

Figure 18. Iso-maximum precipitation contour lines with a 25-yr recurrence

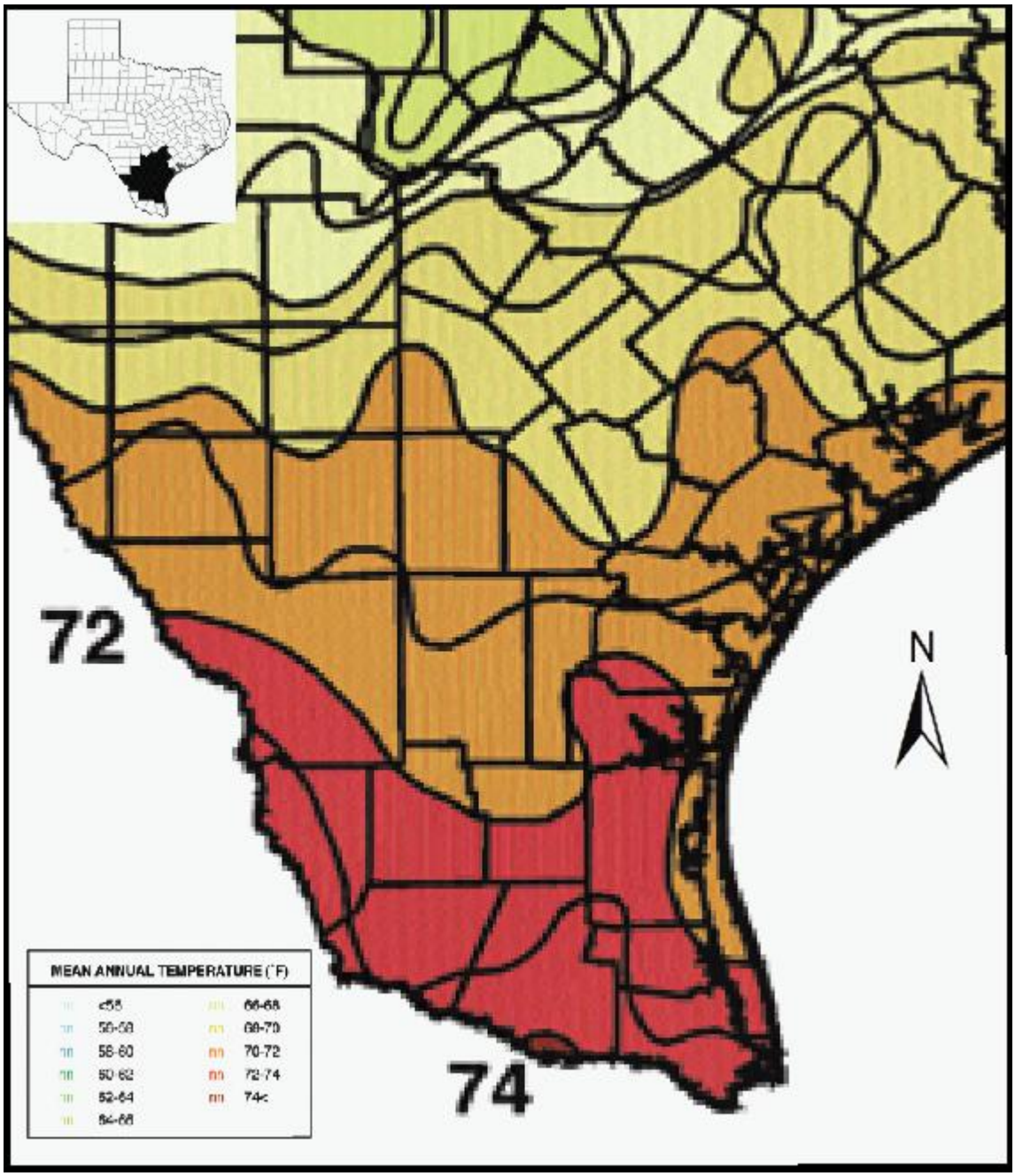

Source: SECO (2008) and
http://seco.cpa.state.tx.us/publications/renewenergy/pdf/c02-texasclimate.pdf

Figure 19. Average annual temperature

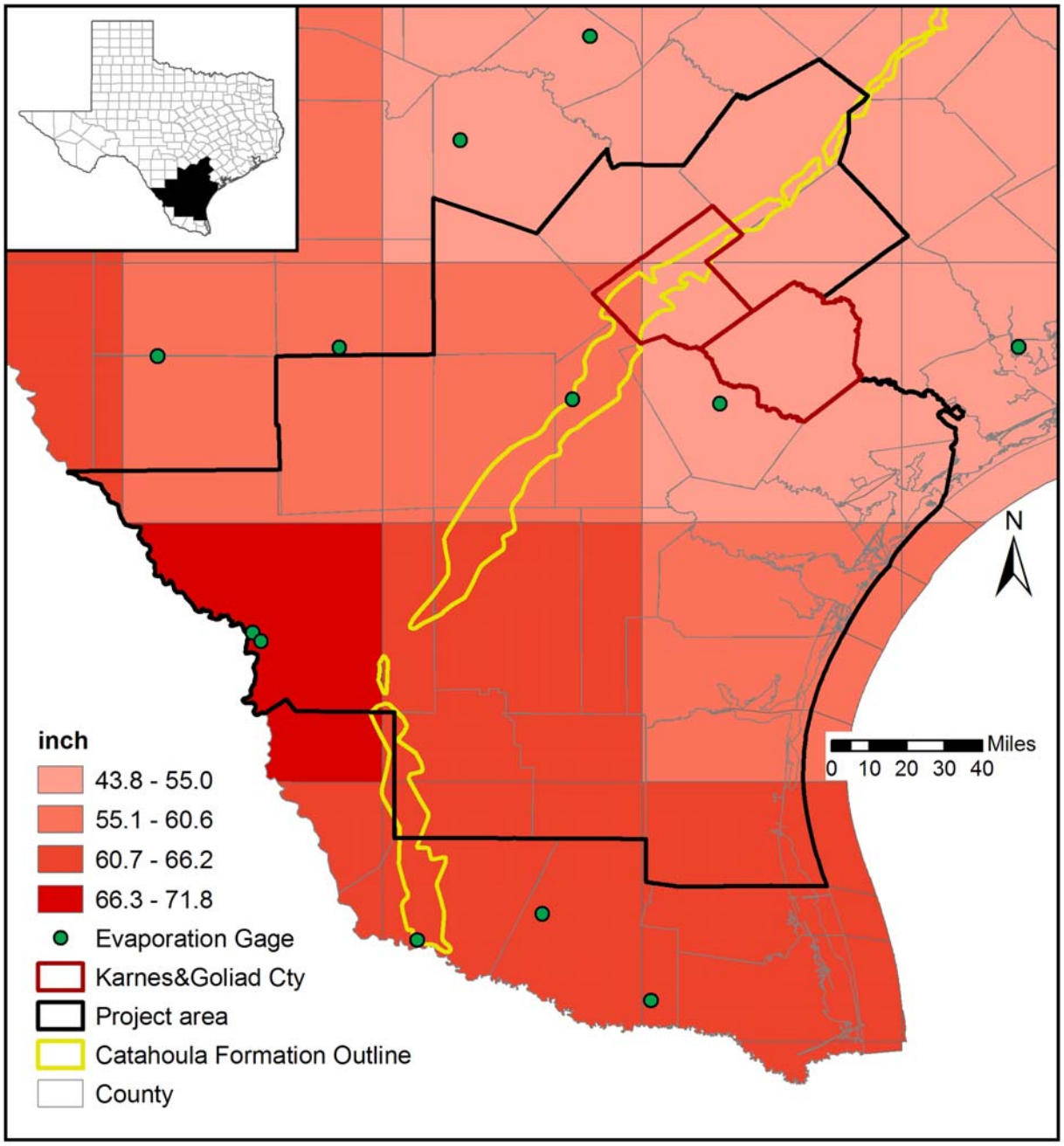

Source: TWDB, evaporation/precipitation data for Texas

Figure 20. Mean gross lake annual evaporation (inches)

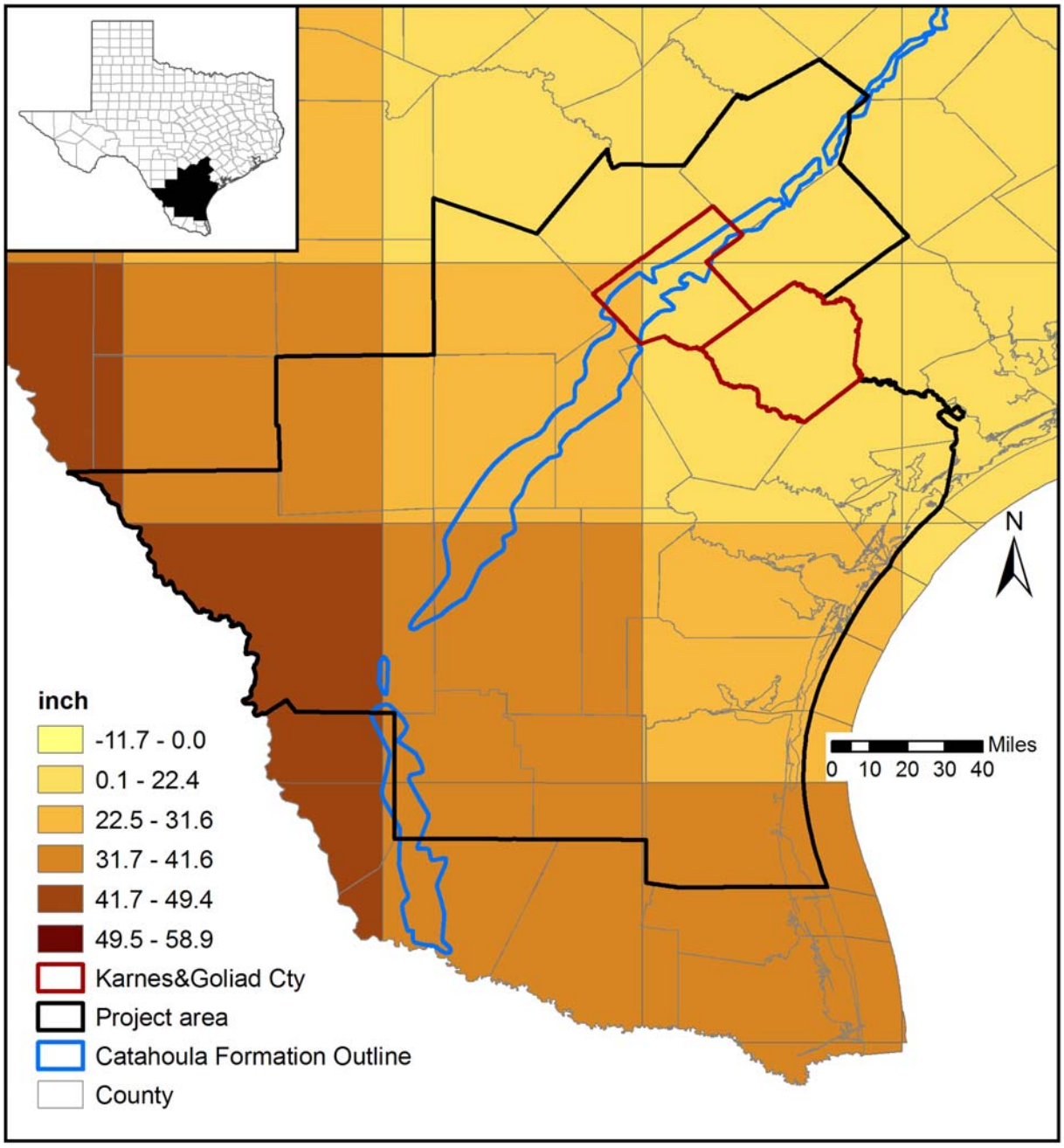

Source: TWDB, evaporation/precipitation data for Texas
Note: no negative net evaporation on the map extent

Figure 21. Net lake annual evaporation (inches)

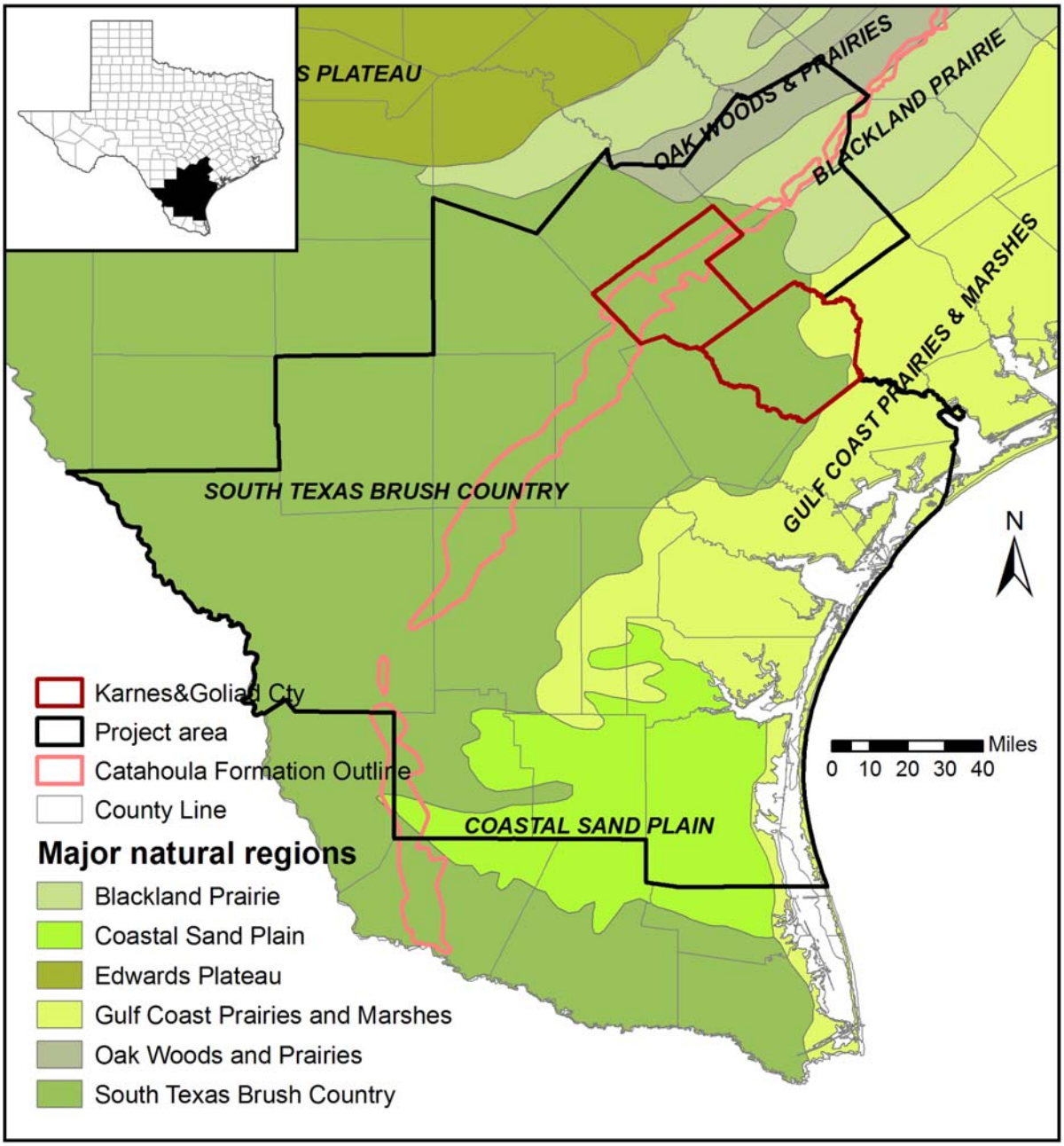

Source: Texas Parks and Wildlife website:
http://www.tpwd.state.tx.us/landwater/land/maps/gis/data_downloads/

Figure 22. Major natural regions in the study area

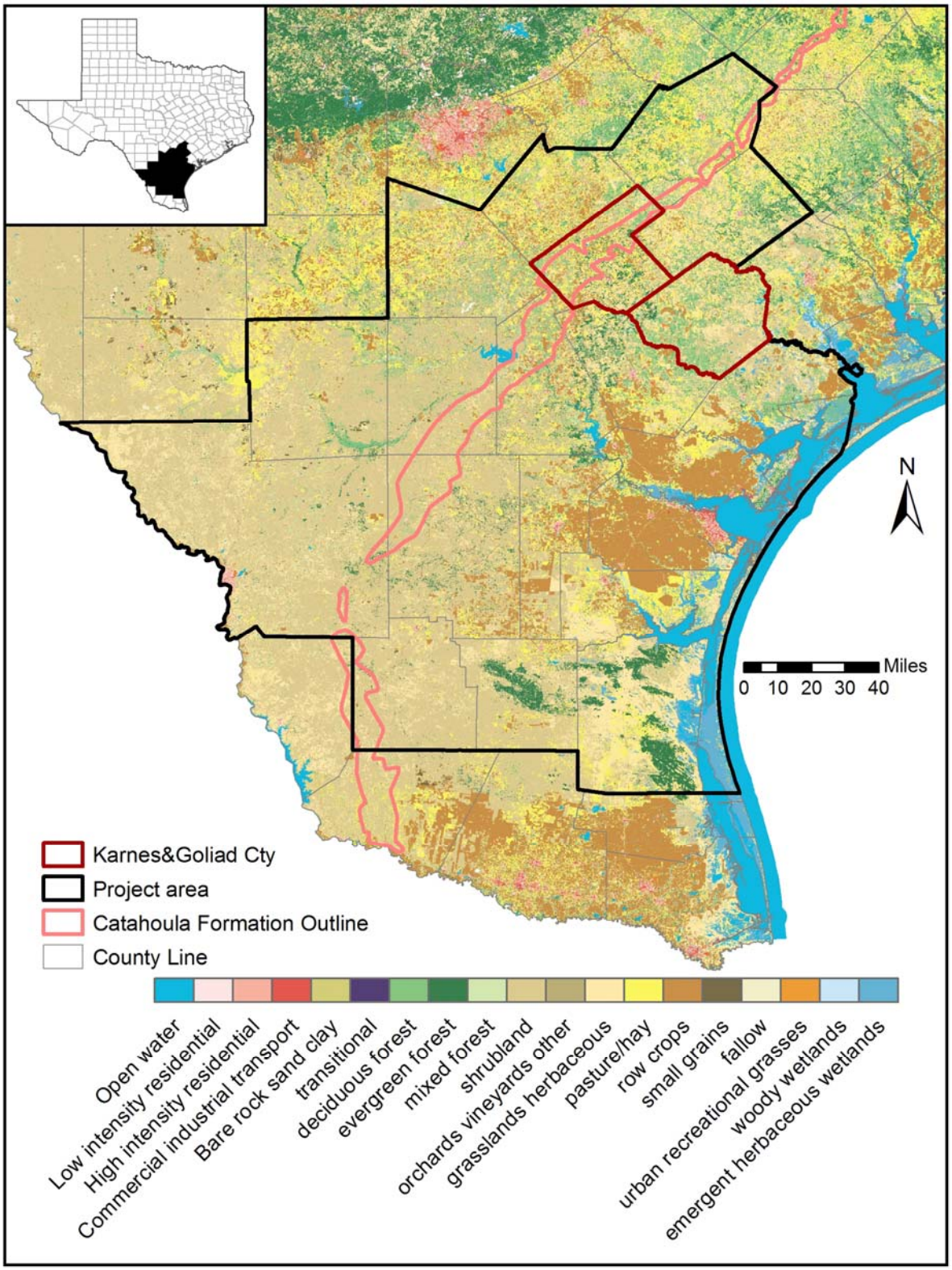

Source: USGS website: http://www.usgs.gov/pubprod/data.html#data

Figure 23. Land use / land cover

III. Geology and Hydrostratigraphy

III-1. Description of Data Sources

Most information presented in this section was obtained from large projects undertaken at the BEG in the 1970's and 1980's in support of oil and gas and uranium exploration. The methodology was always the same: to gather numerous (hundreds to thousands) of geophysical oil and gas or water well logs (generally resistivity and spontaneous potential) and correlate them in dip- and strike-oriented cross sections. Resistivity logs measure salinity of water near the well. Salinity is generally higher and resistivity lower in less permeable rocks such as clays. Complications arise because of the presence of drilling mud, and generally long- and short-range resistivity tools are used in combination. Spontaneous potential measurements detect differences in electrical potential between formation water and drilling mud. Deflection toward lower potential (to the left) suggests that salinity of the formation is lower than that of drilling mud, suggesting a sandy layer ("sand line"). On the other hand, deflection to the right (higher potential) suggests a less-well-flushed, clayey layer ("shale line").

From the well logs, regional maps of lithofacies and inferred depositional systems and total sand thickness were produced. Many reports that document the process and general results related to the Gulf Coast have been published in several publications (Galloway, 1982a; Galloway and Hobday, 1996; Galloway et al., 2000). Fisher and McGowen (1967) introduced the concept of the depositional system in the Gulf Coast area. They defined it as "a three-dimensional, genetically defined physical stratigraphic unit that consists of contiguous, process-related sedimentary facies." The depositional system has become a powerful tool for correlating formation properties in a sophisticated way between well log locations.

III-2. Depositional History and Stratigraphy

III-2-1 General Geology

The importance of describing formations' depositional systems lies in their control of fluid flow, as has been well described in Knox et al. (2007) in a report for the TWDB on the structure of the Yegua-Jackson aquifer. The summary of the depositional history in the Gulf of Mexico, including South Texas provided by Galloway et al. (2000), includes an overview of the lithologic history of the Gulf of Mexico, as well as the STU Province. In the next paragraphs, we summarize relevant points of the geological history of the uranium province.

The geology of the Gulf Coast aquifer in Texas is complex because of cyclic deposition of sedimentary facies. The coastal plains of the Gulf of Mexico basin were formed by downfaulting and downwarping of Paleozoic basement rocks during the breakup of the Paleozoic megacontinent, Pangaea, and the opening of the North Atlantic Ocean in the Late Triassic (Byerly, 1991; Hosman and Weiss, 1991). Three main structural zones can be seen in the study area: the Balcones Fault Zone, the San Marcos Arch, and the Rio Grande Embayment. The Balcones Fault Zone is north of the study area and forms a divide between Upper Cretaceous and Eocene strata (McCoy, 1990). The Balcones Fault Zone consists of mainly normal faults that occur parallel to the trend of the buried Ouachita Orogenic Belt. Along these faults, sediments have been displaced by up to 1,500 ft, moving downward to the Gulf of Mexico. The San Marcos Arch, northeast of the study area between the Rio Grande Embayment and East Texas Basin, is a

broad area of lesser subsidence and a subsurface extension of the Llano Uplift (Chowdhury and Turco, 2006). The arch is crossed by basement-related normal faults that parallel the buried Ouachita Orogenic Belt of Paleozoic age (Ewing, 1991). The Rio Grande Embayment is a small deformed basin that lies between the El Burro Uplift in northeast Mexico and south of the basin-marginal Balcones Fault Zone (Ewing, 1991). Some data indicate that the embayment was possibly compressed during the Laramide Orogeny in the Late Cretaceous–Paleogene (Ewing, 1991).

During the Cretaceous, sediments deposited from shallow inland seas formed broad continental shelves that covered most of Texas. In the Tertiary (starting 65 million yr ago), the Rocky Mountains to the west started rising, and large river systems flowed toward the Gulf of Mexico, carrying abundant sediment, similar to the Mississippi River today. Most of Texas, particularly West Texas, was also uplifted, generating a local sediment source, including erosional debris from the multiple Tertiary volcanic centers in West Texas and Mexico. Six major progradational events occurred in which sedimentation built out into the Gulf Coast Basin (Figure 24). These progradational sequences include, from oldest to most recent, Wilcox, Queen-City, Yegua-Jackson, Vicksburg-Catahoula-Frio, Oakville-Fleming, and Plio-Pleistocene sand-rich wedges (Galloway et al., 2000). The set of depositional systems is the same throughout the Tertiary period: fluvial, deltaic, barrier bar/strandplain, and slope/basin depositional systems. For example, formations hosting uranium mineralizations—late Eocene barrier-lagoon and deltaic systems of the Jackson Group, Oligocene to early Miocene Catahoula Formation fluvial systems, early Miocene Oakville Formation fluvial systems, and Miocene Goliad Formation fluvial systems—embody the general progradation of Gulf Coast sediments transitioning from marine to continental depositional systems. A general stratigraphic column is presented in Figure 25. During most of the Tertiary history of the Texas coast, little variation occurred in the area of the main depocenters, resulting in individualized subbasins. Major fluvial depoaxes occupying the same structural troughs include the Rio Grande Embayment of South Texas and the Houston Embayment, separated by the San Marcos Arch characterized by less abundant sediment influx. This variable sediment input is also true at a smaller scale (Figure 26). Vertical continuity of sand in main depocenters is impacted by lateral migration of channels through time. For example, channel sand bodies vertically stack in rapidly subsiding basins, whereas in a more stable tectonic environment, distributary channels may wander more, resulting in vertically offset sand bodies. Lateral continuity can also be understood in terms of depositional systems (Figure 27). Wave-dominated deltaic and strandplain systems present high lateral continuity and may be thick, whereas fluvial and fluvial-deltaic systems may present abrupt lateral facies change. In addition, sediments from wave-dominated deltaic and strandplain systems are generally well sorted. In general, sand permeability is correlated with sand-body thickness—that is, transmissivity increases more than linearly with thickness. Such considerations have important implications both for explaining location and amount of uranium mineralization and for predicting contaminant migration.

Sediments composing the Gulf Coast Basin have been deposited by river systems flowing from upland areas toward the Gulf of Mexico, resulting in prevailing stratigraphic dip nearly perpendicular to the coastline and general thickening of the beds from inland toward the coast. The basin is bounded updip by the Balcones Fault Zone (a major structural discontinuity; Baker, 1979, 1995) to the northwest and the coastal margin to the southeast (Galloway et al., 1982b). Growth faults, resulting from sediment loading on unstable substrates, periodically develop. Intermittent movement along these growth faults accommodated accumulation of enormous

masses of sediments. Growth faults are mostly syndepositional faults, and zones of growth faulting mark basinward movement of the shelf edge. Fault-bounded reservoir compartments create many structural traps for hydrocarbons in the Tertiary stratigraphic section of the southern Gulf Coast Basin.

Hydrostratigraphic units do not necessarily correspond to stratigraphic units (discussed in Section III-4). The former are defined in terms of flow (i.e., in terms of "permeable" layers vs. "impermeable" or much less "permeable" layers), whereas the latter are defined in terms of age. Three main aquifers define the Gulf Coast aquifer (defined as a major aquifer by the state): the Jasper, Evangeline, and Chicot aquifers, which broadly include the Oakville Sandstone, the Goliad Sand, and Quaternary units, respectively. The Fleming Formation is a confining unit between the Jasper and Evangeline aquifers and is called the Burkeville Confining Unit. A more accurate model would consider that the top of the Catahoula Formation is sometimes included in the Jasper aquifer, just as the top of the Fleming Formation is included in the Evangeline aquifer. The Jackson aquifer, stratigraphically below the Catahoula Formation, is now considered a minor aquifer by the state.

Component geologic units of the Gulf Coast aquifers are, from oldest to youngest, (1) Catahoula Formation; (2) Oakville Sandstone/Fleming Formation; (3) Goliad Formation; (4) Pleistocene formations, the Willis, Lissie, and Beaumont; and (5) Quaternary terrace deposits and alluvium (Doering, 1935; Baker, 1979) (Figure 6). Rocks of the Jackson Group and Frio Formation underlie the Gulf Coast aquifer formations and are pertinent to this study because they contain volcanogenic deposits, which are associated with uranium deposits and, presumably, arsenic concentrations in groundwater. The geologic units range in age from Eocene (Jackson Group) to Recent (see Figure 25). Stratigraphic relationships and definitions are inconsistent and sometimes ambiguous for this group of Tertiary rocks, which are now discussed from oldest to youngest.

III-2-2 Jackson Group

The Jackson Group is part of a major progradational cycle that also includes the underlying Yegua Formation. The Jackson Group includes, from older to younger, the Caddell, the Wellborn, the Manning, and the Whitsett Formations (Eargle, 1959; Fisher et al., 1970). These four formations are well expressed in East Texas but transition to a more complicated nomenclature in Karnes County. Total thickness averages 1,100 ft in the subsurface but becomes thinner in the outcrop area and is characterized by a complex distribution of lagoon, marsh, barrier-island, and associated facies (Figure 28). The so-called Fayette fluvio-deltaic system present in Central and East Texas provided the sand transported to South Texas by longshore drift in a paleogeography analogous to the current coast of the Gulf of Mexico. The lower part of the Jackson Group consists of a basal 100-ft sequence of marine muds (Caddell Formation) overlain by 400 ft of mostly sands: Wellborn / McElroy Formation with the Dilworth Sandstone, Conquista Clay, and Deweesville / Stones Switch (Galloway et al., 1979a, p.45) Sandstone members toward the top. The middle part consists of 200 to 400 ft of mostly muds (including the Dubose Clay Member). Several sand units are present in the 400- to 500-ft-thick upper section, including the Tordilla / Calliham Sandstone overlain by the Flashing Clay Member. As indicated in Figure 7, units from the Dilworth unit on up are grouped under the Whitsett Formation name (classification from Eargle, 1959). Only the latter contains significant amounts of uranium mineralization in the Deweesville and Tortilla sand members (Figure 7). Kreitler et al. (1992,

Section 2) provided more details on these units near the Falls City Susquehanna-Western mill. Uranium mineralization occurs where the strike-oriented barrier sand belt intersects the outcrop. Sand, generally fine and heavily bioturbated by burrows and roots, also contains lignitic material and silicified wood. Discontinuous lignite beds are also present (Fisher et al., 1970).

III-2-3 Frio Clay

Early Oligocene Frio Clay of marine origin (sometimes called the Yeager Formation in the past) blankets the Jackson Group, separates it from the Catahoula Formation, and forms a low-permeability barrier to vertical communication, although the Frio Clay can be locally absent. Alternatively some earlier authors (as mentioned in Baker, 1979, p. 36) suggested the now-discredited hypothesis that the Frio Clay is the nonmarine equivalent of the subsurface Vicksburg Group (see Figure 5). Its maximum thickness is approximately 200 ft (Brown et al., 1976). It marks the top of the third major progradation sequence of the Gulf Coast (Yegua-Jackson, Figure 24). In Karnes County, the clay is bentonitic and slightly calcareous (Anders, 1960, p. G18).

III-2-4 Catahoula Formation

The Catahoula Formation unconformably overlies the Oligocene sediments of the Jackson Group. Catahoula sediments are fluvial rather than marine derived and are composed in varying proportions of sands, clays, and volcanic tuff, depending on location (Figure 29). Several authors suggest that the Catahoula Formation in the southwest of the state should be referred to as the Gueydan Formation (McBride et. al., 1968; Parker, et. al., 1988). In Texas the Catahoula Formation consists of deposits of two major depositional systems: the bed-load Gueydan fluvial system of the Rio Grande Embayment and north of the San Marcos Arch / Llano Uplift the mixed-load Chita-Corrigan fluvial system of the Houston Embayment (Figure 30). These two major depocenters are areas of increased general subsidence. Baker (1979) noted that this unit is often referred to as Catahoula Tuff in the southwest and Catahoula Sandstone northeast of the Colorado River, where it contains more sand and less volcanic material than in the southwest. Only the former is discussed in this document. Contrary to the along-strike sand bodies of the Jackson Group, sand bodies in the Catahoula Formation are mostly dip oriented, consistent with a fluvial depositional system. Sediments of the Catahoula Formation reflect a strong volcanic influence, including numerous occurrences of airborne volcanic ash (Galloway 1977) (Figure 31). Thicknesses of strata at the outcrop range from 200 to 1,000 ft. In the southwestern counties of Duval and McMullen, the Catahoula Formation reaches the maximum thickness of 1,000 ft and contains the coarsest volcanic material of any Gulf Coast Tertiary unit (McBride, et. al., 1968). In this region the Catahoula Formation lies unconformably on either the Frio or Whitsett Formation of the Jackson Group. The formation also thickens gulfward as is typical of other Gulf Coast sequences. However, the Catahoula Formation does so by extremely large amounts, and it transitions to the so-called Frio Formation (only existing in the subsurface and not to be confused with the distinct Frio Clay). Over most of the coastal plain, this transition occurs approximately along the line at which the top of the Catahoula occurs 2,000 ft below the surface (Galloway, 1978, p. 1655). In general, the amount of clay and fine-grained material increases downdip until the pinch-out of the Anahuac Formation is reached (Figure 5), after which point the Frio Formation becomes sandier. In the southwest the Catahoula/Gueydan Formations are unconformably overlain by either the Oakville or the Goliad Formation, whereas in the northeast

toward East Texas, they are overlain by the Fleming Formation (Aronow et. al., 1987; Shelby et. al., 1992).

Sand content ranges from <10% to a maximum of about 50% (Galloway, 1977, p. 10). Fluvial deposition patterns have resulted in highly spatially heterogeneous textural composition, with facies types including channel fill (very coarse), crevasse splay (sandy/silty), floodplain (silty/clayey), and coastal lake (silty). The Gueydan system includes, in vertical succession, the Fant Tuff, Soledad Conglomerate, and Chusa Tuff (all mapped together in Figure 6). The middle member contains the largest amount of coarse clastics, but the two tuff members also include sand units interbedded with massive lenticular units of tuffaceous mudstone and claystone. These units were deposited mostly by sporadic flooding events of large ash-laden streams, ash that was subsequently altered to clay although the units' permeability during deposition or shortly thereafter was likely moderate to high (Galloway, 1977, p. 37). Paleosols are abundant. They sometimes record rapid devitrification of volcanic ash, calichification, and other processes typical of vertisols common to arid to semiarid climates, illustrating a dramatic climate change from the more humid Oligocene period (Cherepon et al., 2007). McBride et al. (1968) described crossbedding in Gueydan strata, which suggests deposition of coarser grained volcaniclastics by streams flowing down a NW-SE-oriented paleoslope in Duval and Karnes Counties. Farther north in Fayette County paleocurrent data suggest more of an east-west flow. Sediments in the lower Catahoula Formation are predominantly gray tuff, whereas pink tuffaceous clay is more common in the upper strata, suggesting a change to more humid climatic conditions during deposition. Volcanic conglomerates and sandstone are most common in midlevels of the unit. Bentonite and opalized clay layers and alteration products of volcanic glass (zeolites, Ca-montmorillonite, opal, and chalcedony) are present throughout the formation and indicate syndepositional alteration of tuffaceous beds. Widespread areas of calichification indicate long periods of exposure to soil-forming conditions at the surface (McBride et al., 1968).

III-2-5 Oakville Sandstone

The Miocene-age Oakville Formation overlies the Catahoula Formation and represents a major pulse in sediments thought to be due to uplift along the Balcones Fault Zone. Galloway et al. (1982a) discussed the Oakville stratigraphy in detail. The Oakville Sandstone is composed of sediments deposited by several fluvial systems, each of which had distinct textural and mineralogical characteristics (Smith et al., 1982a). Together with the overlying Fleming Formation, they formed a major depositional episode. As a nomenclature note, the Fleming is sometimes called the Lagarto Formation in other studies. Galloway et al. (1986, p. 2) also defined a Fleming Group that includes the Oakville and the "Lagarto Formation" These two units are commonly grouped because they are both composed of varying amounts of interbedded sand and clay. In the central part of the Gulf Coast (Brazos River to central Duval County), they are easily recognized as stratigraphically adjacent units because the Oakville is sand rich and the Fleming is more clay rich. To the northeast of the Brazos River, the two units are indistinguishable. Average thickness varies from 300 to 700 ft at the outcrop (Galloway et al., 1982a, p. 4), and the formation is thicker in the subsurface (Henry et al., 1982a, p. 3). Galloway et al. (1982a) identified five principal depositional elements, including four bedload fluvial axes most likely representing areas of peak transmissivity, and a broad interaxial area composed of sediments from smaller, localized stream systems farther north at the limit of the study area (Figure 32, Figure 33, and Figure 34). Each of the elements has distinct thickness, grain-size distribution, and mineralogy resulting from variations in terrain and source material. River

meandering has resulted in a complex sinuous geometry for these channels. The Oakville Sandstone grades into the mixed-load sediments of the overlying Fleming Formation and into the thicker deltaic and barrier systems farther downdip. Sand percentage is high in the paleochannels, whereas finer-grained floodplain deposits are more common in adjacent interchannel environments. Paleosols are not as frequent as in the previous formations, such as the Catahoula Formation and Jackson Group. Most of the uranium mines are located within these axes of high transmissivity ("George West" and "New Davy" axes) (Figure 26). The "George West" axis has a particularly high sand percentage (with minor conglomeratic levels) next to the outcrop where most uranium mines are found. Farther downdip the amount of sand increases as the formation thickens, but the sand fraction decreases because of additional mud facies. The Jackson Group and Oakville Sandstone also display an important contrast in organic material content, abundant in the Jackson sand bodies (which contain their own reducing material), but lacking in that of the Oakville. An important conclusion related to uranium mineralization is that Oakville- and Goliad-hosted deposits need an external reducing factor, namely reducing fluids coming up faults to precipitate uranium.

III-2-6 Fleming Formation

The Oakville Formation is overlain by the Fleming Formation, which is also Miocene in age, and consists of relatively fine-grained, mixed-load-fluvial, and coastal-plain deposits (Galloway et al., 1986). Typically the sediments are complexly interbedded sands, silts, and clays, with intermixed volcaniclastic and tuffaceous material. In South Texas, the Fleming Formation is composed primarily of clays, with sand percentage increasing eastward toward the Sabine River (Chowdhury and Turco, 2006, p. 40). The Fleming Formation is distinguished from the Oakville Formation by its greater percentage of clays, although this distinction is sometimes absent locally. Solis (1981) developed several net-sand and sand-percentage maps of Central Texas (as far south as Duval County), as well as synthetic, depositional systems maps (Figure 35 and Figure 36). He divided the Fleming Formation into two operational units, both having low sand content on average (muddy floodplain deposits), but which can be locally high along river axes (meanderbelt). Sand maps of the Oakville and Fleming Formations are also provided in Galloway et al. (1986, Figs. 9–11).

III-2-7 Goliad Formation

The Goliad Formation overlies the Oakville and Fleming Formations with a low-angle truncation and is the oldest "Pliocene" stratum (Figure 6 and Figure 7). It also has a high proportion of coarse-grained sediments, including sands and cobbles (Hosman, 1996). Thickness is between 900 and 1,800 ft (Brogdon et al., 1977). Note that, according to Galloway (Jackson and Galloway, 1984; personal communication, 2008), the Goliad Formation is actually of Miocene age, not Pliocene, as is so often stated in hydrology-related reports. For consistency and because it has no major impact on the conclusions of this report, we use the common nomenclature. Hoel (1982) mapped the Goliad Formation in detail for her Master's thesis research at UT Austin. She found the Goliad Formation to be genetically and compositionally similar to the underlying Oakville and Catahoula as they exist in the southwest Gulf Coast. Hoel (1982) also showed in preliminary exploration the potential for the Goliad Formation to have economically minable uranium deposits similar to those found in the underlying Oakville Sandstone. Hoel (1982) noted a distinct change in character in the Goliad along a line perpendicular to the coast, just north of the Nueces River, roughly coincident with the San Patricio-Refugio County line. Southwest of

this line the Goliad had been deposited by rivers carrying bedload or very coarse sediments containing a large proportion of orthoclase and plagioclase feldspar crystals and volcanic rock fragments from a "distant western source." Northeast of this line, the rivers carried finer grained sediments composed primarily of calc-lithic particles presumably derived from Edwards Plateau rocks of Central Texas. The upper part of the Goliad includes finer-grained sands that are cemented by calcium carbonate caliche (Hosman, 1996). Clays are interbedded locally. Solis (1981) presented depositional maps of the Goliad Sands, which he mapped in association with the Willis Sands immediately above (Figure 37 and Figure 38). Morton et al. (1988, Figs. 12 and 13) also provided sand maps of the Goliad Sands.

III-2-8 Willis Sand, Lissie Formation, and Beaumont Clay

Above the Goliad are Pliocene- (see earlier note about age of Goliad Sands), Pleistocene-, and Holocene-age deposits that range in depositional environment from high-energy fluvial to deltaic, reflecting glacial cycles and sea-level variations during this period. The fluvial sediments range in texture from gravel to clay and are commonly poorly indurated (unconsolidated). Decreasing dip of the strata toward the coast through time reflects changes in relative uplift of inland areas (southern Rocky Mountains, Great Plains, and Edwards Plateau) and subsidence in the Gulf of Mexico (Doering, 1935; Blum, 1992). Older parts of this depositional sequence are coarser grained and dip 10 to 20 ft/mi (Willis Sand), whereas the younger units are finer grained and dip only approximately 2×10^{-4} (1 ft/mi) (Beaumont Formation) (Doering, 1935). Major Pleistocene to Recent formations along the Texas Gulf Coast, listed from oldest to youngest, include Willis, Lissie, and Beaumont Formations, as well as Quaternary terrace deposits and alluvium (Doering, 1935; Baker, 1979). These units plus Quaternary alluvial deposits are all assigned to the Chicot aquifer. The Lissie Formation and Beaumont Clay are the two dominant subdivisions of the Pleistocene system (Chowdhury and Turco, 2006, p. 43) and were discussed in detail by Sellards et al. (1932). Holocene sediments are localized and widely variable in textural composition. Northeast of the Colorado River, Miocene- to Pliocene-age Fleming Formation clay is unconformably overlain by Willis Sand, which is, in turn, unconformably overlain by sand and clay of the Lissie Formation. South of the Colorado River, the Pliocene-age Goliad Formation is overlain by the Lissie Formation, which consists of clay, silt, sand, and minor amounts of gravel. The Lissie Formation is overlain by clay, silt, and fine-grained sand of the Pleistocene-age Beaumont Formation throughout the Texas Gulf Coast. Although the Beaumont Formation as a whole is much finer grained than directly underlying formations, it contains localized sand channel deposits. The base of the Pleistocene (thought to be the Willis Formation in the northeast Gulf Coast and Lissie Formation in southwest Gulf Coast) is difficult to identify on geophysical logs (Baker, 1979). The base of the Chicot aquifer, which has in the past been defined as the base of the Pleistocene, is therefore ambiguously defined and is often lumped together with the Evangeline aquifer.

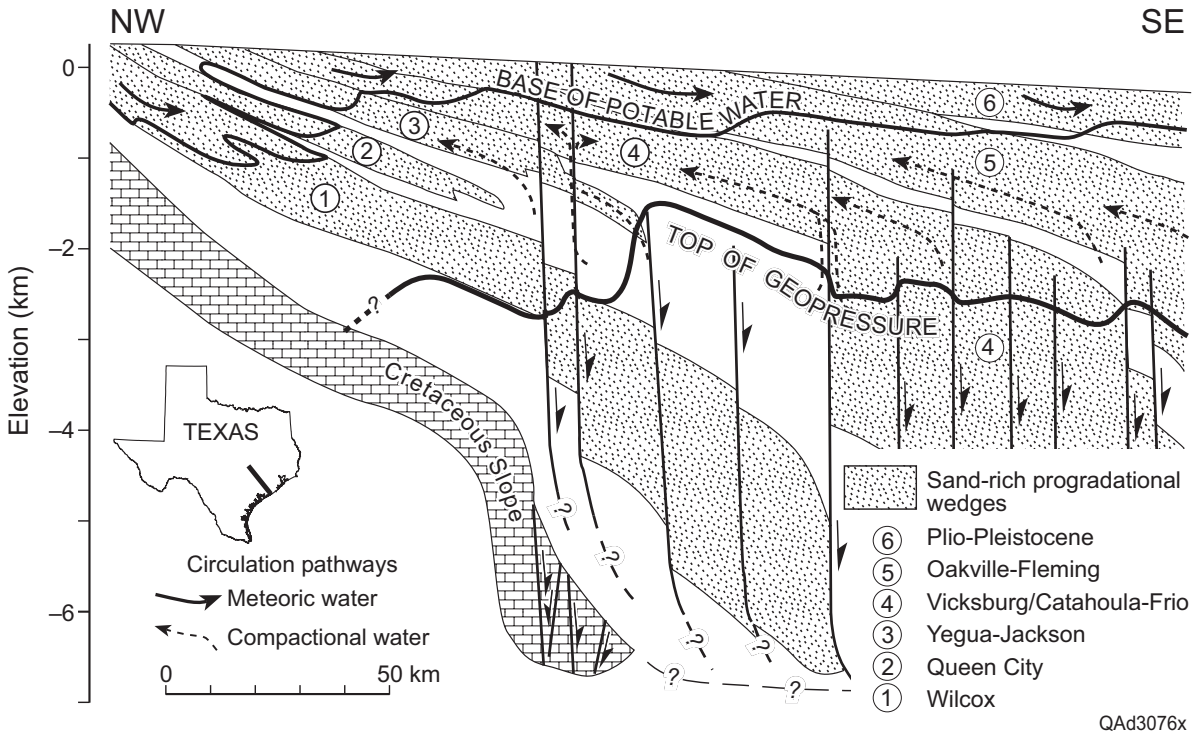

Source: Adapted from Galloway (1982a) and Galloway et al. (1982c). The last major progradation wedge of Plio-Pleistocene age (6) is still active and does not contain uranium deposits.

Figure 24. Southern Gulf Coast major sand-rich progradational packages and growth-fault zones beneath the Texas Coastal Plain

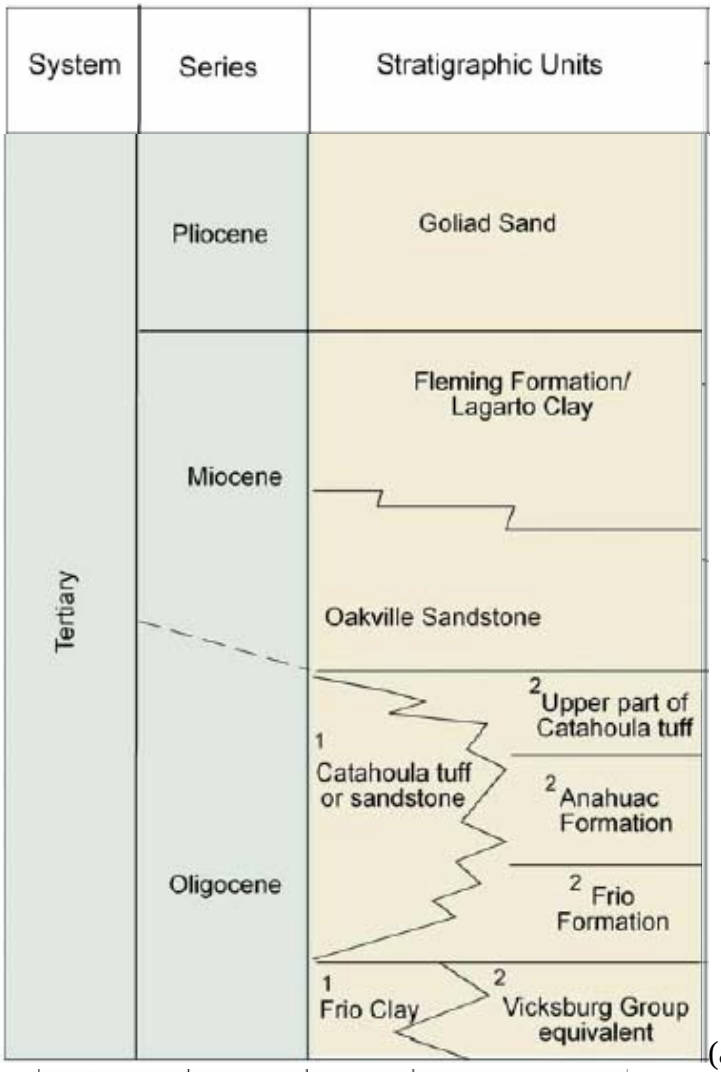

Source: (a) Chowdhury and Mace (2003) (b) and Preston (2006)

Figure 25. Simplified composite stratigraphic section of the STU Province

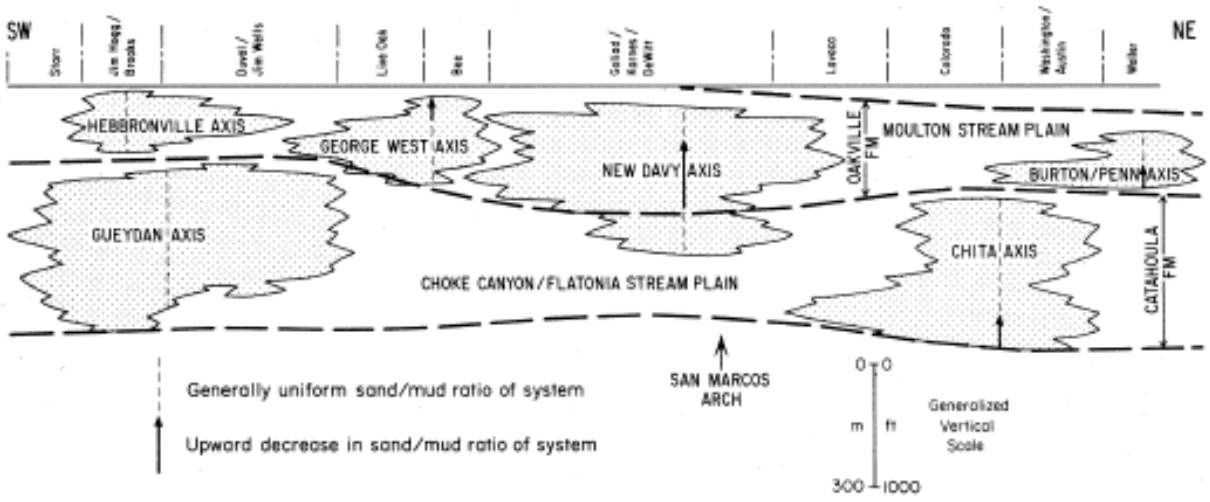

Source: Galloway, 1982b, Fig. 7

Figure 26. Generalized cross section along strike downdip of the Catahoula and Oakville Formation outcrop showing position of the George West (Live Oak County) and New Davy (Karnes County) axes of the Oakville Formation

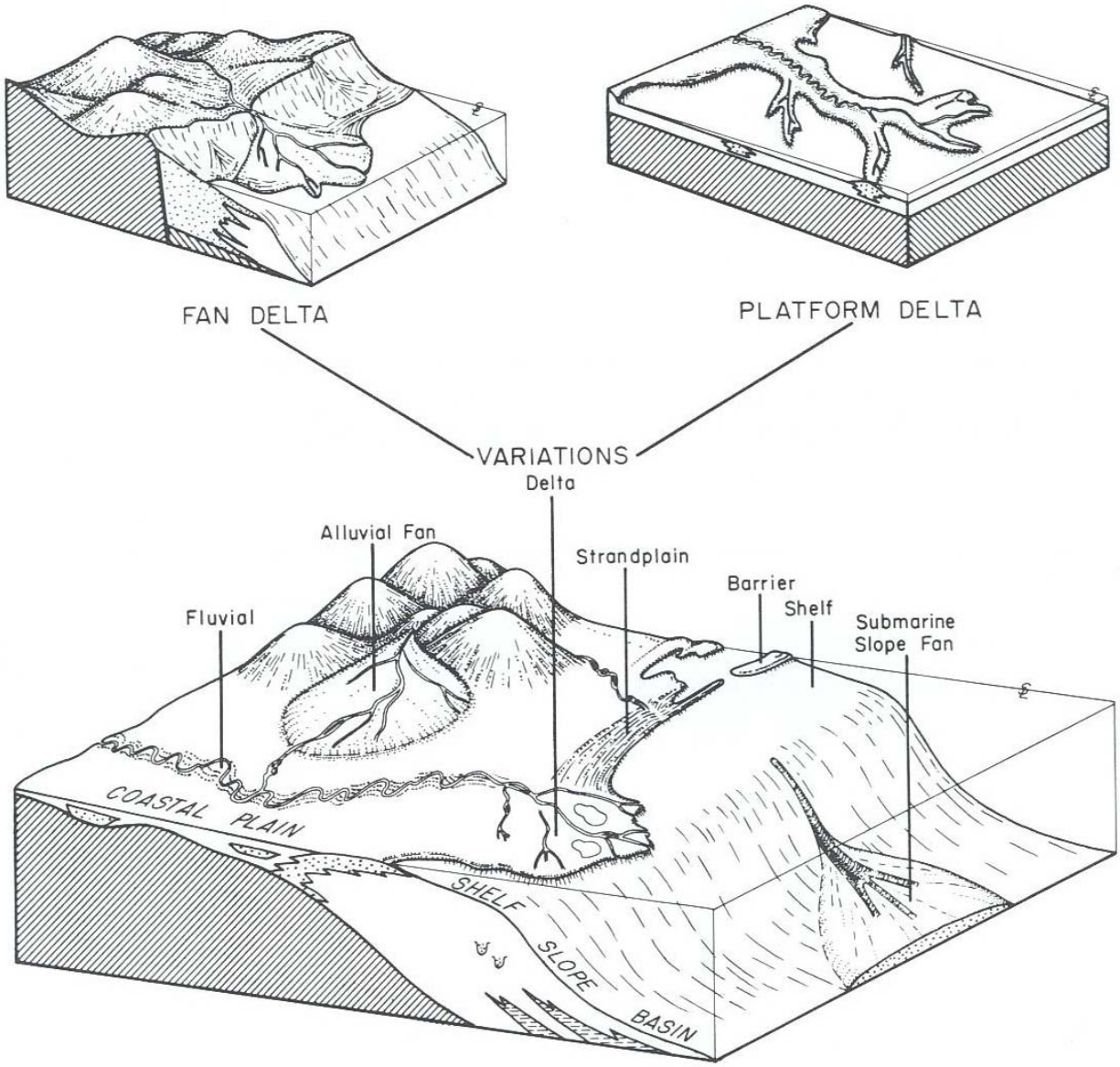

Source: Galloway et al. (1983)
Note: Alluvial-fan depositional environment is not present in the Gulf Coast.

Figure 27. Cartoon of typical Gulf Coast depositional systems

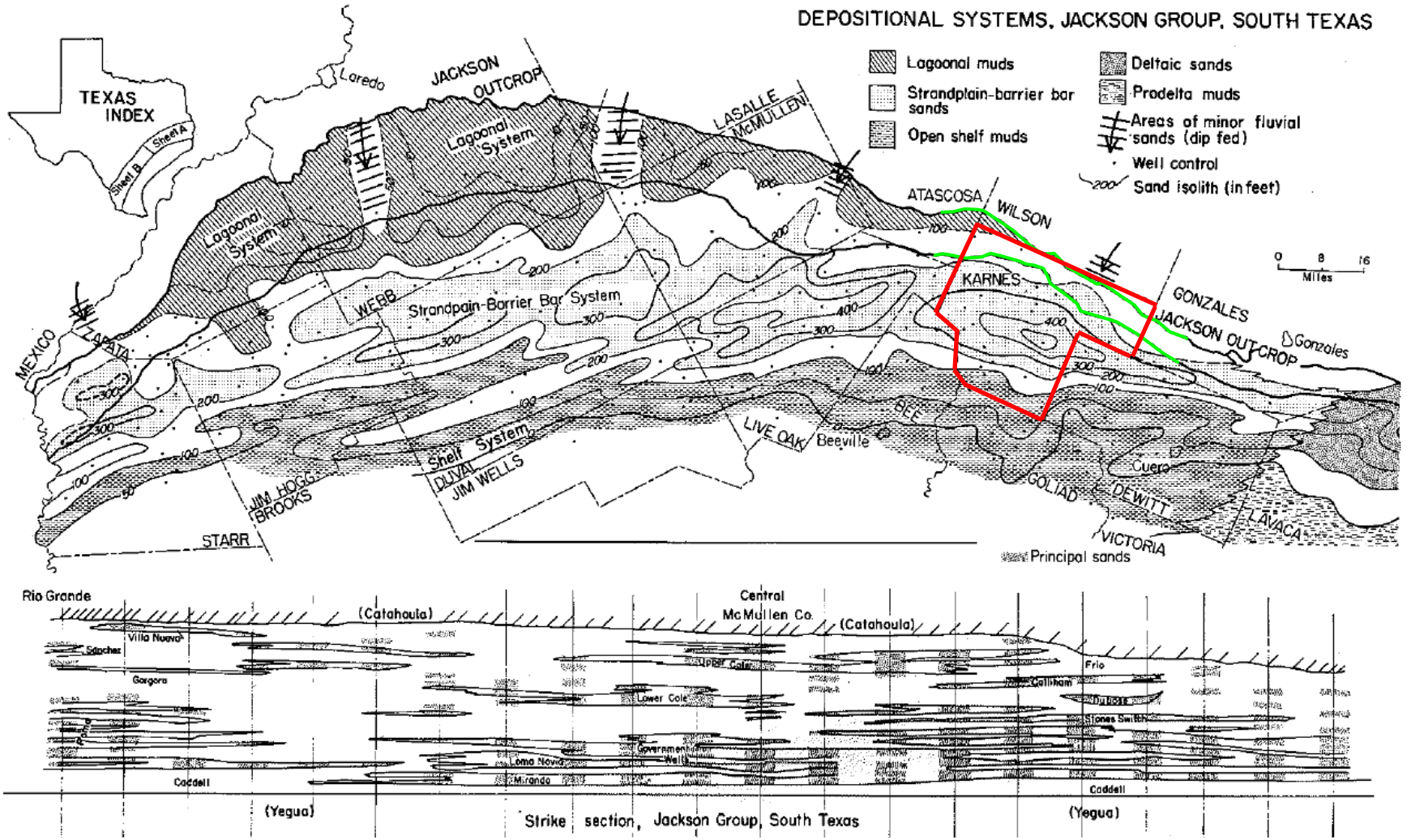

Source: Fig. 1b of Fisher et al. (1970)

Note: Karnes County boundaries are shown in red, and Jackson Group outcrop is highlighted in green across Karnes County.

Figure 28. Net-sand isoliths, principal depositional systems, and strike profile (along maximum sand thickness) of the entire **Jackson Group**. In Karnes County, systems vary from extensive lagoonal facies at the extreme west to strandplain-barrier-bar sands to open-shelf muds in the southeast. The system grades to delta deposits to the northeast, starting in Lavaca County.

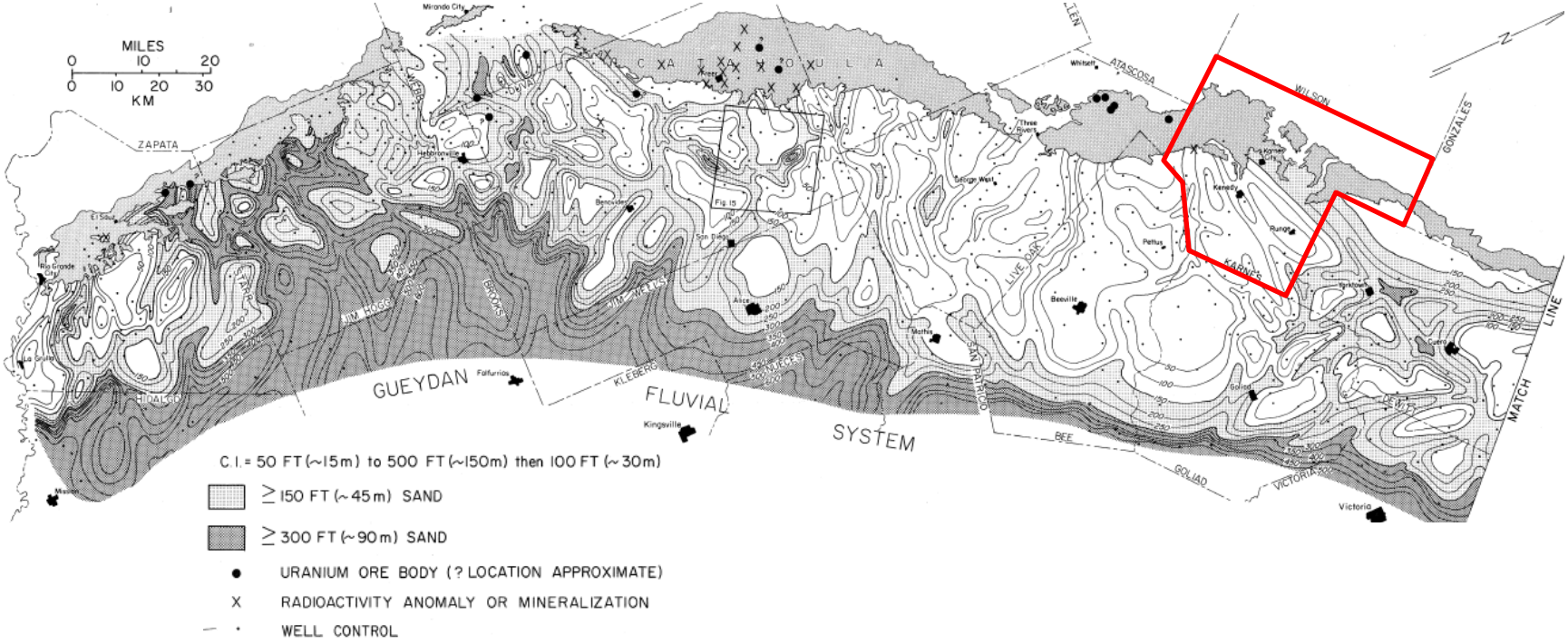

Source: Galloway, 1977, Plate I
Note: Karnes County boundaries are shown in red, and Catahoula Formation outcrop is shown in light-gray.

Figure 29. **Catahoula** net-sand isopachs

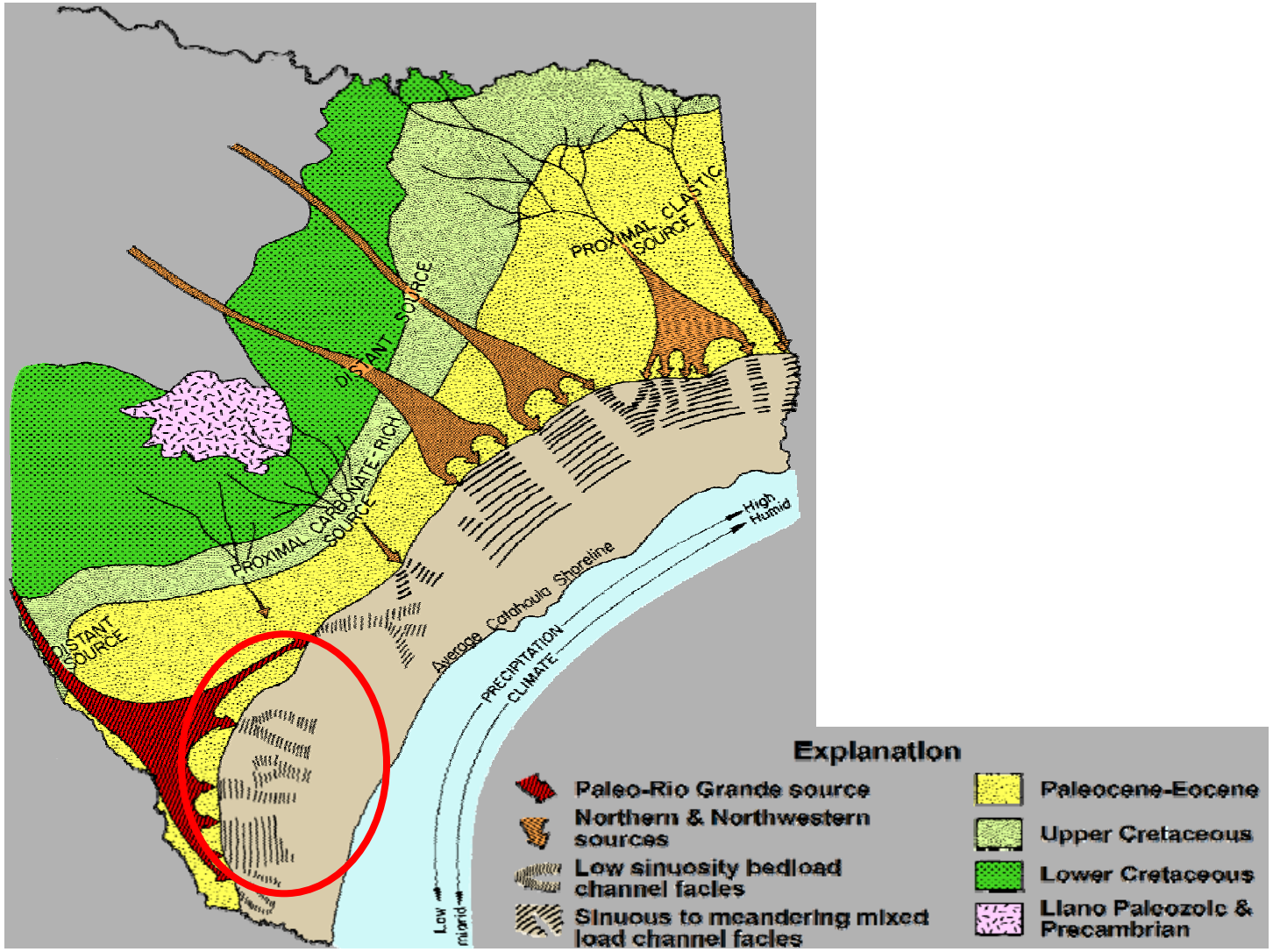

Source: Presentation by W. A. Ambrose, GCAGS, October 23, 2007 (Ambrose, 2007)

Note: Courtesy of Bill Ambrose; red circle denotes location of STU, also suggesting single large fluvial system.

Figure 30. Texas paleogeography during Catahoula deposition times

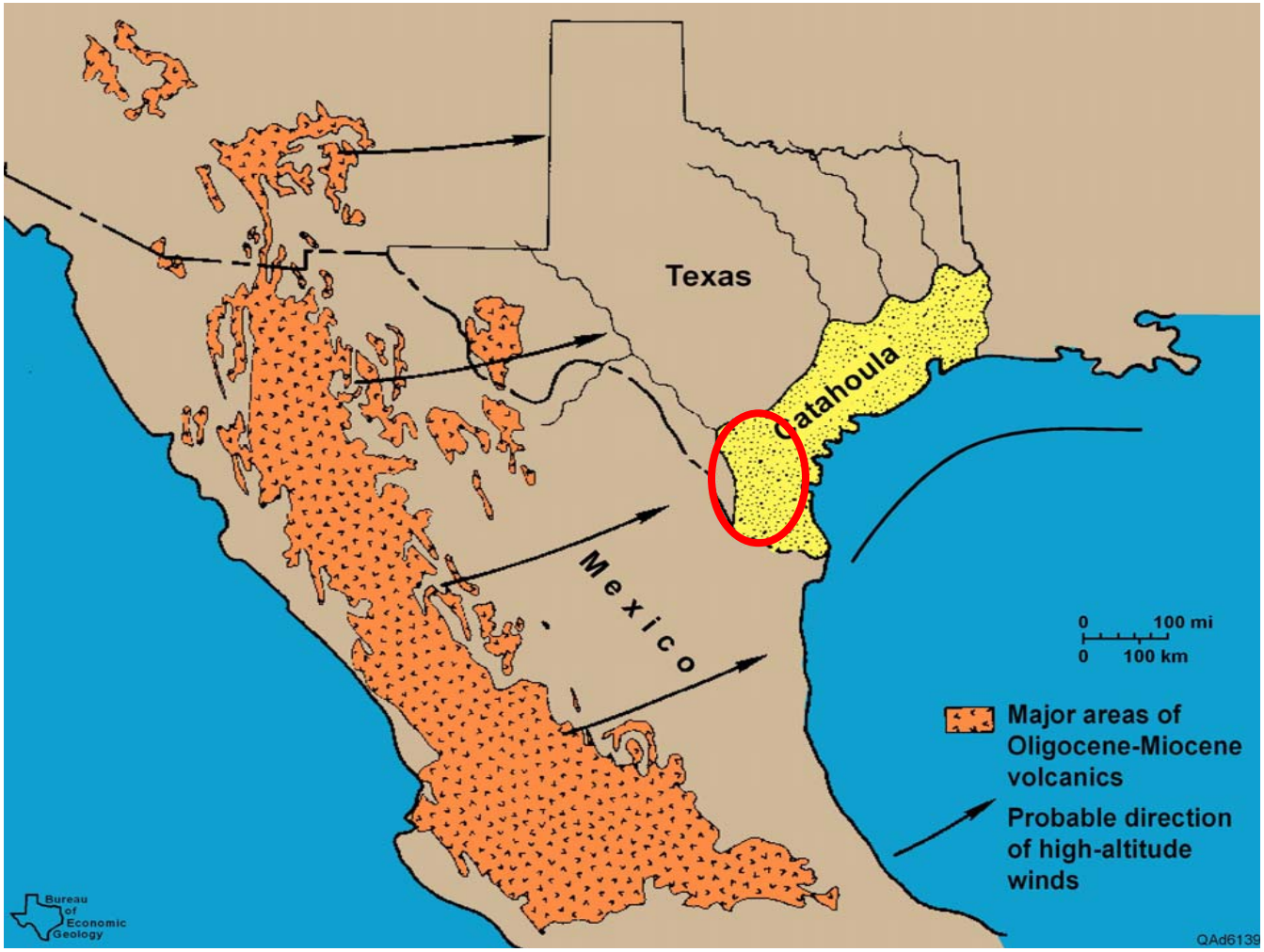

Source: Presentation by W. A. Ambrose, GCAGS, October 23, 2007 (Ambrose, 2007)
Note: Courtesy of Bill Ambrose; red circle denotes location of STU Province

Figure 31. Probable source of Catahoula volcanic ash driven by high-altitude winds

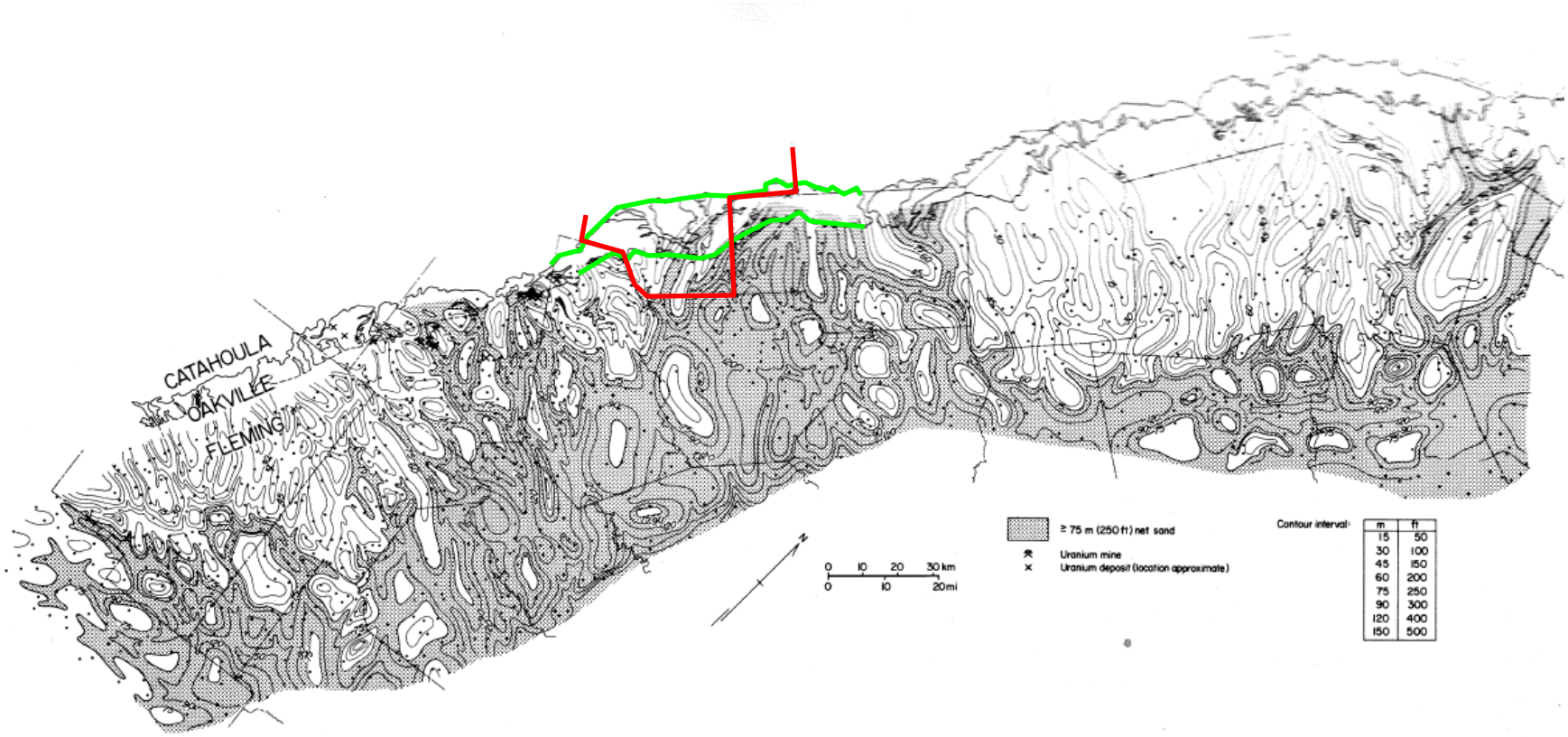

Source: Figure 5 in Galloway et al. (1982a)
Note: Southeastern Karnes County boundaries are shown in red, and Oakville outcrop across Karnes County is highlighted in green.

Figure 32. Net-sand isolith map of the **Oakville** Sandstone

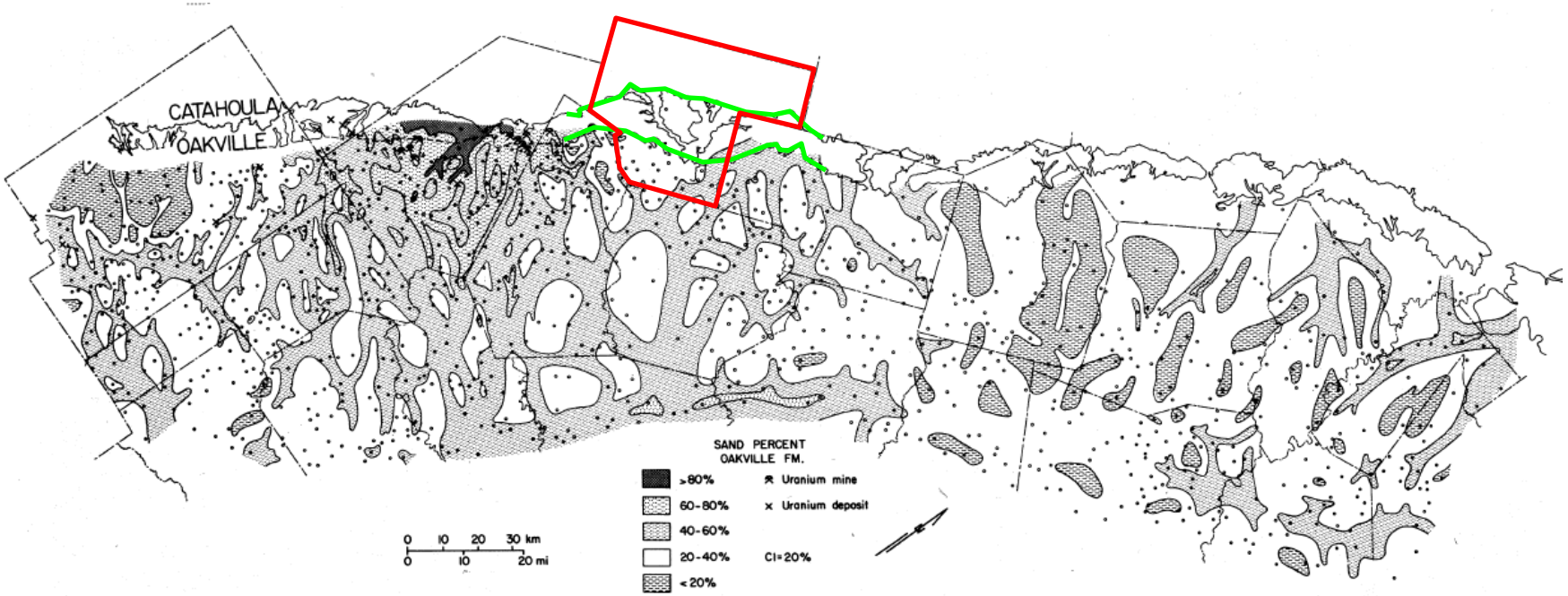

Source: Figure 6 in Galloway et al. (1982a) or Figure 14.7 of Galloway and Hobday (1996)
Note: Karnes County boundaries are shown in red, and Oakville outcrop across Karnes County is highlighted in green.

Figure 33. Sand-percentage map of the **Oakville** Sandstone

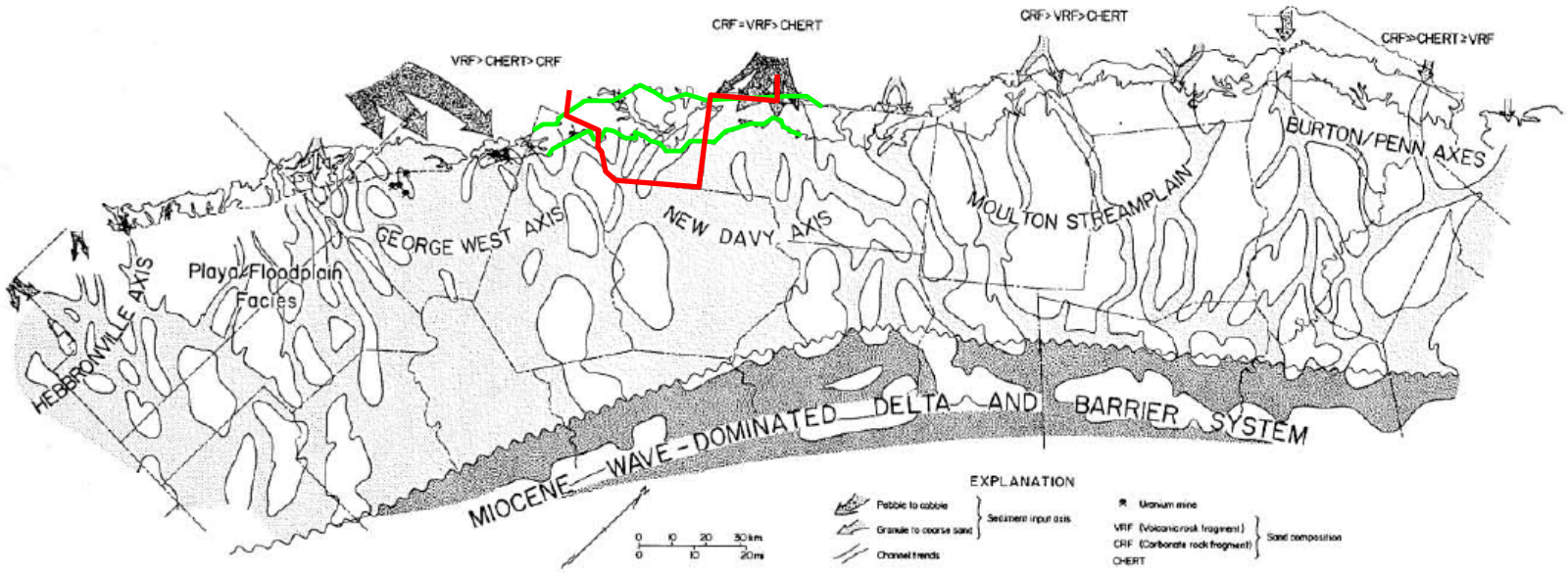

Source: Figure 8 in Galloway et al. (1982a) or Figure 14.7 of Galloway and Hobday (1996)
Note: Southeastern Karnes County boundaries are shown in red, and Oakville outcrop across Karnes County is highlighted in green.

Figure 34. Depositional elements of the **Oakville** fluvial system

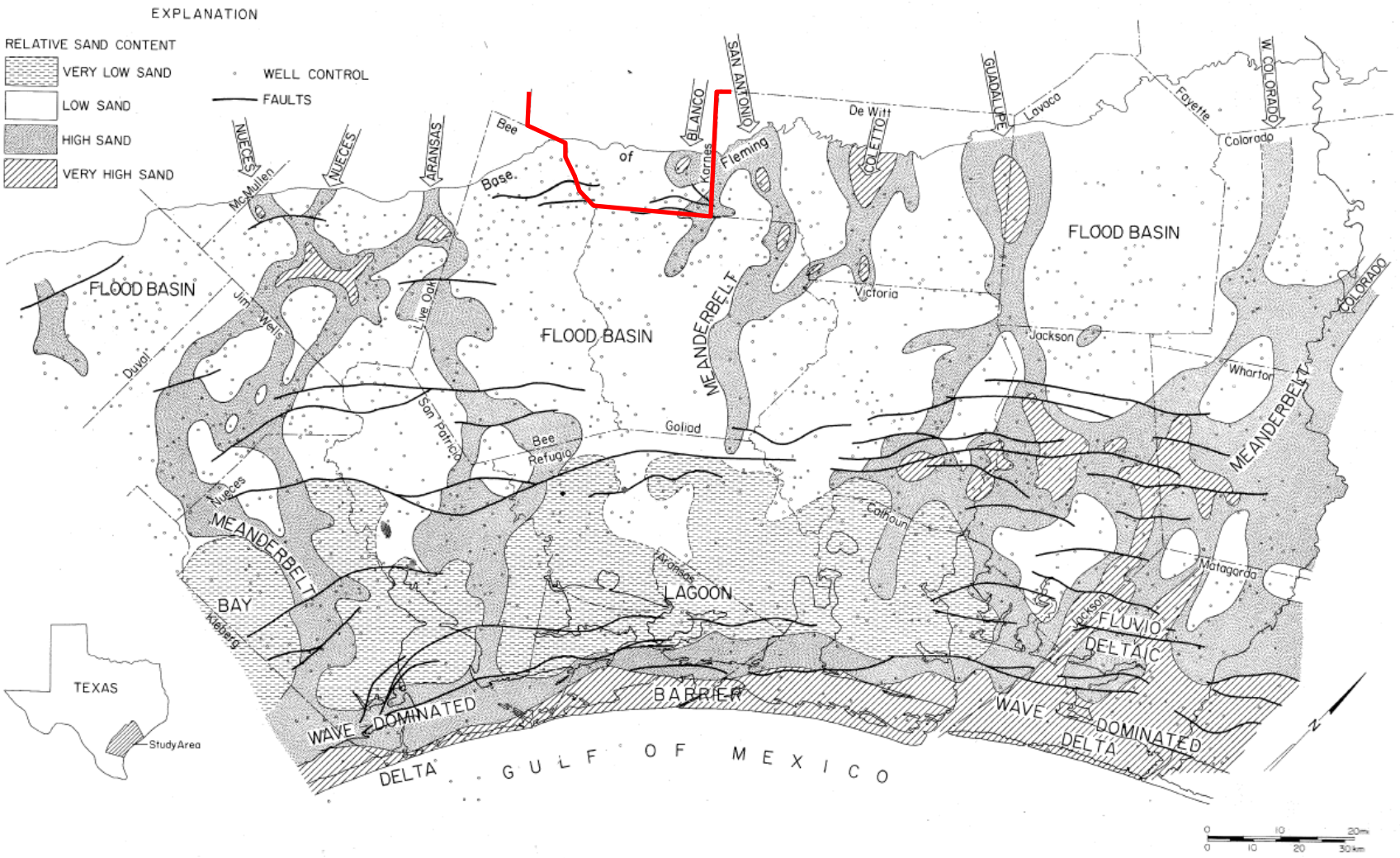

Source: Figure 17 in Solis (1981)
Note: Southeastern Karnes County boundaries are shown in red.

Figure 35. Depositional systems, lower **Fleming** operational unit

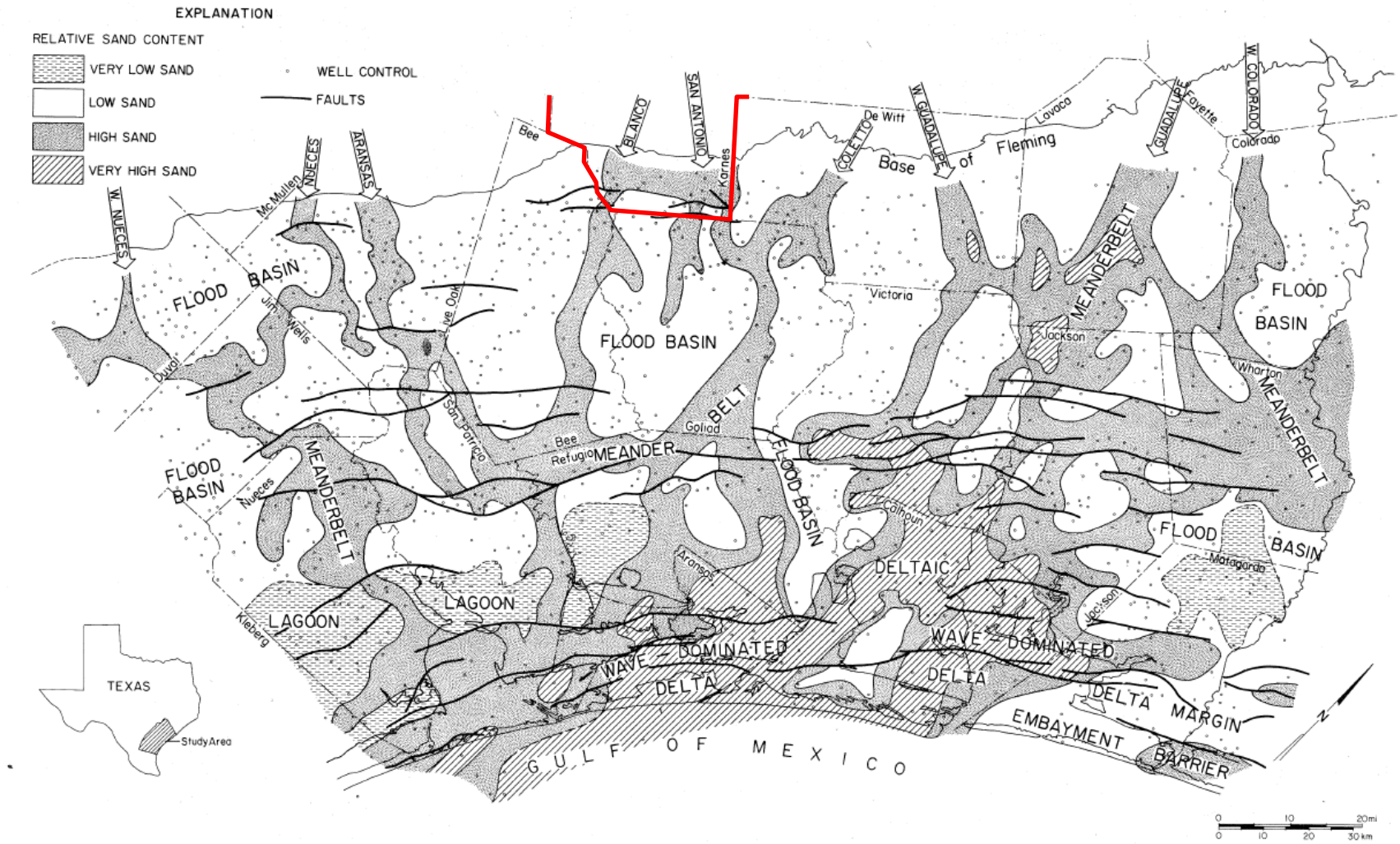

Source: Figure 20 in Solis (1981)
Note: Southeastern Karnes County boundaries are shown in red.

Figure 36. Depositional systems, upper **Fleming** operational unit

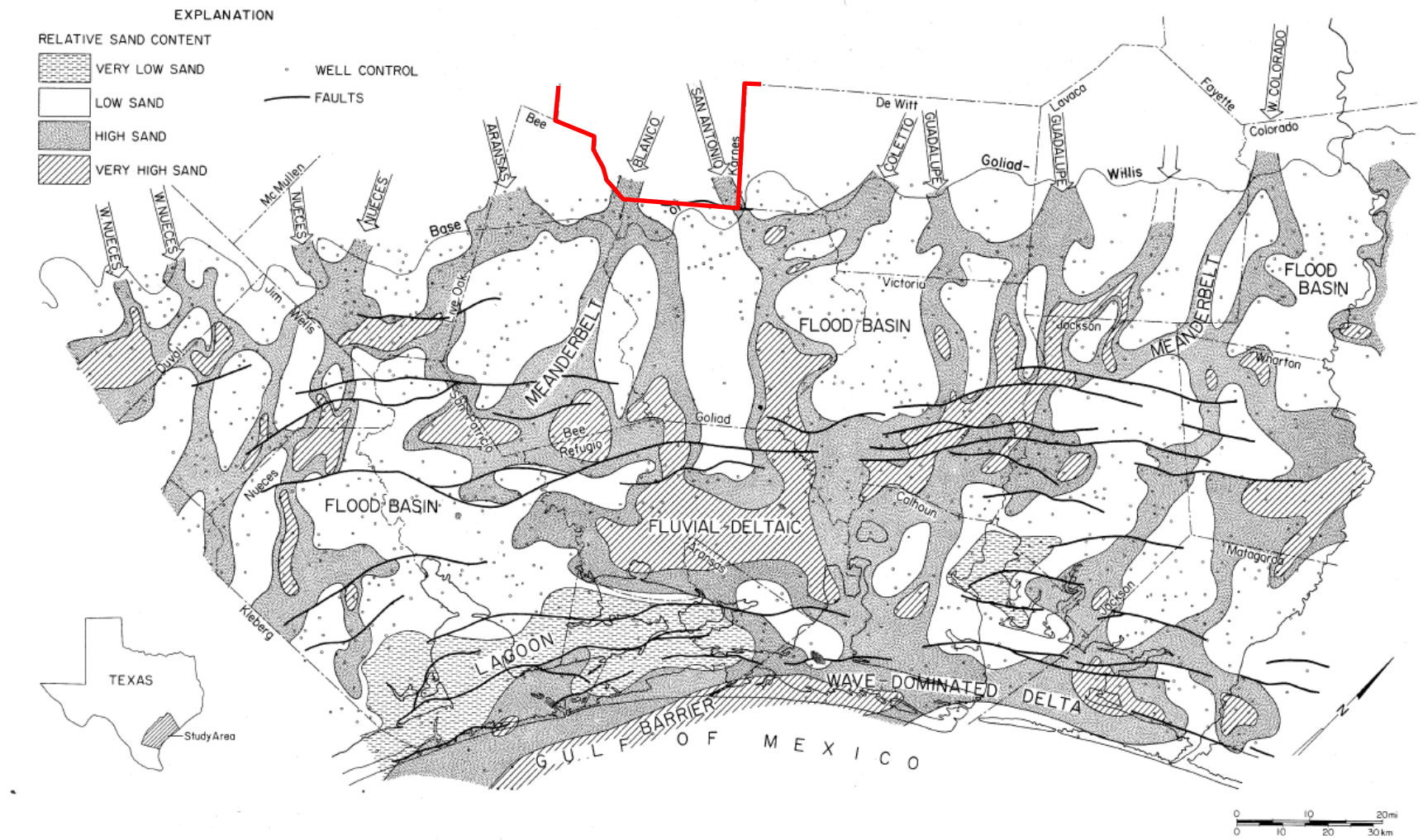

Source: Figure 23 in Solis (1981)
Note: Southeastern Karnes County boundaries are shown in red.

Figure 37. Depositional systems, lower **Goliad**-Willis operational unit

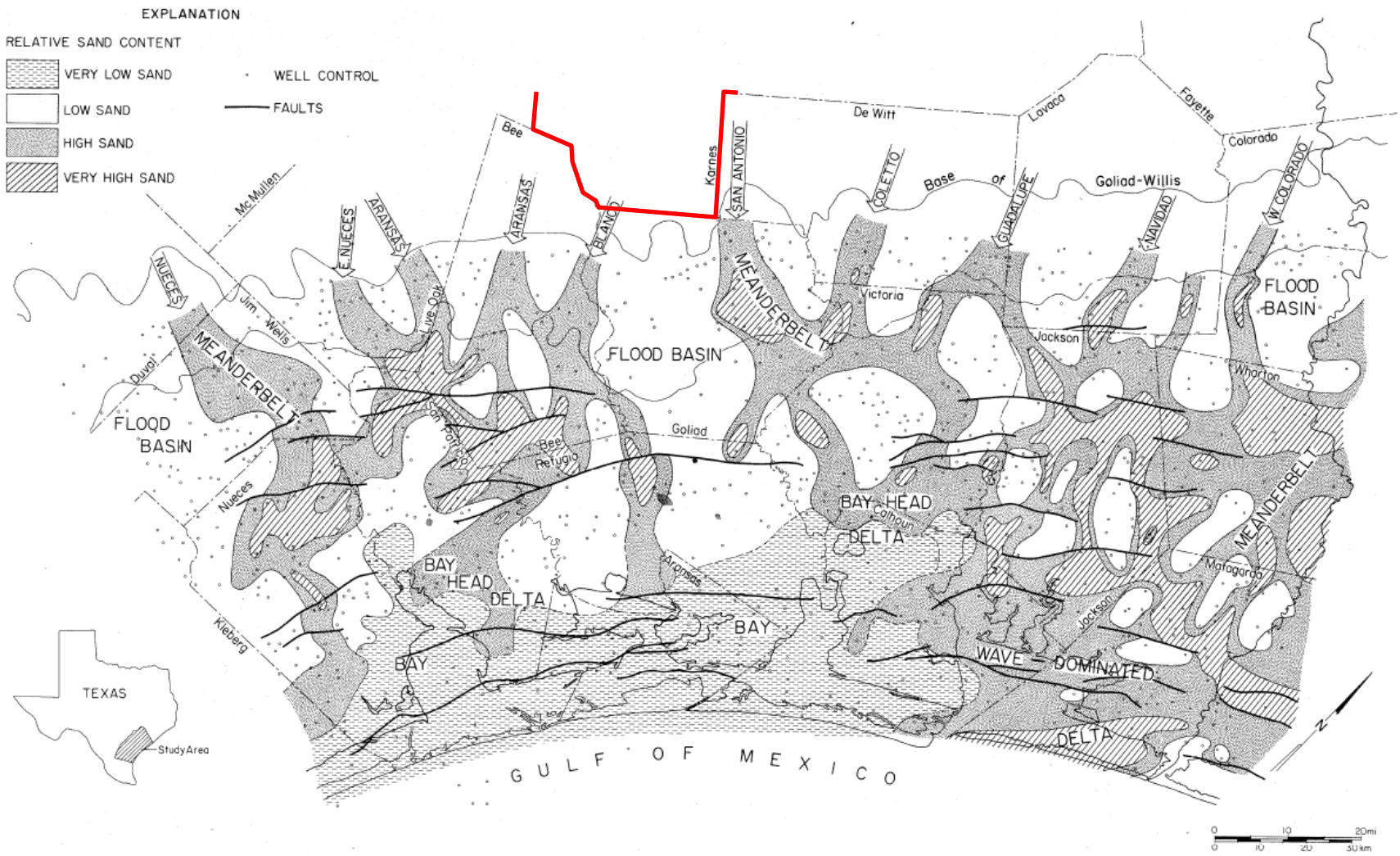

Source: Figure 26 in Solis (1981)
Note: Southeastern Karnes County boundaries are shown in red.

Figure 38. Depositional systems, upper **Goliad**-Willis operational unit

III-3. Structural Information

The structural map of the Gulf Coast area (Figure 39; Ewing, 1991) is dominated by an abundance of growth faults that trend with, or are slightly oblique to, stratigraphic strike, which is more or less parallel to the Gulf of Mexico. Each major progradation package (Figure 24) has a series of growth faults associated with it: Wilcox, Vicksburg, and Frio Fault Zones, located in that order, closer and closer to the current shoreline. The more recent Miocene fault zone is mostly offshore. An interesting feature displayed in Figure 39 (more details in Figure 40) is that the Wilcox Fault Zone impacts the Catahoula Formation and Oakville Sandstone close to their outcrop area (in Live Oak and Duval Counties) in the southwestern Gulf Coast, but no major fault is associated with outcrop of the same formations farther north and in East Texas. More generally, faulting is a prominent secondary feature of Gulf Coast stratigraphy, which affects distribution of uranium mineral deposits and most likely affects groundwater flow, as well as groundwater quality. These faults have throws that increase with depth. Strata on the downthrown side are thicker than those on the upthrown side (Chowdhury and Turco, 2006). Galloway (1977, p. 25) presented a summary of the evolution of a growth fault (Figure 41):

(1) deposition of thick slope and prodelta mud sequences;
(2) loading of thick, uncompartmented muds by a prograding deltaic system;
(3) initiation of down-to-coast syndepositional faults along the delta margin and upper slope;
(4) accentuation of fault displacement and deposition of delta-margin facies on the downthrown side of the fault;
(5) progradation of the delta system beyond the fault zone and activation of younger, basinward zones; and
(6) decreasing activity along the fault zone as successive delta-plain and fluvial systems override the buried delta platform. Catahoula fluvial systems are affected primarily by this final phase of decreasing fault activity.

Verbeek et al. (1979) reported that most of these faults are rooted in the deeper subsurface at depths of 3,200 to 13,000 ft. Solis (1981) concluded that these faults have strongly influenced distribution and orientation of Miocene to lower Pleistocene depocenters containing the thickest sand-bearing unit. Verbeek et al. (1979) found that in the Texas Gulf Coast aquifer, abrupt changes in sediment thickness occur locally over short lateral distances between growth faults. The role of many of these faults in controlling regional groundwater flow is not very clear. Throws across the faults are not large enough to totally offset the hydrogeologic units (Hosman and Weiss, 1991) but some authors (e.g., Kreitler et al., 1977) have suggested that the fault zones may partly compartmentalize groundwater-flow systems locally.

The Fashing fault, which intersects the Jackson Group and Catahoula Formation in Karnes and Gonzales Counties, is downthrown to the northwest (Eargle, 1959). It can be seen as the southwest extension of the Mexia fault. The fault bounds Fashing field hydrocarbon accumulation, but it does not seem to have supplied important quantities of reducing fluids. Uranium accumulation in the Jackson Group tends to be associated with syndepositional organic matter (Ilger et al., 1987).

Many of the local structures, including San Marcos Arch, Rio Grande Embayment, and numerous northeast-southwest-trending faults, began to form prior to the Tertiary period and were generated by a combination of differential subsidence of the basin floor and thick sediments that flowed as viscous fluids on sloping surfaces (Bornhauser, 1958) or by deep-seated vertical

intrusions of salt in the form of narrow ridges pushed up the gulfward-dipping beds to form deep-seated anticlines (Quarles, 1952; Cloos, 1962). A few salt domes intrude the stratigraphic section in the STU Province. However, they are confined to a limited area (Figure 39), and their density is much less than that in East Texas (<10 total). The Palangana Salt Dome caprock reaches 450 ft below ground and severely impacts lower Fleming and older sediments that dip steeply away from the dome (Solis, 1981, p. 19). The local Goliad sediments unconformably overlap Fleming sediments and contain uranium. Although salt rock is not itself a reductant, it can dissolve quickly and build a caprock composed of mostly gypsum/anhydrite, calcite, and, to a lesser extent, native sulfur and metallic sulfides (Hamlin, 2006). The latter two are clearly reductants. In addition, faulting associated with dome growth can create pathways for migration of hydrocarbons or reduced aqueous fluids to the shallow aquifer, where they would encounter uranium-laden oxidizing waters.

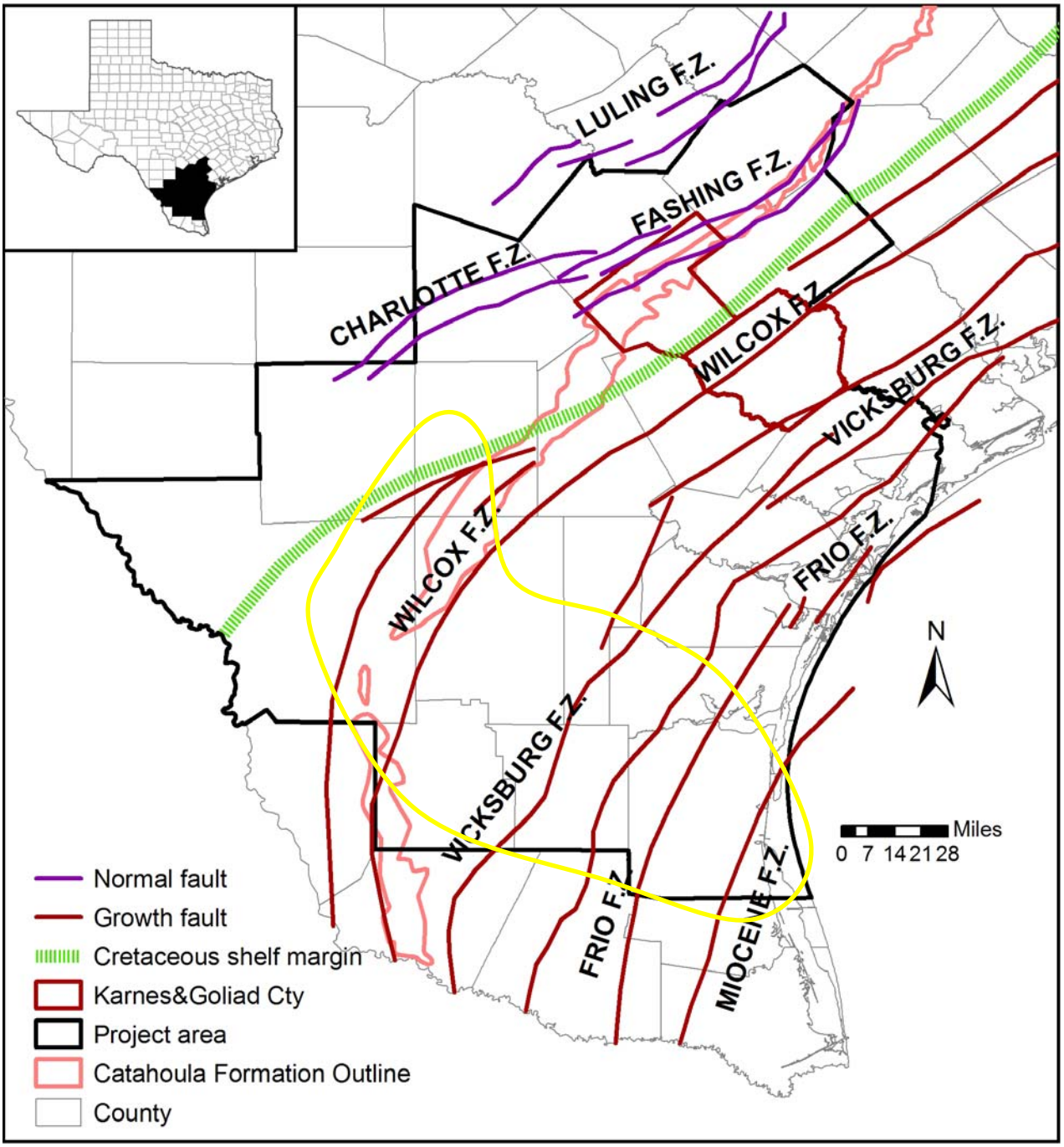

Source: Galloway et al. (1983, Plate I)

Figure 39. Approximate location of fault zones (not necessarily all faults) in the STU Province. South Texas Salt Province is shown in yellow.

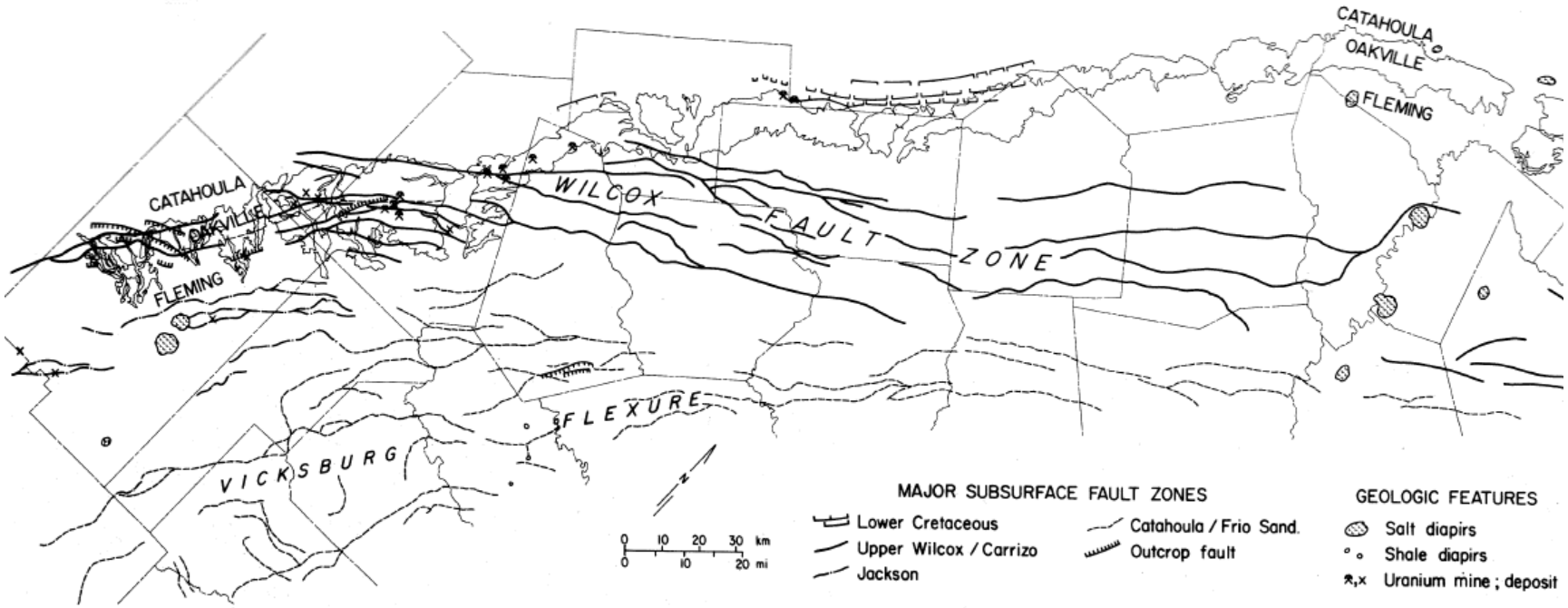

Source: Galloway (1982a, Fig. 22)
Note: Map horizon of fault zones is indicated by line style.

Figure 40. Generalized distribution of faults and diapiric intrusions within or below the Oakville Sandstone

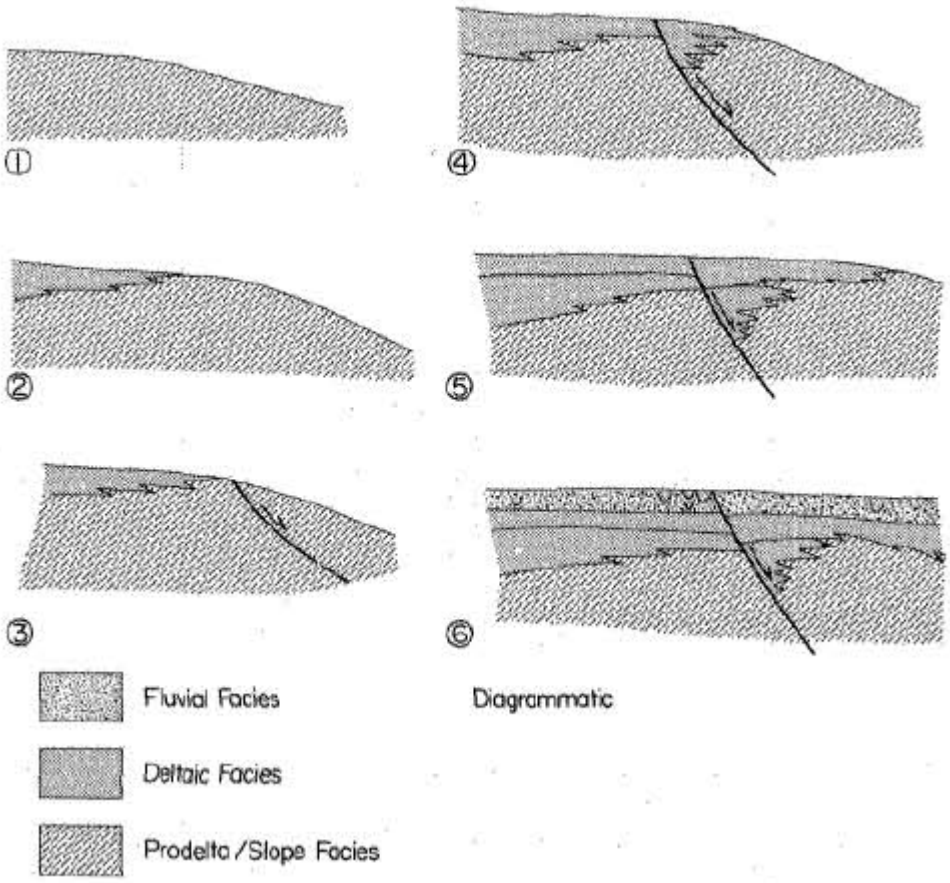

Source: Galloway (1977, Fig. 16)
Note: See text for discussion of individual diagrams.

Figure 41. Growth-fault evolution in the Gulf Coast Basin

III-4. Hydrogeologic Setting

The upper and lower Gulf Coast, east of the Balcones Escarpment, includes several TWDB-designated aquifers (from oldest to youngest): the Carrizo-Wilcox, Queen City-Sparta, Yegua-Jackson, and Gulf Coast (Figure 42 and Figure 43). None of these aquifers corresponds to a single sand body, and they often contain several fresh-water-bearing formations. Several additional aquifers, usually of local importance only, also exist (e.g., in the Jackson Group). Uranium deposits are hosted within the Gulf Coast aquifers but are present also in aquifers from older formations, such as the Catahoula and those of the Jackson Group. Broadly, the Oakville Sandstone, Goliad Sand, and Quaternary units compose the main GCAS aquifers: the Jasper, Evangeline and Chicot aquifers, respectively (Figure 6). The Catahoula Formation often acts as a confining unit at the base of the Jasper aquifer, whereas the Fleming Formation separates the Jasper aquifer from the Evangeline aquifer and is known as the Burkeville Confining System. However, hydrostratigraphic units do not correspond exactly to stratigraphic units because they are defined in terms of flow systems versus age (Figure 44). There is generally a good, but not perfect, match between hydrostratigraphic and stratigraphic units.

Ryder (1988) presented an early set of structure maps (top and bottom elevations of units as well as thickness maps), but the Groundwater availability models (GAMs), encompassing the Gulf Coast formations (Chowdhury and Mace, 2003, 2007; Chowdhury et al., 2004; Knox et al., 2007), contain the most recent and thorough information, albeit at a regional scale not necessarily applicable to local studies. Detailed local studies may require increasing the density of geophysical logs in order to generate structure maps used to develop aquifer geometry. Numerous water wells (Figure 45) tap all aquifers in the STU Province, but large-yield wells are typically dug into the Evangeline aquifer. Figure 46, Figure 47, and Figure 48 provide some insight into the geometry of the GCAS.

III-4-1 Jackson Group

The upper Jackson Group contains several sand bodies and locally functions as an aquifer. A Yegua-Jackson GAM is in progress but has not been released yet (only a report on aquifer geometry is available, Knox et al., 2007). Little is known from this aquifer, and occurrences of good-quality water seem erratic (Preston, 2006). Only outcrop water, often brackish, is used. Farther downdip water quality is poorer, and shallower, more recent units with higher water quality are preferred. As elsewhere in the Gulf Coast, usable aquifers would occur within thick sand bodies well connected to recharge areas. Generally along-strike sand bodies in South Texas (as opposed to along dip farther north) are less conducive to flushing by fresh recharge waters.

III-4-2 Catahoula Formation

The Catahoula Formation, underlying the Oakville Sandstone, is a generally less transmissive zone owing to a greater fine-grained component and is generally regarded as an aquitard. However, it also contains a significant sand fraction and functions as an aquifer in some places. Those sand bodies of the upper Catahoula Formation are often attached to the Jasper aquifer, which is composed mostly of the Oakville Sandstone (see Galloway et al., 1982a, Fig. 23).

III-4-3 Oakville Sandstone/Fleming Formation

Baker (1979, 1986) assigned the Miocene Oakville/Fleming geologic units to the Jasper aquifer, which has been best characterized along the northeastern Texas Gulf Coast, north of the Brazos River. The Jasper aquifer is generally composed of the Miocene-age Oakville Sandstone but includes sections of the Fleming Formation in some places where the Fleming is relatively transmissive. The Oakville Sandstone/Fleming Formations are commonly grouped because they are both composed of varying amounts of interbedded sand and clay. In most of the central part of the Gulf Coast (Brazos River to central Duval County), they are distinguishable as stratigraphically adjacent units because the Oakville Formation is sand rich and the Fleming is relatively more clay rich. Galloway et al. (1982a) described the Oakville in the southwest Gulf Coast as a sand-rich fluvial system overlying the Catahoula Formation. They globally associated the Oakville Sandstone with the Jasper aquifer and the Fleming Formation with the Burkeville Confining System. The match is generally good only in the south part of the study area. Farther north, at intermediate depths, only the lower half of the Oakville Sandstone is part of the Jasper aquifer. The mixed-load muddier top is part of the Burkeville Confining System, whose top corresponds to the middle of the Fleming. The upper part of the Fleming is included in the Evangeline aquifer (Galloway et al., 1982a, p. 27). Farther north, in Fayette and Washington Counties, sands at the top of the Catahoula make up a significant part of the Jasper aquifer. To the northeast of the Brazos River, the Oakville Sandstone and Fleming are indistinguishable.

III-4-4 Goliad Formation

Delineation of the Evangeline aquifer corresponds closely with the extent of the Goliad Formation. The Goliad is entirely within the Evangeline aquifer, and the upper boundary of the Evangeline aquifer closely follows the top of the Goliad Formation where present (Baker, 1979). However, the bottom of the Evangeline aquifer can include sandy units of the Fleming (Baker, 1979, p. 40) fully hydraulically connected to the Goliad Formation.

The Evangeline aquifer is composed of water-bearing zones primarily within the Goliad Sand and secondarily in underlying parts of the Fleming Formation (Ryder and Ardis, 1991, 2002). The Goliad Sand is identified only as an aquifer unit in the TWDB well database within and to the south and west of Lavaca and Jackson Counties. However, the Evangeline aquifer is present throughout the Gulf Coast aquifer in the northeast into Louisiana. Clearly there is a difference in the geologic units that compose the Evangeline aquifer in the southwest and northeast sections of the Gulf Coast aquifer. According to Baker (1979), the Evangeline aquifer was originally defined only as far west as Austin, Brazoria, Fort Bend, and Washington Counties in Texas. He stated that extending the Evangeline farther west is speculative; however, in 1976 the USGS decided to extend the Evangeline to the Rio Grande.

III-4-5 Younger Formations

The Chicot aquifer is composed of the Lissie and Willis Formations, as well as localized Holocene deposits. As noted by Baker (1979), Jorgensen (1975), and Carr et al. (1985), the Chicot aquifer is conceptually distinguished from the Evangeline aquifer by its distinctly greater hydraulic conductivity, which equates to greater sand percent.

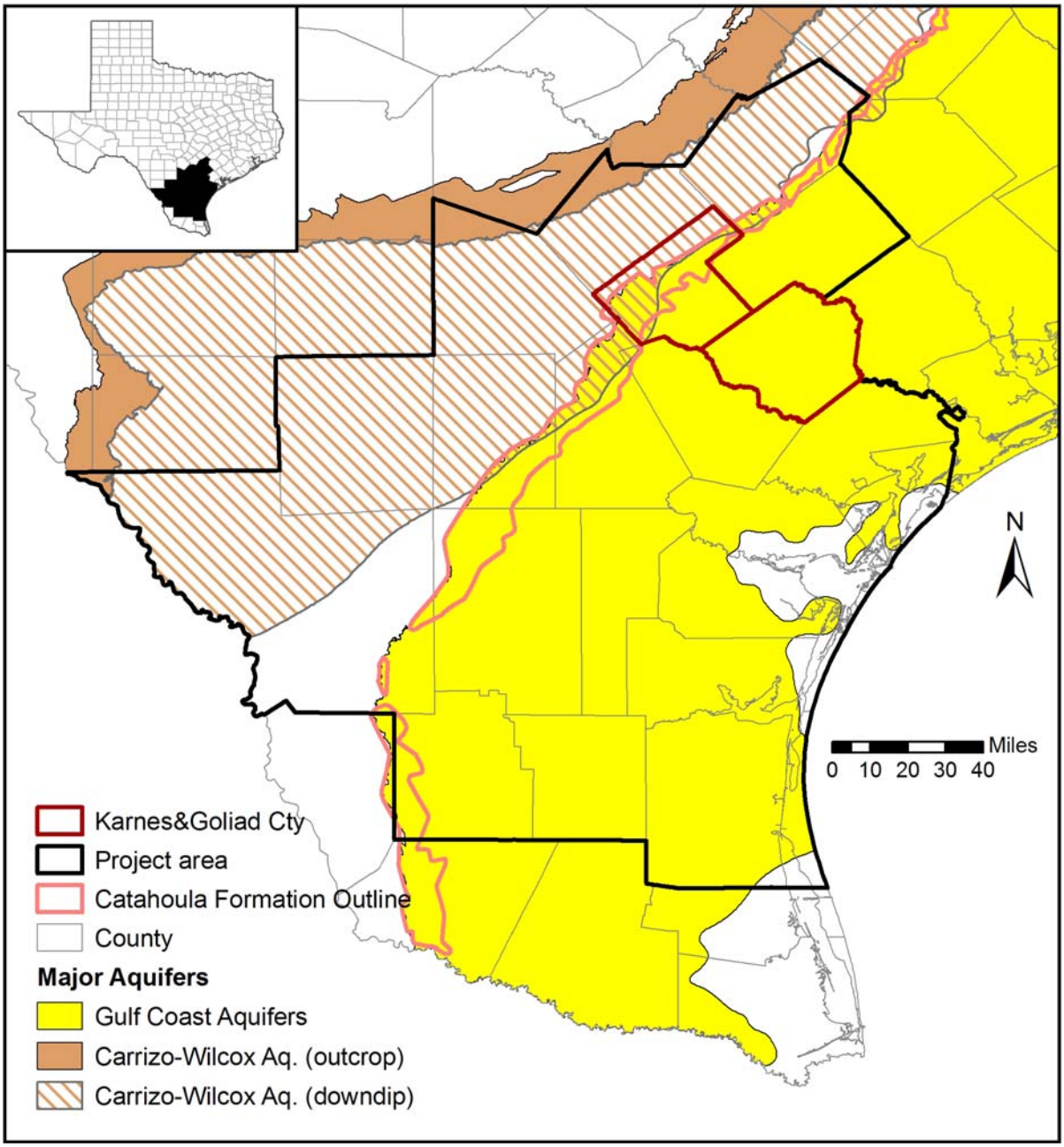

Source: TWDB, http://www.twdb.state.tx.us/mapping/gisdata.asp, January 2009

Figure 42. Map of major aquifers in the study area; downdip limit is 3,000-mg/L TDS contour line

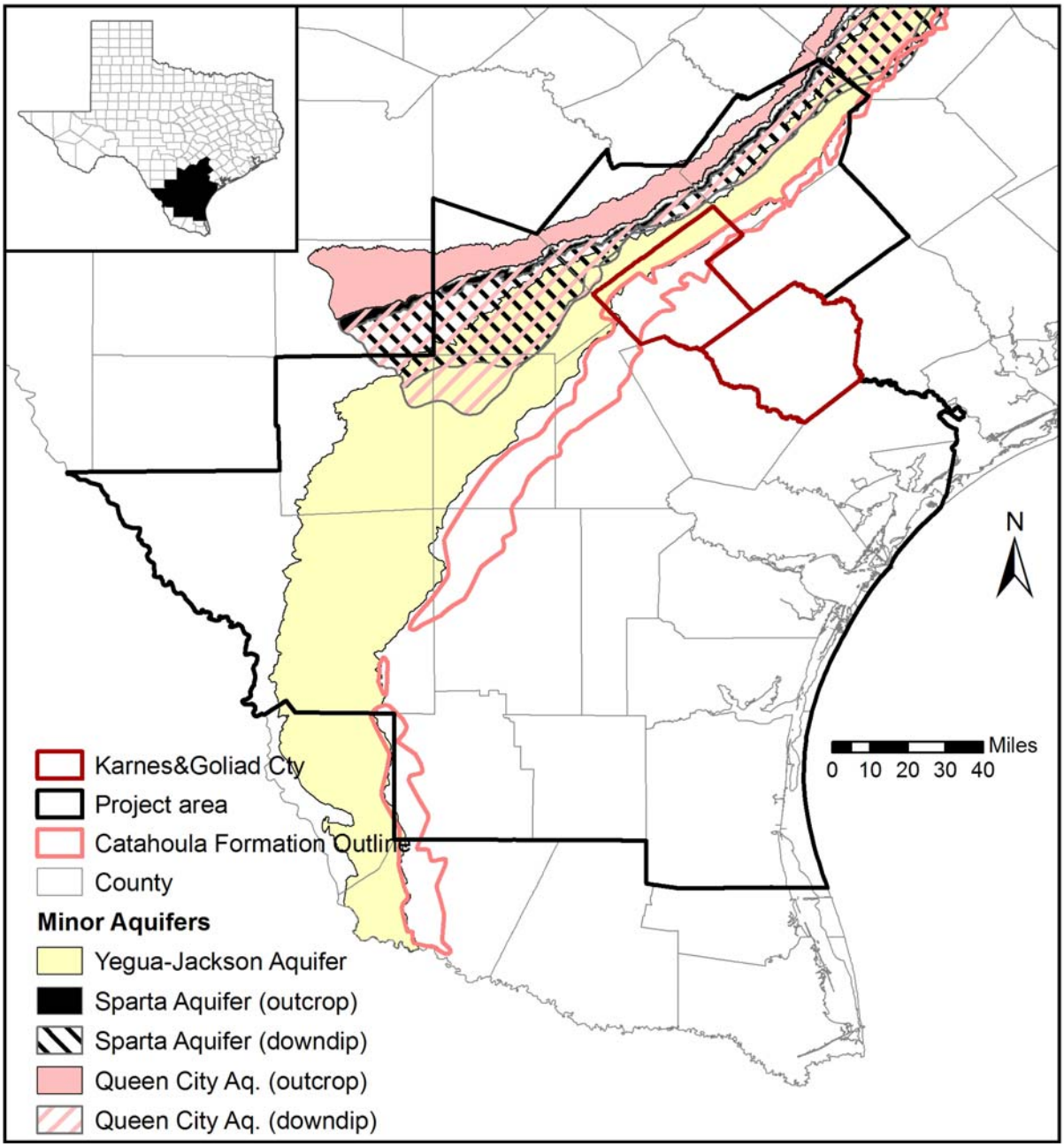

Source: TWDB, http://www.twdb.state.tx.us/mapping/gisdata.asp, January 2009

Figure 43. Map of minor aquifers in the study area; downdip limit is 3,000-mg/L TDS contour line

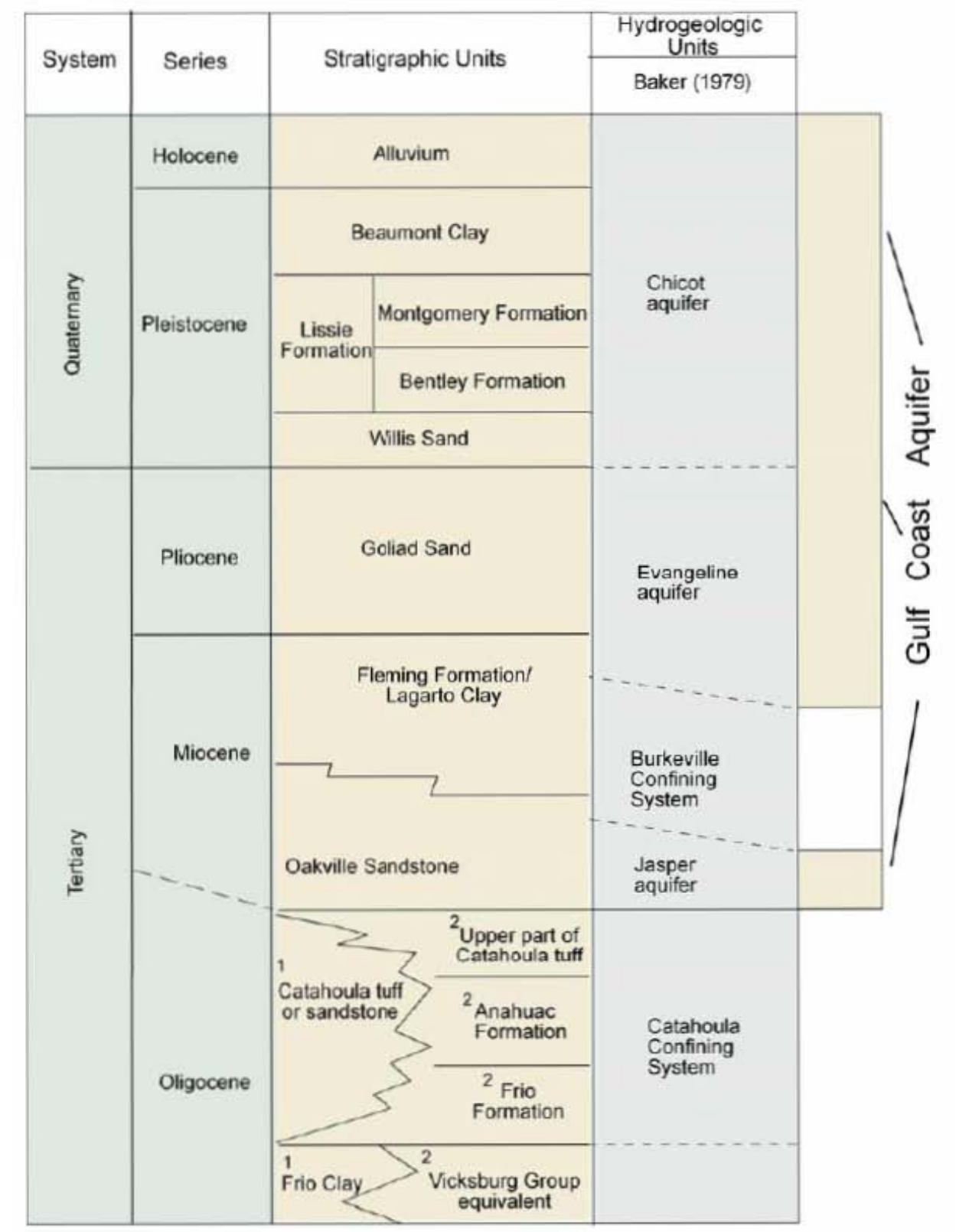

Source: Chowdhury and Mace, 2003

Figure 44. Stratigraphy and hydrostratigraphy of the Gulf Coast aquifers

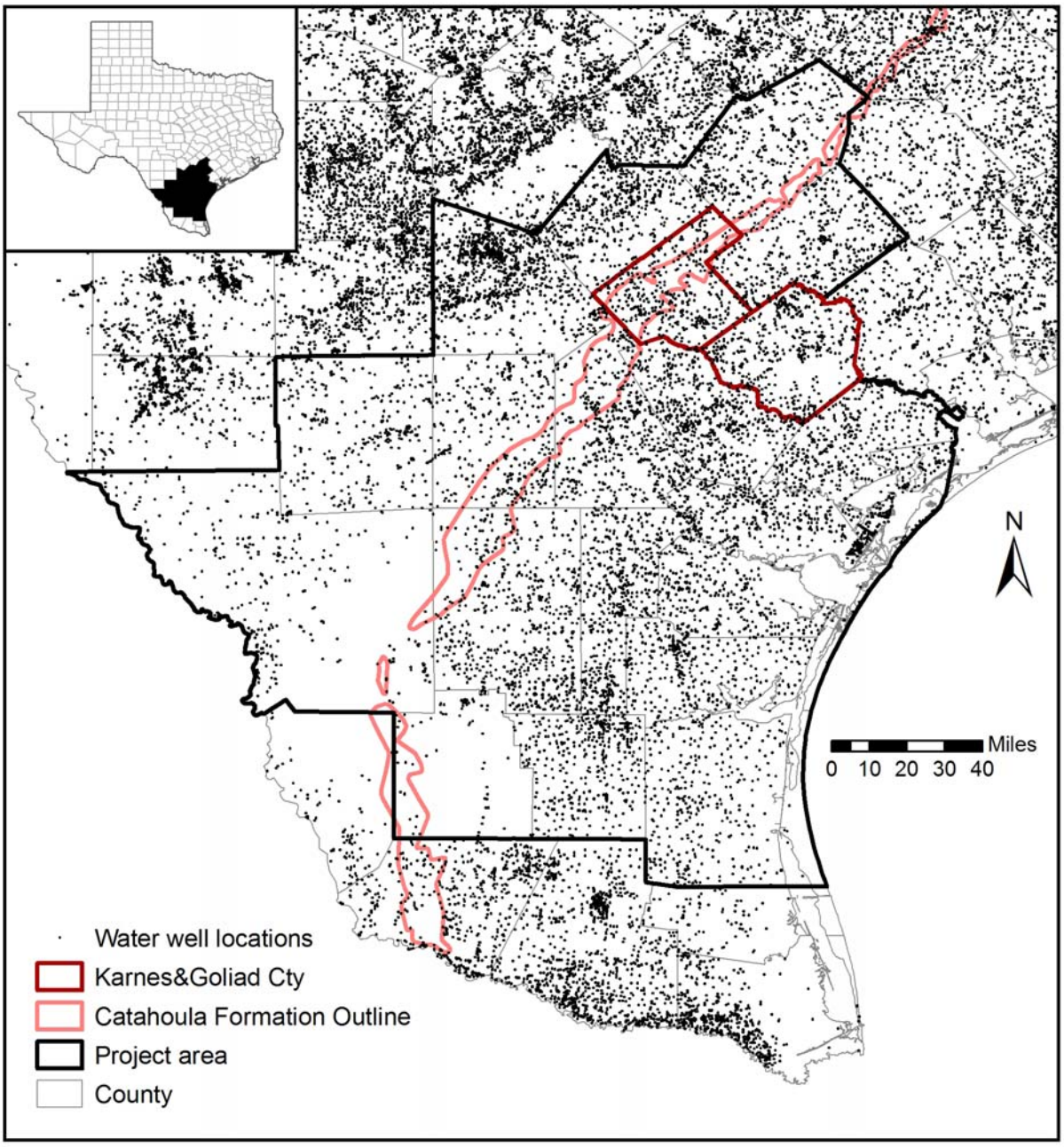

Source: TWDB, http://www.twdb.state.tx.us/mapping/gisdata.asp, January 2009

Figure 45. Water-well locations

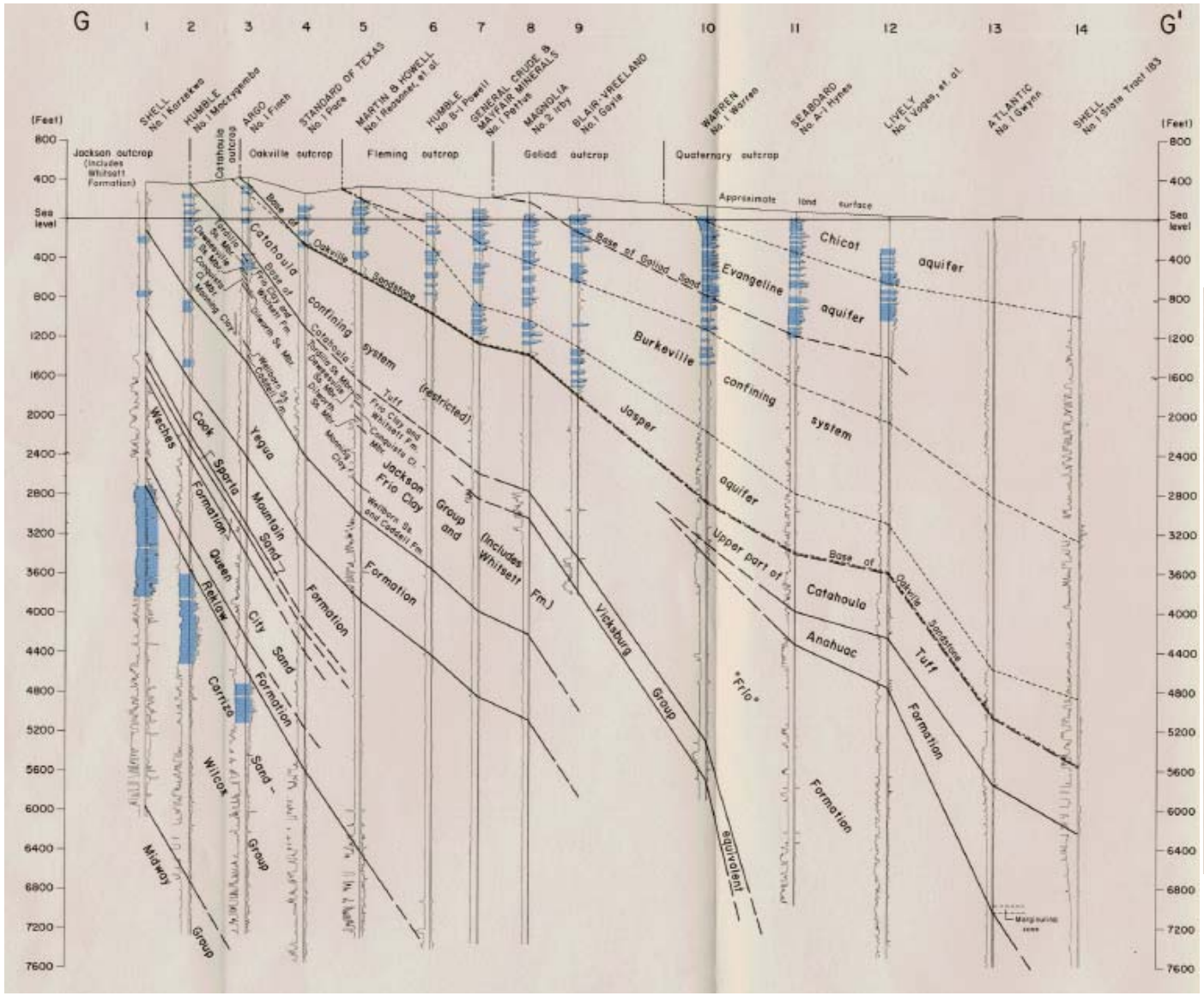

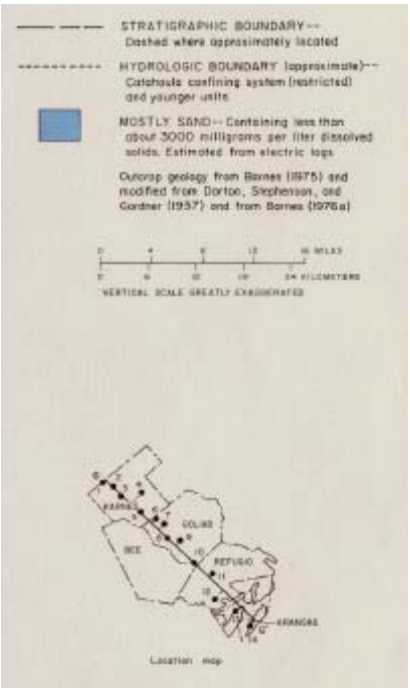

Note: Threshold is 3,000 mg/L.

Figure 46. Stratigraphic and hydrogeologic cross section of Karnes County (from Baker, 1979, Fig. 8)

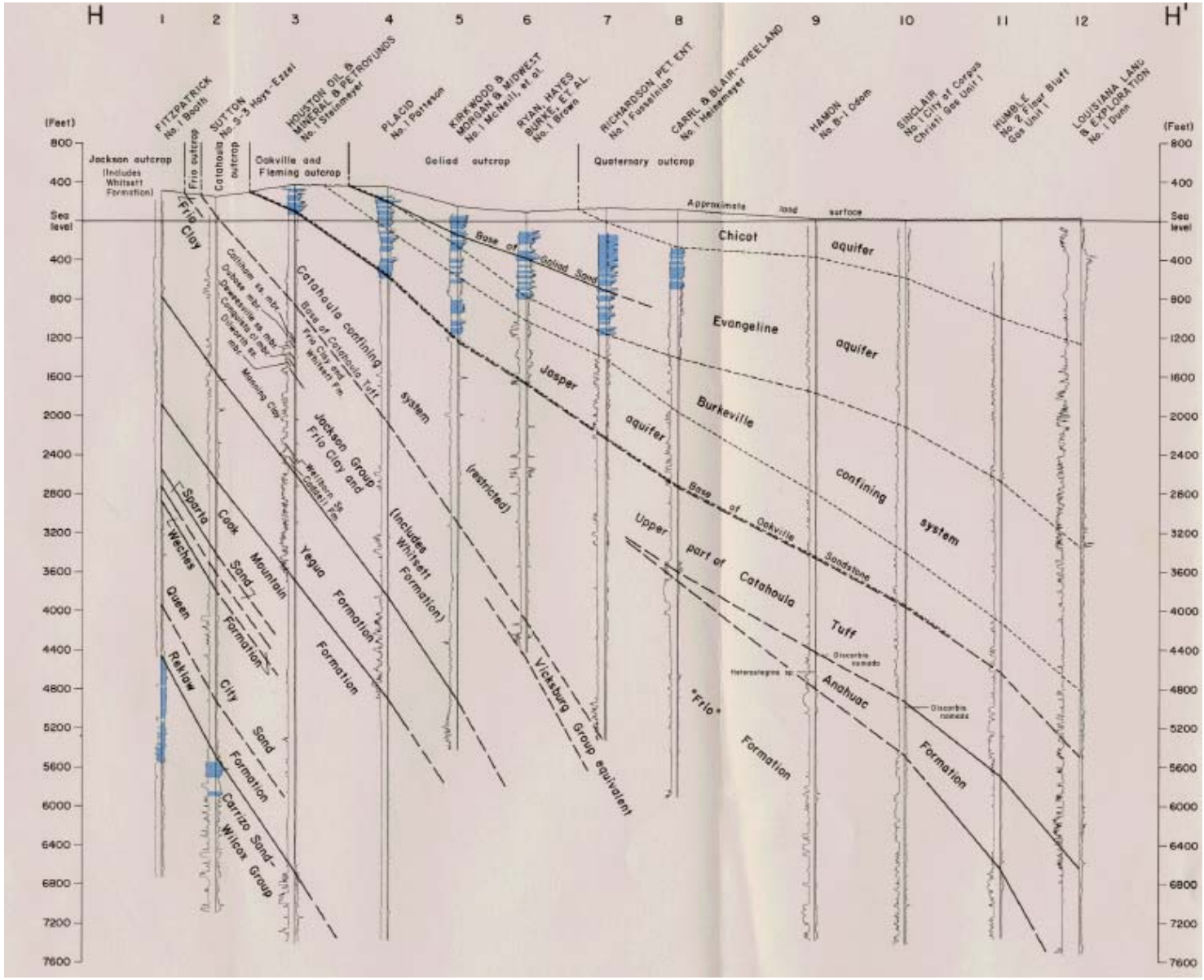

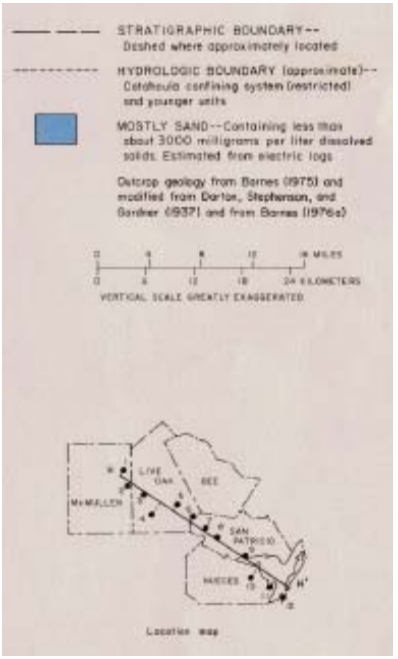

Note: Threshold is 3,000 mg/L.

Figure 47. Stratigraphic and hydrogeologic cross section of Live Oak County (from Baker, 1979, Fig. 9)

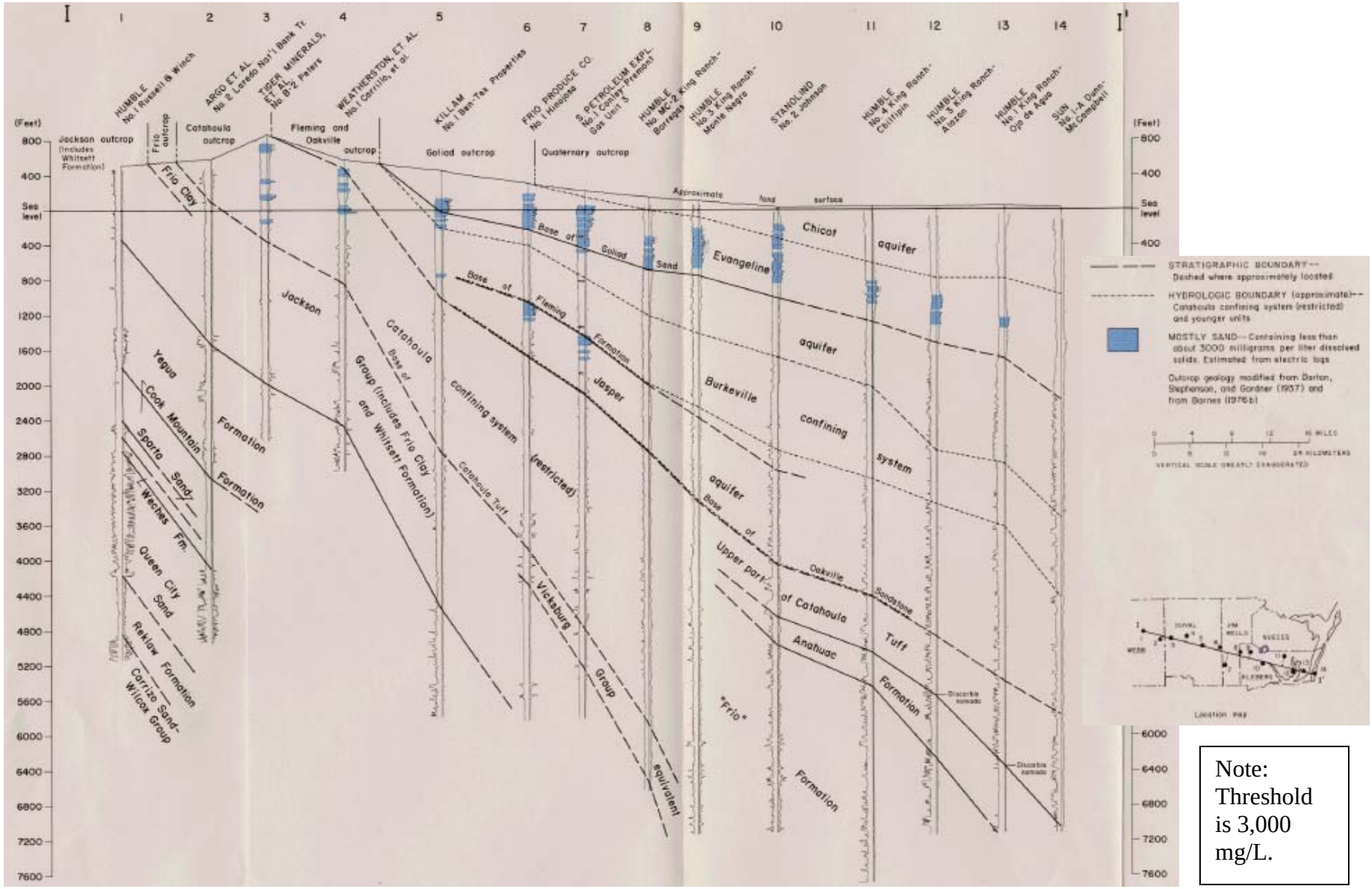

Figure 48. Stratigraphic and hydrogeologic cross section of Duval County (from Baker, 1979, Fig. 10)

IV. Soils and Unsaturated Zone

IV-1. Soils

Usual sources of general information about soils across the U.S. come from two databases: SSURGO (http://soils.usda.gov/survey/geography/ssurgo) county soil survey data and STATSGO (http://soils.usda.gov/survey/geography/statsgo/), both of which are managed by the U.S. Department of Agriculture. Regional maps are too crude to show the variety of soils over the study. Soil nature and classification depend on topography, base-rock lithology, and climate. A finer resolution is needed to represent the complexity and intricacies of these combined variations.

Understanding the nature of a soil helps in quantifying recharge and in understanding chemical processes subjected to rainwater impacting its composition and, ultimately, the chemical composition of shallow groundwater. A few reports document and discuss topography and surface hydrology of the STU. For example, Okerman and Petri (2001) documented agricultural conditions of Nueces and Kleberg Counties. Henry and Kapadia (1980, p. 2) discussed the soils of the Karnes and Live Oak uranium districts. They noted that soil types largely reflect the compositions of underlying substrates and that the same type of soil can occur in different formations. Four distinct soil-type groupings were discerned:

(1) Clay-rich soils developed on muddy parts of the Whitsett, Catahoula, and, to a lesser extent, the Oakville Formation. These include the Monteola clay, Tordia clay, Pawelek clay loam, and Clairville clay loam. They are common throughout the outcrop area of the Catahoula Formation in Karnes and Live Oak Counties. These soils have low permeability and are alkaline and calcium rich, commonly featuring caliche at shallow depths.

(2) Sandy to rocky soils developed on sands and indurated sands of the Whitsett Formation. These include Picosa loam, Weigang silty clay loam, Wilco loamy fine sand, and Cestohowa fine sandy loam. These have a broad textural range, including some sandstone rock fragments. The pH ranges from less than 7 in sandier soils to above 8 in clayier soils.

(3) Soils developed on the nonindurated sands of the Oakville Formation. Representative soils are the Runge fine sandy loam, Wilco loamy fine sands, Sarnosa fine sandy loam, and Danjer clay loam. Upper sections of the sandiest soils are acidic, whereas deeper and finer strata are alkaline and calcareous.

(4) Bottom-land soils on Quaternary alluvium. These are found along drainages and are largely determined by composition of soils of the adjacent drainage areas. They are mostly alkaline, clay rich, and poorly drained.

Quartz, feldspar, and rock fragments dominate the mineralogical composition of sandy soils, whereas montmorillonite, with minor kaolinite and illite, is abundant in clayey soils, reflecting the composition of the parent material. All soil types contain caliche nodules or caliche layers.

IV-2. Trace Elements in Soils

Typical whole-rock trace-metal content is given in Table 2, showing different sources with higher concentrations in shales based on global average values reported by Hem (1985). Typical uranium concentrations are in the 1- to 3-ppm range, which is also the typical concentration in rock-building minerals such as quartz and feldspars (e.g., Bradshaw and Lett, 1980). Shales generally accumulate more trace metals than other sedimentary rocks because of their slow accumulation and the properties of clay minerals. Other elements of interest, such as arsenic, molybdenum, and selenium, are also present within the same order of magnitude of a few ppm. Vanadium and fluorine are typically one to two orders of magnitude higher, 10 to 100 and 100 to 800 ppm, respectively.

Soils in general concentrate metals, although concentrations often reflect concentrations in the parent material. Rock-degradation products, such as iron and other metal oxides and clays, are more abundant in soils and scavenge oxyanion compounds. Shacklette and Boerngen (1984) provided average abundance of selected elements in soils (Table 3). Average arsenic concentration in soils is about 7 ppm, higher than in whole rock. Interestingly, average uranium concentration in soils at 2.6 ppm is not significantly different from that in whole-rock samples, denoting a difference in behavior. The national geochemical database (http://tin.er.usgs.gov/geochem/) developed by the USGS (2004, 2008) contains more recent information on average elemental abundance in surficial soils and sediments at the county level for the conterminous U.S. (Table 5). U.S averages for both studies compare well, 7.2 and 6.6 for arsenic and 0.39 and 0.34 ppm for selenium, for older and more recent studies, respectively. Note that STU county averages are lower by approximately 50% for all selected trace elements compared with U.S. averages (Figure 49), hence the danger of averaging at a scale much larger than the stratum of interest. For example, outcrop of the Catahoula Formation always represents a small fraction of the total area of a county. Table 6 displays similar values for specific locations in the STU Province (sample location in Figure 50).

Henry and Kapadia (1980) studied concentrations of As, Cu, Se, and Mo (but not U) in soils in the southwestern Gulf Coast area, both in background samples (256 samples) and near mines (182 samples). Samples originated from Atascosa, Bee, Dewitt, Karnes, and Live Oak Counties. Cu is not an oxyanion and behaves differently from other metals. Table 4 presents baseline concentration for trace elements in the southwestern Gulf Coast and elsewhere in the U.S. Most soils in South Texas have Mo, As, and Se concentrations similar to those of natural soils elsewhere, except perhaps molybdenum in the Whitsett Formation. (most likely resulting from small uneconomic accumulations). However, sampling of mined and mineralized areas shows much higher concentrations. Samples were taken in close proximity (<½ mi) to the mining areas. Above-background concentrations may be due to (1) naturally higher concentrations next to shallow economic deposits or (2) human-made increases related to mining activities. Henry and Kapadia (1980) also claimed that sampling results do not support windblown dust as the origin of increased concentration in soils. However, they concluded that high soil concentrations are due to either shallow mineralization or runoff from excavated material. These shallow mineralized areas are present mostly in the Whitsett Formation of the Jackson Group and not so much in the Catahoula and Oakville Formations. (Henry and Kapadia, 1980, p. 30). Stream sediment contamination from postclosure runoff, and also from direct pit discharge before it was prohibited in the 1970's, may run for miles.

Table 2. Average abundance of uranium and companion elements for different rock types

Element (mg/kg)	Igneous	Sandstone	Shale	Carbonate
Arsenic	1.8	1	9	1.8
Boron	7.5	90	194	16
Fluoride	715	220	560	112
Molybdenum	1.2	0.5	4.2	0.75
Antimony	0.5	0.8	0.1	0.2
Selenium	0.05	0.5	0.6	0.3
Uranium	2.8	1.	4.5	2.2
Vanadium	149	20	101	13

Source: Hem (1985, Table 1)

Element	Crust Average[A]	Crust Average	Crust Average[D]
Arsenic	(0.8–2.2)		2.1
Boron			8.7
Fluoride			540
Molybdenum	1.5 (0.25–1.5)		1.1
Antimony			0.2
Selenium	0.05		0.05
Uranium	1.8 (0–3.3)	2.6[B] 1.7[C]	1.8
Vanadium	30 -225		190
Thorium	(0–18)	10[B]	6

[A] Guilbert and Park (1986, Tables 3.4 and 3.5) average (and range)
[B] Burns and Finch (1999, p.270)
[C] Cuney and Kyser (2009, p.23)
[D] University of Sheffield, UK, 2009, http://www.webelements.com/geology.html

Table 3. Average abundance of uranium and associated elements in soils in the U.S. (mg/kg)

Element	Geometric Average[A]	Range[A]	"Background Values"[B]
Arsenic	7.2	<0.1–97	10
Boron	33	<20–300	30
Fluoride	430	<1 –3,700	300
Molybdenum	~1	<3–15	3
Antimony	0.66	<1 – 8.8	1
Selenium	0.39	<0.1–4.3	0.3
Uranium	2.7	0.3–11	1
Vanadium	80	<7–500	55

[A] Shacklette and Boerngen (1984, Tables 1 and 2)
[B] Moon et al. (2006, Table 8.2)

Table 4. Current uranium and companion element concentration in southwestern Gulf Coast soils (A and B horizons). Arithmetic mean (range) in mg/kg

Formation	Arsenic	Molybdenum	Selenium	Uranium
Whitsett	5.3 (0.6–17)	2.1 (0.2–4.6)	0.18 (0.01–0.90)	
Catahoula	3.4 (0.2–6.9)	0.9 (0.2–4.0)	0.13 (0.01–0.60)	2–3*
Oakville	No Data	0.9 (0.3–2.0)	0.17 (0.01–0.38)	
U.S. average	~5–6	1-2	0.1–0.5	

NOTE: From a total of about 300 samples
Data from Table 4 of Henry and Kapadia (1980); arithmetic mean + composite range
* From Galloway (1977, p. 39) and Galloway and Kaiser (1980, p. 14)

Table 5. County average soil concentration of selected trace elements (As, Se, Hg, Pb, Zn, Cu)

County	As	σ_As	Se	σ_Se	Hg	σ_Hg	Pb	σ_Pb	Zn	σ_Zn	Cu	σ_Cu
Aransas	2.682	1.055	0.147	0.033	0.014	0.004	9.215	2.414	25.666	5.255	5.380	1.186
Atascosa	6.358	1.409	0.224	0.092	0.015	0.005	14.670	2.752	38.936	6.140	7.241	2.255
Bee	3.082	0.855	0.235	0.076	0.014	0.004	11.523	4.037	29.475	8.595	7.636	2.175
Brooks	5.052	3.336	0.160	0.043	0.021	0.014	11.078	4.962	17.714	6.828	4.529	1.386
De Witt	4.955	1.153	0.339	0.078	0.012	0.002	10.883	3.263	26.132	5.788	7.746	1.706
Duval	4.461	1.114	0.190	0.080	0.018	0.015	13.503	5.731	44.480	13.040	10.437	3.569
Goliad	4.912	2.164	0.300	0.077	0.016	0.006	14.137	3.180	28.250	3.617	7.017	1.535
Gonzales	5.033	1.159	0.243	0.082	0.015	0.006	11.092	2.726	24.947	4.756	5.059	1.847
Jim Hogg	3.761	0.979	0.199	0.063	0.013	0.003	16.105	3.133	47.597	9.108	9.169	1.061
Jim Wells	3.472	0.773	0.154	0.041	0.020	0.017	11.563	2.321	33.099	7.060	8.012	1.934
Karnes	5.223	1.625	0.282	0.055	0.013	0.004	12.873	3.463	33.126	6.593	7.104	1.707
Kenedy	2.084	0.159	0.121	0.026	0.010	0.000	22.211	3.116	22.592	3.533	5.282	1.055
Kleberg	3.878	1.819	0.137	0.038	0.015	0.008	16.463	6.134	29.784	10.407	6.859	2.921
La Salle	6.022	1.441	0.192	0.050	0.026	0.019	16.512	3.097	49.798	9.426	10.856	2.591
Live Oak	4.262	1.214	0.231	0.048	0.020	0.009	20.733	6.959	43.722	9.447	10.005	1.779
McMullen	4.526	0.554	0.161	0.041	0.012	0.002	23.139	5.594	46.346	9.918	10.891	2.540
Nueces	5.330	1.658	0.140	0.028	0.018	0.011	16.941	5.007	35.384	12.682	7.866	2.541
Refugio	3.774	1.835	0.212	0.054	0.018	0.006	12.061	3.806	29.378	4.153	6.360	1.572
San Patricio	4.072	1.007	0.141	0.032	0.011	0.002	12.281	2.721	26.656	2.807	6.229	1.369
Webb	5.396	1.307	0.194	0.090	0.017	0.009	13.287	3.245	45.082	7.066	9.160	2.905
Wilson	5.044	1.117	0.307	0.159	0.015	0.005	15.352	4.038	32.591	10.546	5.468	2.494
Average	**As**		**Se**		**Hg**		**Pb**		**Zn**		**Cu**	
STU	4.447		0.205		0.016		14.553		33.845		7.538	
Texas	5.408		0.244		0.017		16.680		39.558		10.323	
United States	6.611		0.338		0.061		25.128		59.741		14.457	

Source: http://tin.er.usgs.gov/geochem/doc/averages/countydata.htm; file “county-averages.xls”
Note: All data in ppm

Table 6. Trace-element analysis (in ppm—mg/kg) of selected soil samples in the STU province (see Figure 50 for location)

Sample#	County	Hor.	Name	As	Cu	Mo	Pb	Sb	U	V	Th	Zn	F	Se
Sample close to the Catahoula outcrop														
D174197	Duval	B	S.	3.1	10		10	<1	1.9	30	5.3	26	600	0.18
D198564	Duval	A	D.		15		10		5.5	100	14.9			
D174311	Jim Hogg	B	S.	1.7	5			<1	0.8	7		10	<400	0.14
D198573	Karnes	A	D.		20		10		1.8	30	11.0			
D198574	Karnes	B	D.		20		10		1.7	30	10.7			
D198575	Karnes	B	D.		20		10		1.7	50	11.7			
D198576	Karnes	C	D.		10		10		2.3	30	8.0			
D198577	Karnes	C	D.		15				2.1	30	9.9			
D142685	Live Oak	B	S.	6.0	7		10		1.8	30	3.8	32	90	0.19
D159214	McMullen	A	D.		20		15		2.3	50	11.3			
D159213	McMullen	B	D.		3		10		1.0	10	2.1			
D159235	McMullen	A	D.		30		15		9.9	100	8.7			
D174357	McMullen	B	S.	8.1	15		15	<1	2.0	70	15.8	54	<400	0.34
Other samples														
D142686	Aransas	B	S.	3.0	7		20		1.3	20	7.1	22	180	0.11
D174237	Brazoria	B	S.	2.0	10		10	<1	2.3	20	7.3	26	<400	0.40
D142687	Calhoun	B	S.	5.3	15		15		2.3	30	7.5	22	140	0.36
D142681	Cameron	B	S.	13.0	20		15		3.8	100	8.7	97	550	0.27
D174319	Cameron	B	S.	2.6	5		10	<1	1.2	20		14	<400	<0.1
D142675	Dimmit	B	S.	2.1	5		10		2.0	20	4.8	22	20	<0.1
D174300	Hidalgo	B	S.	3.5	10		10	1.5	1.9	30		26	<400	0.19
D142683	Kenedy	B	S.	10.0	5		10		0.9	10		11	50	<0.1
D142688	Matagorda [Victoria?]	B	S.	4.3	10		10		2.1	30	6.7	14	30	0.33
D142684	San Patricio	B	S.	4.2	7		15		1.7	20	5.7	21	180	0.15
D142679	Starr	B	S.	11.0	7		20		5.0	30	8.1	61	180	0.15
D142676	Webb	B	S.	6.4	3		15		2.7	20	4.9	42	90	0.13
D142677	Webb	B	S.	11.0	5		30		4.2	30	7.8	80	170	0.61
D142682	Willacy	B	S.	6.2	20		15		2.6	50	8.2	69	320	0.26
D142678	Zapata	B	S.	4.2	5		10		1.9	30	4.9	34	30	0.12

Note: Hor. = soil horizon (A, B, or C); Name = sampling submitted by either H. T. Shacklette (“S.”) or K. A. Dickenson (“D”). Empty cell means no analysis was performed (Shacklette and Boerngen, 1984).

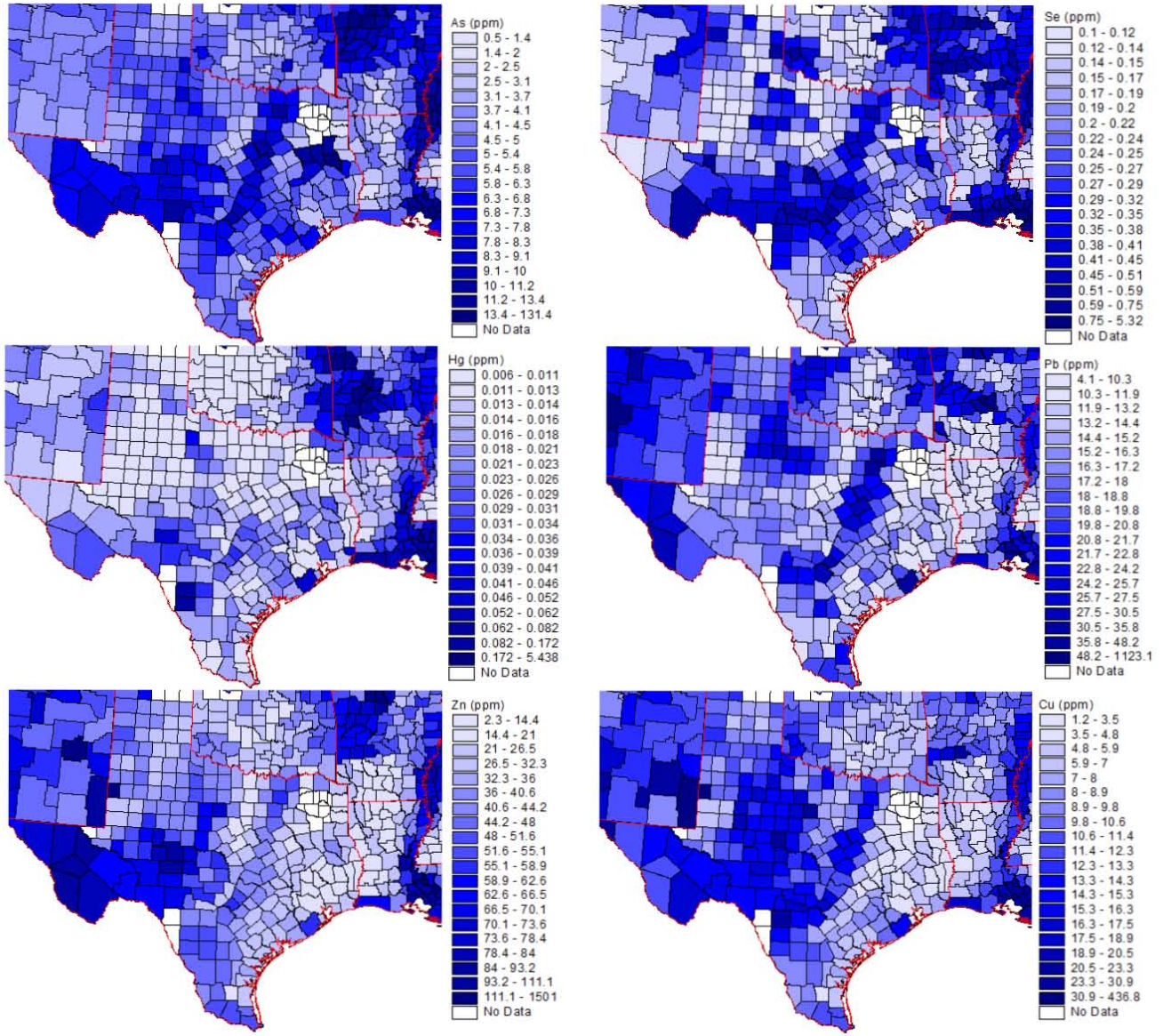

Figure 49. National Geochemical Database by county for selected elements (As, Se, Hg, Pb, Zn, Cu)

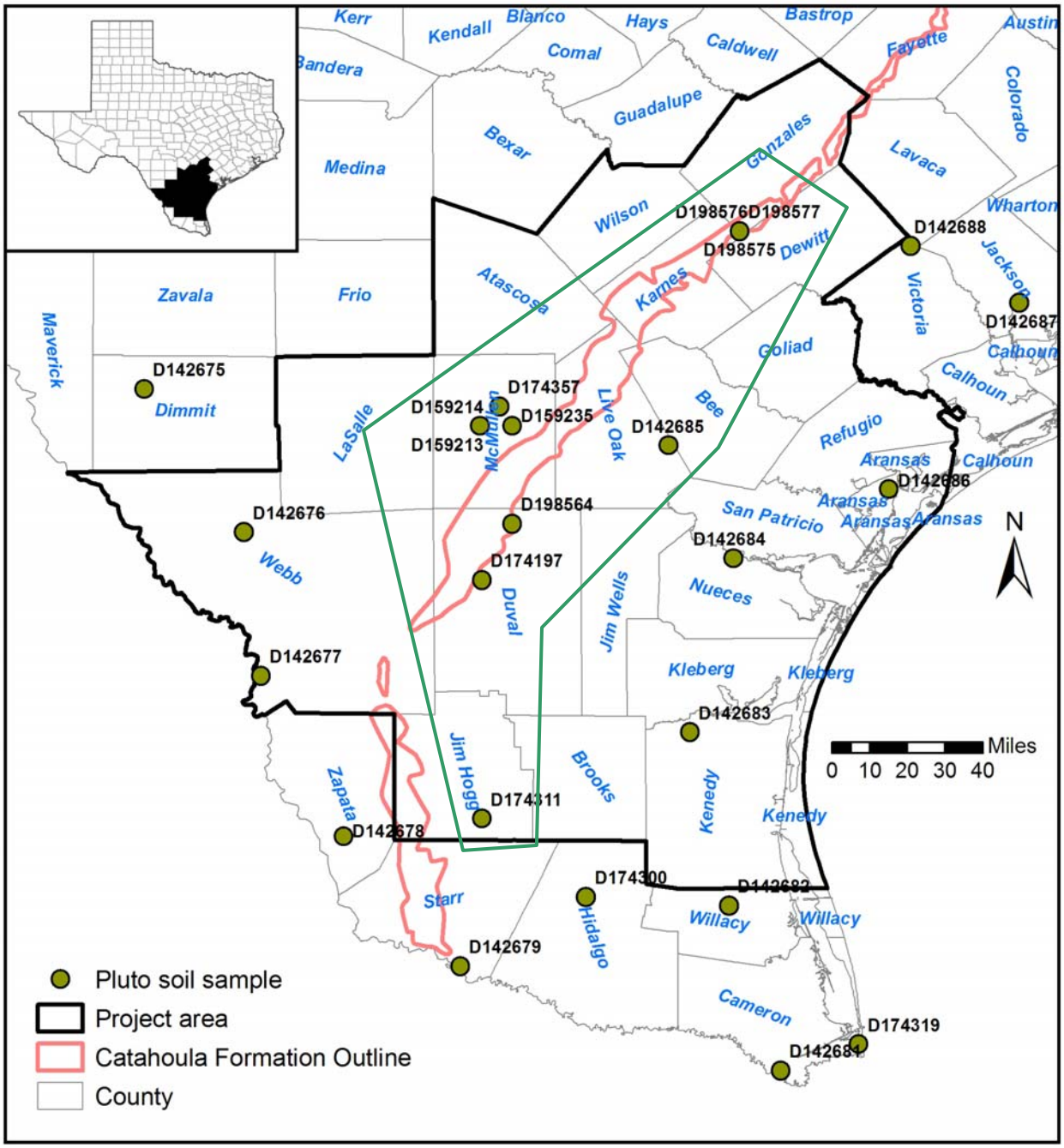

Source: Pluto database, http://tin.er.usgs.gov/metadata/plutosoil.faq.html; most data were originally submitted by H. T. Shacklette (most likely published in Shacklette and Boerngen, 1984); some in McMullen and Karnes Counties submitted by K. A. Dickinson

Figure 50. Location of PLUTO soil samples for trace-element analysis (see Table 6)

V. Groundwater and Aquifer Description

This section forms the core of the report and documents hydrogeology and features of STU flow systems and geochemistry and trace element behavior, as well as processes that led to STU mineral accumulations.

V-1. Description of Data Source

This section provides a summary of the sources of data presented in later subsections of Section V but is not necessarily comprehensive. Data on hydrogeology and aquifers were obtained from TWDB county and regional reports and USGS regional studies (Ryder, 1988; Ryder and Ardis, 1991; RASA models). TWDB and its predecessor agencies have produced numerous so-called county reports describing sources of groundwater at the county level (Table 7). In the past, USGS also published county-level reports. Century-old reports are included as well because they often help in determining predevelopment natural conditions. More recently, TWDB has also embarked on a more quantitative estimation of state water resources through the GAM program (Chowdhury and Mace, 2003; Chowdhury et al., 2004; Knox et al., 2007; Chowdhury and Mace, 2007). Most of these reports are available from the TWDB website. Many earlier, regional reports have also been published by the TWDB (Baker, 1979; Muller and Price, 1979; McCoy, 1990; more are listed in Chowdhury and Mace, 2006). Most are also available through the TWDB website.

Information on aqueous geochemistry across the state, particularly on the Gulf Coast, can be obtained through State agencies and the USGS and was compiled from the following databases: (1) Texas Water Development Board (TWDB) database available at http://www.twdb.state.tx.us/DATA/waterwell/well_info.asp, (2) Texas Commission on Environmental Quality (TCEQ) Public Water System (PWS) database not publicly available (http://www.tceq.state.tx.us/, (3) National Uranium Resource Evaluation (NURE) database available for the State of Texas at http://pubs.usgs.gov/of/1997/ofr-97-0492/state/nure_tx.htm, and (4) U.S. Geological Survey (USGS) National Water Information System (NWIS) database available at http://waterdata.usgs.gov/nwis/.

TWDB conducts ambient groundwater-quality monitoring. All major and selected minor aquifers are sampled on a 5-yr rotating basis. At the state level, water-quality data are available for 55,000 groundwater sites (wells, springs), resulting in a total of 104,000 analyses, each analysis including major anions and cations. The earliest water chemistry data available are from the late 19th century. Groundwater-quality information includes State well number, date of sampling event, time, collection remarks, reliability of sampling-method remarks, collecting agency, indication of whether the sample is chemically balanced, lab-calculated pH, phenol and total alkalinity, hardness, specific conductance, sodium adsorption ratio (SAR), residual sodium carbonate (RSC), total dissolved solids (TDS), and major anions and cations (Ca, Mg, K, Na, Sr, SO_4, HCO_3, CO_3, Cl^-, F, NO_3, SiO_2). In some instances, analyses are performed for infrequent constituents (metals), organics, nutrients, and radioactive constituents. Approximately 500,000 infrequent constituent analyses (each corresponding to one single constituent) have been entered in the database. Additional well information is provided in the database, including well depth, main aquifer, and groundwater level. The TWDB database includes some, but not all, water-quality data in the USGS database, which are provided as a Microsoft Access file and can be

downloaded from the TWDB website. Note that information from the TWDB database is not always accurate, especially earlier samples, despite TWDB's best quality-assurance efforts.

The TCEQ PWS database includes water-quality data for all public water systems in the state. Water sources of public water systems include surface water, groundwater, and/or mixed sources. Water-chemistry data in the PWS database represent water-entry points, which may represent a blend of groundwater from different wells, groundwater and surface water, or surface water. For this study, we are interested only in raw groundwater chemistry data; therefore, we selected water-quality samples that can be associated with a single well and included raw and entry-point data. The database obtained from TCEQ is a subset of the larger PWS database that includes only inorganic chemical constituents of concern, including arsenic. Constituents in this modified database include specific conductance, TDS, alkalinity, total hardness, pH, Al, An, Be, N, NH_3, As, Ba, Ca, Cd, Cl, Cr, Cu, Fl, Fe, Pb, Mg, Mn, Hg, Ni, NO_3, NO_2, K, Se, Ag, Na, SO_4, Th, Zn, U, Rd, radium 226 and radium 228, gross beta, tritium, gross alpha, and Sr_{90}. Additional well information in the database includes well depth, screened interval, aquifer designation, and geology. Well depth is available for most wells, but screen depth and geologic descriptions are not available for all wells in the database. TCEQ PWS has limited spatial coverage because it excludes rural areas. The database is provided as a Microsoft Access file.

The National Uranium Resource Evaluation (NURE) database is based on hydrogeochemical and stream sediment reconnaissance studies and includes data from stream sediments, soils, groundwater, and surface water over the entire U.S. The reconnaissance survey began in 1975 and ended in 1980 under the responsibility of four DOE national laboratories: Lawrence Livermore National Laboratory (LLNL), Los Alamos National Laboratory (LANL), Oak Ridge Gaseous Diffusion Plant (ORGDP), and Savannah River Laboratory (SRL) (Smith, 2001; USGS, 2004). The purpose of the program was to explore for undiscovered uranium. This database provides chemical data for Ag, Al, As, Au, B, Ba, Be, Bi, Br, Ca, Cd, Ce, Cl, Co, Cr, Cs, Cu, Cy, Eu, F, Fe, Ga, He, Hf, Hg, K, La, Li, Lu, Mg, Mn, Mo, Na, Nb, Ni, P, Pb, Pt, Rb, Sb, Sc, Se, Si, Sm, Sn, Sr, Ta, Tb, Th, Ti, U, V, W, Y, Yb, Zn, Zr, PO_4 (phosphate), NO_3 (nitrate), SO_4 (sulfate), methane, ethane, propane, and butane in samples of stream sediment, spring sediment, lake or pond sediment, soil, rock, well water, stream water, and spring water. In addition, the database provides location and descriptive information for each sample. The NURE database has gaps in the southwestern Gulf Coast and, more important, does not allow easy attribution to aquifers. The USGS database includes water-quality data for selected areas of Texas, but mostly in the Houston area.

Specific information about mining districts and mining-related information comes from the 10+ BEG Reports of Investigations published in the 1970's and 1980's, during the peak of uranium production in the STU Province. The USGS also published abundant literature on the STU and other U.S. uranium provinces. Most reports cited in this document are available for free from the USGS "publications warehouse" (http://pubs.er.usgs.gov/).

V-2. Hydrogeology and Hydrogeochemistry

Relative geometry of the different water-bearing units was described in Section III-4. The general regional flow system in the Gulf Coast consists of recharge in the outcrop areas, with shallow systems rejecting most of the recharge relatively quickly into local streams and rivers. The slow, regional, deep recharge moves downdip and slowly flows back up through more recent units. In other words, in a system at equilibrium, recharge enters the formations through a rather

narrow band and is balanced by water leaving the same formation both through very short flowpaths in the outcrop and diffusely through the footprint of their confined sections (e.g., Reedy et al., 2009). Pumping that has been taking place in the past half-century captures water either in the short outcrop path to rivers and streams (for generally low yield irrigation or domestic wells) or in the confined section (for higher yield irrigation or municipal wells).

Recharge to the STU Province water-bearing units occurs in outcrop zones of the respective units through infiltrating rainfall (generally in higher elevation areas) and losing streams (especially in the south). Groundwater then flows downdip and downgradient, as determined by hydraulic-head levels, which generally mirror regional topography. High- and low-transmissivity zones associated with paleochannels and interfluves, respectively, may funnel or deflect flows locally, but the overall pattern is increasing groundwater residence times with distance downdip (perpendicular to the coast) and with depth below the water table. Flow can be locally or regionally perturbed, with some flowpaths leading to discharge into streams and river valleys. Fault zones may also affect flow patterns; for example, displacement along some faults is adequate to physically separate individual sand channels, possibly reducing transmissivities locally. Discharge is to rivers, streams (gaining streams), and springs, and eventually to the Gulf of Mexico, according to Toth (1963)'s model of shallow ("quick" local discharge to local streams—order of years or decades), intermediate, and regional (deep and slow—order of several millennia) flow systems. In addition, fresh water flows deeper along channels and other high-transmissivity zones and slowly returns to the surface by leakage through overlying formations. Modern pumping may disrupt natural flow lines.

V-2-1 Flow Models

Given the high average population density and economic importance of the Texas Gulf Coast, many hydrogeologic-flow numerical models have been published in the past 50 yr. The most notable models at the supraregional scale include the federally sponsored and USGS-developed 5- × 5-mi^2 cell RASA model (Ryder, 1988; Ryder and Ardis, 1991). The model includes 14 layers covering all major aquifers of the upper and lower Gulf Coast, from the Wilcox at the base to recent aquifers of Pleistocene and Holocene age at the top. Begun in the early 1990's, another series of numerical models, although state sponsored and regional in scale, include the same formations. The 1- × 1-mi^2 cell GAM models represent the achievement of decades of incremental groundwater flow modeling by state geologists and their consultants (http://www.twdb.state.tx.us/gam/index.htm). When finished, GAM coverage will include at least three models in the STU province: the southern Gulf Coast (Chowdhury and Mace, 2003, 2007), the central Gulf Coast (Waterstone, 2003; Chowdhury et al., 2004), and the Yegua-Jackson (Knox et al., 2007, modeling part in progress). GAM models are periodically updated to include new data. Local numerical flow models have also been produced (e.g., Adidas, 1991; Hay, 1999; Arredondo and Thomann, 2005; undoubtedly many more exist)

V-2-2 Flow Parameter Distribution

Although the Gulf Coast aquifer has been extensively pumped, predicting yield from the aquifer is difficult. This uncertainty in estimating yield is due to the relative unpredictability of the distribution of sand-shale content, pore-fill cements, depositional facies, and compaction from overlying sediments at the local scale. The ease with which water can move through pore spaces or fractures in the sediments and how much water the sediments can store are controlled by its

hydraulic properties. For example, water can flow more readily through coarser sediments—such as sand and gravel—than finer sediments—such as silt and shale. Hydraulic conductivity depends on intrinsic permeability of the sediments and on degree of water saturation. Transmissivity, a product of hydraulic conductivity and aquifer thickness, describes the ability of an aquifer to transmit water through its entire thickness. If hydraulic conductivity is uniform from point to point, an aquifer is considered homogeneous. If hydraulic conductivity is not uniform, an aquifer is considered heterogeneous. Trending heterogeneity results from sediment accumulations in specific depositional environments (e.g., from deep-sea muds to beach sands to lagoonal muds), and layered heterogeneity develops when beds with high and low permeability occur together (Freeze and Cherry, 1979). Storativity describes the capacity of an aquifer to transfer water to and from storage (Anderson and Woessner, 1992). The capacity of an aquifer to transfer water can be described by the following parameters: specific storage, storage coefficient, and specific yield. Specific storage is equal to the volume of water released from storage within a unit volume of porous material per unit decline in hydraulic head. The storage coefficient is the product of specific storage and aquifer thickness and represents the volume of water released per unit area per unit decline in hydraulic head. Specific yield is the volume of water released by gravity drainage per unit area of the aquifer per unit decline in water level (Anderson and Woessner, 1992). In confined aquifers, storativity is controlled by compression of the water and the porous medium. In unconfined aquifers, storativity / specific yield approximates effective porosity of the aquifer material.

Hydraulic conductivity and, hence, an aquifer's transmissivity and potential water yield are closely related to grain-size distribution of the aquifer (e.g., Masch and Denny, 1966). Zones of sand (or coarser) grain sizes are good indicators of high-yield zones. Bedload-dominated fluvial systems exhibit high transmissivities because of coarse grain size and high sand content. On the other hand, suspended-load fluvial systems generally translate into poor aquifers because of the lack of continuity in transmissive elements (Galloway et al., 1979b, p. 246). Older BEG reports mention conductivity and pump tests, but GAM models are the authoritative source of information on flow properties. Note that hydrogeologic systems are not permanent but are dynamic, and they evolve with geologic time. For spatial distribution of trace-element aqueous concentrations to be understood, therefore, paleohydrology needs to be understood. Evidence shows that current hydrological conditions are different from those that occurred during ore formation—for example, at the Panna Maria mine (Galloway et al., 1979a, p. 45).

STU aquifers show considerable variation in well yields over a short distance primarily owing to the occurrences of trending heterogeneity. Although the Gulf Coast aquifer has been extensively pumped, yield from the aquifer is difficult to predict. This uncertainty in estimating yield is due to unpredictability in determining distribution of sand-shale content, pore-fill cements, depositional facies, and compaction from overlying sediments. Prudic (1991) examined 1,500 aquifer test analyses and more than 5,000 specific-capacity tests for the entire Gulf Coast aquifer, extending from Texas to Louisiana. He found that hydraulic conductivity is highly variable, ranging from 1 to 1,000 ft/d. Geometric mean for hydraulic conductivity was 55 ft/d from pumping tests and 71 ft/d from specific-capacity tests. He noted that hydraulic conductivity is more dependent on depth to the middle of the screened interval than sand-bed thickness. He also observed that hydraulic conductivity decreased as a function of depth.

In the supraregional RASA model, GCAS horizontal hydraulic conductivity averaged over all cells of the same layer ranged from 15 to 25 ft/d (Ryder and Ardis, 1991, Table 3). Average

transmissivity values varied from about 7,770 to about 10,250 ft^2/d. Vertical conductivity varied from 1.1×10^{-4} to 1.3×10^{-3} ft/d in confining layers (Ryder and Ardis, 1991, Table 4). However, vertical conductivity variability was much larger in the aquifers and varied from 5.3×10^{-6} to 5.0×10^{-2} ft/d. The horizontal to vertical permeability ratio typically increases with scale of the model because cells get bigger and are more likely to incorporate barriers to flow. Integrating properties of a larger and larger volume of rock to obtain a single or just a few values is called *upscaling* and is one of the grand challenges of flow in the subsurface. In essence and in practice, vertical permeability values are averaged according to a harmonic average rule, which gives more weight to the lowest value, whereas horizontal-permeability averages are obtained through the arithmetic average (more weight to the largest value).

The following paragraphs give an overview of aquifers relevant to the STU. GAM models developed by the TWDB provide the most comprehensive information, often summarizing all previous work on these same aquifers.

Aquifers from the Jackson Group—No report is dedicated solely to describing flow properties of all Jackson Group aquifers. Kreitler et al. (1992) provided local information on the different small aquifers present near the Susquehanna-Western mine tailings near Falls City. TWDB (Adidas, 1991) did a groundwater study near the town of Bruni in southeastern Webb County, stating that "fluvial sand to gray-green clay sedimentary deposits yield variable amounts of highly mineralized water" from upper Jackson Group rocks. As was the case in predevelopment conditions in many Gulf Coast aquifers, heads were described as artesian in the 1930's. Fewer than half a dozen wells on the west edge of the Gulf Coast aquifers in Webb County penetrate upper Jackson Group rocks, and arsenic concentrations in these wells were below detection limits.

Most reports that include the Jackson aquifer mostly discuss the underlying Yegua aquifer. Preston (2006) reported that known well yields range from a few gallons per minute (gpm) to over 300 gpm at the "Yegua-Jackson" aquifer, and properly located, designed, and constructed wells sited in the most productive areas might produce up to 500 to 600 gpm. Although the occurrence, quality, and quantity of water from this aquifer are variable, domestic and livestock supplies are available from shallow wells over most of its extent. Locally water for municipal, industrial, and irrigation purposes is available. Yields of most wells are small, less than 50 gpm, but in some areas, yields of adequately constructed wells may range to more than 500 gpm (Ashworth and Hopkins, 1995). Harris (1965) reported that the Jackson aquifer yields only small quantities (<50 gpm) of slightly to moderately saline water to wells in La Salle and McMullen Counties.

Aquifers from the Catahoula Formation—The Catahoula Formation contains groundwater near the outcrop in relatively restricted sand layers. A study by Adidas (1991) near Bruni, Webb County, detected six water-bearing units in the Catahoula Formation with yields varying from 5 to 30+ gpm (always <100 gpm). The base of the lowermost unit is about 300 ft below ground surface. The water is slightly brackish, however. Hydraulic conductivity of the Catahoula is on the order of 19 ft/d, and the storage coefficient is about 0.0008 (Adidas, 1991). Harris (1965) reported that the Catahoula Tuff yields small quantities (<500 gpm) of slightly to moderately saline water to wells in McMullen and La Salle Counties. Catahoula sandstones lying directly below Oakville sandstones are included in the Oakville aquifer.

Jasper Aquifer—The Jasper aquifer is relatively coarse grained near the outcrop and becomes finer grained downdip. Although pumpage from the Jasper aquifer is not significant, the aquifer is capable of yielding 3,000 gpm or more of water to wells in certain areas (Baker, 1986). Transmissivity of the Jasper aquifer ranges from less than 2500 ft^2/d to about 35,000 ft^2/d. Water in the Jasper aquifer downdip from the outcrop is discharged upward through the Burkeville Confining System. The effective vertical-hydraulic conductivity of the Burkeville Confining System is a function of composite intergranular flow characteristics of the predominantly silt and clay beds that compose this hydraulic unit. Vertical hydraulic conductivity ranges from 1.0×10^{-5} to 2.5×10^{-3} ft/d. In the GAM, average horizontal hydraulic conductivity of 0.5 ft/d; specific yield, 0.05; and storativity, 5.2×10^{-5} to 3.5×10^{-3} are used for the Jasper aquifer (Chowdhury et al., 2004), although actual values ultimately depend on location of the cell/sample within the depositional system. For example, the Karnes County uranium mining district falls within a sand-rich area that Galloway et al. (1982a) labeled as the New Davy Fluvial Axis. This axis abuts the George West Axis, which is thought to have been one of two principal areas of entry of a large river onto the Gulf Coastal Plain during the Miocene. Sand percentage ranges up to about 50% and decreases downdip, with remaining fractions composed of silt and clay. Distribution of high sand percentage areas is characterized by sinuous, interweaving belts downdip, typically between 2 and 8 km in width. The most abundant sedimentary facies can be characterized as conglomeratic bedload and mixed-load channel fill, which features a wide range of coarse grain sizes (from sand to conglomerate), interspersed with clay-rich, fine-grained lenses locally. This complicated stratigraphic setup results in very heterogeneous, but overall highly transmissive, conditions in the aquifer. Harris (1965) reported that the Lagarto and Oakville Formations yield only small quantities (<50 gpm) of fresh to moderately saline water to wells in La Salle and McMullen Counties.

Evangeline Aquifer—The Evangeline aquifer is similarly variable with respect to transmissivities because of its fluvial depositional history. Huge quantities of water were pumped from the Evangeline aquifer for municipal supply, industrial use, and irrigation in some areas. Large-capacity wells yield from 1,000 to more than 3,000 gpm and average about 2,000 gpm in the Houston area (Baker, 1986). The Goliad Formation unconformably overlies the Soledad Volcanic Conglomerate Member of the Catahoula Formation in the study area. The Goliad is composed of fine- to coarse-grained sand and sandstone, which in many areas contains gravel interbedded with silty and sandy clay and clay. Anders and Baker (1961) reported that generally the Goliad Sand contains the highest quality water of any formation in Live Oak County except the Carrizo Sand. Water from the Goliad Sand is fresh to moderately saline and commonly rather hard, and it contains appreciable quantities of sodium (Anders and Baker, 1961). The rocks of Goliad and younger age yield very small amounts of water (<10 gpm) to a large number of domestic and stock wells in Live Oak County. The formation also yields large volumes of water to a few irrigation wells. In general, the Goliad Sand is capable of yielding 500 to more than 1,000 gpm to properly constructed wells where 100 ft or more of the formation is saturated (Anders and Baker, 1961). Londsdale and Day (1937) reported that a ranch located southwest of Bruni had seven wells reported to have yielded 120,000 gpd (5,000 gpm) by 1937. Windmills yielded 2 to 20 gpm from the Goliad Formation, whereas industrial supply wells yielded 35 gpm (Adidas, 1991). In the GAM models (Chowdhury et al., 2004), horizontal hydraulic conductivity calibrated ranges from 1.25 to 2.5 ft/d, and vertical hydraulic conductivity from 1.1×10^{-8} to 2.1×10^{-4} ft/d. Specific yield is 0.001, and storativity ranges from 1×10^{-6} to 3.5×10^{-3}.

According to Carr et al. (1985) transmissivity values vary from 3,000 to 12,000 ft^2/d in the Evangeline aquifer. Ryder (1988) assigned a constant hydraulic conductivity of 60 ft/d to the lower Pliocene-upper Miocene permeable zone (Evangeline aquifer) to calibrate his predevelopment model. Hay (1999) assigned much lower hydraulic conductivity values to calibrate his model than what was previously used in the Gulf Coast aquifer (0.4 to 7 ft/d for the Evangeline aquifer). The model was verified using water levels and pumpage data for 1985. A lower hydraulic conductivity required a lower annual recharge rate of 0.078 inches. Vertical hydraulic conductivity in a sand aquifer is controlled primarily by low-permeability clay lenses contained within a sand sequence. Estimated vertical hydraulic conductivity is highly variable (10^{-7} to 1 ft/d) in the GCAS in the Houston area (Jorgensen, 1975). In a regional study of the entire Gulf Coast aquifer, Ryder (1988) calibrated vertical hydraulic conductivities that range from 1×10^{-5} ft/d for a confining unit to 1×10^{-2} ft/d for the four aquifers and permeable zones. In a more localized study of Matagorda and Wharton Counties, Dutton and Richter (1990) used calibrated vertical hydraulic conductivity values of 2.27×10^{-5} to 2.63×10^{-1} ft/d (mean = 5.58×10^{-4} ft/d) for the Evangeline aquifer.

Storativity values of the Evangeline aquifer range from 0.0005 to about 0.1 (Carr et al., 1985). Meyer and Carr (1979) reported storativity values that range from 0.001 to 0.01 in the unconfined areas and 0.0004 to 0.001 in the confined areas of the Evangeline aquifer. Dutton and Richter (1990) reported a much lower range of storativity for the Evangeline aquifer in Matagorda and Wharton Counties (6.28×10^{-6} to 8.89×10^{-1}). Chowdhury and Mace (2007) reported that the hydraulic conductivity of the Gulf Coast aquifer in the Lower Rio Grande Valley is nearly log-normally distributed. Hydraulic conductivity from specific-capacity tests for the GCAS has a geometric mean of 11 ft/d (TCEQ data, 720 data points) to 15 ft/d (TWDB data, 77 data points). The geometric mean of hydraulic conductivity from these two combined sources is 3 ft/d for the Evangeline aquifer. Pumping tests result in higher hydraulic conductivity values in the Rio Grande Alluvium section of the Chicot aquifer. Chowdhury and Mace (2007) used a semivariogram to determine spatial correlation of hydraulic conductivity. A semivariogram is a measure of the spatial correlation of a parameter. Samples taken close together are typically more alike than samples separated by larger distances. The semivariogram represents this change in variance with increasing separation distance. Chowdhury and Mace (2007) reported a range of 50,000 ft, a nugget of 0, and a sill of 0.5 (units of $[\log(ft/d)]^2$) for the hydraulic conductivities of the Evangeline aquifer using a spherical theoretical semivariogram that fits the experimental variogram. *Sill* defines the variance, *range* is the distance at which the variogram reaches the sill, and *nugget* is caused by errors in the data owing to measurement value, location assigned, or lack of data. In addition they suspected that the poor to moderate spatial correlation of hydraulic conductivity is controlled primarily by heterogeneity of the aquifer material commonly encountered in a fluvial-deltaic depositional sequence.

Chicot Aquifer—Transmissivity values range from 3,000 to 18,000 ft^2/d in the Chicot aquifer in the Houston area (Meyer and Carr, 1979). In a later report, Carr et al. (1985) also found similar transmissivity values (3,000 to 25,000 ft^2/d in the Chicot aquifer). Ryder (1988) assigned a constant hydraulic conductivity of 170 ft/d to the Holocene-upper Pleistocene permeable zone (upper Chicot aquifer), and 20 ft/d to the lower Pleistocene-upper Pliocene permeable zone (lower Chicot aquifer). Chowdhury and Mace (2007) observed that the geometric mean of hydraulic conductivity is 18 ft/d for the Chicot aquifer. Pumping tests result in higher hydraulic conductivity values in the Rio Grande Alluvium section of the Chicot aquifer. They also found a range of 65,000 ft, a nugget of 0.2 (units of $[\log(ft/d)]^2$), and a sill of 0.25 (units of $[\log(ft/d)]^2$)

for the hydraulic conductivities of the Chicot aquifer using a spherical theoretical semivariogram to fit the experimental variogram. Storativity of the Chicot aquifer ranges from 0.0004 to 0.1 (Meyer and Carr, 1979; Carr et al., 1985). Dutton and Richter (1990) reported a slightly higher range of storativity values in the Chicot aquifer in Matagorda and Wharton Counties (3.11×10^{-2} to 2.39×10^{-1}).

V-2-3 Recharge

Most recharge to the GCAS is by infiltrating rainfall and losing streams, occurring mostly in outcrop zones of the respective units, as well as possibly through irrigation return flow. Downdip of the outcrop zone, aquifers become confined, and little if any recharge is received from overlying units, although interaction among aquifer units is possible through fractures or locally absent confining units. The regional groundwater-flow conceptual model allows for recharge from below, although as upward leakage from underlying aquifers.

Accurate computation of recharge is notoriously difficult but is related in a complex way to precipitation amount (Figure 16), evaporation (Figure 20), and other factors. Different researchers have generated vastly different values, varying by more than one order of magnitude. Relatively small outcrop areas of the Jackson, Catahoula, and Jasper aquifers limit the amount of recharge compared with the much wider Goliad outcrop. However, an intense calichification may prevent much recharge from reaching the aquifer. Chowdhury et al. (2004, Section 1.3) reviewed recharge estimates to the GCAS. They vary from about 0.1 to 4 inches/yr. Table 8 provides more detailed information.

V-2-4 Discharge and Pumping

Natural discharge is through base flow to streams, rivers, and springs through evapotranspiration from phreatophytes whose roots reach the water table and through leakage to overlying layers. Relatively distributed pumping includes domestic wells that follow population density (Figure 8), to which irrigation wells must be added, leading to a rather high density of water wells (Figure 45). Domestic wells generally tap the shallowest fresh-water unit, whereas large irrigation wells can extend deeper to more productive horizons. Large water withdrawals operating for extended periods create regional cones of depression clearly visible on regional maps (as opposed to local drawdown resulting from a few wells or a single well), particularly in the confined section of the aquifer. When deep, a cone of depression can be transmitted to the next overlying or underlying aquifer, albeit attenuated. Once pumping is reduced or stops, the aquifer recovers and water levels rebound. The Evangeline aquifer displayed two such cones of depression in 1989 in Kleberg and Victoria Counties, with a smaller third one on the Jim Wells/Kleberg County line, as a result of industrial pumping from a local refinery (Chowdhury et al., 2004, Fig. 7). The Victoria cone had recovered by 1999, but that of Kleberg County, centered in the City of Kingsville, is still prominent (Chowdhury et al., 2004, Fig. 9), although it has decreased from 200 to 150 ft. The overlying Chicot aquifer also showed two cones of depression in 1989 in Jim Hogg and Jackson/Matagorda Counties (Chowdhury et al., 2004, Fig. 6). Recovery was mostly complete by 1999 (Chowdhury et al., 2004, Fig. 8). Less to no pumping occurs in the confined section of the Jasper aquifer because water quality decreases rapidly downdip (Chowdhury et al., 2004, p. 25).

Most pumping occurs for irrigation, and it is consequently skewed toward the summer months. Maps of pumpage in 1999 (Figure 51 and Figure 52) show that most pumping is in surficial

aquifers (Evangeline and Chicot) and very little in underlying formations and then mostly in the outcrop area. However, overall, compared with the amount extracted from the same aquifers farther north, the STU Province experiences relatively little pumping. In addition to a lower population density, the water is often brackish (Figure 53).

V-2-5 Water Types, Major Element Distribution, and Chemistry

Aquifer subunits of the GCAS are, from oldest to youngest, the Jasper, Evangeline, and Chicot aquifers. Older, relevant, water-bearing formations include the Catahoula Formation and those of the Jackson Group. A high-level TWDB report (LBG-Guyton & Associates, 2003) presents salinity distribution of major and minor aquifers in Texas (Figure 53). TDS thresholds of 1,000, 3,000, and 10,000 mg/L are approximately contoured. The fresh-water zone for the Jasper aquifer does not extend very deep, and this observation confirms statements made in the previous sections on the Evangeline aquifer (Goliad Sands) being the large-yield aquifer of the STU Province. The same LBG-Guyton & Associates (2003) report also presents results on the Yegua-Jackson aquifers, although without a cross section in the area of interest. Given the maps presented, however, in the STU Province footprint, water quickly becomes brackish in the downdip area in these formations or sometimes even in the outcrop area. Additional information on water quality can be found in USGS reports (Wesselman, 1983; Pettijohn, 1988; Pettijohn et al., 1988) and in a Core Laboratories Inc. (1972) report. The latter provides maps of salinity of upper and lower Gulf Coast formations but relies only on depth interval, not formation. The GAM reports also discuss groundwater quality in general terms.

When aquifer TDS needs to be mapped from actual field data, it is sometimes difficult to reconcile well depth and aquifer. The TWDB has a list of seven- to eight-character aquifer codes for most water-bearing units in Texas (Nordstrom and Quincy, 1999; recently revised as Rein and Hopkins, 2008). These codes were defined using either rock- or hydrostratigraphic-unit names. Of the wells sampled for arsenic by TWDB, each of the three aquifer subunits of the GCAS (Jasper, Evangeline, and Chicot) contains as many as eight different aquifer codes. Geologic and hydrologic units that compose the GCAS vary in name and character and are not consistently identified from one area to another. For example, two wells near La Gloria, Texas, in Starr County that were drilled 1 yr apart have the same total depth and are separated horizontally by only 50 m. One of the wells has an aquifer designation of 122OKVL (Oakville), which is in the Jasper aquifer, whereas the other well is labeled 121EVGL, which is in the Evangeline aquifer (R. Smyth, BEG, personal communication).

Groundwater chemistry is quite variable (but within some general limits, as indicated by the Piper plot of Figure 54) and generally reflects the water-rock interaction that has occurred since recharge. Groundwater of the GCAS is generally of Ca-HCO_3, Ca-Na-HCO_3-Cl, or Na-HCO_3 hydrochemical facies (Chowdhury et al., 2006). In outcrop areas, bicarbonate HCO_3 is frequently the most abundant anion, indicating the strong influence of carbonates. Mining areas and subeconomic mineralization do not seem to impact regional hydrochemistry. Other parameters are at play, particularly depth (deep/shallow) and depositional systems. Several panels in Figure 55 display the spatial distribution of TDS: for all formations combined (panels a and b) and for each of the Yegua-Jackson, Catahoula, Jasper, Evangeline, and Chicot aquifers (panels c to f). The maps show the extent of brackish water in all aquifers and the transitioning to fresher water north of the study area for all aquifers. As noted earlier, only the Evangeline aquifer seems suitable as a large-yield fresh-water source. The most recent groundwater-sample analysis was

used to draw the maps and no time-series analysis was done. The overall brackish nature of shallow aquifers in the STU Province suggests poor flushing and possible buildup of toxic elements.

Typical downflow evolution follows a common pattern for most GCAS: from calcium to sodium and from bicarbonate to chloride with an increase in TDS. Geochemical processes are: (1) cation exchange on clays of calcium for sodium, (2) leaching of chloride from sediment, and (3) mixing with connate water or with water discharging from underlying formations. The chemical pattern is modified by the permeability of the formation, with low-TDS water extending farther downdip along fluvial channels. In the southwestern Gulf Coast, geochemical evolution reflects the impact of both Ca/Na cation exchange on clay and fault discharge, possibly from different depths. Following a pattern similar to that of TDS, Eh conditions vary from strongly oxidizing in the recharge area (470 mV) to reducing farther downdip (-170 mV), with variations due to conductivity changes and proximity to faults. The decrease is not progressive but moves through plateaus at about 400, 50 and 100 mV (Galloway, 1982a, p. 21 and his Fig. 18). Values of pH increase more or less regularly from about 7 to 8. In another example, the modern Catahoula Formation (Gueydan segment) seems to be directly impacted by sodium-chloride brines even in the shallow subsurface, and the typical pattern described earlier is not developed in this formation. Gates et al. (2008, 2009) studied a sampling transect across Karnes and Goliad Counties sampling shallow groundwater in the Catahoula, Jasper, and Evangeline aquifers (Figure 54). Although the studies focus on arsenic distribution, they also examine major geochemical processes taking place in the aquifers. Consistent with results from earlier authors, they include carbonate and silicate weathering, as well as cation exchange.

The following paragraphs detail water quality by aquifer. Note that presence of brackish water does not necessarily translate into nonusable water. Slightly brackish waters are considered a resource across Texas, especially in dry climates such as those in South Texas, and are good candidates for inland desalination (Kalaswad and Arroyo, 2006).

Jackson Group: Jackson Group aquifers have a relatively high TDS in the STU (but the water is fresher toward the north), even in the outcrop area where it is often >3,000 mg/L (Pettijohn et al., 1988; LBG-Guyton & Associates, 2003, p. 136) seemingly erratically (Preston, 2006, p. 54).

Catahoula Formation: The Catahoula Formation in southwest Texas has relatively high TDS, attributed to the impact of deep water, except in sandy lobes following major depositional sandy channels (Galloway and Kaiser, 1980, p. 25). Current water composition of the Catahoula Formation is dominated by sodium-bicarbonate-chloride- and sodium-chloride-type water (Galloway and Kaiser, 1980, p. 19). High chloride content in the shallow subsurface suggests the long-term influence of deep brines mixing with recharging waters. The formation pH varies from neutral to alkaline, with values locally >10 in ash beds (Galloway and Kaiser, 1980, p. 27). Large areas enriched in chloride, sulfate, and sodium result from mixing with deeper water brought up from deeper horizons by faults associated with the Wilcox Trend (Figure 39).

Oakville Sandstone / Jasper Aquifer: The Oakville Sandstone / Jasper aquifer is typical of GCAS. A thin, oxidizing recharge zone is in the formation outcrop, whereas groundwater slowly becomes more reducing downdip. In the southwestern Gulf Coast area, the Oakville Sandstone, between 100 and 200 m thick in the outcrop (Smith et al., 1982a), consists of sandy deposits from several major fluvial systems and grades downdip into finer deposits. Axes of higher transmissivity, such as George West in Live Oak County, include most of the uranium mines.

TDS in the Oakville are generally in the brackish range (>1,000 mg/L) because of the impact of fault discharge (Smith et al., 1982a, p. 10) except in the outcrop area and initially along high-transmissivity zones. High concentrations of sulfate and chloride are associated with those faults (Figure 39, Wilcox Fault Zone, and Figure 2 of Henry et al., 1982a). Sulfate could also originate from dissolution of evaporites locally present in playa-floodplain facies (Henry et al., 1982a). In the northeastern Gulf Coast, the same aquifer does not show such high TDS and remains mostly below 1,000 mg/L (Henry et al., 1982a). Hydrochemical facies evolution ranges from calcium bicarbonate in the recharge zone to sodium bicarbonate chloride farther downdip, with a strong sulfate component (Smith et al., 1982a, p. 13–14) in the southwestern Gulf Coast, whereas in the northeastern Gulf Coast, the hydrogeochemical composition is in the sodium bicarbonate range. Henry et al. (1982a) also postulated that some high chloride concentration may be due to evaporites from uncommon playalike deposits.

Burkeville Confining System: Water quality in the Burkeville Confining System (mostly Lagarto Clay) is variable. Anders (1963) stated that, in Karnes County, sand bodies in the outcrop area contain fresh water sometimes tapped for domestic use, but elsewhere the water is mostly slightly brackish (>1,000 and <3,000 mg/L).

Goliad Sands / Evangeline Aquifer: The Evangeline aquifer represents an important source of fresh water in South Texas, as illustrated by pumpage data (Figure 52), and is mostly fresh to a depth of >1,000 ft, particularly along depositional features such as dip-oriented fluvial channels.

Table 7. List of TWDB county-level groundwater resources reports in the study area

County	Reference	USGS/TWDB Report
Aransas	Shafer (1970)	Report 124
Atascosa	Lonsdale (1935); Sundstrom and Follett (1950); Alexander and White (1966)	USGS Water Supply Paper 676; USGS Water Supply Paper 1079; Report 32
Bee	Myers and Dale (1966)	Report 17
Brooks	Myers and Dale (1967)	Report 61
Calhoun	Marvin et al. (1962)	Bulletin 6202
De Witt	Follett and Gabrysch (1965)	Bulletin 6518
Duval	Sayre (1937); Shafer (1974)	USGS Water Supply Paper 776; Report 181
Goliad	Dale et al. (1957)	Bulletin 5711
Gonzales	Shafer (1965)	Report 4
Jackson	Baker (1965)	Report 1
Karnes	Anders (1960); Anders (1963); Alexander et al. (1964)	Bulletin 6007; USGS Water Supply Paper 1539; Bulletin 6409
Kleberg	Livingston and Bridges (1936); Shafer and Baker (1973)	USGS Water Supply Paper 773; Report 173
Kenedy	Shafer and Baker (1973)	Report 173
Jim Hogg	No county-level report	
Jim Wells	Shafer and Baker (1973)	Report 173
Lavaca	Loskot et al. (1982)	Report 270
LaSalle	Deussen and Dole (1916); Harris (1965)	USGS Water Supply Paper 375; Bulletin 6520
Live Oak	Anders and Baker (1961)	Bulletin 6105
McMullen	Deussen and Dole (1916); Harris (1965)	USGS Water Supply Paper 375; Bulletin 6520
Nueces	Shafer (1968)	Report 73
Refugio	Mason (1963)	Bulletin 6312
San Patricio	Shafer (1968)	Report 73
Starr	Dale (1952)	Bulletin 5209
Victoria	Marvin et al. (1962)	Bulletin 6202
Webb	Lonsdale and Day (1937); Lambert (2004)	USGS Water Supply Paper 778; USGS SIR 2004-5022
Wilson	Anders (1957)	Bulletin 5710
Zapata	No county-level report	

Note: Most of these reports are available on the USGS or TWDB website (last accessed March 2009) http://pubs.er.usgs.gov, http://www.twdb.state.tx.us/publications/reports/SGWReports.asp or http://www.twdb.state.tx.us/publications/reports/GroundWaterReports/bulletins/Bulletins.asp; there are also many older records of wells, test-well and drillers' logs, etc., from before WWII at http://www.lib.utexas.edu/books/landscapes/texa.php.

Table 8. Recharge rates in the study area

Location (County/Area)	Aquifer	Recharge rate (in/yr)	Reference	Technique
Matagorda, Wharton	Beaumont, Chicot, Evangeline	0.0–0.4	Dutton and Richter, 1990	Groundwater modeling
Duval, Jim Wells	Evangeline	0.1	Groschen, 1985	Groundwater modeling
Aransas, Bee, Brooks, Calhoun, De Witt, Duval, Goliad, Hidalgo, Jackson, Jim Hogg, Jim Wells, Karnes, Kenedy, Kleberg, Lavaca, Live Oak, McMullen, Nueces, Refugio, San Patricio, Starr, Victoria, Webb, Willacy	Chicot, Evangeline, Jasper	0.0004–0.12	Hay, 1999	Groundwater modeling
Colorado, Lavaca, Wharton	Chicot, Evangeline	1.2–1.3	Loskot et al., 1982	Darcy's Law
Jim Wells	Evangeline	< 0.1	Mason, 1963	Darcy's Law
Brooks	Evangeline		Myers and Dale, 1967	Darcy's Law
Nueces, San Patricio			Shafer, 1968	Darcy's Law
Gulf Coast			Muller and Price, 1979	Groundwater modeling
Gulf Coast		0.7 (0.0–6.0)	Ryder, 1988	Groundwater modeling
Gulf Coast		0.0–0.7	Williamson et al., 1990	Groundwater modeling
Southern Gulf Coast GAM		0.09–0.15	Chowdhury and Mace (2004)	Groundwater modeling

Source: *recharge_rates.xls* at http://www.twdb.state.tx.us/gam/resources/resources.htm, complemented by GAM data

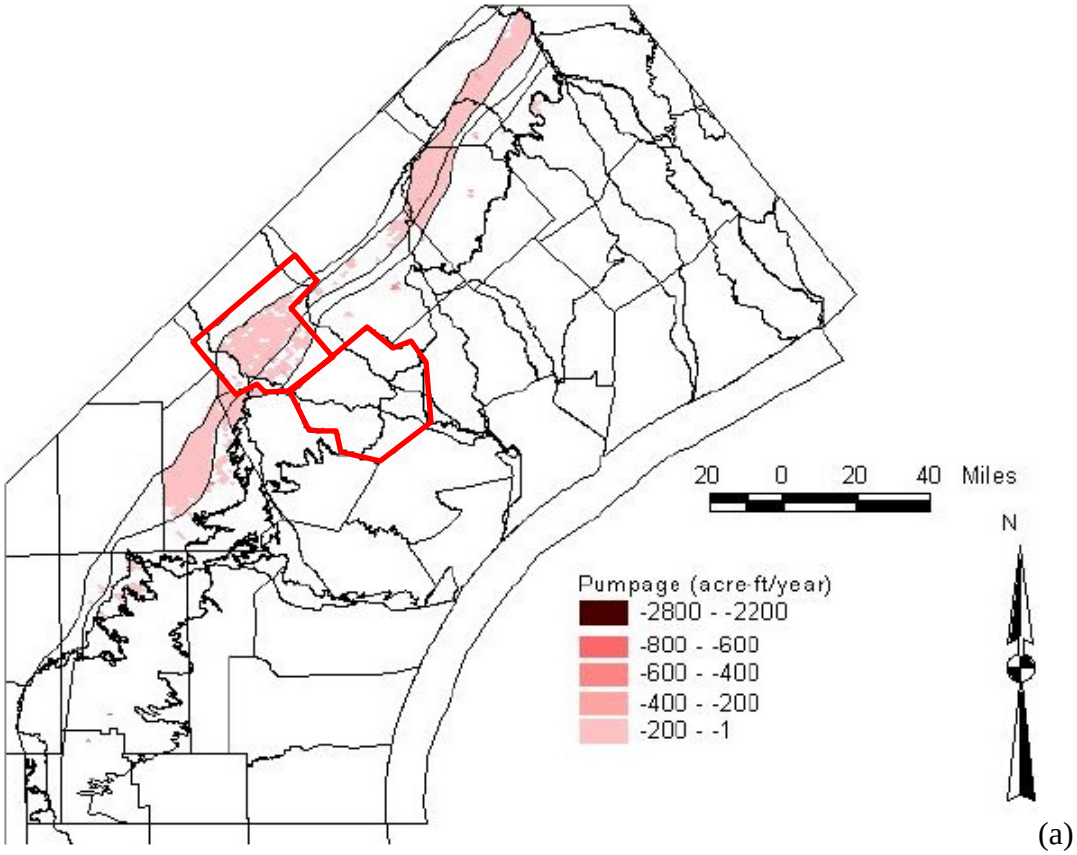

(a)

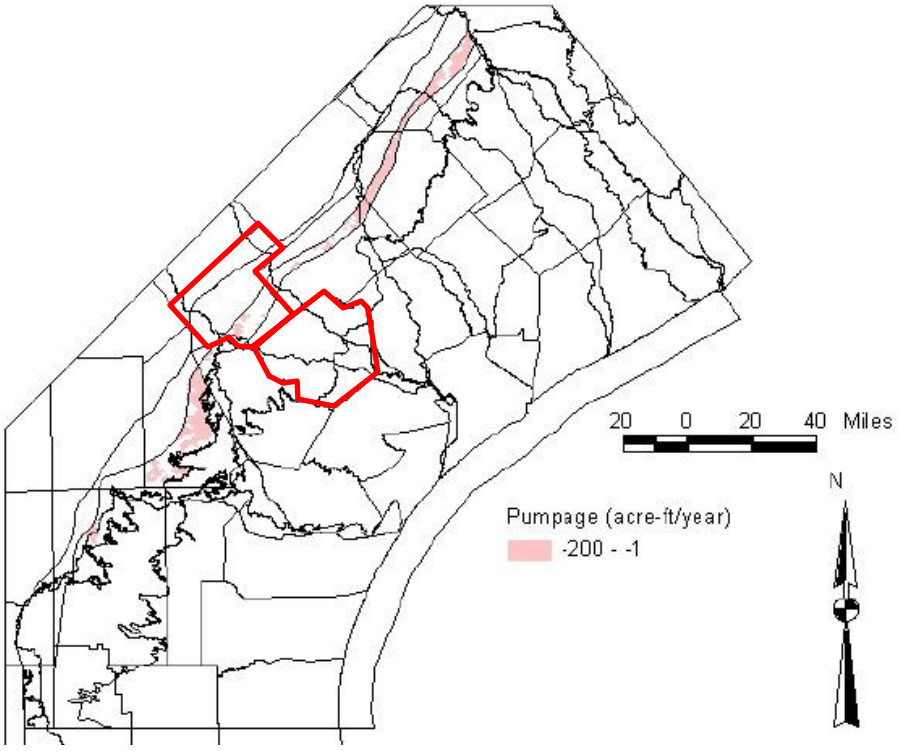

(b)

Source: Chowdhury et al., 2004, Figs. 19 and 20

Figure 51. Groundwater pumpage distribution (year 1999) in the (a) Jasper aquifer and (b) Burkeville Confining System; Karnes and Goliad Counties outlined in red

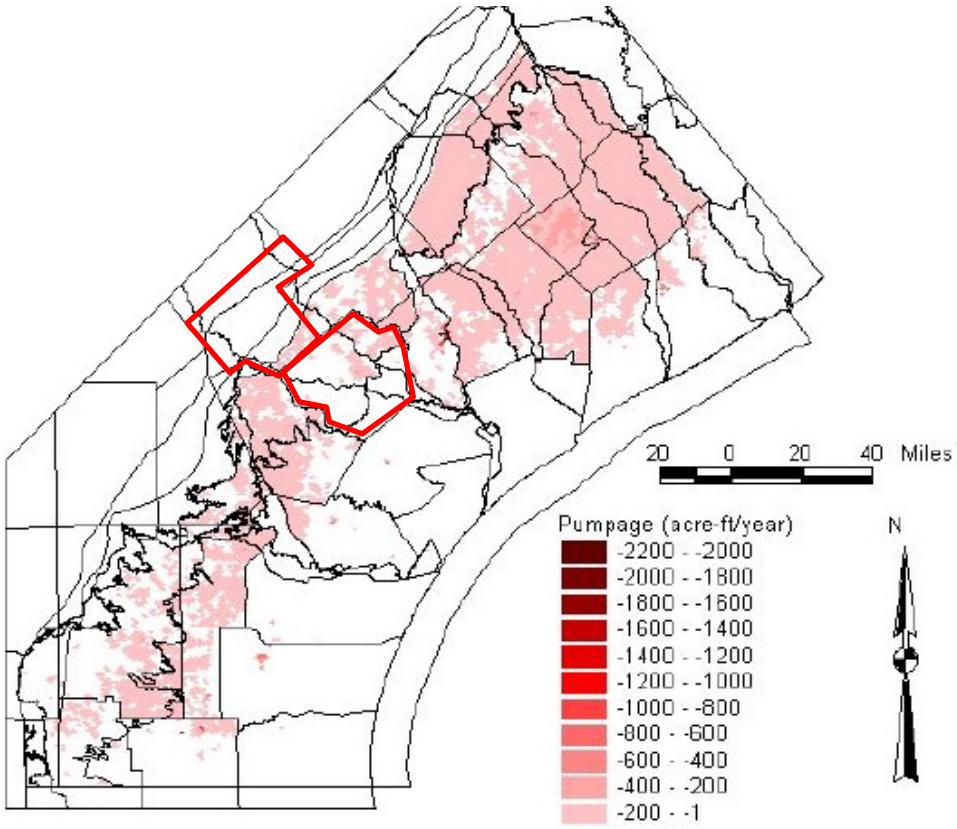

(a)

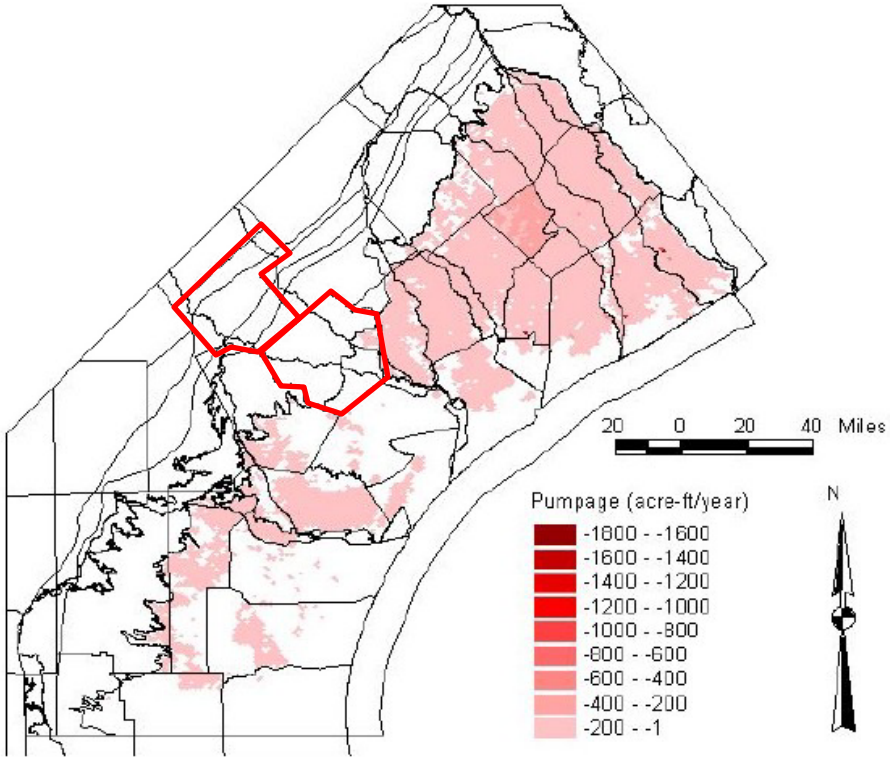

(b)

Source: Chowdhury et al., 2004, Figs. 17 and 18

Figure 52. Groundwater pumpage distribution (year 1999) in the (a) Evangeline aquifer and (b) Chicot Confining System; Karnes and Goliad Counties outlined in red

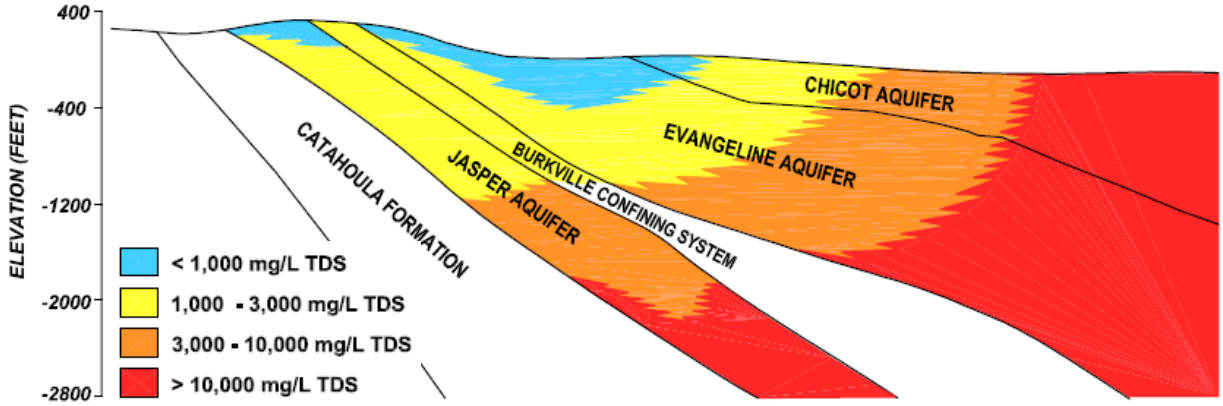

Source: LBG-Guyton & Associates (2003, Fig. 28); cross section initially from Baker (1979)
Note: Section length is approximately 100 mi.

Figure 53. Idealized NW-SE cross section of Live Oak and San Patricio Counties to the coast showing TDS variations along profile and with distance

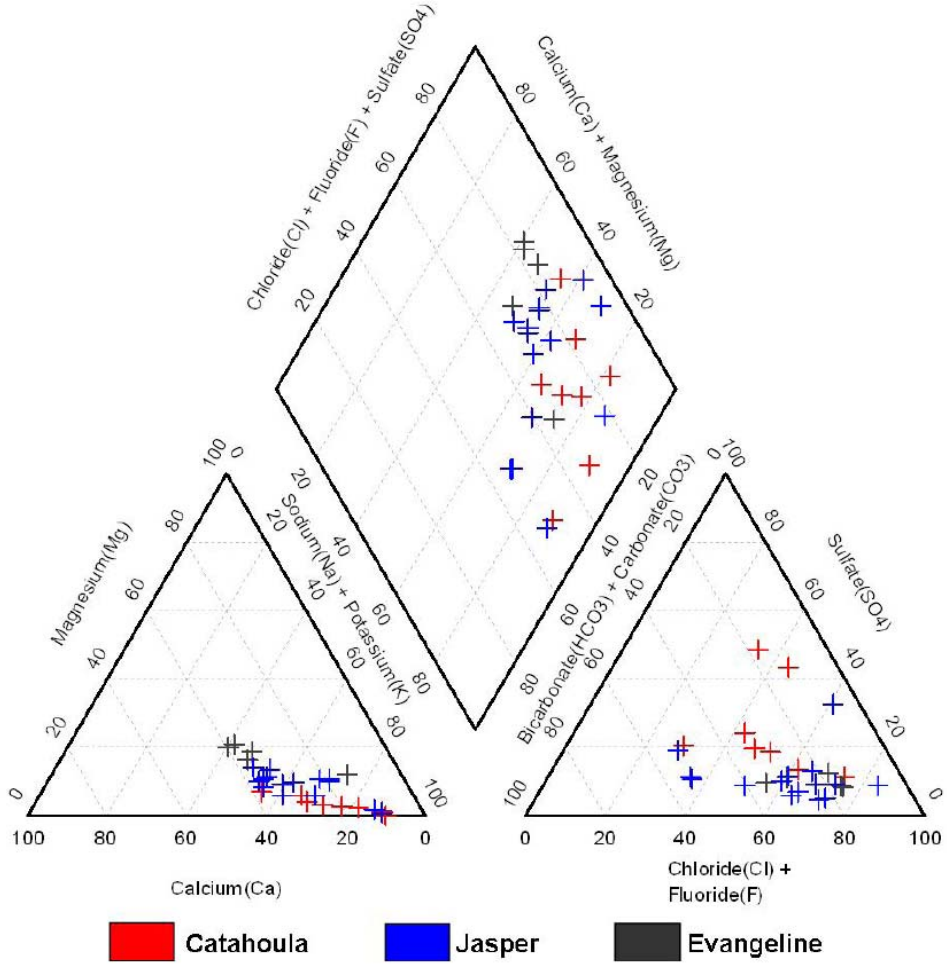

Source: Gates et al. (2009)

Figure 54. Piper plot of groundwater samples from a transect across Karnes and Goliad Counties

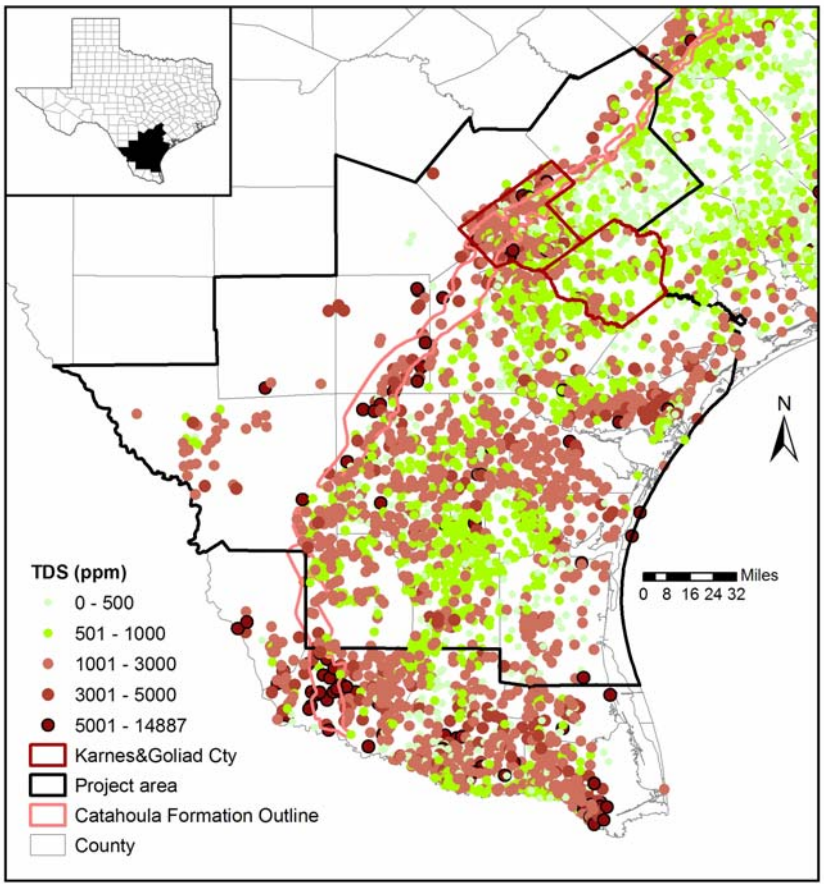

(a)

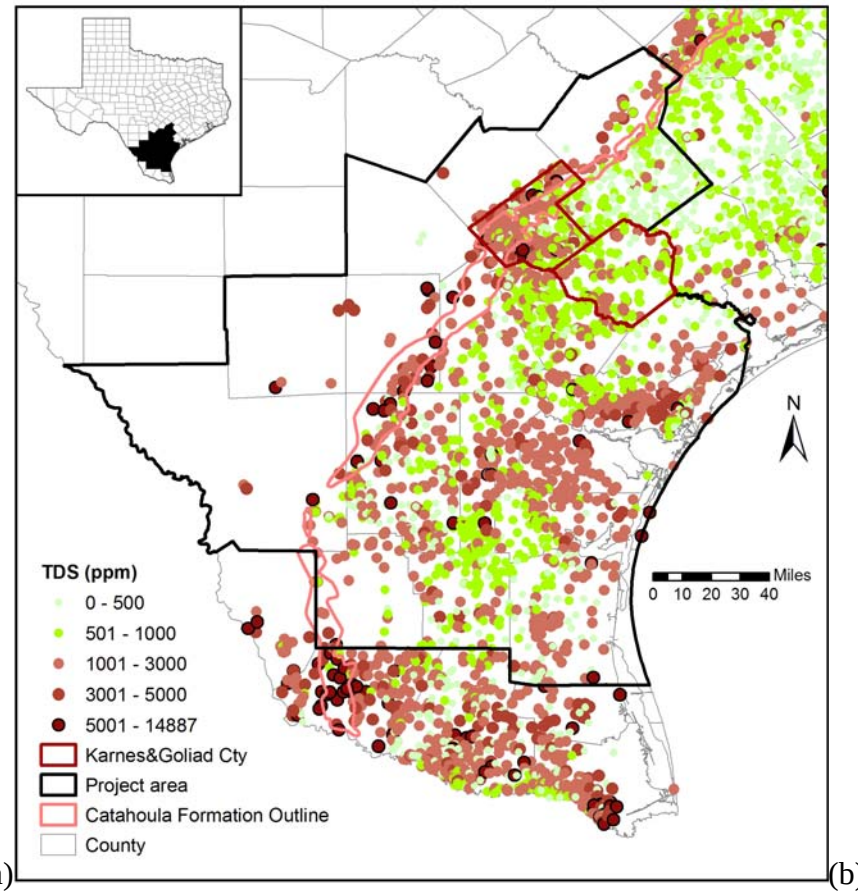

(b)

Source: TWDB database (downloaded Feb. 2009) and NURE database for (a)

Figure 55. TDS distribution in aquifers of the STU province: (a) all aquifers TWDB and NURE databases; (b) all aquifers (TWDB database only); (c) Yegua-Jackson aquifers; (d) Catahoula aquifers; (e) Jasper aquifer; (f) Evangeline aquifer; and (g) Chicot aquifer.

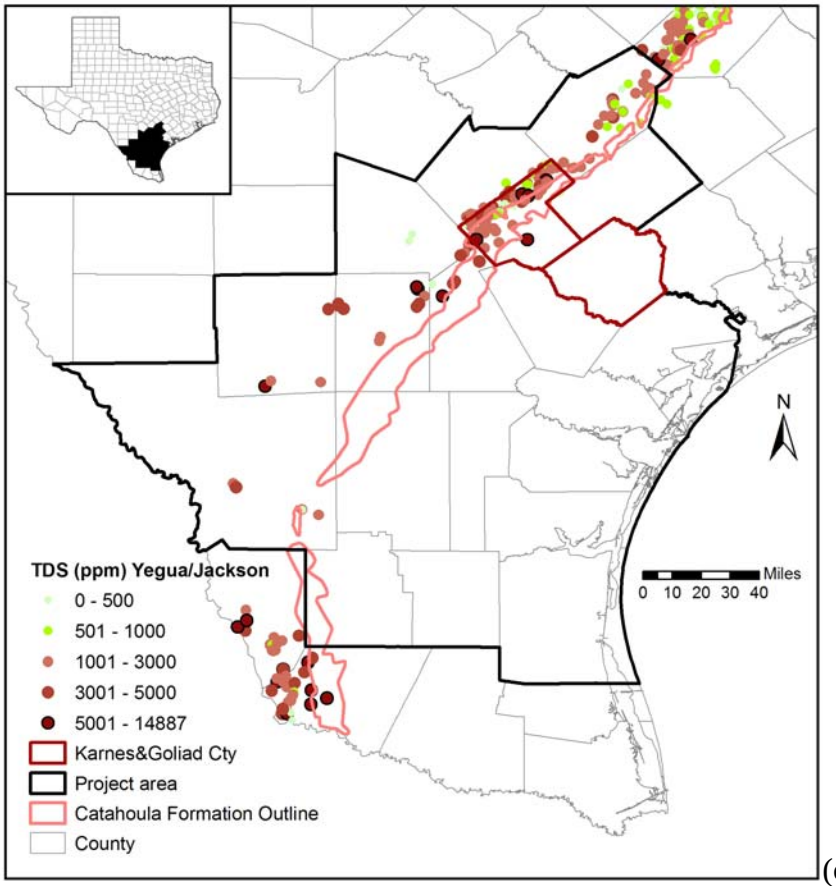

(c)

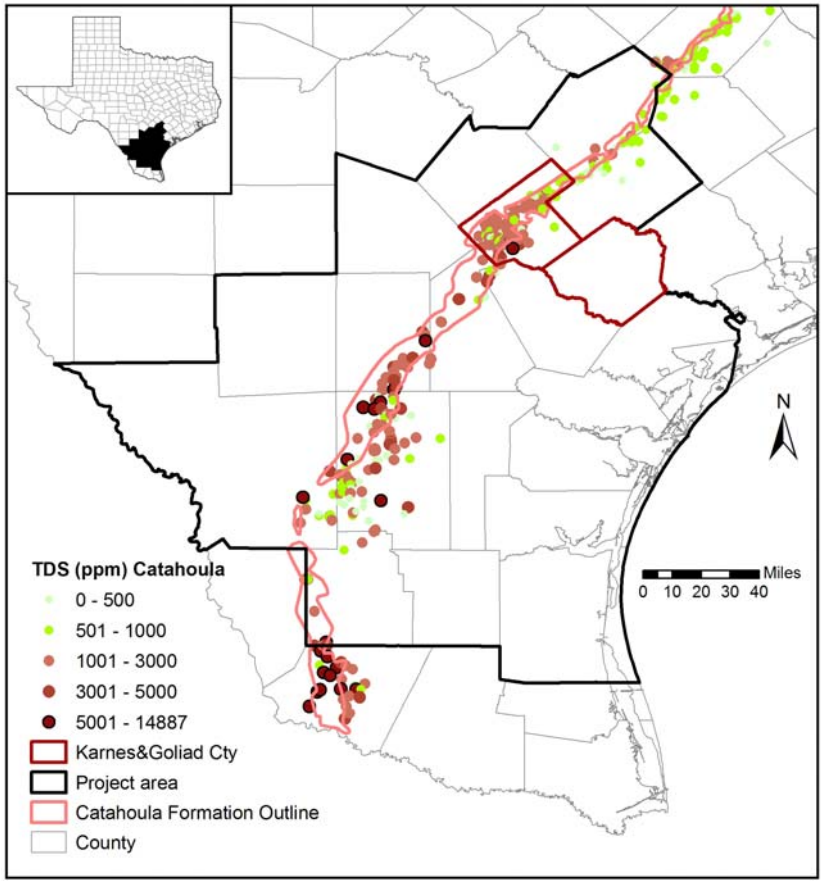

(d)

Source: TWDB database (downloaded Feb. 2009)

Figure 55. TDS distribution in aquifers of the STU province: (a) all aquifers TWDB and NURE databases; (b) all aquifers (TWDB database only); (c) Yegua-Jackson aquifers; (d) Catahoula aquifers; (e) Jasper aquifer; (f) Evangeline aquifer; and (g) Chicot aquifer

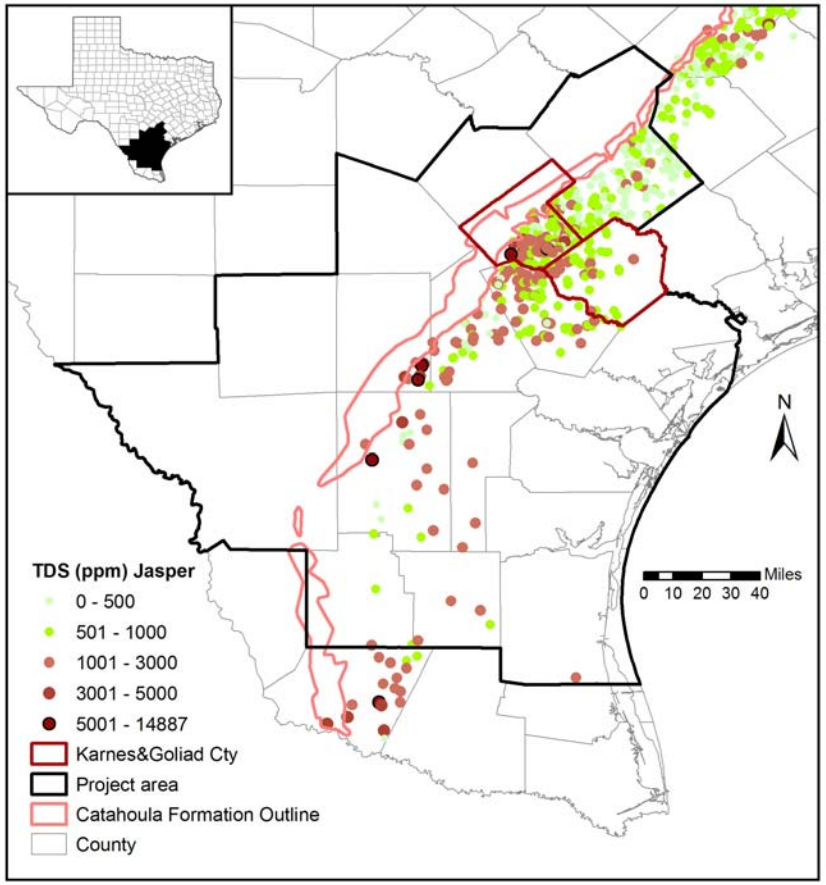

(e)

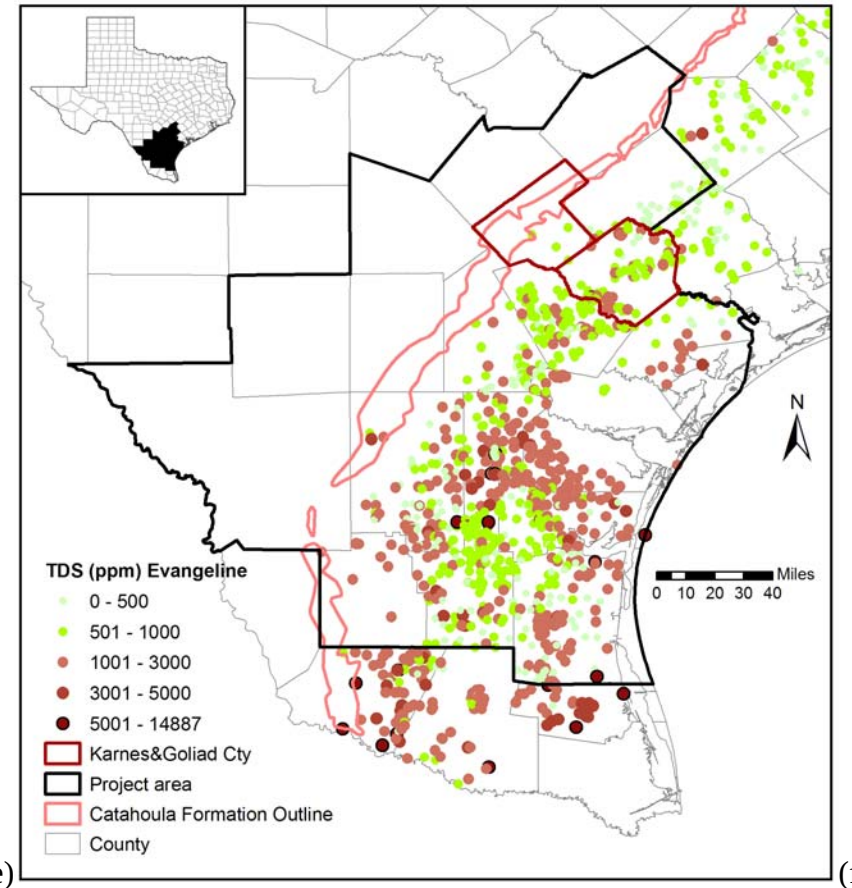

(f)

Source: TWDB database (downloaded Feb. 2009)

Figure 55. TDS distribution in aquifers of the STU province: (a) all aquifers TWDB and NURE databases; (b) all aquifers (TWDB database only); (c) Yegua-Jackson aquifers; (d) Catahoula aquifers; (e) Jasper aquifer; (f) Evangeline aquifer; and (g) Chicot aquifer

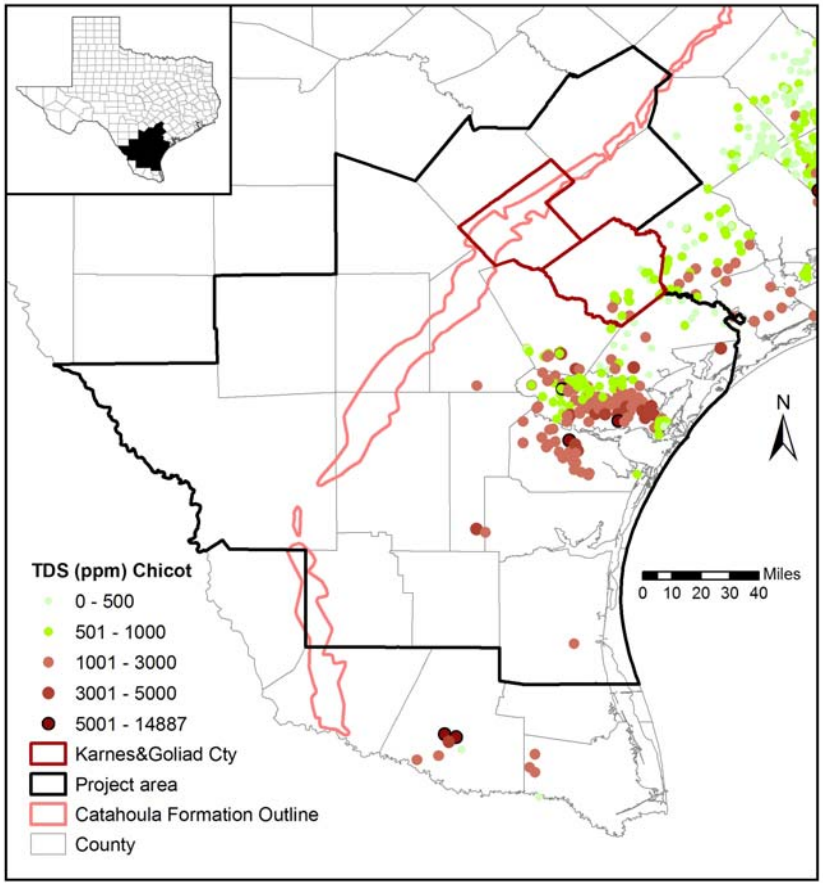

(g)

Source: TWDB database (downloaded Feb. 2009)

Figure 55. TDS distribution in aquifers of the STU province: (a) all aquifers TWDB and NURE databases; (b) all aquifers (TWDB database only); (c) Yegua-Jackson aquifers; (d) Catahoula aquifers; (e) Jasper aquifer; (f) Evangeline aquifer; and (g) Chicot aquifer

VI. Environmental Chemistry

This section summarizes information about mineralogy, chemistry, and ore-forming processes of the STU Province. Origin of STU Province deposits has been the topic of many publications. Little has been published on the STU since the end of commercial uranium production in the 1980's, however. Adams (1991) summarized the evolution of concepts of uranium deposits in the STU Province and elsewhere in the U.S. Note that hydrogeochemical characteristics prevalent during the active phase of uranium deposition may have been different from current characteristics. In fact, Miocene Catahoula waters were clearly very different from today's (Galloway and Kaiser, 1980, p. 18). Ash dissolution would lead to higher TDS overall, with high silica as well as a richness in calcium, sodium, bicarbonate, chloride, and sulfate, as opposed to the current composition of mostly sodium bicarbonate chloride.

VI-1. Overview of Uranium Ore-Body Formation

An understanding of STU Province uranium mineralization requires an understanding of the key process of redox reactions in aquifers, which are linked closely to current and paleoflow systems. As often observed in upper and lower Gulf Coast aquifers, maximum water flux corresponds to major channel / fluvial axes and extends farther downdip in tongues, leaving islands of lower permeability (and lower redox potential) within or between tongues. Depending on the water flux, the redox front may be moving downdip as fresh oxidized water continues to dissolve upstream portions of the reduced accumulation to precipitate it a little farther downdip—a process that can concentrate and disperse accumulations (both uneconomic and commercial). On the other hand, a limited water flux will be unable to move the front, which becomes essentially passive and fossilized. The general model of uranium mineralization involves a host rock deposited in oxidizing conditions reduced during diagenesis or later and invaded by uranium-rich oxidizing waters that precipitate at the redox interface as uraninite (UO_2) or pitchblende (amorphous UO_2) or coffinite ($USiO_4.nH_2O$). Both minerals contain tetravalent uranium [U(IV)], which is much less soluble than hexavalent uranium [U(VI)], the typical redox state of uranium in oxidizing conditions. Accessory metals include molybdenum, selenium, and arsenic. Vanadium is also present in the STU Province but in general did not precipitate. The common association of Mo, Se, V, As, and U is used in mining exploration (e.g., Rose and Wright, 1980). Other common ore-body minerals include marcasite, pyrite, clinoptilolite, clays, and calcite. Uranium minerals generally occur as grain coatings and fillings of intergranular spaces (e.g., Bomber et al., 1986); sorbed uranium increases as uranium grade decreases. Perhaps the mineralization begins as a sorption process exceeding the substrate capacity (TiOx, montmorillonite, organic debris) (Galloway and Kaiser, 1980, p. 54). The mineralized zone often appears as crescent- or C-shaped rolls in cross section, with the "nose" pointing down the hydraulic gradient—hence the name "roll-front deposit." However, it can have a sinuous, irregular shape in plan view following permeability and reducing-material patterns (Figure 56 and Figure 57). Normal faults provided fluids that reduced the host rock. Periodic discharge occurred from deep fluids through faults owing to compaction of deeper sediments in a dynamic basin (Galloway et al., 1979b, p. 130; Galloway, 1982a). Reynolds and Goldhaber (1983) suggested that some brines were enriched in sulfides coming from deep-buried sour hydrocarbons (e.g., at Benavides, Webb County), whereas other brines might have been rich in sulfate (and, presumably, hydrocarbons) that was then reduced by local microbial activity. These

fluids do not seem to be particularly enriched in metals (Galloway, 1982a, p. 19, 27). Abundant detrital titano-magnetite ($Fe_{3-a}Ti_aO_4$) / ilmenite ($FeTiO_3$) and hematite (αFe_2O_3) provided the iron source for generation of reduced pyrite (Goldhaber et al., 1978; Reynolds and Goldhaber, 1978). Ti oxides (anatase and rutile) are left behind (e.g., Bomber et al., 1986). Pyrite is required because depositional environments of the host sandstones are mostly fluvial, generally "clean," and they need the extrinsic reducing material brought up by the faults. For example, Goldhaber et al. (1978, Table 1) mentioned a very low organic carbon content (<0.16%) in the Benavides, Webb County, ore samples. They also cited values of less than 0.1% for deposits in Karnes and Live Oak Counties. However, some sands deposited in floodplains or barrier lagoons (particularly formations of the Jackson Group—Ilger et al., 1987) often contain abundant carbonaceous material (or diagenetic pyrite following bacterial use of the organic matter) (Reynolds et al., 1982; Maynard, 1984). Reynolds et al. (1982) reported an average value of 0.42% for the Panna Maria deposit hosted by Jackson Group rocks. Pyrite of microbial or abiotic origin can be discriminated because it deviates in its shape (framboidal and euhedral) and isotopic sulfur composition (-20 to 0 permil and >10 permil) for diagenetic and pre-ore pyrites, respectively (Galloway and Kaiser, 1980, p. 39; Reynolds and Goldhaber, 1983). Ore-stage marcasite, another iron sulfide, is also generally present in deposits not containing organic matter. Deposit shapes are more complicated and less predictable in the Eocene Jackson Formation because they depend more on syndepositional organic-matter distribution.

Galloway and Hobday (1996) and Galloway (1982a, 1977) explained the process of forming uranium ore bodies in detail (Figure 56 and Figure 57). During the constructional phase (Figure 56), (1) uranium and other trace elements are released from updip interbedded or overlying material, mostly through pedogenesis of ash-fall material (either direct deposition or reworked by streams) in the unsaturated zone (Figure 58). Uranium and these trace metals are initially recaptured by sorbing processes but are now a lot more accessible than when trapped in the glass shards of the volcanic ash (Galloway and Kaiser, 1980, p. 14). (2) Some uranium is efficiently mobilized and moves along recharging water in the groundwater system. If it is locally discharged into drainage, it is lost to the system. (3) Otherwise, uranium moves downdip with oxidizing waters. (4) Uranium precipitates when it encounters reducing zones—for example, pods of organic material or boundaries with finer-grained material. In a second modification phase (Figure 57), mineralization is redistributed or further altered following (5) compaction and regional flow changes, including maturation to a fully confined system. Further changes can occur, such as (6) exposure of deposits to weathering as a result of erosion or invasion of parts of the aquifer by reducing reactive waters coming from deeper flow regimes.

Leaching—Uranium and associated trace elements are leached and mobilized from silicic volcanic rocks through a pedogenic process when the sediment is still porous and favorable to fluid flow (Smith et al., 1982b; Stewart et al., 2006). The ash undergoes extensive argillation and releases uranium and other trace elements in the process, then hexavalent U travels as a carbonate complex. Studies by Zielinski et al. (1980) and Walton et al. (1981), leaching experiments by Trentham (1981), and observations by Galloway et al. (1979a, p. 62) have shown that U is mobilized from volcanic ash under unsaturated conditions and that volcanic glass alters to smectite but that under saturated conditions volcanic glass transforms to zeolites, leading to much lower U mobilization. Contrasting Catahoula Tuffs and mostly alluvial volcanic sediments of far West Texas, Walton et al. (1981) demonstrated that uranium mobilization is commensurate with intensity of unsaturated-zone and pedogenic processes. Maynard (1984) insisted on the importance of unsaturated conditions because, according to this author, diagenetic reactions on

ash in the zone of saturation generally produce zeolites that typically sequester uranium. For example, the Jackson Formation has zeolitically altered tuffs (Adams, 1991, Table 4). Henry and Walton (1978, p.VII-10 to -13) detailed the different mineralogical changes of increasing alteration of ash-fall material. They hypothesized that volatiles sorbed on the glass pumice surface are the first to be desorbed. Uranium may be associated with these volatiles as UF_6 because of its affinity for fluoride. However, accepting that such a process could occur in more silicic ash, Walton et al. (1981) disputed this hypothesis for the Catahoula Tuff and suggested instead that congruent volcanic glass dissolution is the most likely mechanism. They then hypothesized that either uranium remained mobile over long distances or it was bound again to diagenetic and/or detrital minerals while remaining easily accessible so that it could be released more slowly. The unsaturated/saturated nature of the alteration determines the nature of the newly formed minerals and their ability to release uranium.

Galloway and Kaiser (1980) determined that paleosols in the Catahoula Formation have only about 50% of the U content relative to that of nonweathered sections of the formation at the time of deposition. A useful indicator of U leaching is the Th:U ratio—elements that are generally associated but because Th is rather immobile, it is not mobilized as U is leached (Dickinson, 1976; Rose and Wright, 1980). Initial U content of the Catahoula glass was >10 ppm (Galloway and Kaiser, 1980, p. 16), and about half was mobilized. Additional evidence of this lies in the contrast in uranium concentration between highly weathered paleosols (2 ppm on five samples) and the relatively unweathered lacustrine deposits of the same material (9 ppm in 22 samples) (Galloway and Kaiser, 1980, p. 15).

Deposition and Ore Body—Change from oxidizing to reducing conditions is generally recognized as the primary mineralization mechanism, but others, such as change in pH, can also concentrate uranium and molybdenum in particular (Galloway et al., 1982a, p. 31; Nicot, 2008). Trapping by zeolite minerals is another of these mechanisms, and these processes should not necessarily be a priori ruled out. Galloway and Kaiser (1980, p. 49) also tentatively described a small deposit in which uranium probably occurs as urano-organic complexes or sorbed but without a clear mineral phase. When the roll-front deposit is actively growing, uranium and other metals are constantly / periodically dissolved by incoming oxidizing waters, themselves charged, possibly, with uranium and precipitating slightly farther downdip as they encounter fresh reducing material (Figure 59). Although it varies, Osmond and Cowart (1981) estimated front migration on the order of 1 m in 10,000 to 100,000 yr at two New Mexico deposits.

Historical deposits were mined within the Jackson Group and Catahoula and Oakville Formations, not too far from the Catahoula Formation outcrop. However, uranium deposits also exist in the younger Goliad Sand Formation. Uranium Energy Corporation is developing an ISR operation in Goliad County near the intersection of Dewitt and Victoria Counties (Carothers, 2007, 2008), which is much farther east than all open-pit deposits. The presumed ore bodies are in the Goliad Formation. According to Carothers (2008), the ore bodies are not C shaped but, rather, tabular. Carothers (2008) hypothesized that the origin of the deposit may be similar to those of the Catahoula / Oakville Formations or a variation in which the source of uranium would be erosion of older deposits. Other deposits in the same Goliad Formation include several salt-dome-related deposits, such as the Kingsville Dome in Kleberg County (Arredondo, 1991) and the Palangana Salt Dome in Duval County (Blackstone, 2005). The latter deposit occurs at a depth of 250 to 400 ft, wrapping around the dome, which provided the reducing material, which

was most likely provided by leaking hydrocarbons or H_2S along the salt-dome edges or dome-related faults.

The Catahoula Formation records a peak in deposition in ash/tephra across the Gulf Coast but continued volcanic activity during the Miocene-deposited air-fall-ash sediments in the Oakville Formation. Deposits hosted in the Whitsett or Catahoula Formations could have been eroded and uranium remobilized under oxidizing conditions, as demonstrated by the existence of shallow (in modern times) deposits in the Jackson Group. This secondary origin of uranium is likely for deposits hosted by the Goliad Formation.

Postdeposition and Late Evolution—Some deposits (e.g., Ray Point district) are fossilized by secondary postore resulfidization, which overwhelms the redox front and oxidized tongue and stops the roll-front migration and, in essence, fossilizes it such in a way as is seen in Lamprecht and Felder in Live Oak County (Goldhaber et al., 1983). The latest sulfidization event has been dated at 5 m.y. at the Felder deposit in Live Oak County (Ludwig et al., 1982).

Deposits can also be exhumed or otherwise exposed to oxidizing conditions. Exposure by erosion of deposits previously confined in reducing conditions remobilizes the ore, with uranium redox state moving from tetra- to hexavalent and development of a more varied uranium mineralogy depending on local aqueous geochemistry (phosphates, vanadates, etc.) and other alteration minerals (limonite, jarosite). They were the earliest deposits discovered. In such a situation, secondary hexavalent minerals make up the bulk of the uranium-bearing phases—uranyl humates in the Jackson Group (Mohan et al., 1991). Autunite (hydrated calcium uranyl phosphate) is the most abundant secondary mineral (Bunker and MacKallor, 1973); tyuyamunite (hydrated calcium uranyl vanadate) and carnotite (hydrated potassium uranyl vanadate), although present, are not common because of the low vanadium concentration compared with that of other deposits in the American west. Uranophane (hydrated calcium uranyl silicate) is also common (Henry et al., 1982a, p. 18).

Individual deposits are described in a variety of mostly BEG and USGS reports (Table 9). Most deposits show a polarity Se-U-Mo that can be used to infer direction of (paleo)flow but, in general, discussion of As and V is lacking (except locally, e.g., in Galloway and Kaiser, 1980, p. 49; up to 1,510 ppm As is described). The most likely reason that As and V are not discussed may be that they remain soluble even under reducing conditions and typically precipitated from solutions only for more extreme reducing conditions than typically occur at the STU Province.

Paleohydrology—The paleohydrology differs from the current hydrology (Figure 60). Permeability of ash layers was much higher during metal mobilization before the ash was altered to mostly clays. Permeability of the sand was also likely higher (Adams, 1991). The syndepositional groundwater composition in the Catahoula Formation was likely oxidizing, slightly basic, and bicarbonate rich, with a relatively high TDS because of ash dissolution (Galloway and Kaiser, 1980, p. 19). The dissolved solid charge would have consisted of sodium, calcium, chloride, and sulfate, in addition to bicarbonate. Silica would likely have been high too. In such a chemical environment, uranium would be soluble as a uranyl-carbonate complex. Modern groundwater composition in the Catahoula Formation is described in Section V-2-5. It is dominated by sodium bicarbonate-chloride water and farther downdip by sodium-chloride water. Note that roll front is not impeding and is not a dam or barrier to flow (e.g., Guilbert and Park, 1986, p. 913), and the permeable sandstone pores are not plugged by mineralization.

Knowledge of paleohydrology is important for an understanding of the mineralization history of the STU Province. For example, source of uranium in the Jackson Group is unlikely to be interbedded volcanic layers because the Jackson Group was an area of general discharge at the time of its deposition and any mobilized uranium would have been flushed out of the system (and possibly accumulate in black shales farther out in the basin). Rather, Jackson Group mineralization results from mobilization of more recent Catahoula-age ash falls. Another example of the importance of paleohydrology is the observation that mobilized uranium needs to reach a reducing zone to precipitate. Presence of the Frio Clay prevented adequate fluid circulation and mineralization in the Jackson Group sandstones below it (Galloway et al., 1979a, p. 39). Jackson Group-hosted ore bodies in Karnes County exist only when the Frio Clay is absent (likely eroded). In addition, Jackson-hosted deposits are strike-elongated deposits following barrier-island cores (Cherepon et al., 2007) following main permeability zones. The opposite is true for younger formations where high-permeability axes are oriented along dip.

Current Processes—The ash-leaching process has ceased for a long time, modern waters contain little U, and typical shallow groundwater concentrations are not high enough to be ore forming (Galloway, 1982a, p. 29). However, uranium is still being mobilized and transported today in part of the formations with oxidizing conditions and where pH is at least slightly basic. Deposits can become disconnected from the main aquifer by faulting—for example, Ray Point (Galloway et al., 1979a, p. 76) or House-Seale (Galloway and Kaiser, 1980, p. 41)—and stop migrating and/or growing, a process called *entombment*. Understanding of disequilibrium conditions suggests that some roll fronts are still active. Deposits such as House-Seale (Galloway and Kaiser, 1980, p. 45) are disconnected from the general flow system, are in radiometric equilibrium, and, consequently, are dead/passive. Other accumulations in clear radiometric disequilibrium are most likely moving the front farther down flow or redistributing it (Galloway and Kaiser, 1980, p. 49).

The East Texas Case—The question often arises as to why East Texas does not have the same level of mineralization of uranium and trace metals as South Texas, despite similar geology. The most likely explanation was presented by Henry et al. (1982a, p. 46) and also by Huang (1978) and revolves around the concept of flushing and climate. Geological evidence suggests that contrasts between the climates in East and South Texas have not changed much since Eocene times: more humid and gaining streams in the east and drier and losing streams in the south. It follows that for an equivalent level of metal mobilization, most metal would flow directly to the ocean (where metals could be further concentrated but through other mechanisms) without encountering reducing conditions on land. It also follows that drier climate with thick unsaturated zones is more appropriate for uranium mobilization. According to Galloway and Hobday (1996), more humid climates are not as suitable because of the high organic activity generating reducing conditions at the surface and numerous opportunities for mobilized uranium to discharge into local streams. Ledger (1981) and Ledger et al. (1984) presented a similar case. McCulloh (1982) advanced the same arguments for Louisiana.

Summary—Uranium ore bodies exist in the STU Province because source, transport, and trapping mechanisms occur together. Thick sequences of air-fall volcanic ash provide the uranium, which is mobilized as a result of a relatively dry climate. Uranium is then precipitated when it encounters reducing material deeper in the section along a transmissive flow system.

Table 9. BEG and other references providing thorough description of specific mines and/or districts

Deposit/mine/district	**County**	**Reference**
Panna Maria	Karnes	Galloway et al. (1979a, p. 42) Reynolds et al. (1982) Reynolds and Goldhaber (1983)
Ray Point District	Live Oak	Galloway et al. (1979a, p. 68) Galloway et al. (1982a, p. 32) Galloway et al. (1982b, p. 162, 219) Galloway (1982a) Henry et al. (1982a, p. 28) Henry et al. (1982b, p. 23)
George West District	Live Oak	Galloway et al. (1982a, p. 38) Galloway et al. (1982b, p. 179, 216) Galloway (1982a) Henry et al. (1982a, p. 34) Henry et al. (1982b, p. 20)
Bruni/Benavides	Webb	Adidas et al. (1991) Reynolds and Goldhaber (1983) Galloway and Kaiser (1980, p. 35)
House-Seale	Live Oak	Galloway and Kaiser (1980, p. 41)
Lamprecht	Live Oak	Goldhaber et al. (1979) Fishman et al. (1982) Reynolds and Goldhaber (1983)
Felder	Live Oak	Reynolds et al. (1980) Fishman et al. (1982) Reynolds and Goldhaber (1983)
Franklin	Karnes	Cossey and Frank (1983)

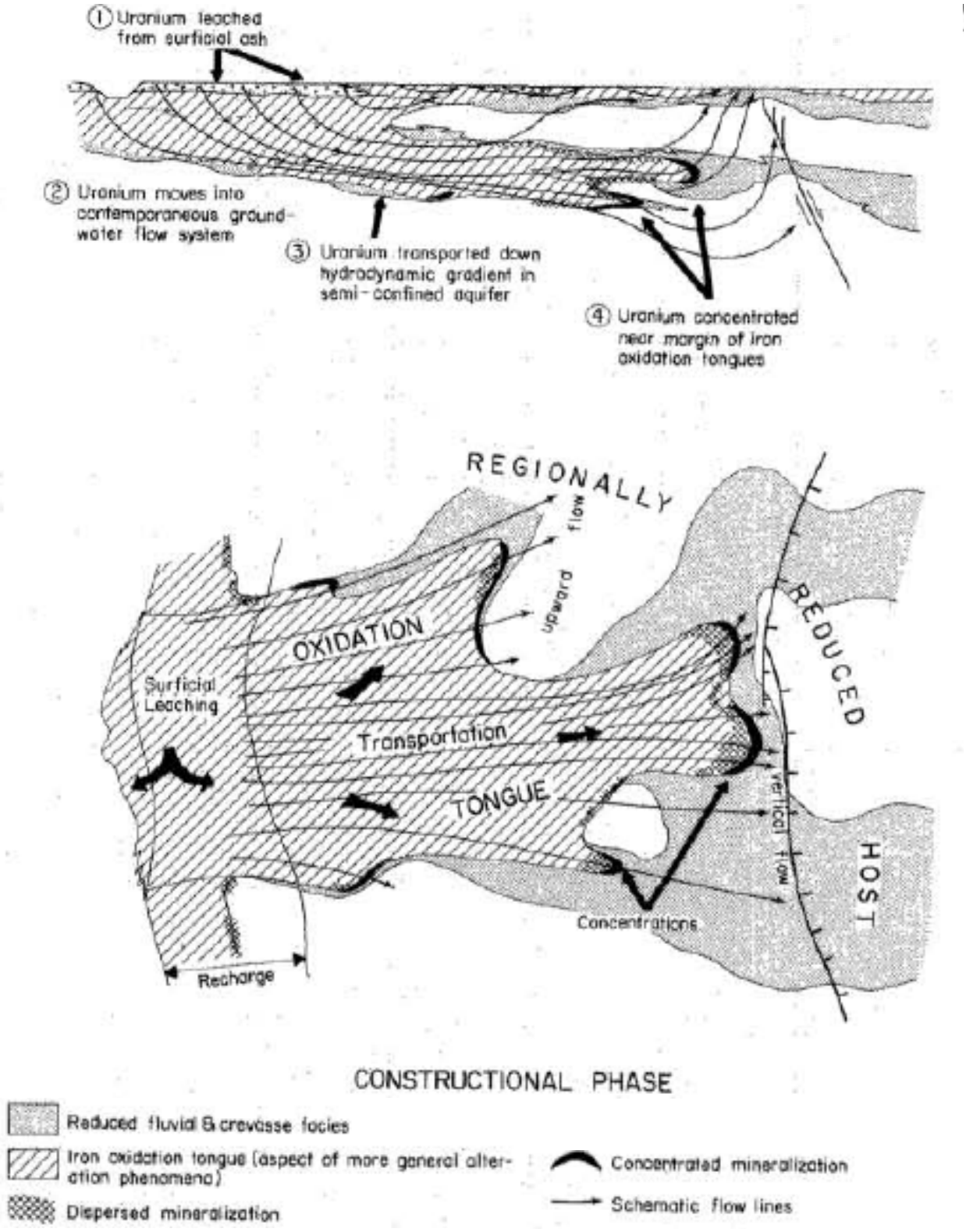

Source: Galloway (1977)
Note: Dimensions along flow lines can vary from 5 to 50 mi, depending on the system.

Figure 56. Constructional phase of uranium mineralization

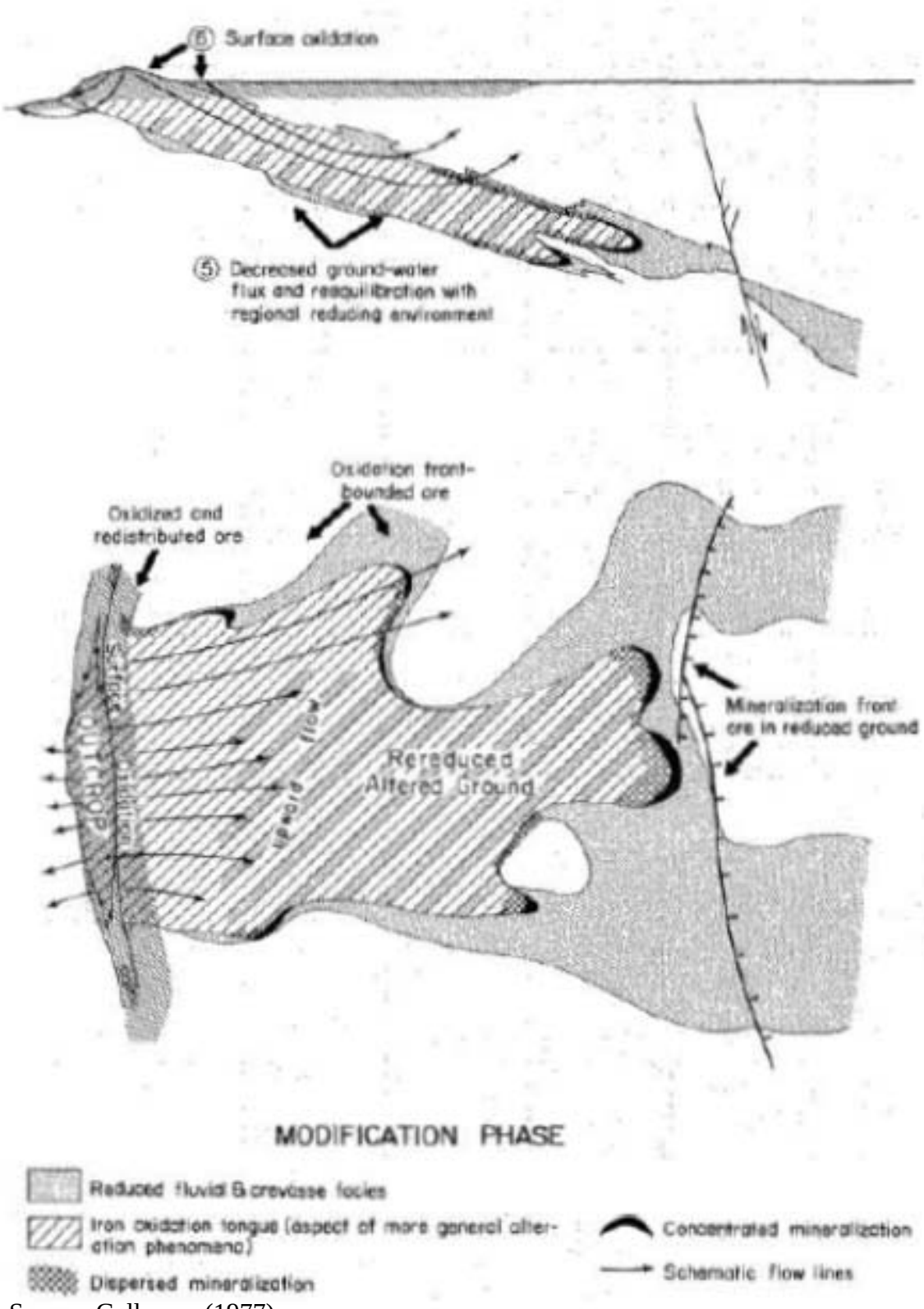

Source: Galloway (1977)

Note: Dimensions along flow lines can vary from 5 to 50 mi, depending on the system.

Figure 57. Modification phase of uranium mineralization

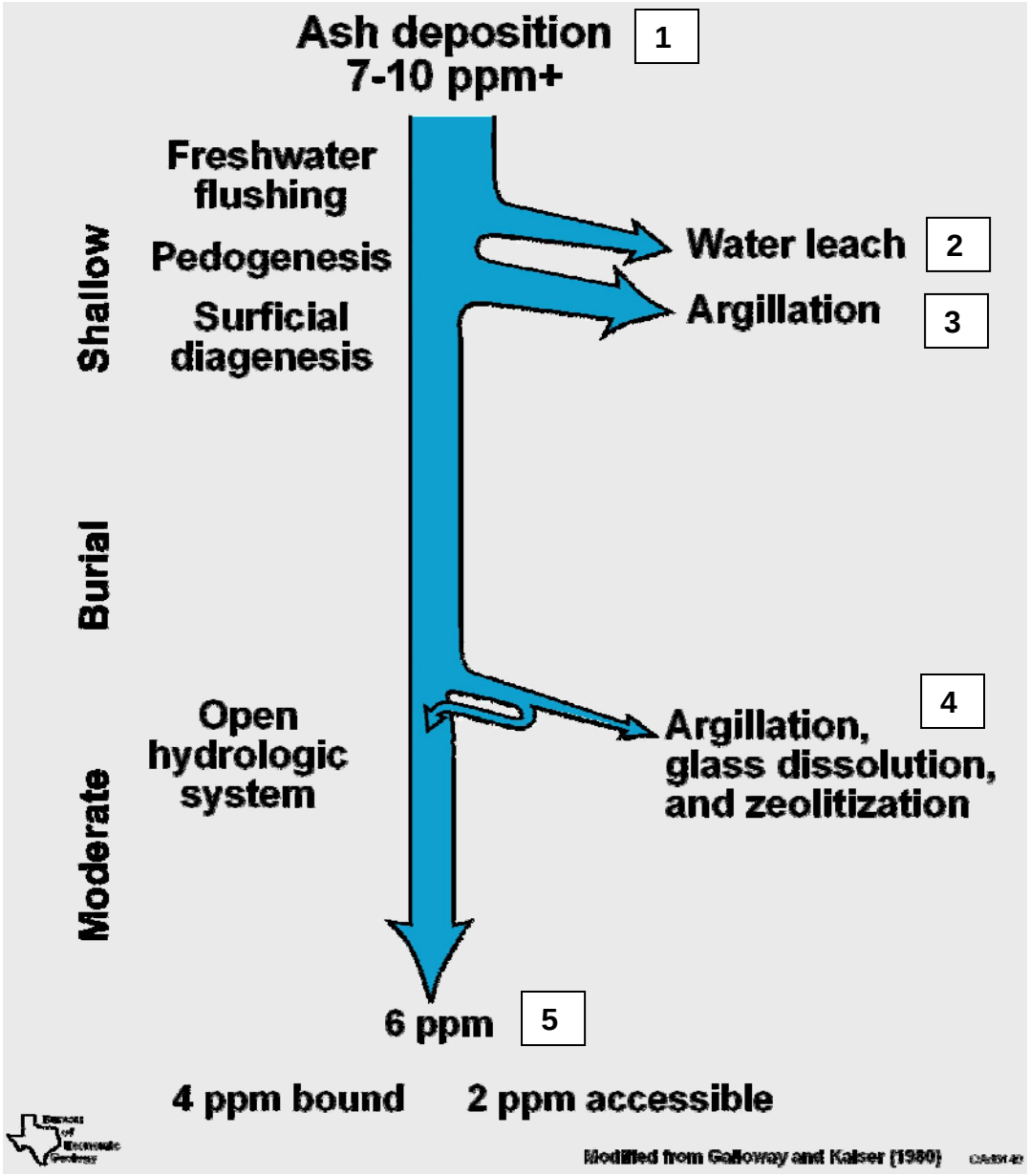

Source: Ambrose (2007) modified from Galloway and Kaiser (1980)
Note: (1) STU ash is enriched relative to other ash deposits; (2) some uranium is leached immediately; (3) some uranium was leached, sorbed, and released in early diagenesis (10,000 yr?); (4) subordinate long-term release; and (5) current uranium status in Catahoula tuffs. Between 1 and 4 ppm was released.

Figure 58. Volcanic-ash leaching processes

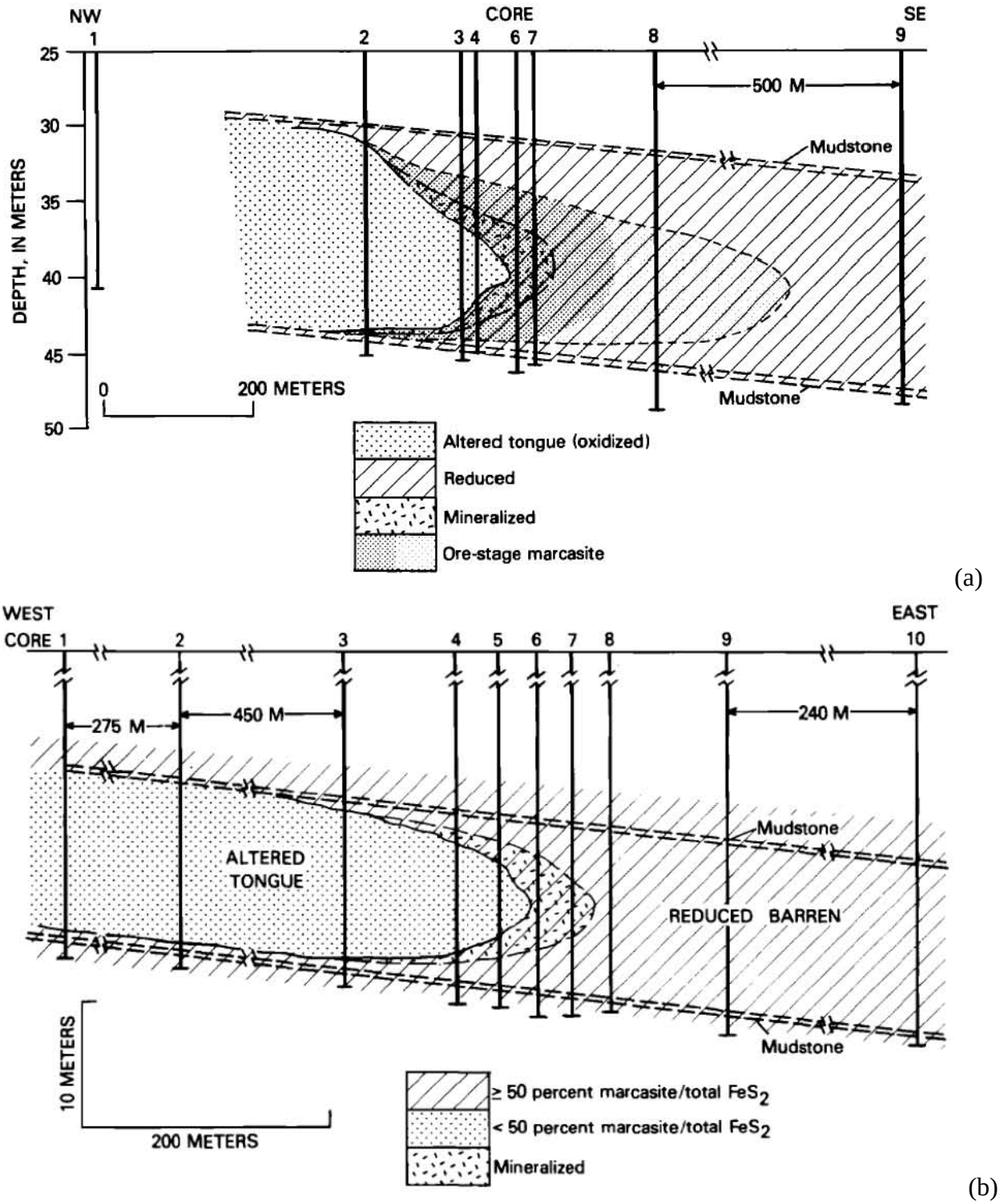

Source: Reynolds and Goldhaber, 1983

Figure 59. Cross-section of uranium deposits: (a) Benavides, Webb County; (b) Lamprecht, Live Oak County; (c) Felder, Live Oak County; and (d) Panna Maria, Karnes County.

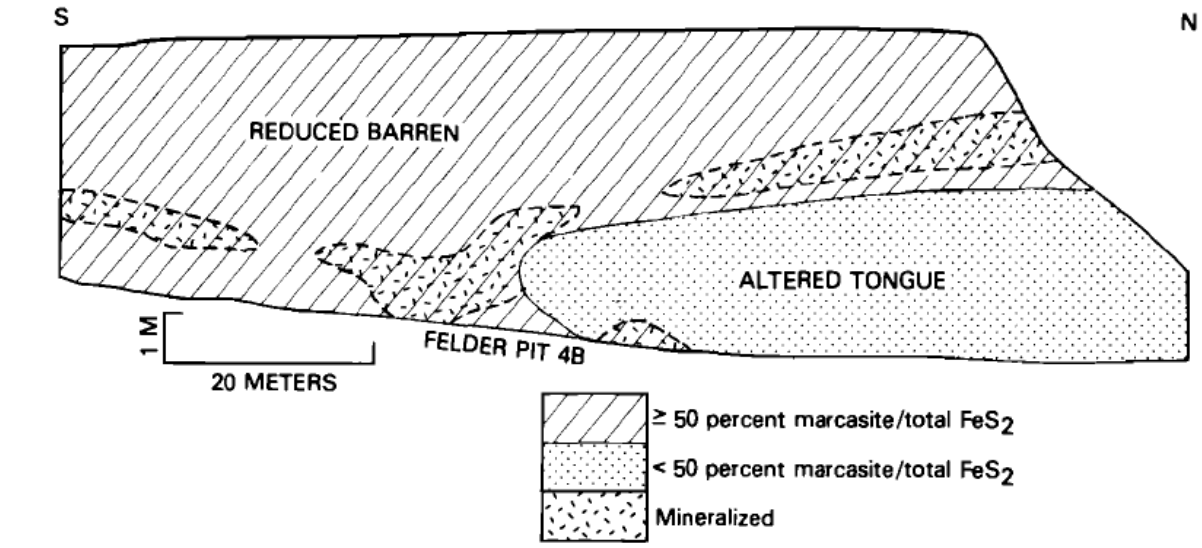

(c)

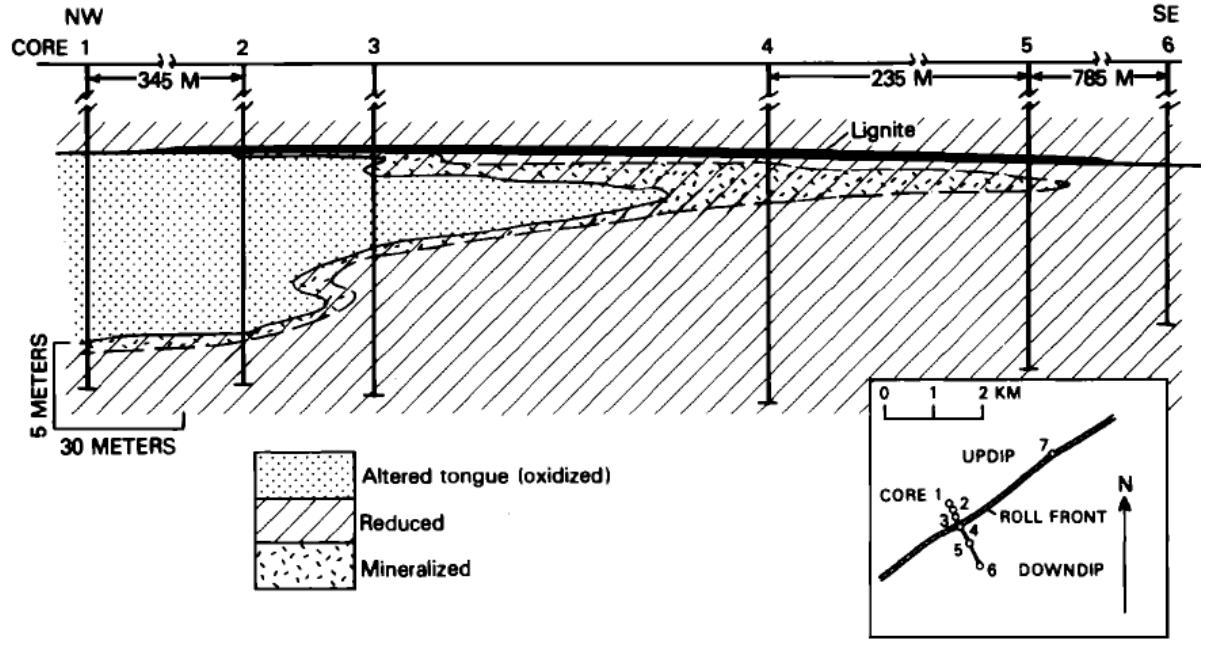

(d)

Source: Reynolds and Goldhaber, 1983
Note: Benavides, Lamprecht, and Felder deposits occur in fluvial channel environment with no carbon material whereas the Panna Maria deposit occurs in coastal barrier environment in which organic material is abundant.

Figure 59. Cross-section of uranium deposits: (a) Benavides, Webb County; (b) Lamprecht, Live Oak County; (c) Felder, Live Oak County; and (d) Panna Maria, Karnes County. (continued)

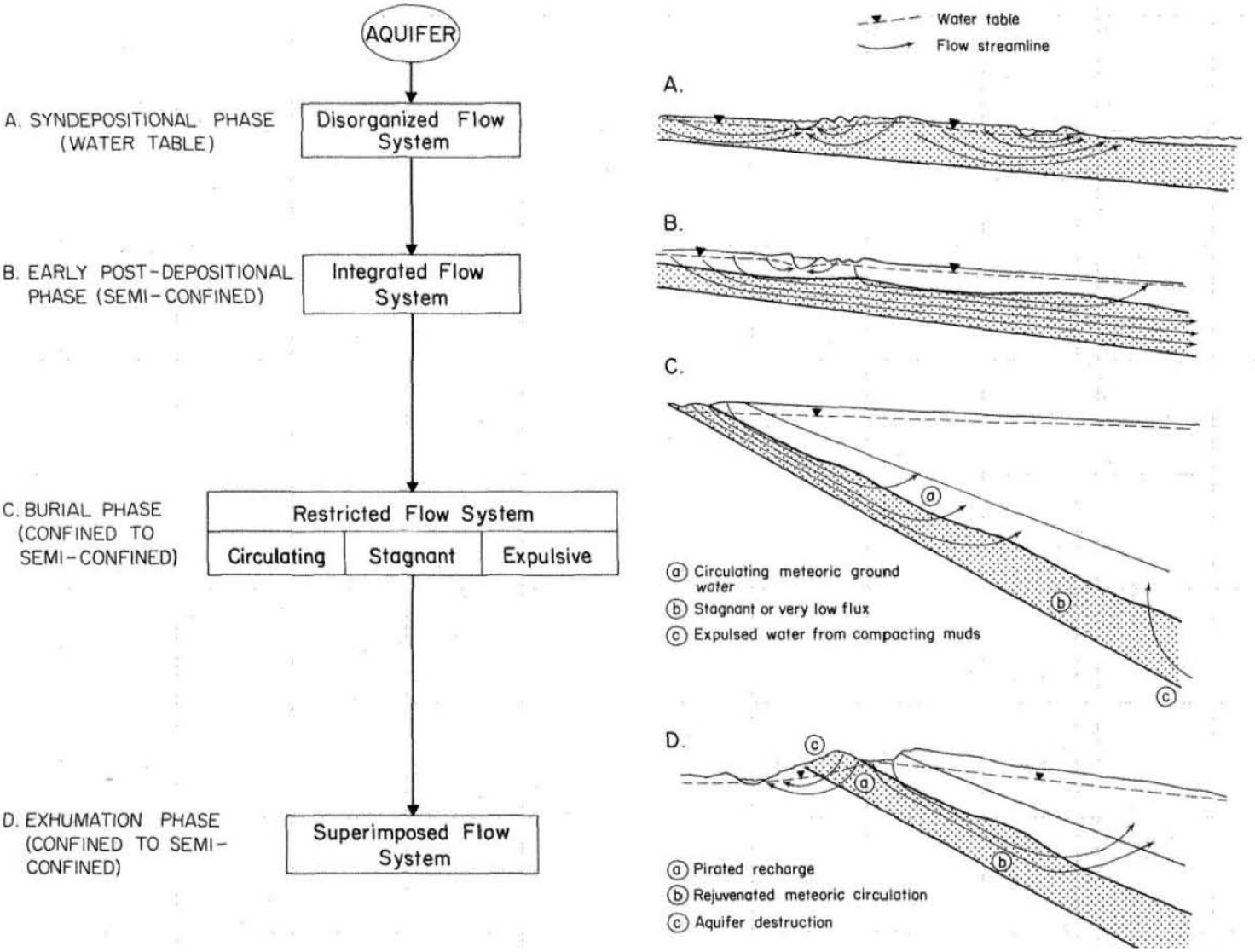

Source: Galloway (1977)

Figure 60. Geological phases of a Gulf Coast aquifer

VI-2. Matrix Mineralogy

Knowledge of matrix mineralogy is important in determining reactions in the subsurface and transport properties of easily sorbed oxyanions. Permeable formations in the STU Province can be qualified as "more or less dirty sandstones," tending toward the arkosic pole and sometimes including many rock fragments. Feldspars, particularly plagioclase minerals, tend to be reactive and are subject to several alteration pathways.

Jackson Group. Strandplain deposits tend to be well-sorted clean sands (Hamilton, 1994, p. 8), transitioning both updip and downdip to mudstones.

Catahoula Formation Catahoula sandstones are dominated by plagioclase feldspar and volcanic rock fragments (Galloway, 1977, p. 23), all in subequal proportions (feldspathic litharenite or lithic arkose, according to Folk's classification, 1974) (Figure 61). They also include many tuffaceous mud grains of local origin and carbonate rock fragments. Finer sandstones contain a larger proportion of quartz and feldspar. Sandstones also contain heavy minerals, including up to 4% magnetite/ilmenite (Galloway, 1977, p. 23). McBride et al. (1968, p. 33) stated that the heavy mineral fraction ranges from 3 to 11 weight percent, 66 to 90% of which are opaques (probably mostly FeOx and related oxides). Composition of clay minerals in the clayey petrofacies consists mostly of a mixed calcium-sodium montmorillonite resulting from alteration of volcanic ash rather than reworking of older units. The absence of detrital illite suggests that all clays are derived from ash-layer alteration, consequently providing a much larger source of uranium than if some of the rock volume had been barren illite. Subsequent diagenesis decreased permeability of the sand as a result of clay coating and calcite cement. Clayey facies have low permeability, although before alteration they may have had much higher permeability, allowing leaching of uranium and other trace metals soon after deposition. Current trace-metal concentrations in the Catahoula Formation rocks show no particular enrichment, suggesting that leaching occurred early after deposition. Sand grains are rimmed by calcium carbonate, montmorillonite, and clinoptilolite (Galloway, 1977, p. 37—see Galloway and Kaiser, 1980, p. 11, for pictures or p. 27 for sketch), the latter two providing good sorbing material. Organic material is not frequent in the Gueydan system (Catahoula), but silicified wood is not uncommon (Galloway, 1977, p. 38). McBride et al. (1968) presented comprehensive petrographic descriptions of the different units.

Oakville Formation The Oakville sands consist of quartz-poor litharenites or feldspathic litharenites (classification of Folk, 1974) (Galloway et al., 1982a, p. 23). They consist mostly of a mixture of quartz, carbonate rock fragments, and volcanic rock fragments, in order of abundance. Chert and feldspar are present in lesser, but also considerable, amounts (Galloway et al., 1982a). Solis (1981, p. 6) stated the following average composition: quartz (40%), chert (25%), and considerable amounts of feldspar and calcite cement. He also reported observations of silicified wood. Galloway (1982a, p. 2–3) and Galloway et al. (1982a, p. 24) suggested that sediments were deposited in an arid environment in a typical redbed system with hematitic alteration. Clay mineralogy is dominated by montmorillonite, with minor components of kaolinite and illite. Galloway et al. (1982a, p. 23) suggested that montmorillonite is derived from older strata rather than an alteration product of ash material, but both origins likely exist. Diagenetic calcic materials are abundant in association with both fine- and coarse-grained components. The most common minor constituents include iron oxyhydroxides and iron-titanium oxides. Whole-rock analyses suggest that iron oxides are common in the subsurface (2% in Table 1 of Galloway, 1982a). Silica cementation sometimes reduces porosity of framework sands

(Galloway et al., 1982a, p. 24). The formation contains no bedded organic deposits (Galloway et al., 1982a, p. 25). Organic carbon is described as low in most aqueous samples of the Oakville sand (<0.01%).

Goliad Formation Approximately 80% of the formation is sand and gravel. Hoel (1982) reported that the formation is similar to the Catahoula and the Oakville sandstones and contains a large proportion of orthoclase and plagioclase feldspars and volcanic rock fragments, particularly south of the San Patricio-Refugio County line (bedload rivers) (Chowdhury and Mace, 2006).

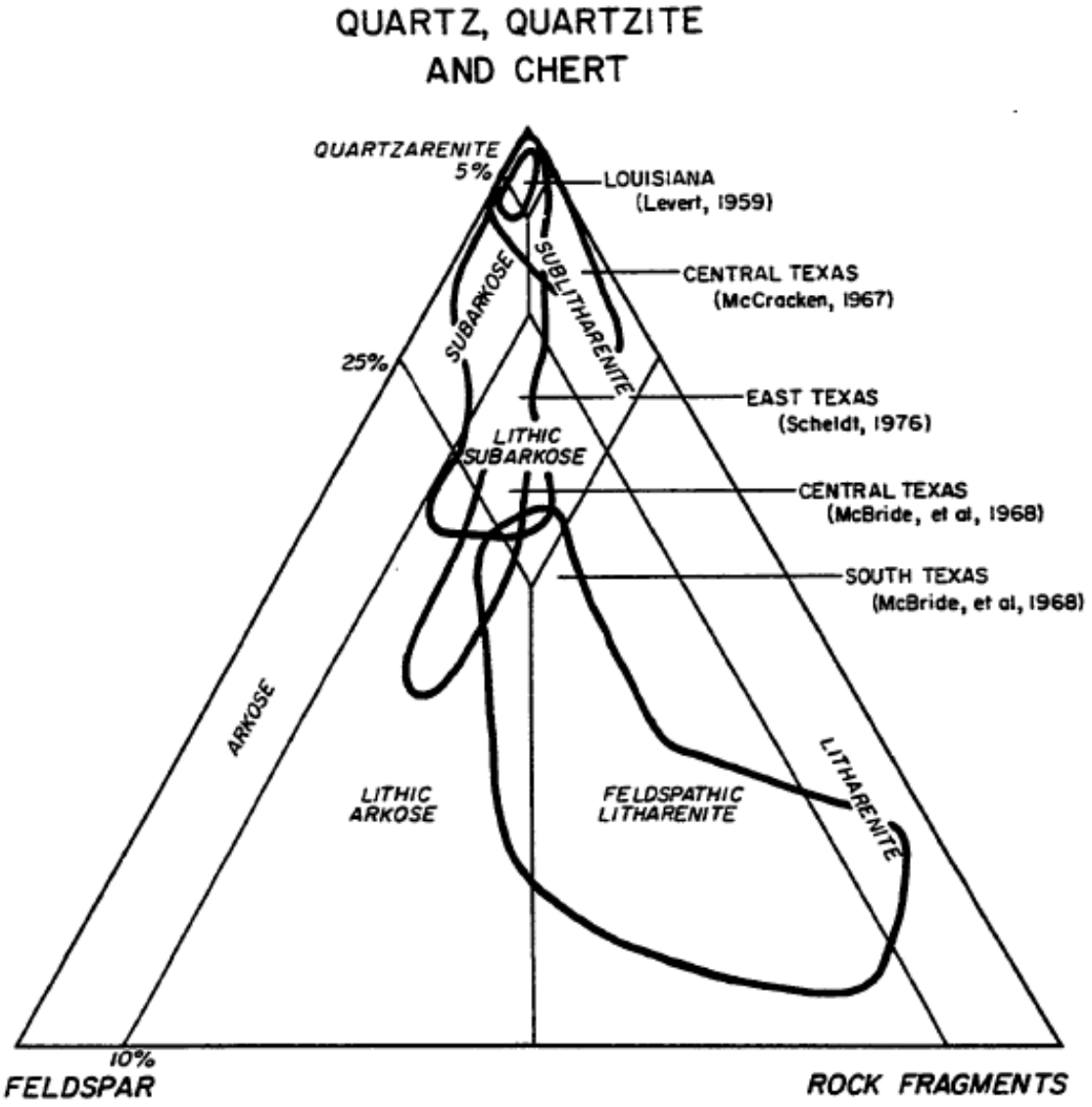

Source: Ledger, 1981, Fig. 7

Figure 61. Ternary diagram of solid phase composition of Catahoula sediments

VI-3. Minor and Trace-Element Distribution and Chemistry

Gates et al. (2008, 2009) reviewed distribution in the southern Gulf Coast of several prominent dissolved trace elements, including arsenic, uranium, vanadium, and others, following up on previous work by Scanlon et al. (2005). In general, concentrations of trace elements are significantly higher in the STU Province than in northern equivalents of the same formations. This observation has puzzled researchers for some time but may be connected to paleoclimate and ancient and current rates of flushing (see Section VI-1). Concentrations also tend to decrease with decreasing aquifer age (Oakville then Evangeline then Chicot). This section focuses on the regional distribution of trace elements. The RRC has a program in place to sample water from open-pit mines and to track water quality. Although no comprehensive study has been performed to the authors' knowledge, it seems that there is no regional impact from legacy mining. Lack of regional impact does not necessarily translate into a lack of contamination, natural contamination in particular. Economic mineralizations do not exist in a vacuum but are the epitome of a larger set of mineralized areas, possibly leading to elevated background values and possible natural contamination at the subregional level (i.e., high concentration dispersion from deposits [possibly uneconomical]). Galloway et al. (1982b) and Henry et al. (1982b) discussed impact of in situ leaching on aquifer groundwater quality. They also discussed the impact of leach-fluid uncontrolled excursions. Kreitler et al. (1992) and Adidas et al. (1991) discussed a TWDB-sponsored study initiated after concerns from residents of Bruni, Webb County, that a leach operation was contaminating the aquifer. Consensus was that immediately after cessation of operations, degradation was localized and decreased with restoration activities. Collecting information about elemental fractionation between U and Th234 and isotopic fractionation between U234 and U238 can generate a detailed understanding of the deposit (both Th234 and U234 are steps of the U238 decay series) (Cowart and Osmond, 1977; San Juan, 1982). In the next paragraphs, we evaluate mechanisms controlling trace-element distribution, describe in general terms trace elements of concern, and comment on their spatial distribution in individual formations.

Uranium in sedimentary deposits is generally accompanied by a suite of oxyanions, such as selenium, molybdenum, arsenic, and vanadium, as well as, possibly, fluoride and boron. These are well-known associations and have been documented in recent BEG work both in the Texas High Plains and in the southern Gulf Coast area (Scanlon et al., 2005; Gates et al., 2008, 2009). For example, these studies have made clear that in the vast majority of cases, elevated arsenic in groundwater is natural, not anthropogenic, and not related to cotton-farming activities (which, in the past, used arsenic-based chemicals as a defoliant before cotton was harvested). Therefore, any study of uranium contamination must also provide an explanation for the distribution of all associated oxyanions.

Trace elements, by definition, do not impact water geochemistry because of their low concentration but are, rather, fully controlled by it, particularly by Eh and pH conditions. In general, when considering trace-element behavior, three broad groups of conditions must be considered, as well as interactions among them: (1) environmental conditions, chiefly Eh and pH; for example, in oxidizing conditions, uranium is much more soluble in alkaline environments because it forms strong complexes with carbonate ions; (2) sorption opportunities, particularly on metal oxides and clays; for example, Galloway and Kaiser (1980, p. 60) stated that greatest sorption of uranyl ion on montmorillonite occurs at a pH of 6; and (3) precipitation opportunities; in general, precipitation as an individual phase is unlikely unless concentrations

are high, although precipitation in solid solutions with minor and major elements occurs; for example, arsenic can enter and be stable within pyrite (FeS_2) and not necessarily precipitate as arsenopyrite (FeAsS); (4) the chemical form of the element under various environmental conditions, and also, more generally, the possibility of complexation by ligands; for example, Se, Mo, V, and As exist in various deprotonated states of the following weak acids: H_2SeO_3, H_2MoO_4, H_3VO_4, $H_3As_2O_3$, and H_3AsO_4, respectively. Uranyl ion (UO_2^{2+}) is positively charged but forms negatively charged complexes with inorganic ligands, such as carbonate, fluoride, and hydroxyl ions. In oxidizing conditions, trace-element concentrations are not typically controlled by mineral precipitation, except perhaps immediately adjacent to oxidizing deposits (Galloway et al., 1982b, p. 139). A clear zonation across the redox gradient can, however, be seen as Eh decreases with Se, U, and Mo minerals (precipitating in that order), whereas their respective aqueous concentration drops. Aqueous concentrations of As and V are not sensitive to Eh drop (within the Eh range typically present in Gulf Coast aquifers) but, rather, to the presence of sorption sinks. Se, Mo, V, and As are all known to form negatively charged oxyanions. Iron oxides (FeOx) sorb oxyanions and uranium very well except at basic pH (~8–9), at which point a change in the oxide surface charge releases the ions. Overall, trace-element concentration is generally determined by sorption behavior. The actual amount sorbed is a function of the amount of complexing ligands in solution, the balance being determined by thermodynamics.

From a practical standpoint, note that earlier geochemical modeling performed by investigators in the 1970's and 1980's was not satisfactory relative to trace-element behavior (e.g., Galloway et al., 1982b, p. vii) because thermodynamic data were largely missing. Henry et al. (1982a) presented an extensive discussion on trace-element geochemistry. However, the state of knowledge has advanced significantly since then (e.g., Burns and Finch, 1999; Arthur et al., 2006), thanks to the federally funded Yucca Mountain Project, although some knowledge gaps still exist. The past decades have also brought to light the importance of microbes in subsurface, even deep subsurface, processes. Min et al. (2005) put forward arguments suggesting that roll fronts could be biomediated, with U(VI) being used as an electron acceptor; in the process it precipitated as U(IV). Cuney and Kyser (2009, p.32) also emphasized this paradigm shift.

Elements of Concern Table 10 presents typical and average trace-element concentration in aquifers. Uranium, arsenic, molybdenum, and selenium often occur together at a regional scale because they derived from the same source (ash-fall leaching). Fluoride and boron are also frequently associated with these four elements. Radioactive decay of uranium generates radium and radon, which behave differently from the previous elements but which are also found in areas where uranium is present. This report is too general to provide detailed discussions of the relevant geochemistry that could be developed in a future, more focused, report. Some salient aspects of their geochemistry are presented later; Chowdhury et al. (2006) presented more details on the geochemistry of some of these elements. From a spatial distribution standpoint, most elements show a higher aqueous concentration closer to the Catahoula outcrop then decreases both eastward away from the outcrop and with decreasing depth in more recent formations: uranium (Figure 62 and Figure 64), arsenic (Figure 63 and Figure 65), selenium (Figure 67), and vanadium (Figure 68). Molybdenum (Figure 66) and fluorine (Figure 69) show deviations from this general rule.

In addition to Scanlon et al. (2005) and Gates et al. (2008), several reports and papers discuss in detail these elements' distribution. Concentration range for major, minor, and trace elements from Gates et al. (2009) is displayed in Figure 70. Langmuir and Chatham (1980) presented

aqueous concentration profiles of trace elements across Catahoula and Oakville Formations. Smith et al. (1982a, their Figs. 19 and 21–23) discussed spatial distribution of uranium, molybdenum, selenium, and arsenic with inferred isopleths in the Jasper aquifer. All ions increase from the northeastern to the southwestern Gulf Coast. Galloway (1982a, his Fig. 18) presented a typical downflow evolution, with uranium and selenium decreasing downdip while Mo remains high. Henry et al. (1982a, p. 1) stated that very high aqueous concentrations of trace elements occur only within ore zones, but that sampling within mining districts yields trace-element concentrations similar to those in the regional background. An analysis by Henry et al. (1982a) (also described and discussed in Galloway et al., 1982b) of 58 water samples along 10 dip-oriented profiles (6 in the study area) showed that uranium concentrations varied from <0.2 to 10 ppb, except in four samples (highest 99 ppb). All but four samples contained <5 ppb selenium. Molybdenum and arsenic concentrations ranged from <0.2 to 57 ppb and from <1 to 39 ppb, respectively. They also presented results of sampling near the open pit with no clear deviation from the background. According to Henry et al. (1982a, p. 46), this strongly suggests that there is no active source of elements (leaching) and that the source has been depleted.

Arsenic (As): Arsenic typically occurs in two redox states, both soluble in Gulf Coast environmental conditions—As(III) and As(V) as arsenite (H_3AsO_3) and arsenate (H_3AsO_4), respectively. The molecules remain fully protonated at low pH but lose all H at high pH. At neutral to slightly alkaline pH, arsenite is a neutral molecule (H_3AsO_3), whereas arsenate is partly deprotonated ($HAsO_4^{2-}$), allowing arsenate to sorb more easily on (positively) charged mineral surfaces. Neither of these two states forms complexes in typical conditions. Minerals having As(III) or As(V) in their structure generally precipitate only at high-As concentrations.

Boron (B): Boron forms the oxyanion borate (H_3BO_3), which is a fully protonated neutral molecule in most common environmental conditions. Being a neutral molecule, boron is not extensively sorbed and is fairly mobile. In addition, boron-based minerals do not precipitate easily.

Fluorine (F): Fluorine exists in only one redox state (F^-) but often acts as a ligand complexing other ions, especially at lower pH; at higher pH, F^- tends to be substituted by the hydroxyl ion OH^-. Fluorite (CaF_2) has a rather low solubility and can control fluorine aqueous concentration. Fluoride can also sorb significantly to oxides, especially aluminum oxides and clays.

Molybdenum (Mo): Molybdenum forms oxyanions in its oxidizing Mo(VI) state (molybdate, H_2MoO_4) but is fairly insoluble in its other common state, Mo(IV), precipitating typically as molydbenite (MoS_2).

Radium (Ra): Radium, an element of the uranium decay series, has a chemical behavior similar to that of Ca and Ba. Radium sulfate has a solubility product lower than that of barite. Ra often precipitates with barite and, perhaps, gypsum (solid solution). Sulfate-poor water will have a higher Ra concentration. However, it also sorbs strongly to iron oxides, clays, and organic matter.

Radon (Rn): Radon is gas that will travel in a dissolved form, and although radon (Cech et al., 1987, 1988) does not seem to be a problem, Beaman and Tissot (2004) thought otherwise. Surface risk due to radon has been described as low, despite the presence of uranium, because soil permeability is generally low when uranium is abundant (Schumann, 1993, p. 155). However, there is an important caveat: areas of potentially high radon concentrations may be masked by larger areas at much lower concentrations (Duval, 2005).

Selenium (Se): Selenium is another oxyanion whose behavior is similar to that of arsenic and molybdenum (including sorption). It exists under two redox states—Se(VI) and Se(IV) (selenite, H_2SeO_3, and selenate, H_2SeO_4, respectively). The main difference between selenium and arsenic is that the slightly reduced form, Se(IV), is insoluble and precipitates under mildly reducing conditions.

Uranium (U): Uranium generally exists naturally in two redox states: a reduced tetravalent form U(IV) and an oxidized hexavalent form U(VI). Uranium(VI) in oxidizing conditions exists as the soluble, positively charged uranyl UO_2^{++}. Solubility is higher at acid-pH levels, decreases at neutral pH, and increases slightly at alkaline pH. However, the uranyl ion, in contrast to oxyanions, can easily form aqueous complexes, including with the hydroxyl, fluoride, carbonate, and phosphate ligands. Hence, in the presence of carbonates (alkaline pH), uranium solubility is considerably enhanced in the form of uranyl-carbonate (UO_2CO_3) and other higher order carbonate complexes: uranyl-di- and uranyl-tri-carbonates ($UO_2(CO_3)_2^{-2}$ and $UO_2(CO_3)_3^{-4}$ (e.g., Langmuir, 1997, Chapter 13; EPA, 1999; Brady et al., 2002). Uranyl complexes can sorb on clays, Fe-TiOx grains, and organic matter if present. Transition between the two forms occurs at relatively high redox potential, similar to that of the ferrous/ferric transition. In that state, however, uranium has low solubility and precipitates as uraninite (UO_2), coffinite ($USiO_4.nH_2O$) (if SiO_2 >60 mg/L, Henry et al., 1982a, p. 18), or related minerals. In the southwestern Gulf Coast, there is no mineral controlling uranium solubility in oxidizing conditions. However, uranite and coffinite are the controlling minerals if Eh drops below 0 to 100 mV.

Vanadium (V): Vanadium is another oxyanion existing mostly as V(V) vanadate (H_3VO_3), mobile in oxidizing conditions, but it can sorb on metal oxides and other favorable mineral surfaces. The next redox state V(IV) exists only in conditions more reducing than that of the Gulf Coast.

The question of how far the presence of a deposit can be felt geochemically is of importance both from an exploration standpoint and from an environmental standpoint. It depends on the local redox state of groundwater flow. If groundwater is reducing, there is little incentive for uranium and allied elements to be mobilized. However, if conditions are oxidizing, a large halo can extend far downdip. Uranium decay products (He, Rn, Ra, Pb, Th), some of concern, have also variable mobility (Figure 71). He and Rn are not sensitive to redox conditions, and Th is not mobile. In addition, aerial radiometric surveys have shown that the uranium anomaly is not limited to the ore but extends hundreds of feet from the ore and that a low-intensity anomaly of radioelements also exists (Moxham, 1964, p. 317). These observations (made preproduction) suggest that uranium concentration in rocks is higher than average in a widespread area. However, this does not seem to translate into higher concentration in the surrounding water.

Table 10. Typical dissolved concentration in groundwater

Element	Value or Range (ug/L)	Source	Drinking Water MCL (ug/L)
Antimony	~<5	Hem (1985, p. 145)	6
Arsenic	1–50 1–50 <10	Hitchon et al. (1999) Welch et al. (2000, Fig. 2) Smedley and Kinninburgh (2002, p. 525)	10
Boron	50–1000	Hitchon et al. (1999)	600*
Fluoride	10–1,500 <1,000	Hitchon et al. (1999) Hem (1985, p. 120)	4,000
Molybdenum	~<10 (?)	Hem (1985, p. 140)	
Radium (combined)	<1 pCi/L		5 pCi/L
Radon			
Selenium	0.1–10 <1	Hitchon et al. (1999) Hem (1985, p.145)	5
Thorium	0.01–1	Hem (1985, p. 149)	100? 15 pCi/L (max excluding U and Rn, that is, mostly Th)
Uranium	0.1–10 0.1 (humid climate) 1.0 (arid climate)	Hem (1985, p. 148) Rose and Wright (1980) Rose and Wright (1980)	30
Vanadium	<10	Hem (1985, p. 138)	250**

*: Advisory maximum level

**: No MCL, Superfund Removal Action level

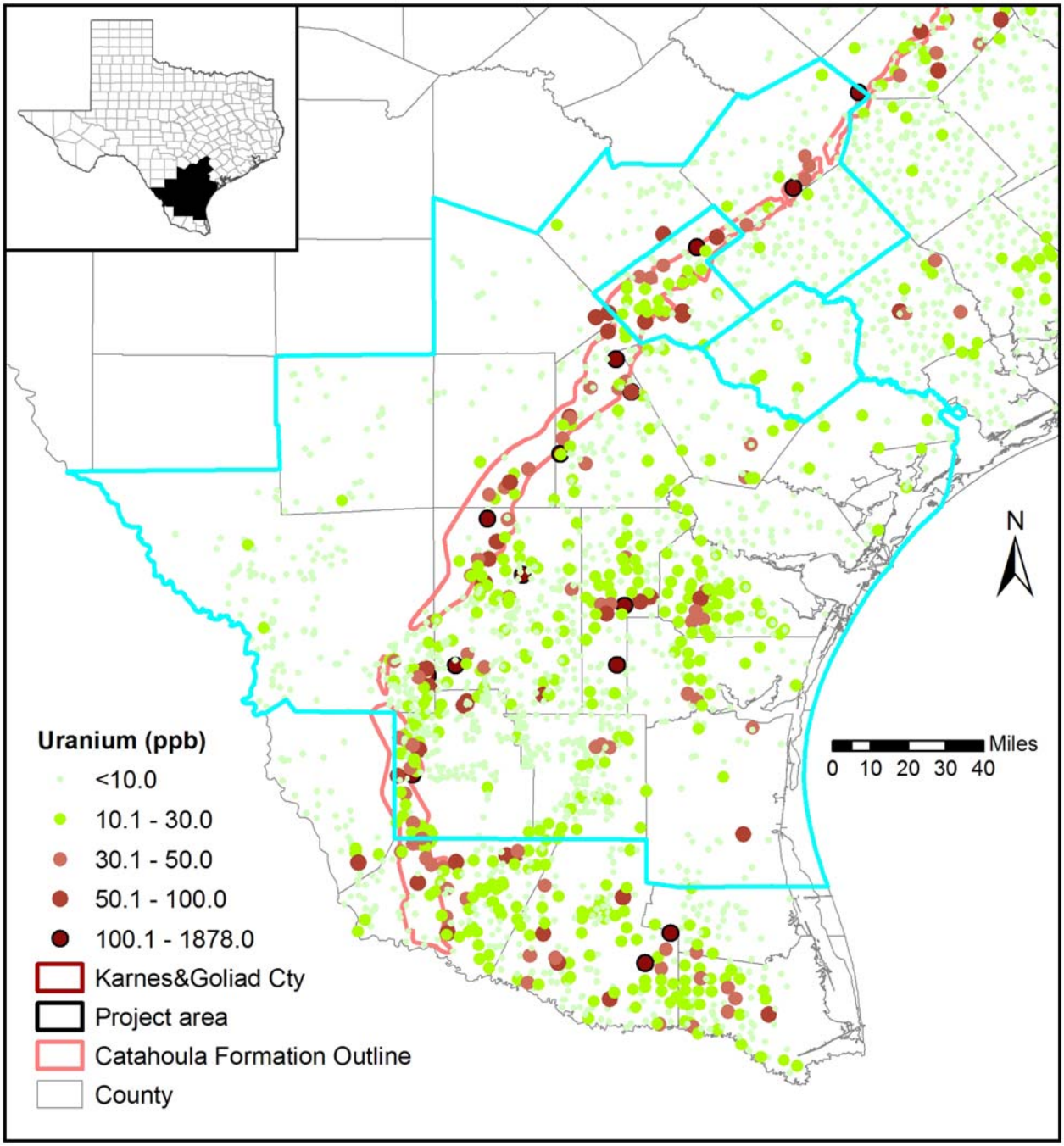

Source: TWDB database (downloaded Feb. 2009) and NURE database

Figure 62. Uranium aqueous uranium distribution in South Texas Uranium province

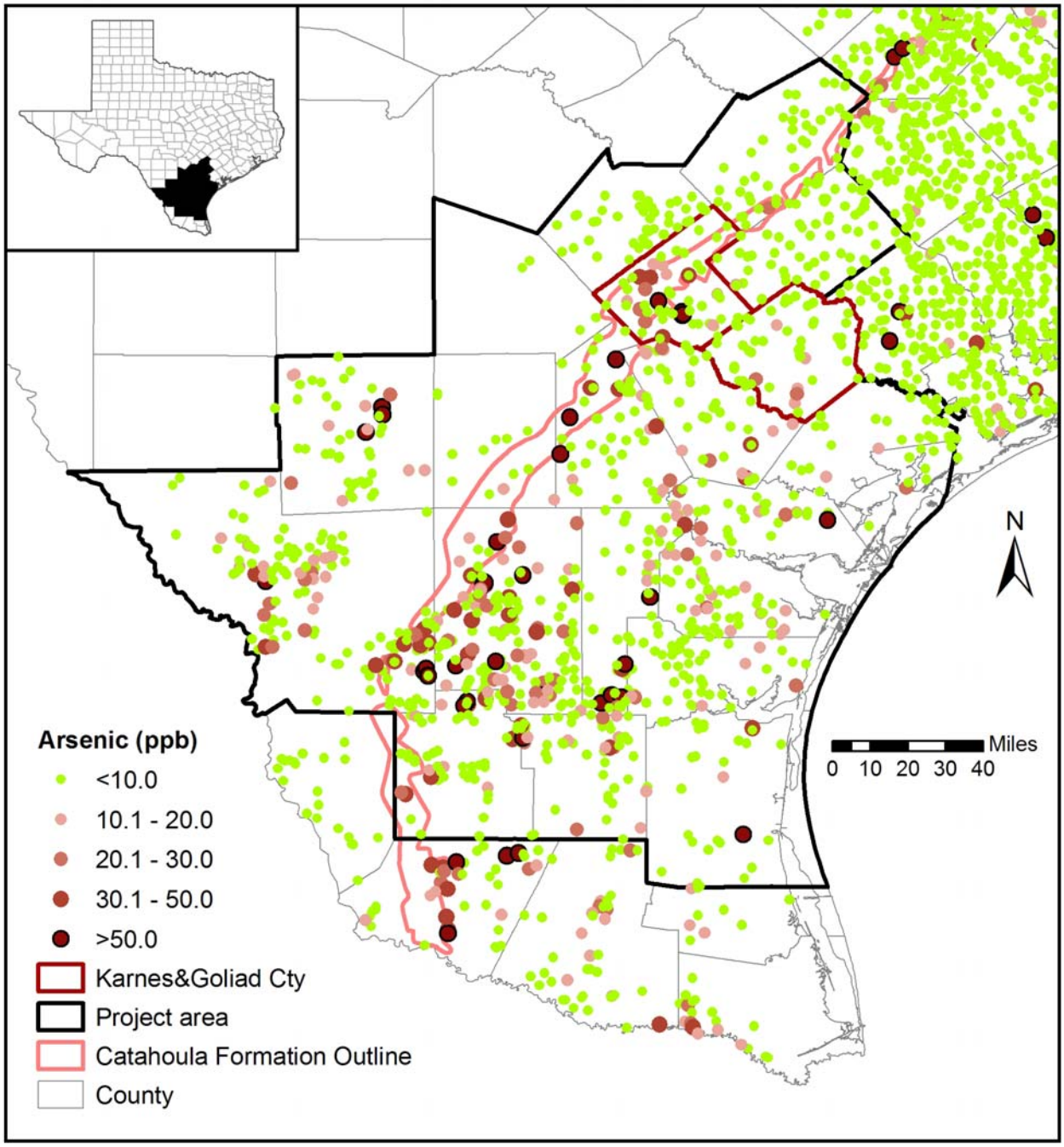

Source: TWDB database (downloaded Feb. 2009) and NURE database

Figure 63. Arsenic aqueous uranium distribution in South Texas Uranium Province

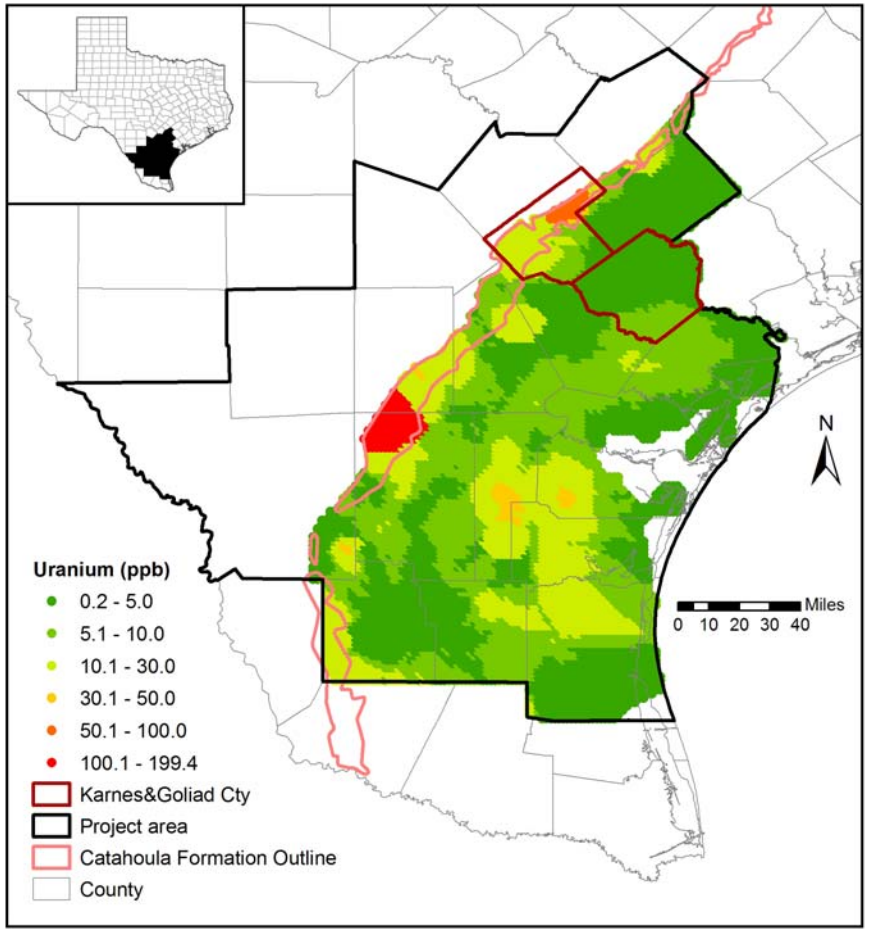

Source: Modified from Gates et al. (2008)

Figure 64. Interpolated map of uranium concentrations in Catahoula and Jasper aquifers

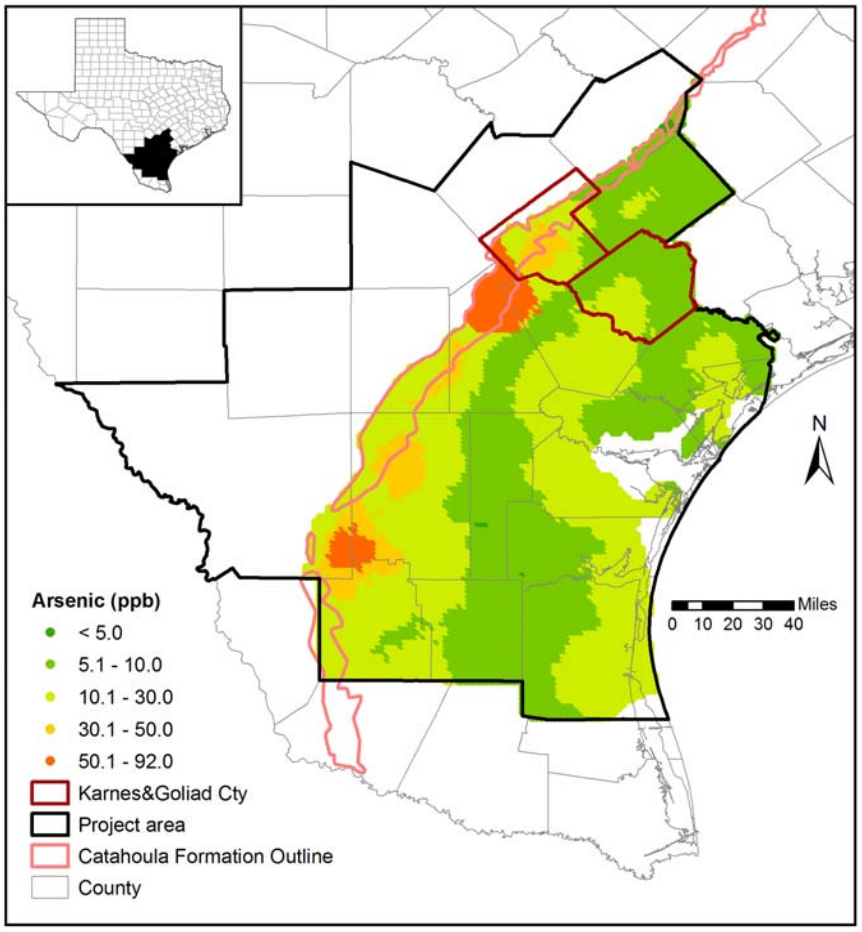

Source: Modified from Gates et al. (2008)

Figure 65. Interpolated map of arsenic concentrations in Catahoula and Jasper aquifers

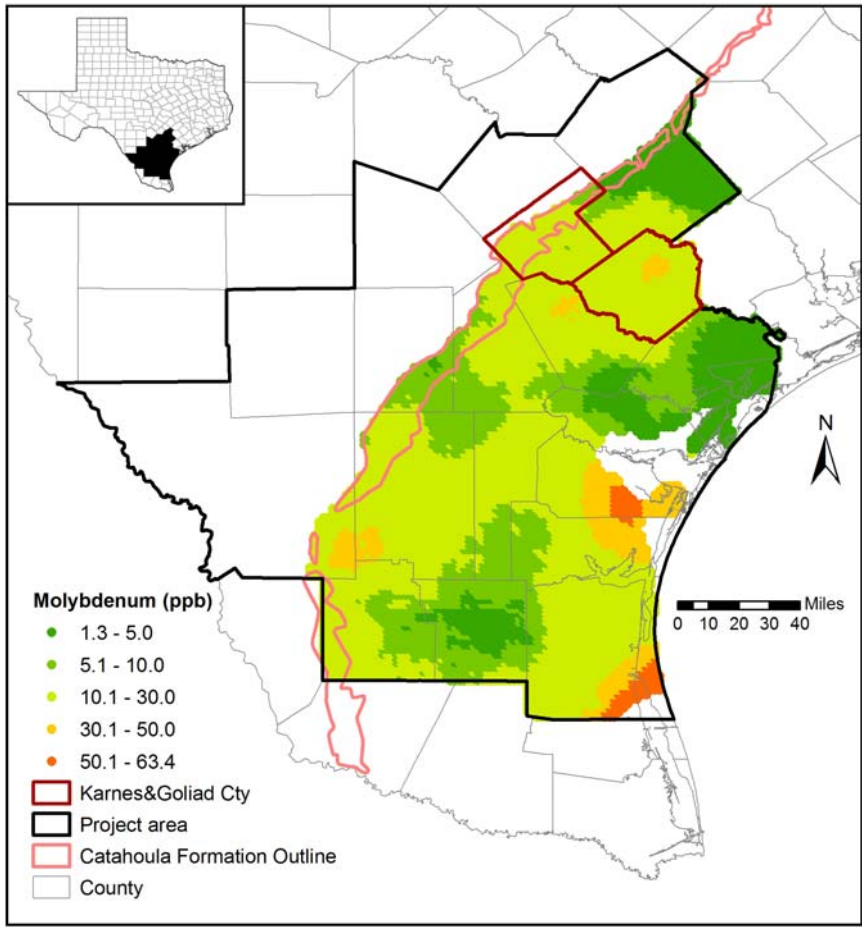

Source: Modified from Gates et al. (2008)

Figure 66. Interpolated map of molybdenum concentrations in Catahoula and Jasper aquifers

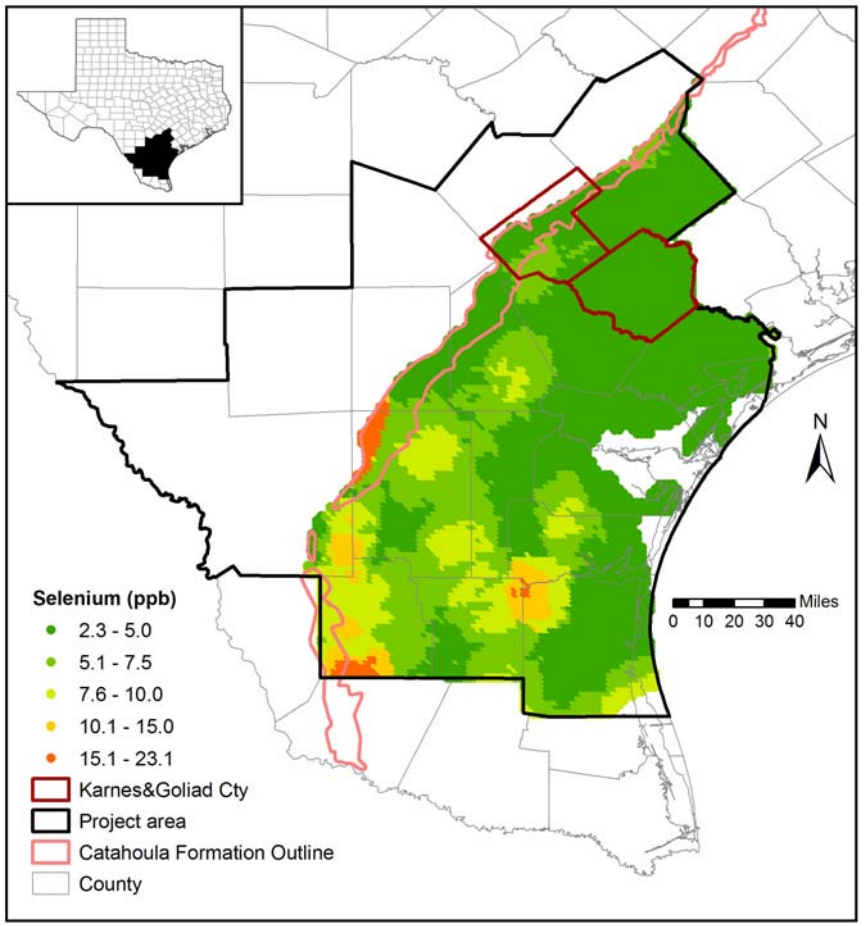

Source: Modified from Gates et al. (2008)

Figure 67. Interpolated map of selenium concentrations in Catahoula and Jasper aquifers

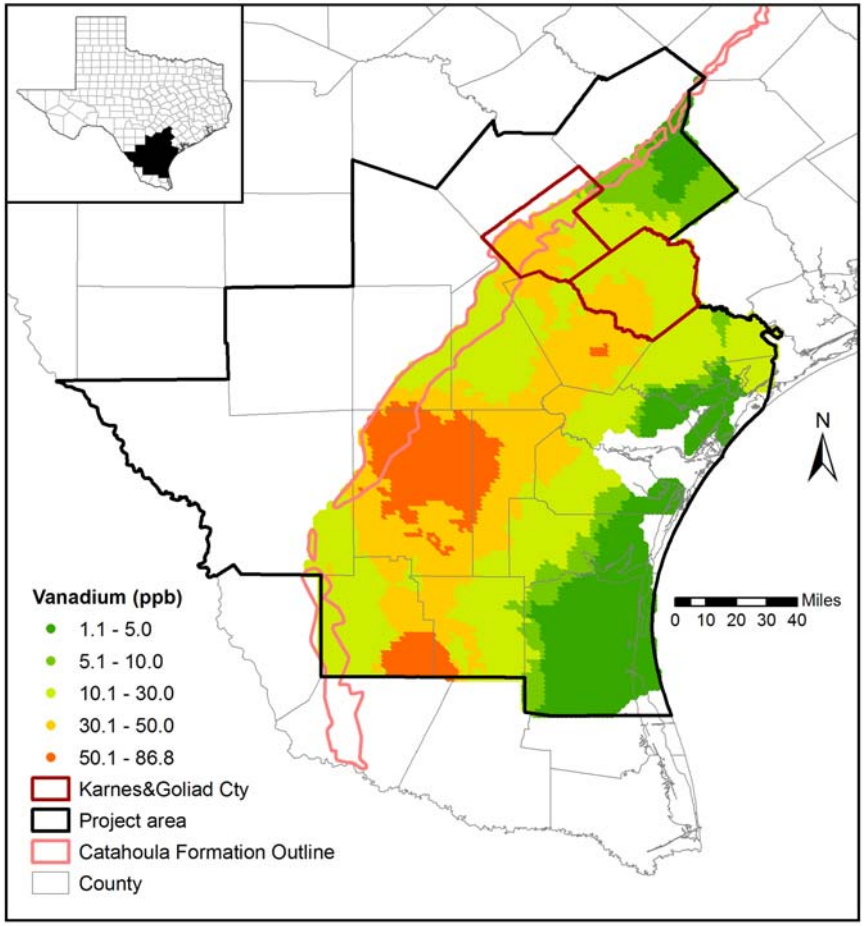

Source: Modified from Gates et al. (2008)

Figure 68. Interpolated map of vanadium concentrations in Catahoula and Jasper aquifers

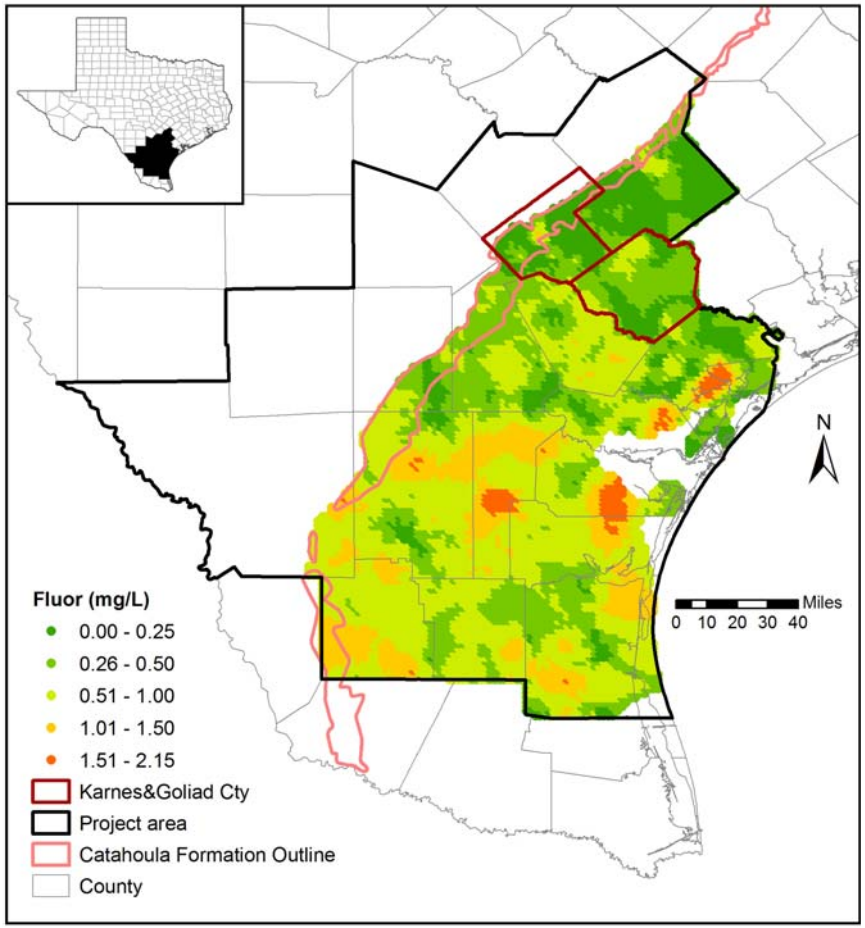

Source: Modified from Gates et al. (2008)

Figure 69. Interpolated map of fluorine concentrations in Catahoula and Jasper aquifers

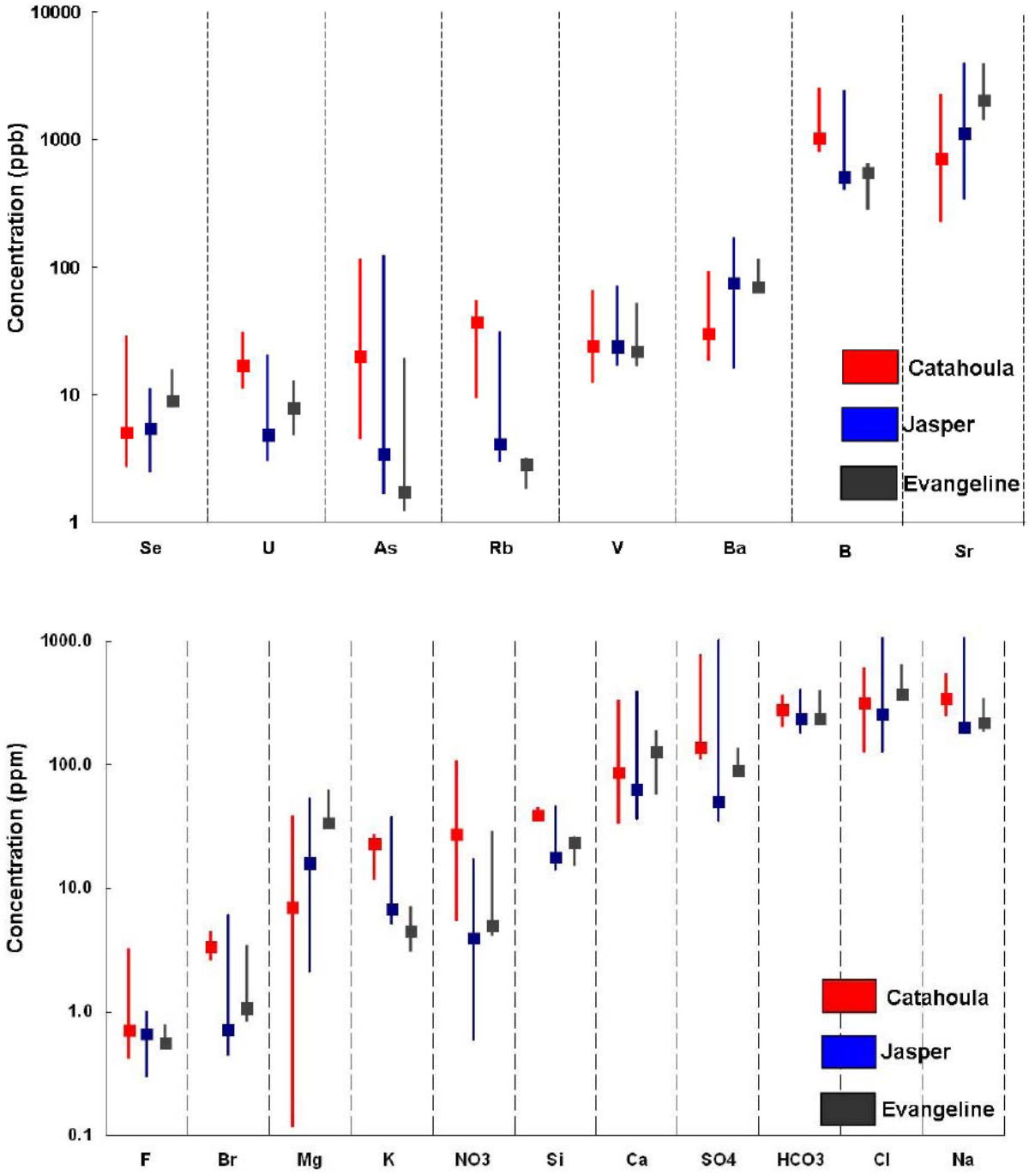

Source: Gates et al. (2009)

Figure 70. Box whisker plot of (a) trace elements and (b) major/minor ions for groundwater samples from a transect across Karnes and Goliad Counties

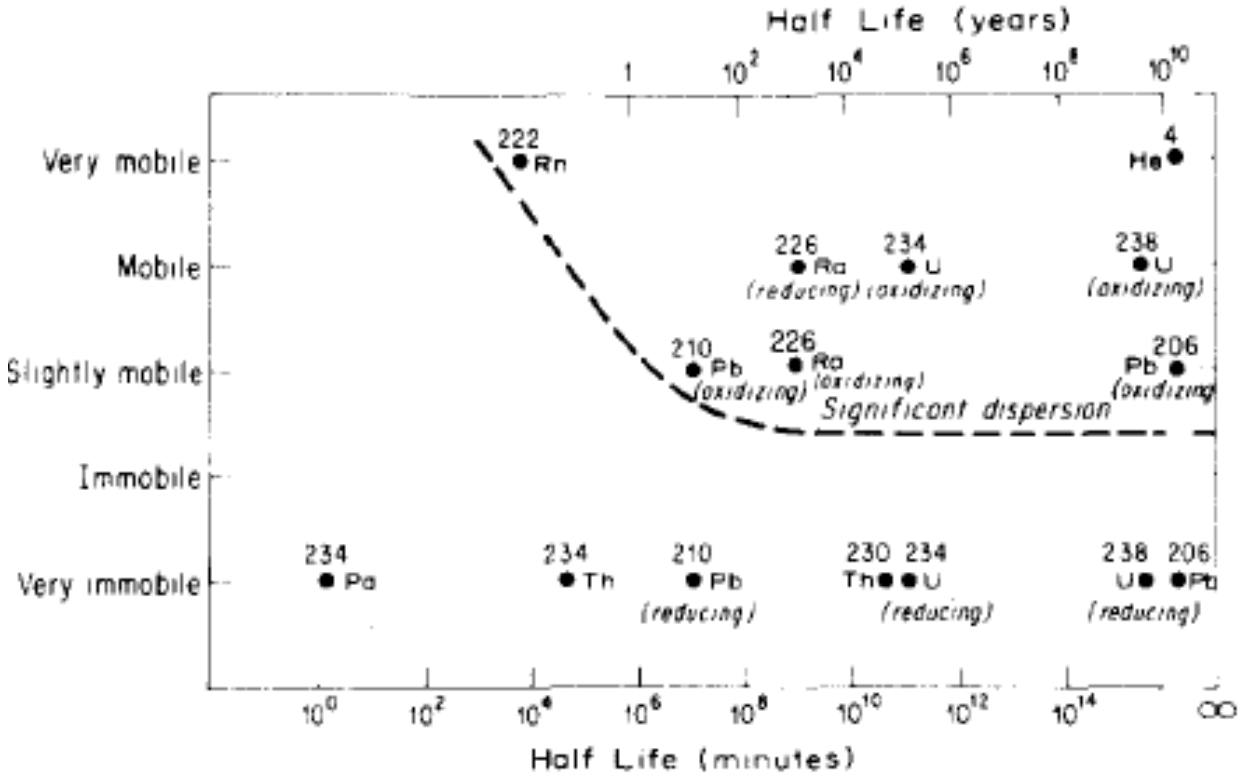

Source: Rose and Wright (1980)

Figure 71. Mobility of uranium decay products

VII. Geologic Hazards

This section describes other geologic features that might impact or be impacted by uranium activities (exploration, production, remediation). They include extraction of other resources, seismic activity, and weather hazards.

VII-1. Petroleum and Mineral Extraction

Oil and gas production is from a combination of stratigraphic/structural traps in the downdip Oligocene and Miocene in units that do not crop out at the surface (Vicksburg and Frio Formations) and from salt-dome structures (Figure 72 and Figure 73). Oil and gas production has resulted in high well density (Figure 74)—among the highest in the U.S. and in the world. A general map with reservoirs arranged by play (Figure 75) shows that, in the STU Province, reservoirs can be sorted into two categories: (1) those near the Jackson/Catahoula/Oakville outcrop and (2) those much farther downdip. Category 1 includes reservoirs of Cretaceous to Eocene age (Yegua, Jackson, Wilcox), whereas the Oligocene Vicksburg and Frio Formations host most reservoirs of category 2. Although the map represents only major reservoirs (cumulative production >10 million barrels of oil or standard cubic feet of gas), it gives a good estimate of location, age, and depth of all reservoirs. Reservoirs are mostly deep (Figure 76), except in Duval, Jim Hogg, and Webb Counties and, to a lesser degree, in Goliad and Bee Counties.

The barrier-strandplain depositional systems of the Yegua-Jackson Formations host significant hydrocarbon accumulations in Duval, Jim Hogg, and Webb Counties (Figure 75). Multiple reservoirs exist at relatively shallow depths (<4,000 ft) and are formed by anticlinal nosing through differential compaction and by updip pinch-out in heterogeneous assemblages (Seni and Choh, 1994, p.1–2). The deltaic and fluvio-deltaic plays in the Wilcox Formation are located at depths >6,000 ft, except for Weigang field (on Karnes / Atascosa County line) at 3,900 ft. The trapping mechanism is generally linked to a fault (connected to the unstable boundary of one of the Cretaceous margins). The Cretaceous-age oil and gas reservoirs (Person, Panna Maria) in Karnes County (in the Catahoula/Jackson Formation footprint) are contained in the Edwards Formation at a depth of about 11,000 ft (Cook, 1979; Galloway et al., 1983, p. 39; Kosters et al, 1989, p. 17) and are associated with a regional fault. Frio reservoirs (Galloway, 1982c) are located deeper. They abut faults such as the Vicksburg or the Frio Fault Zone or are trapped in rollover anticlines associated with fault systems.

In addition to uranium and oil and gas, other mineral commodities are also extracted from the STU (Figure 77). They include aggregate, industrial sand, etc. operations, as well as the San Miguel lignite open-pit mine in Atascosa County (e.g., CCGS, 1975). Coal seams belong to the lower Jackson Group, claystones and mudstones of mostly volcanic origin separating the coalbeds. Warwick et al. (1994) noted that average whole-coal concentrations of As, Be, Sb, and U in the lignite samples are greater than published averages for these elements in other U.S. lignite deposits.

VII-2. Seismic Stability

The U.S Geological Survey developed seismic hazard maps (Figure 78) and calculated the seismic hazard at several spectral accelerations (SA, periods 0.2, 0.3, 0.5, 0.75, 1.0, and 2.0 s)

and peak horizontal ground acceleration (PGA). The hazard curves were then interpolated at 0.00211, 0.00103, and 0.00040 annual rate of exceedance to obtain the 10-, 5-, and 2-% probability of exceedance in 50 yr, respectively, finally resulting in national seismic hazard maps. The hazard model assumes Poisson (time-dependent) event occurrence (Petersen et al., 2008a). Note that these maps were based on uniform firm-rock-site conditions, defined as a site with average shear-wave velocity of 760 m/s in the upper 30 m of the crust (Petersen et al., 2008a).

The entire regions of Central and East Texas have predicted probabilities for ground damage of less than 6% *g*, with both 2 and 10% chance of exceedance in 50 yr, according to USGS seismic hazard data, and, therefore, the study area overall has very low seismic risk, with minimal historical seismic activity and no historical earthquakes. The nearest areas of significant seismic risk are the New Madrid Fault Zone in northern Arkansas/Mississippi and southern Missouri/Illinois.

VII-3. Weather Hazards: Hurricanes and Tornadoes

The study area is located near the Gulf Coast and may pose an undue risk of damage by hurricanes. Figure 79 is a map of the site designation by the U.S. Landfalling Hurricane Probability Project (2010). The study area does not pose an undue risk of damage by tornadoes. Figure 80 uses the Fujita (F) scale to provide the number and intensity of tornadoes classified as F2 and higher that have occurred within 1,000 mi^2 (2,600 km^2) of the area encompassing the proposed site over the last 5 yr. The number that occurs is approximately one every 5 yr. Estimated property damage due to tornadoes is relatively low in the study area.

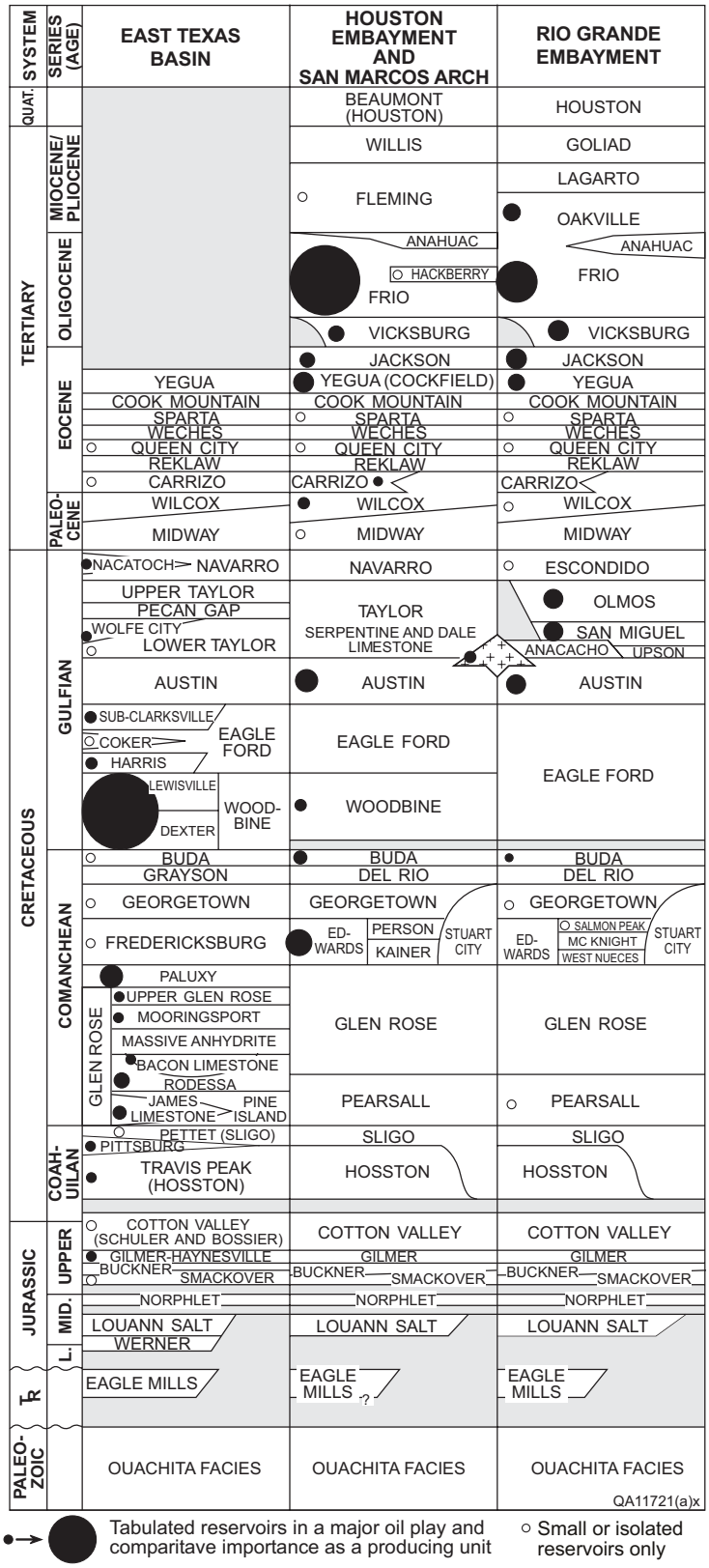

Figure 72. Stratigraphic column and relative oil production for Gulf Coast and East Texas Basins (after Galloway et al., 1983)

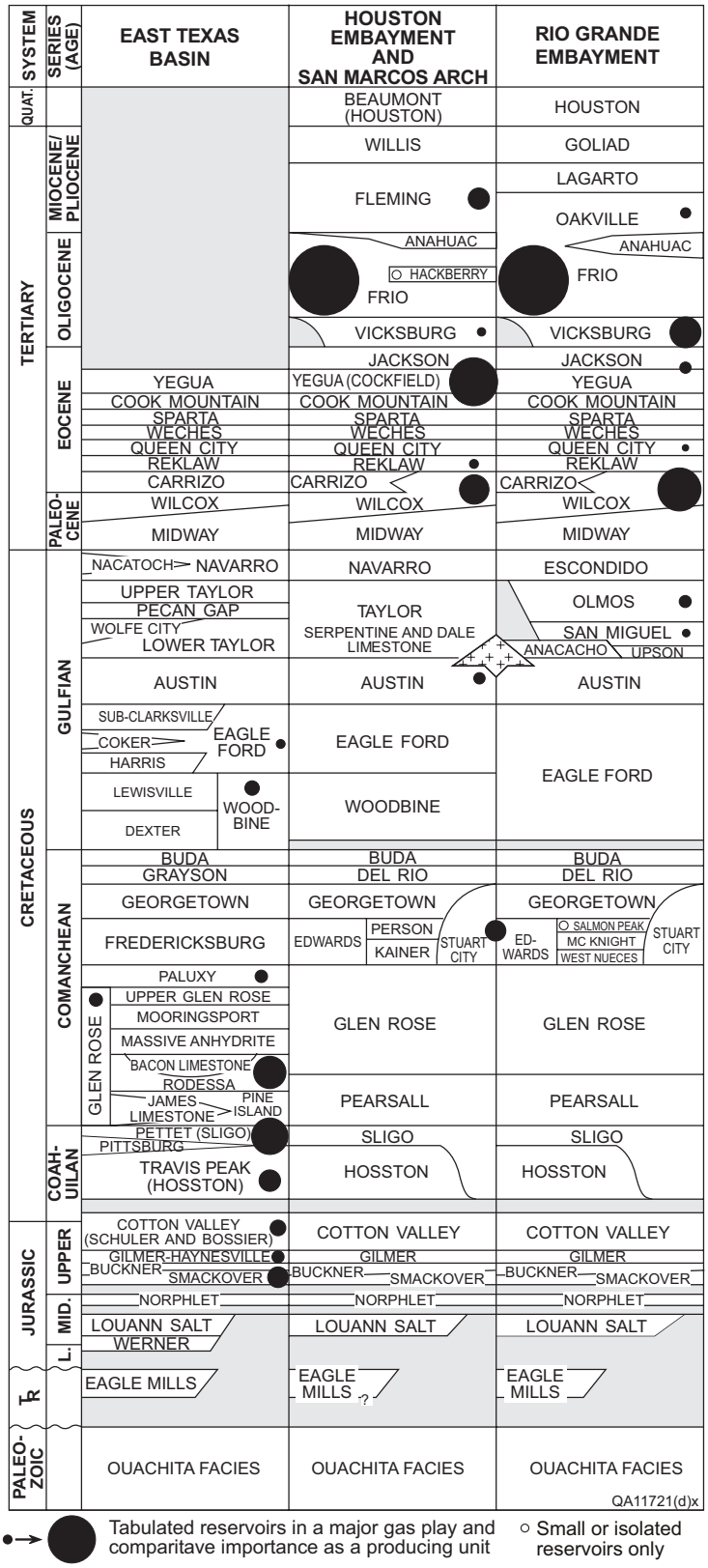

Figure 73. Stratigraphic column and relative gas production for Gulf Coast and East Texas Basins (after Kosters et al., 1989)

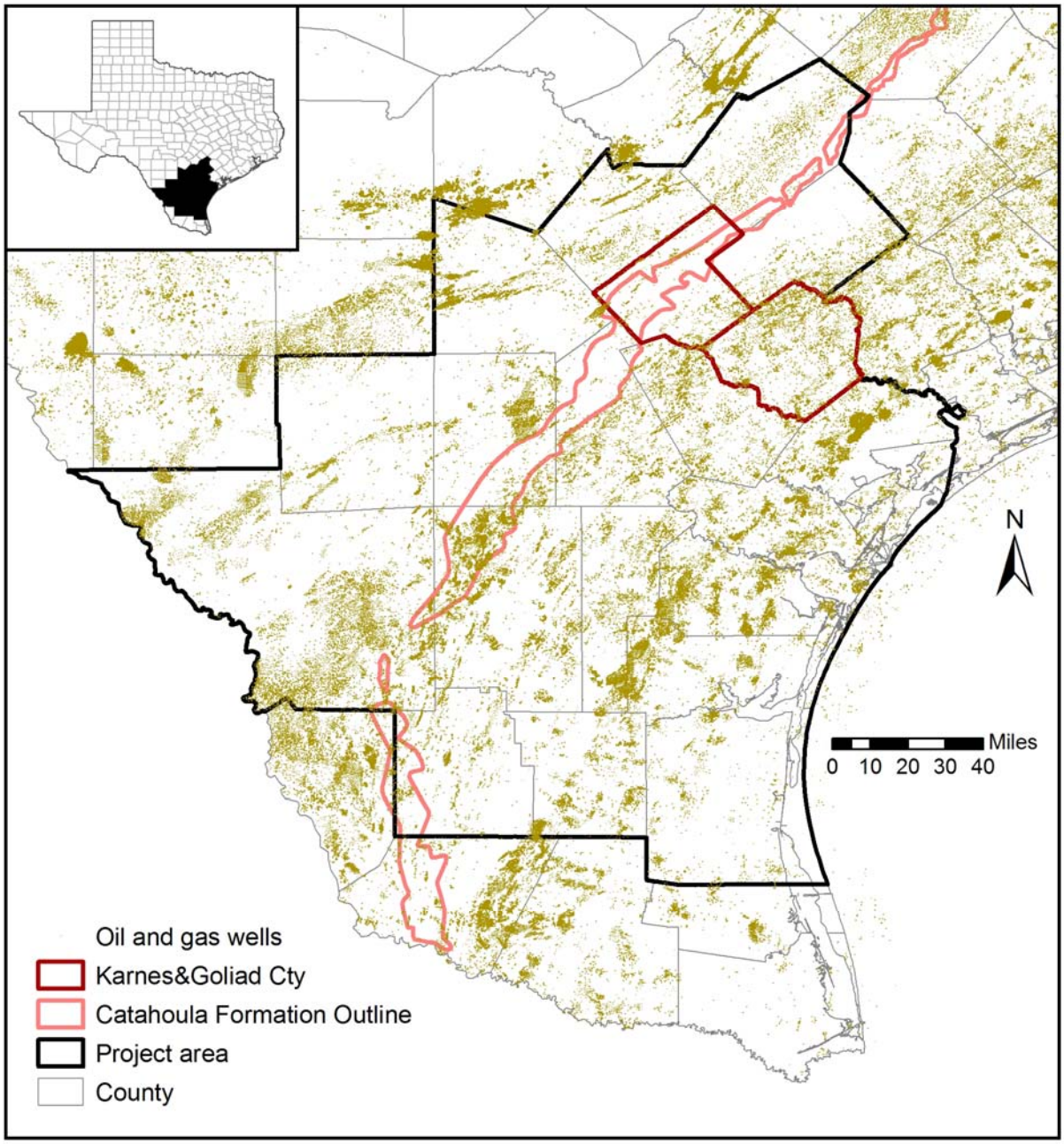

Source: RRC

Figure 74. Surface location of oil and gas wells

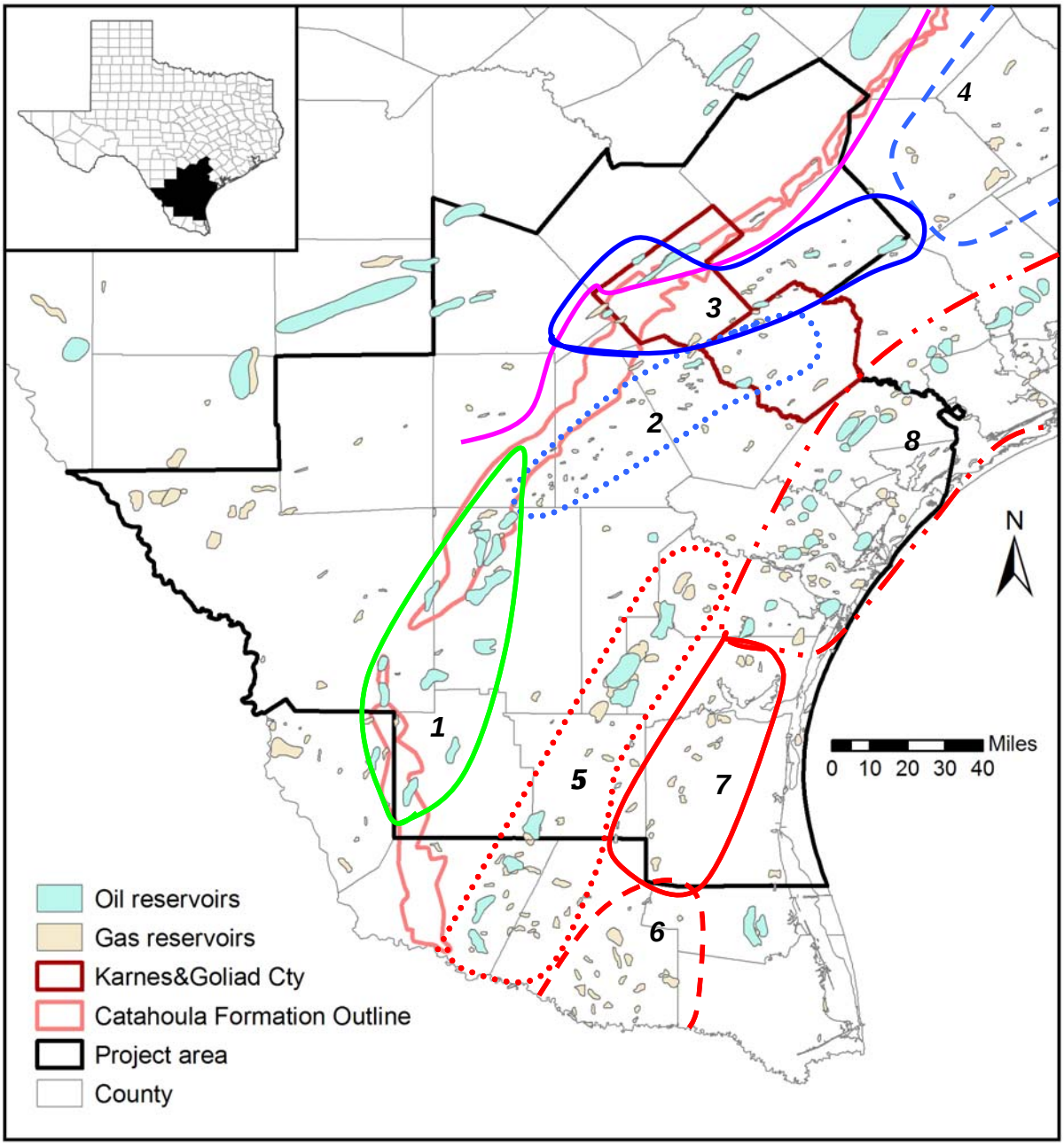

Approximate south boundary of Cretaceous-age reservoirs
Jackson-Yegua Barrier/Strandplain Sandstone play (1)
Wilcox Deltaic Sandstone play (Rio Grande Embayment) (2)
Wilcox Fluvio-Deltaic Sandstone play (3)
Wilcox Deltaic Sandstone (Houston Embayment) play (4)
Vicksburg Fault Zone Vicksburg and Frio Fluvial/Deltaic Sandstone play (5)
Frio Delta-Front/Shoreline Sandstone (Rio Grande Embayment) play (6)
Proximal Frio Deltaic Sandstone play (7)
Frio Barrier/Strandplain Sandstone play (8)

Source of reservoir footprint: Galloway et al. (1983) and Kosters et al. (1989)

Figure 75. Approximate location of major oil and gas fields

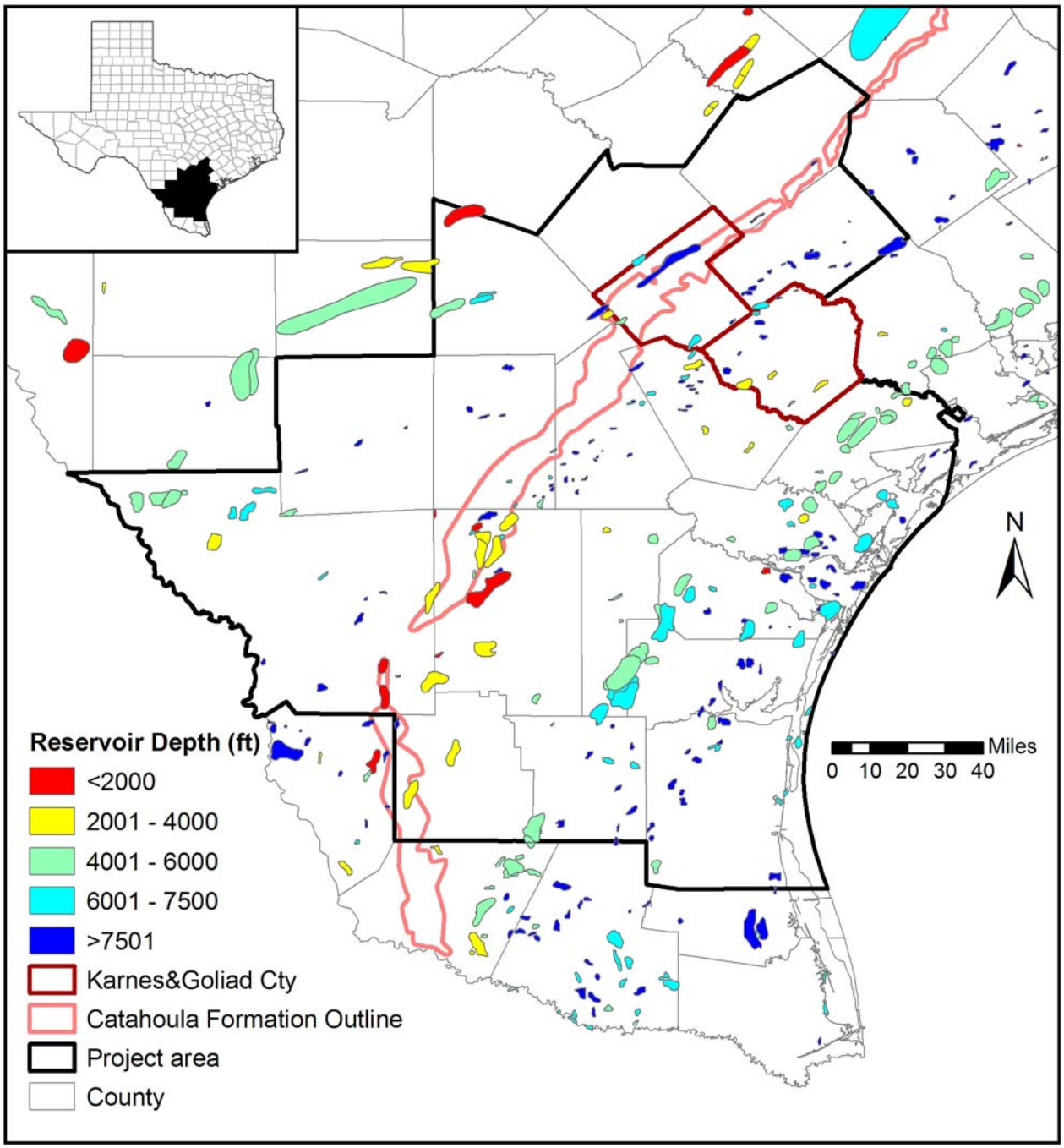

Source of reservoir footprint and depth information: Galloway et al. (1983) and Kosters et al. (1989)

Figure 76. Color-coded map of oil and gas reservoir depth

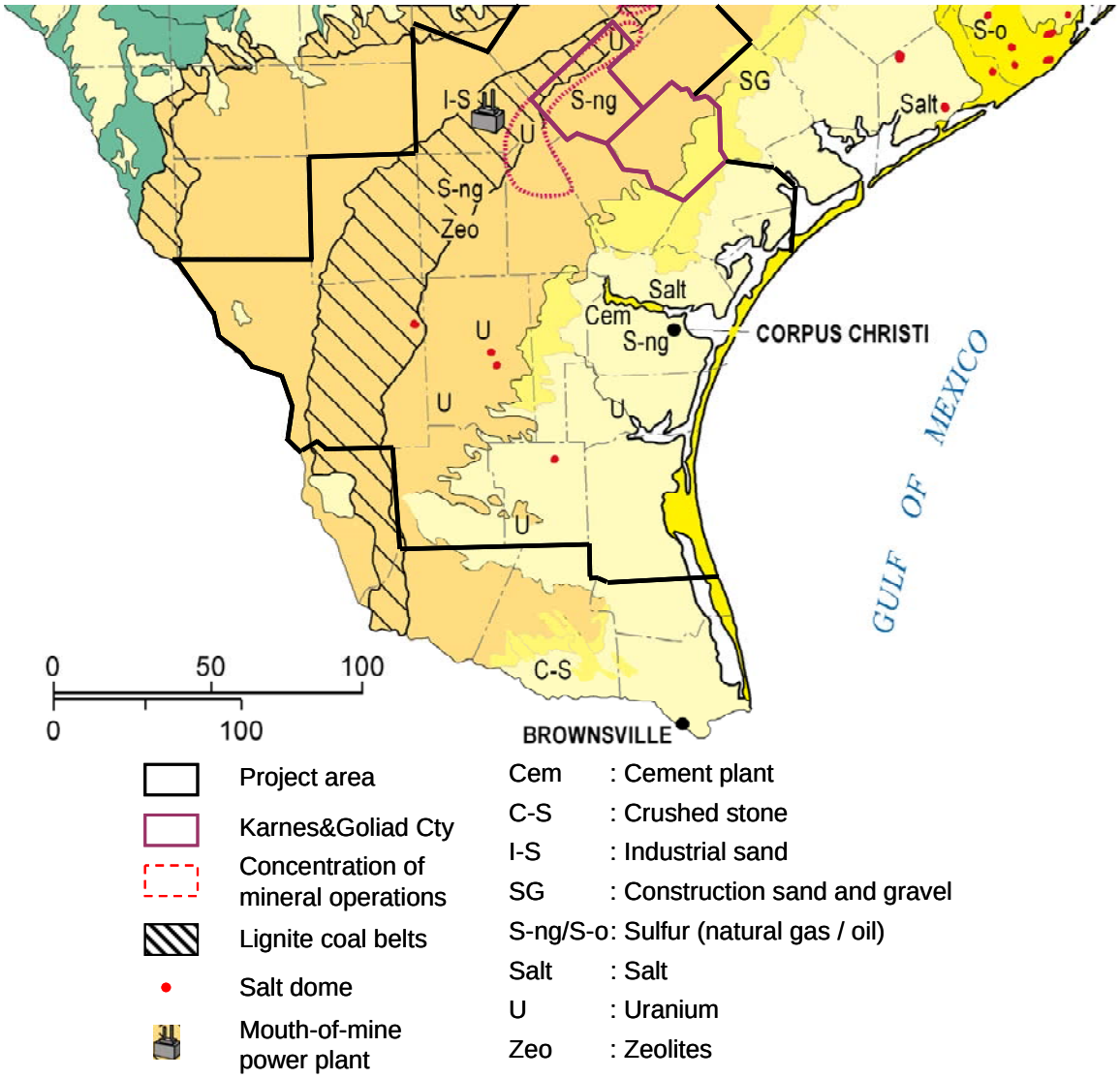

Source: Kyle (2008)

Figure 77. Map of industrial minerals in South Texas

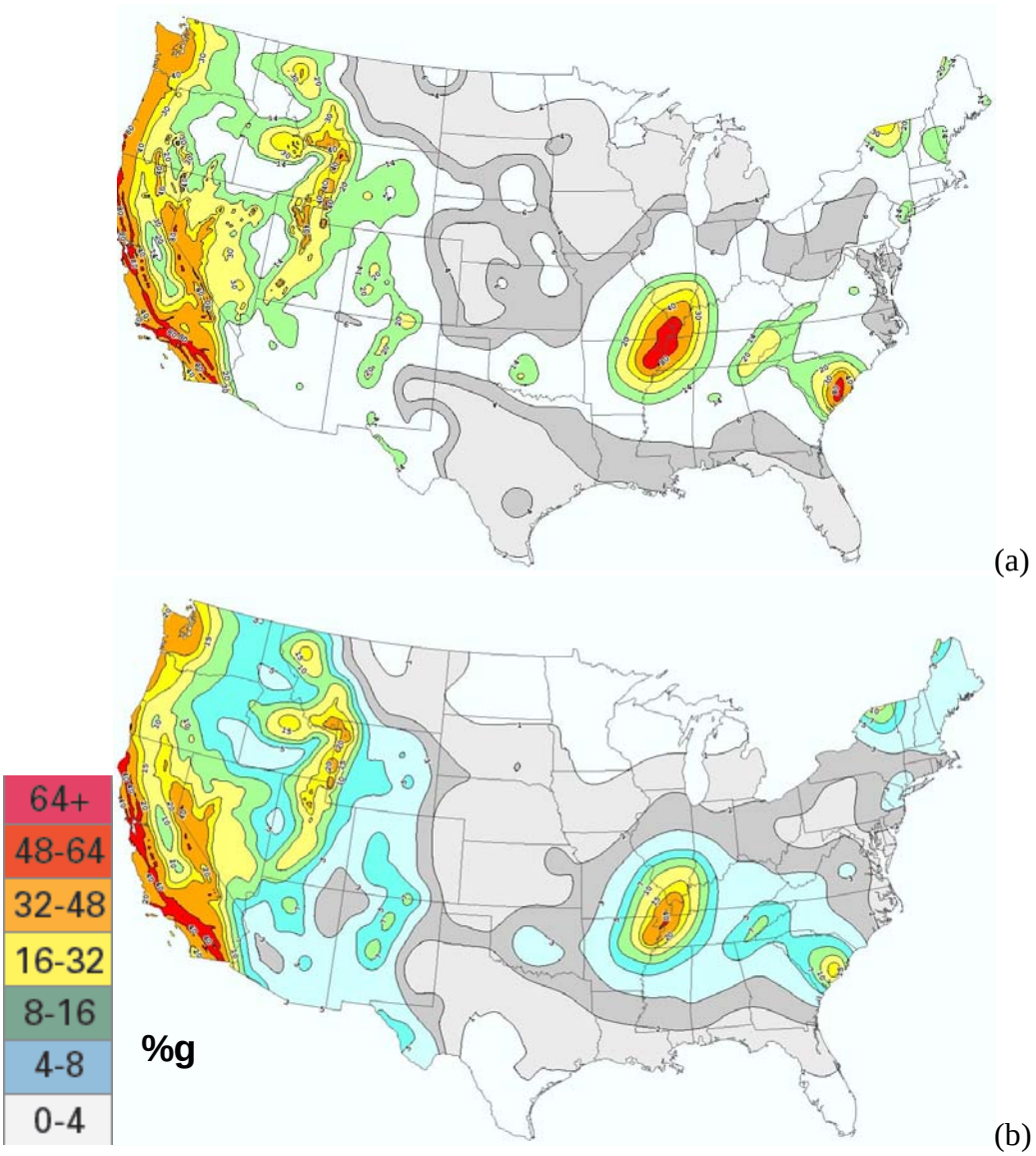

Source: Petersen et al. (2008a, b) and Rukstales (2008) for details

Figure 78. Peak horizontal acceleration (%g) with (a) 2% and (b) 10% probability of exceedance in 50 yr in the continental U.S.

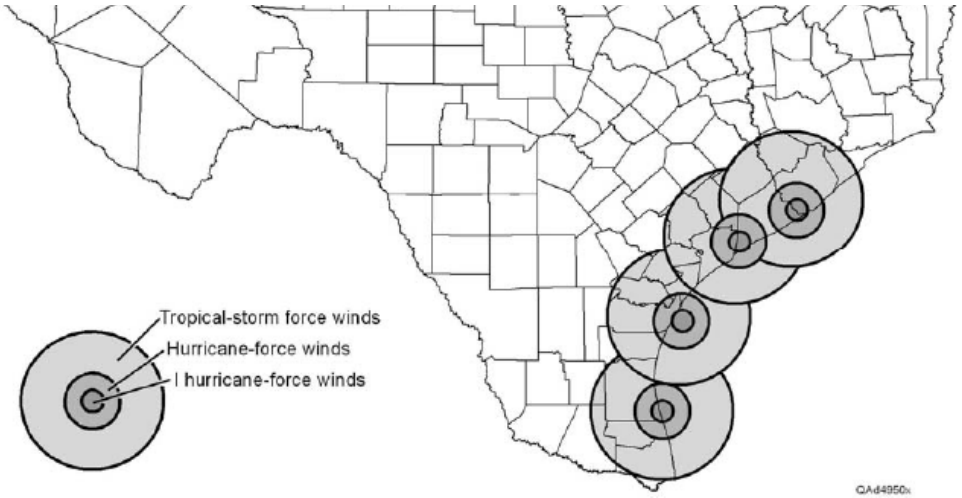

Source: U.S. Landfalling Hurricane Probability Project (2010) and FutureGen Texas (2007)

Figure 79. Site designation by U.S. Landfalling Hurricane Probability Project

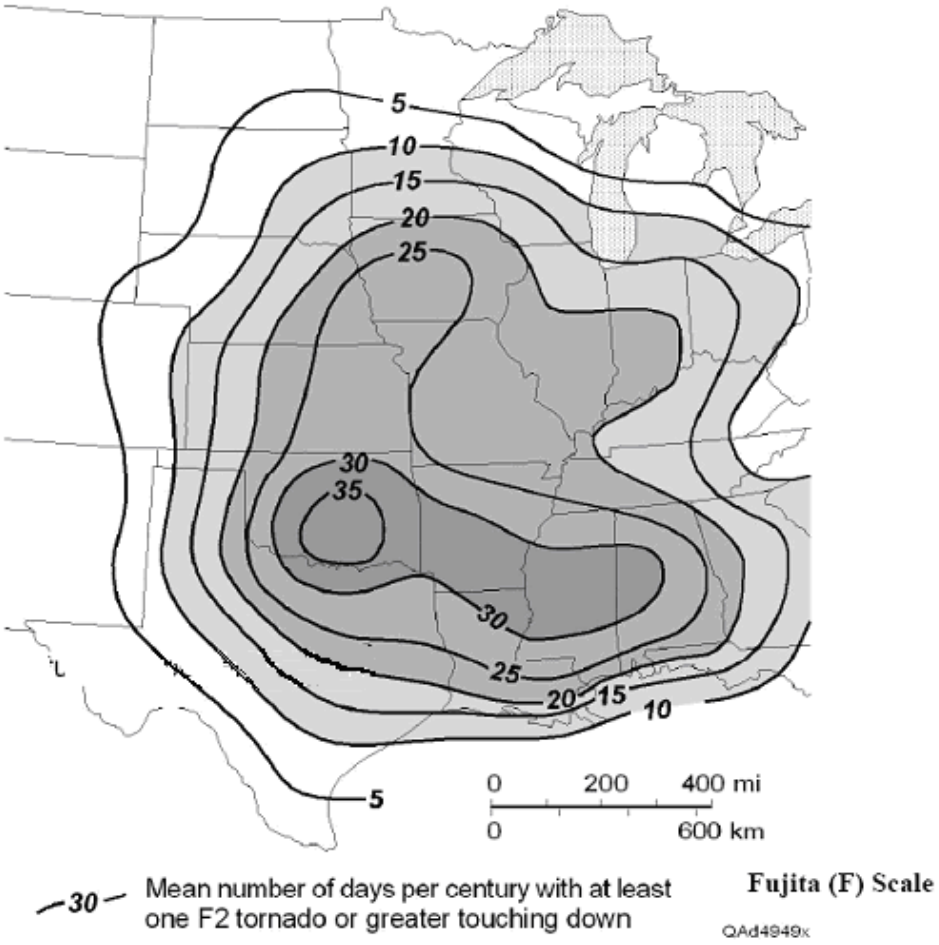

Source: FutureGen Texas (2007)

Figure 80. Contour plot of tornado intensity based on years 2002–2006

VIII. Uranium Exploration

Uranium exploration is not different in principle from exploration for other mineral resources (e.g., Moon et al., 2006). In broad terms, the process involves several steps—from regional studies, to prospects, to reserves estimation in individual deposits. Exploration techniques typically use geology, geophysics, and geochemistry at different spatial scales. Mineral exploration in a given province is generally thought of as consisting of four broad phases: (1) preliminary studies, (2) reconnaissance-phase airborne geophysics and stream / lake sediment geochemistry (the NURE program), (3) reconnaissance follow-up, and (4) detailed evaluation. Fundamentals of uranium exploration have not changed significantly since they were laid out by, for example, Dickinson and Duval (1977) for the STU Province. Galloway (1977, p. 49) outlined exploration potential of the whole Gulf Coast. A postaudit analysis would be required to determine whether his educated guesses were correct. His interpretation was geological and relied mostly on orientation of sand axes relative to dip of the formation (strike-oriented—no potential downdip; dip-oriented—deep potential).

In the earliest steps of a uranium exploration program, explorationists generally follow a conceptual genetic model but stay open minded about possible deviations from the model. In other words, regional studies are often chosen as a function of the prevalent conceptual model. In the STU Province, the model, applicable to the Catahoula, Oakville, and Goliad Formations, consists of looking for structural controls (e.g., faults and salt domes) intersecting with permeable fluvial channels (Galloway, 1977, p. 47). Structural controls are less obvious for uranium deposits in the Jackson Group, and an appropriate conceptual model would involve looking for organic-rich facies. More generally, uranium source, enrichment mechanism, pyrite or organic matter abundance, and redox front location are all elements to be considered. And yet geological considerations are not enough because not all favorable structures / traps are mineralized. Presence of abundant pyrite does not necessarily translate into economic accumulation or even into uranium concentrations higher than background. Similarly, looking for the current position of the redox front may not be useful in finding resulfidized accumulations (i.e., fossilized paleoredox fronts). Another example of deviation from the accepted accumulation model might be found in East Texas. According to the current conceptual model, this area would not be a good region to look for roll-front-type uranium deposits because current understanding of the roll-front genetic model suggests that East Texas lacks a concentration mechanism. Whereas because uranium was also leached from local East Texas volcaniclastics, looking for black shales of the same age in a distal depositional environment might make sense. Black shales (rich in organic matter) are known to scavenge metals and host several large deposits worldwide.

The first step is sometimes skipped because more companies simply build on discoveries made by first-entrant companies. Because mineral deposits often occur in clusters, however, follower-entrant companies could secure leases near known deposits and be successful as well. In the reconnaissance mode, airborne surveys and stream sediments (commonly either heavy-mineral- or fine-fraction sorbing metals) help define broad areas of interest. Airborne (airplane, helicopter) radiometrics (gamma-ray spectroscopy) measuring uranium, thorium, and potassium in surficial material are generally combined with aeromagnetic surveys (which typically provides information on depth to basement or igneous bodies). In 1954, an airborne radiometric survey of oil structures (Bunker and MacKellor, 1973) led to the discovery of uranium deposits and

initiated uranium production in the STU Province. Radiometric response is a function of potassium content and elements of the uranium and thorium decay series (Dickinson and Duval, 1977). By accounting for thorium's being separated from uranium at the source and being immobile while uranium remains mobile, workers can map equivalent uranium signal over equivalent thorium signal and help pinpoint uranium potential concentrations. Aerial photographs and remote sensing studies can provide finer structural maps and surface features, such as supergene alteration (e.g., alteration zone, if there is abundant pyrite). Thermal imaging is another aerial technique, which can discriminate formation types, including mineralized areas and their alteration halo (it is unclear whether it has been applied to the STU Province). Geochemical regional studies generally look for a pathfinder element or indicator mineral. The problem with uranium exploration is that associated elements (selenium, arsenic, molybdenum, vanadium, and decay products such as radium, radon, and helium) occur at concentrations barely above that of uranium and are not necessarily more mobile than uranium itself (Rose and Wright, 1980). Uranium is generally considered its own indicator, although mobility of uranium can be limited by easy adsorption of uranyl ions on metal oxides and clays and by formation of secondary uranium minerals (e.g., Cuney and Kyser, 2009, p. 32). Reconnaissance surveys by the NURE program relied on pathfinder elements such as V, Se, Mo, and As, as discussed earlier in the document, but also on Rn and He, which are decay products (as mentioned earlier, Ra is mobile except in the presence of sulfate or large amounts of sorbing material).

Radiometrics can also be effective at the local scale (at outcrops, during borehole logging, or even when they are car borne). Soil-gas measurements of radon and helium can also be a successful technique for locating uranium accumulations. Kreitler et al. (1992, p. 19) postulated that daughter elements such as radium and lead (including radioactive elements visible in radiometric studies) stay behind as the roll front migrates because of the difference in chemical behavior. Cowart and Osmond (1977) noted the importance of calculating the U234:U238 ratio from aqueous samples in order to locate the position of the uranium accumulation—the radioactive halo can therefore be much larger than the chemical uranium accumulation. Geochemical samples can originate from soils, stream sediments, or subsurface or surface-water bodies. Bradshaw and Lett (1980) and Rose and Wright (1980) detailed geochemical exploration techniques for sandstone-type/roll-front deposits. These techniques apply to whole rock/soil, stream sediment, and aqueous samples. Butz (1977) provided examples of successful geochemical exploration targets in the STU Province as part of the NURE program. Biogeochemistry (sampling of plant parts such as roots, leaves, twigs, etc.) has been used for uranium exploration but not extensively in the STU Province to the authors' knowledge (these samples are not on the list of NURE sample types). The technique has worked in the past; for example, Dunn (2007) reported Canadian deposits (not roll-front deposits) at a depth of 300 m with a clear biogeochemical anomaly. Anecdotal biological exploration by sampling vegetation and observing cattle impacted by high trace-element concentration such as molybdenum and arsenic (Henry and Kapadia, 1980) suggests that the method might work in South Texas.

Hydrogeochemistry is not used as often because it requires knowledge of external factors such as pH and Eh for an accurate interpretation of the results, although buried deposits using downhole measurements in water wells could be located following this technique (it is unclear whether it has been applied in the STU Province). The solution-mineral equilibria approach, through computation of saturation indices of common roll-front minerals such as uraninite and coffinite has the potential of pinpointing accumulations (Langmuir and Chatham, 1980; Pirlo and Giblin, 2004). In unrelated studies, Runnells and Lindberg (1981) and Langmuir and Chatham (1980)

proposed computing saturation index values of common uranium minerals. Langmuir and Chatham (1980) found that the approach could detect a significant accumulation 300 m away from the ore body. A similar approach, although focusing on saturation indices of clays, zeolites, and other minerals associated with uranium deposits, was also suggested by Galloway and Kaiser (1980, p. 62). But whether it was ever implemented in the STU Province is unclear.

Surface and downhole geophysics is useful at intermediate and detailed study stages. Electric, induced polarization (IP) or self-potential (SP) methods can provide information about the location vis a vis reducing fluid conduits because they can reveal pyrite-rich areas.

In the last stage of determining the exact extent of accumulation, drilling follows oxidizing conditions downdip then goes along strike to define the extent of the deposit (e.g., Blackstone, 2005; Carothers, 2007, 2008, 2009). These authors discussed ISL development of uranium accumulations at depths of 200 to 500 ft. This relative shallowness in the STU Province allows for extensive drilling, either for exploration purposes or to prove up reserves.

IX. Conclusions

This report provides an overview of the geological and geographical attributes of the South Texas Uranium Province. It relies heavily on the extensive work conducted in the 1970's and 1980's by the BEG and the USGS. More recently, BEG has performed some additional investigations targeting trace elements, particularly arsenic (Scanlon et al., 2005; Gates et al., 2008, 2009). Note that uranium mineralization does not exist in a vacuum and that an accurate description of uranium geochemical behavior must necessarily also explain field observations and measurements of associated elements.

Uranium accumulations and higher-than-average aqueous concentrations of associated elements (arsenic, selenium, molybdenum, vanadium, boron, and fluorine) are generally well understood. Economic uranium deposits resulted from the early leaching of sediments of volcanic origin, followed by transport under oxidizing conditions in high-transmissivity sections of aquifers (stacked fluvial channels). Uranium precipitates from solution when a sharp redox gradient is encountered in the form of some reducing material that is, in most cases, iron sulfides. Associated elements either precipitate from solution with uranium (selenium and molybdenum) or remain in solution and move farther downdip. When reexposed to oxidizing conditions, either through natural erosion or through open-pit mines, uranium reverts back to a soluble state and can migrate according to flow gradients. In oxidizing conditions, uranium and other trace elements are sensitive to pH variations that, in particular, impact sorption on clays and iron and metal oxides.

X. References

Adams, S. S., 1991, Evolution of genetic concepts for principal types of sandstone uranium deposits in the United States, *in* R. W. Hutchinson and R. I. Grauch (eds.), Historical perspectives of genetic concepts and case histories of famous discoveries: Economic Geology Monograph 8, p. 225-248.

Adams, S. S., and R. B., Smith, 1981, Geology and recognition criteria for sandstone uranium deposits in mixed fluvial-shallow marine sedimentary sequences, South Texas: Grand Junction, Colorado, U.S. Department of Energy, Report GJBX-4(81), 154 p. NURE program.

Adidas, E. O. 1991, Ground-water quality and availability in and around Bruni, Webb County, Texas: Austin, Texas Water Development Board, Report LP-209, 51 p.

Alexander, W. G, Jr., B. N. Meyers, and O. C. Date, 1964, Reconnaissance investigation of the groundwater resources of the Guadalupe, San Antonio, and Nueces river basins, Texas: Texas Water Commission Bulletin 6409.

Alexander, W. G, Jr., and D. E. White, 1966, Ground-water resources of Atascosa and Frio Counties, Texas: Texas Water Commission Report No. 32.

Ambrose, W. A., 2007, Depositional systems of uranium in south Texas: Gulf Coast Association of Geological Societies Transactions, 57, p. 5-16.

Anders, R. B., 1957, Ground-water geology of Wilson County, Texas: Texas Water Commission Bulletin 5710.

Anders, R. B., 1960, Ground-water geology of Karnes County, Texas: Texas Water Commission Bulletin 6007.

Anders, R. B., 1963, Ground-water geology of Karnes County, Texas: U.S. Geological Survey Water Supply Paper 1539-G, 40 p.

Anders, R. B., and E. T. Baker, 1961, Ground-water geology of Live Oak County, Texas: Texas Water Commission Bulletin 6105.

Anderson, M. P., and W. W. Woessner, Applied groundwater modeling: San Diego, Academic Press, 1992.

Arthur R. C., T. Iwatsuki, E. Sasao, R. Metcalfe, K. Amano, and K. Ota, 2006, Geochemical constraints on the origin and stability of the Tono Uranium Deposit, Japan: Geochemistry: Exploration, Environment, Analysis, 6(1), p.33-48.

Aronow, S., T. E. Brown, J. L. Brewton, D. H. Eargle, and V. E. Barnes, 1987, Beeville-Bay City Sheet: The University of Texas at Austin, Bureau of Economic Geology Geologic Atlas of Texas, scale 1:250,000.

Arredondo, A. G., 1991, Geology and hydrogeology of the Kingsville Dome in situ leach uranium mine: Texas A&I University, Master's thesis.

Arredondo, A. G., and W. F. Thomann, 2005, A computer simulation and evaluation of groundwater resources in the Evangeline aquifer in the area of Kleberg County, Texas: The Texas Journal of Science, 57(2), p.115-136

Ashworth, J. B. and J. Hopkins, 1995, Major and minor aquifers of Texas: Austin, Texas Water Development Board, Texas Report 345.

Asquith, W. H., and M. C. Roussel, 2004, Atlas of depth-duration frequency of precipitation annual maxima for Texas: U.S. Geological Survey Scientific Investigation Report 2004-5041, 114 p.

Baker, E. T., Jr., 1965, Ground-water resources of Jackson County, Texas: Texas Water Development Board Report 1.

Baker, E. T., 1979, Stratigraphic and hydrogeologic framework of part of the Coastal Plain of Texas: Texas Department of Water Resources, Austin, Texas Report No. 236, 43 p.

Baker, E. T., Jr., 1986, Hydrology of the Jasper aquifer in the southeast Texas Coastal Plain: Texas Water Development Board, Austin, Texas Report 295, 64 p.

Baker, E. T., Jr., 1995, Stratigraphic nomenclature and geologic sections of the gulf coastal plain of Texas: U.S. Geological Survey Open-File Report 94-461, 34 p.

Beaman, M., and W. M. McGee, 2002, Geodatabase of the South Texas Uranium District: Gulf Coast Association of Geological Societies Transactions, 52, p.39-42.

Beaman, M., and P. Tissot, 2004, Radon in ground waters of the South Texas Uranium District: Proceedings of the 2004 ESRI Education User Conference, San Diego, California, August 9–13, 2004, http://proceedings.esri.com/library/userconf/proc04/docs/pap1842.pdf

Blackstone, R. E., 2005, Technical report on the Palangana and Hobson uranium in-situ leach project, Duval and Karnes Counties, Texas, prepared for Standard Uranium Inc., Vancouver, BC, 77 p.

Blum, M. D., 1992, Modern depositional environments and recent alluvial history of the lower Colorado River, Gulf Coastal plain of Texas: The University of Texas at Austin, Ph.D. dissertation.

Bomber, B. J., E. B. Ledger, and T. T. Tieh, 1986, Ore petrography of a sedimentary uranium deposit: Live Oak County, Texas: Economic Geology, 81, p.131-142.

Bornhauser, M., 1958, Gulf coast tectonics: American Association of Petroleum Geologists Bulletin, v. 42, p. 339-370.

Bradshaw, P. M. D. and R. E. W. Lett, 1980, Geochemical exploration for uranium using soils, *in* R. H. Carpenter (ed.), Geochemical exploration for uranium: Journal of Geochemical Exploration, 13, p. 305-319.

Brady, P. V., C. F. Jove-Colon, G. Carr, and F. Huang, 2002, Soil radionuclide plumes, *in* P .C. Zhang and P. V. Brady (eds.) Geochemistry of soil radionuclides: Soil Science Society of America, SSSA Special Publication No. 59, p.165-190.

Brandenberger, J. P. Louchouarn, B. E. Herbert, and P. Tissot, 2004, Geochemical and hydrodynamic controls on arsenic and trace metal cycling in a seasonally stratified U.S. sub-tropical reservoir: Applied Geochemistry 19, p. 1601-1623.

Brogdon, L. D., C. A. Jones, and J. V. Quick, 1977, Uranium favorability by lithofacies analysis, Oakville and Goliad Formations, South Texas: Gulf Coast Association of Geological Societies Transactions, 27, p. 32-40.

Brown, T. E., N. B. Waechter, F. Owens, I. Howeth, and V. E. Barnes, 1976, Crystal City-Eagle Pass sheet: The University of Texas at Austin, Bureau of Economic Geology, Geologic Atlas of Texas, scale 1:250,000.

Bunker C. M. and J. A. MacKallor, 1973, Geology of the oxidized ore uranium deposits of the Tordilla Hill-Deweesville area, Karnes County, Texas: a study of a district before mining: U.S. Geological Survey Professional Paper 765, 37 p.

Burns, P. C., and R. Finch, 1999, Uranium: mineralogy, geochemistry and the environment: Mineralogical Society of America, Reviews in Mineralogy, 38, 679 p.

Butz, T.R., 1977. Uranium geochemical survey of the Crystal City—Beeville quadrangles, Texas: U.S. Department of Energy, Open-File Report GJBX-77 (77), p. 99-132.

Byerly, G. R., 1991, Nature of igneous activity, *in* A. Salvador, editor, The Gulf of Mexico basin: Boulder, Colorado, The Geology of North America, Geological Society of America, v. J., p. 91-108.

Carothers, T. A., 2007, Technical report for Uranium Energy Corp.'s Goliad project in situ recovery uranium property, Goliad County, Texas, prepared for Uranium Energy Corp., Austin, TX, October 4, variously paginated,

Carothers, T. A., 2008, Technical report for Uranium Energy Corp.'s Goliad project in situ recovery uranium property, Goliad County, Texas, prepared for Uranium Energy Corp., Austin, TX, March 7, 2008, variously paginated; last accessed February 2009 http://www.uraniumenergy.com/_resources/reports/goliad_ni43-101.pdf ,

Carothers, T. A., 2009, Technical report for Uranium Energy Corp.'s Nichols project, Karnes County, Texas, prepared for Uranium Energy Corp., Austin, TX, January 21, 2009, variously paginated.

Carr J. E., W. R. Meyer, W. M. Sandeen, and I. R. McLane, 1985, Digital models for the simulation of ground-water hydrology of the Chicot and Evangeline aquifers along the gulf coast of Texas: Texas Department of Water Resources Report 289.

CCGS (Corpus Christi Geological Society), 1975, Triple energy field trip, Duval, Webb & Zapata Counties, Texas: uranium, coal, gas, guidebook of April 18–19, 1975 field trip, 23 p.

Cech, I., C. W. Kreitler, H. M. Prichard, A. Holguin, and M. Lemma, 1988, Radon distribution in domestic water of Texas: Ground Water, 26(5), p. 561-569.

Cech, I. M., H. M. Prichard, A. Mayerson, and M. Lemma, 1987, Pattern of distribution of radium 226 in drinking water of Texas: Water Resources Research, 23(10), p. 1987-1995.

Cherepon, A. J., J. E. Brandt, and W. E. Galloway, 2007, Geology of the Karnes Uranium District: Austin Geological Society Field Guidebook 27, 85 p.

Chowdhury, A. H., R. Boghici, and J. Hopkins, 2006, Hydrogeochemistry, salinity distribution, and trace constituents: implications for salinity sources, geochemical evolution, and flow systems characterization, Gulf Cost aquifer, Texas, *in* R. E. Mace, S. C. Davidson, E. S. Angle, and W. F. Mullican (eds.), Aquifers of the Gulf Coast of Texas: Texas Water Development Board, Report 365, p. 81-128.

Chowdhury, A. H., and R. E. Mace, 2003, A groundwater availability model of the Gulf Coast aquifer in the Lower Rio Grande Valley, Texas: numerical simulations through 2050: Texas Water Development Board Report, October, 171 p.

Chowdhury, A. H., and R. E. Mace , 2006, Groundwater models of the Gulf Coast aquifer of Texas, *in* R. E. Mace, S. C. Davidson, E. S. Angle, and W. F. Mullican (eds.), Aquifers of the gulf coast of Texas: Texas Water Development Board, Report 365, p. 173-203.

Chowdhury, A. H., and R. E. Mace. 2007, Groundwater resource evaluation and availability model of the Gulf Coast aquifer in the Lower Rio Grande Valley of Texas: Texas Water Development Board, Report 368, 119 p.

Chowdhury, A. H., and M. J. Turco, 2006, Geology of the Gulf Coast aquifer, Texas, *in* R. E. Mace, S. C. Davidson, E. S. Angle, and W. F. Mullican (eds.), Aquifers of the gulf coast of Texas: Texas Water Development Board, Report 365, p. 23-50.

Chowdhury, A. H., S. Wade, R. E. Mace, and C. Ridgeway, 2004, Groundwater availability model of the central Gulf Coast aquifer system: numerical simulations through 1999: Texas Water Development Board Report, September 2004, 108 p

Cloos, E., 1962, Experimental analysis of gulf coast fracture patterns: American Association of Petroleum Geologists Bulletin, v. 52, p. 420-444.

Cook, T. D., 1979, Exploration History of South Texas Lower Cretaceous Carbonate Platform, AAPG Bulletin, 63(1), p. 32-49

Core Laboratories Inc., 1972, A survey of the subsurface saline water of Texas: Texas Water Development Board, Report 157, Vol. 1, 113 p.

Cossey, S. P. J. and H. J. Frank, 1983, Uranium mineralization and use of resistance log character in deltaic point bars: Franklin mine, Karnes County, Texas: AAPG Bulletin, 67(1), p. 131-151.

Cowart, J. B. and J. K. Osmond, 1977, Uranium isotopes in groundwater: their use in prospecting for sandstone-type uranium deposits: Journal of Geochemical Exploration, 8, p.365-379.

Cuney, M., and K. Kyser (eds.), 2009, Recent and not-so-recent developments in uranium deposits and implications for exploration: Mineralogical Association of Canada, Quebec, Canada, 257 p.

Dale, O. C., 1952, Ground-water resources of Starr County, Texas: Texas Water Commission Bulletin 5209.

Dale, O. C., E. A. Moulder, and T. Aranow, 1957, Ground-water resources of Goliad County, Texas: Texas Water Commission Bulletin 5711.

De Soto, R. H. 1978. Uranium geology and exploration: lecture notes: Colorado School of Mines, March, 396 p.

Deussen, A. and R. B. Dole, 1916, Ground water in LaSalle and McMullen Counties, Texas, *in* U.S. Geological Survey Water Supply Paper 375, p. 141-177

Dickinson, K. A., 1976, Geologic controls of uranium deposition, Karnes County, Texas: U.S. Geological Survey Open File Report 76-331, 16 p.

Dickinson, K. A., and J. S. Duval, 1977, Trend areas and exploration techniques—South-Texas uranium: geologic controls, exploration techniques, and potential, *in* Geology [and environmental considerations] of alternate energy resources, uranium, lignite, and geothermal energy in the south central states, Chapter 2: Houston Geological Society , p. 45-66.

Doering, J., 1935, Post-Fleming surface formations of southeast Texas and south Louisiana: American Association of Petroleum Geologists Bulletin, 19(5), p. 651-688.

Dunn, C. E., 2007, Biogeochemistry in mineral exploration: handbook of exploration and environmental geochemistry series, v. 9, 460 p.

Dutton, A. R., and B. C. Richter, 1990, Impact of surface- and ground-water management strategies on ground-water resources of the Gulf Coast aquifer in Wharton and Matagorda Counties, Texas: The University of Texas at Austin, Bureau of Economic Geology, report prepared under contract IAC (88-89)0910 for Lower Colorado River Authority, 66 p.

Duval, J. S., 2005, Radon in soils of parts of Cameron, Hidalgo, and Willacy Counties, Texas: U.S. Geological Survey Open-File Report 2005-1423, online report only, last accessed December 2009, http://pubs.usgs.gov/of/2005/1423/,

Eargle, D. H., 1959, Stratigraphy of Jackson Group (Eocene), South-Central, Texas: American Association of Petroleum Geologists Bulletin, 43, p. 2623-2635.

EIA, 2003, U.S. Uranium reserves estimates by state, http://www.eia.doe.gov/cneaf/nuclear/page/reserves/uresst.html, last accessed February 2009.

EPA, 1999, Understanding variation in partition coefficient, Kd, values: review of geochemistry and available Kd values for cadmium, cesium, chromium, lead, plutonium, radon, strontium, thorium, tritium (3H), and uranium: EPA 402-R-99-004B, vol. 2, variously paginated, http://www.epa.gov/radiation/cleanup/402-r-99-004.html, last accessed February 2010.

EPA, 2006, Uranium location database compilation: EPA 402-R-05-009, August, 26 p., http://epa.gov/radiation/tenorm/pubs.html, last accessed February 2009.

Ewing, T. E., 1990, Tectonic map of Texas: The University of Texas at Austin. Bureau of Economic Geology, scale 1:750000, 4 sheets.

Ewing, T. E., 1991, The tectonic framework of Texas: The University of Texas at Austin. Bureau of Economic Geology, 36 p.

Finch, W. I., 1996, Uranium provinces of North America—their definition, distribution, and models: U.S. Geological Survey Bulletin 2141.

Finch, W. I., 1997, Uranium, its impact on the national and global energy mix—and its history, distribution, production, nuclear fuel-cycle, future, and relation to the environment: U.S. Geological Survey Circular 1141.

Fisher, W. L. and J. H. McGowen, 1967, Depositional systems of the Wilcox Group of Texas and their relationship to occurrence of oil and gas: Gulf Coast Association of Geological Societies Transactions, 17, p. 105-125.

Fisher, W. L., C. V. Proctor, W. E. Galloway, and J. S. Nagle, 1970, Depositional systems in the Jackson Group of Texas-Their relationship to oil, gas, and uranium: Gulf Coast Association of Geological Societies Transactions, 20, p. 234-261.

Fishman, N. S., R. L. Reynolds, and M. B. Goldhaber, 1982, Geochemical and mineralogic data from the Lamprecht and Felder uranium deposits, Live Oak County, Texas U.S. Geological Survey Open-File Record 82-749, 32 p.

Folk, R. L., 1974, The petrology of sedimentary rocks: Austin, Texas, Hemphill Publishing Co., 182 p.

Follett, C. R., and R. K. Gabrysch, 1965, Ground-water resources of Dewitt County, Texas: Texas Water Commission Bulletin 6518.

Freeze, R. A., and J. A. Cherry, 1979, Groundwater: Englewood Cliffs, NJ, Prentice-Hall, 604 p.

FutureGen Texas, 2007, Final submission to FutureGen Industrial Alliance, Inc., for FutureGen Facility host site request for proposal by The University of Texas at Austin, Bureau of Economic Geology.

Galloway, W. E., 1977, Catahoula Formation of the Texas coastal plain: depositional systems, composition, structural development, ground-water flow history, and uranium deposition: The University of Texas at Austin, Bureau of Economic Geology Report of Investigations No. 87, 59 p.

Galloway, W. E., 1978, Uranium mineralization in a coastal-plain fluvial aquifer system, Catahoula Formation, Texas: Economic Geology, 73, p. 1655-1673.

Galloway, W. E., 1982a. Epigenetic zonation and fluid flow history of uranium-bearing fluvial aquifer systems, south Texas uranium province: The University of Texas at Austin, Bureau of Economic Geology Report of Investigations No. 119, 31 p.

Galloway, W. E., 1982b, Depositional architecture of Cenozoic Gulf Coastal Plain fluvial systems: The University of Texas at Austin, Bureau of Economic Geology, Geological Circular 82-5, 29 p. Reprinted from SEPM Special Publications 31, *Recent and ancient non-marine depositional environments: Models for exploration*, August 1981.

Galloway, W. E., T. E. Ewing, C. M. Garrett Jr., N. Tyler, and D. G. Bebout, 1983, Atlas of major Texas oil reservoirs: The University of Texas at Austin, Bureau of Economic Geology, 139 p.

Galloway, W. E., R. J. Finley, and C. D. Henry, 1979a, South Texas uranium province geologic perspective: The University of Texas at Austin, Bureau of Economic Geology Guidebook No. 18, 79 p.

Galloway, W. E., P. E. Ganey-Curry, X. Li, and R. T. Buffler, 2000, Cenozoic depositional history of the Gulf of Mexico basin: AAPG Bulletin, 84, p. 1743-1774.

Galloway, W. E., C. D. Henry, and G. E. Smith, 1982a, Depositional framework, hydrostratigraphy, and uranium mineralization of the Oakville sandstone (Miocene), Texas coastal plain: The University of Texas at Austin, Bureau of Economic Geology Report of Investigations No. 113, 51 p.

Galloway, W. E., C. D. Henry, and G. E. Smith, 1982b, Predicting response of an aquifer system to uranium extraction: Oakville aquifer, Texas Coastal Plain: The University of Texas at Austin, Bureau of Economic Geology, report prepared for U.S. Environmental Protection Agency under grants No. R805357010 and R805357020, 308 p.

Galloway, W. E., and D. K. Hobday, 1996, Terrigenous clastic depositional systems: Springer, 2nd edition, 489 p.

Galloway, W. E., D. K. Hobday, and K. Magara, 1982c, Frio Formation of Texas Gulf Coastal-Plain—Depositional systems, structural framework, and hydrocarbon distribution: AAPG Bulletin, 66, p. 649-688.

Galloway, W. E., L. A. Jirik, R. A. Morton, and J. R. Dubar, 1986, Lower Miocene (Fleming) depositional episode of the Texas Coastal Plain and continental shelf: structural framework, facies, and hydrocarbon resources: The University of Texas at Austin, Bureau of Economic Geology Report of Investigations No 150, 50 p.

Galloway, W. E., and W. R. Kaiser, 1980, Catahoula Formation of the Texas coastal plain: origin, geochemical evolution, and characteristics of uranium deposits: The University of Texas at Austin, Bureau of Economic Geology Report of Investigations No. 100, 81 p.

Galloway, W. E., C. W. Kreitler, and J. H. McGowen, 1979b, Depositional and ground-water flow systems in the exploration for uranium, a research colloquium, September 8–9, 1978: The University of Texas at Austin, Bureau of Economic Geology, 267 p.

Gates, J. B., J.-P. Nicot, B. R. Scanlon, and R. C. Reedy, 2008, Evaluation of elevated arsenic levels in the Gulf Coast aquifer: The University of Texas at Austin, Bureau of Economic Geology, final report prepared for Texas Commission on Environmental Quality, under contract no. 263404-22, 104 p.

Gates, J. B., J.-P. Nicot, B. R. Scanlon, and R. C. Reedy, 2009, Evaluation of elevated arsenic levels in the Gulf Coast aquifer: The University of Texas at Austin, Bureau of Economic Geology, report prepared for Texas Commission on Environmental Quality under Contract No. 582-8-75374, 22 p. + tables and figures.

Goldhaber, M .B., R. L. Reynolds, and R. O. Rye, 1978, Origin of a South Texas roll-type uranium deposit: II. sulfide petrology and sulfur isotope studies: Economic Geology, 73, p.1690-1705.

Goldhaber, M .B., R. L. Reynolds, and R. O. Rye, 1979, Formation and resulfidization of a South Texas roll-front uranium deposit: U.S. Geological Survey Open-File Report 79-1651, 41 p.

Goldhaber, M .B., R. L. Reynolds, and R. O. Rye, 1983, Role of fluid mixing and fault-related sulfide in the origin of the ray-point uranium district, South Texas: Economic Geology, 78, p. 1043-1063.

Groschen, G. E., 1985, Simulated effects of projected pumping on the availability of freshwater in the Evangeline aquifer in an area southwest of Corpus Christi, Texas: U.S. Geological Survey, Water Resources Investigations Report 85-4182, 103 p.

Guilbert, J. M., and C. F. J. Park, 1986, The geology of ore deposits: New York, W. H. Freeman and Company.

Hamilton, D. S., 1994, Increased oil recovery potential from barrier/strandplain reservoirs, Jackson-Yegua trend, by geologically targeted infill drilling: examples from Seventy-Six West and Colmena Hill fields, South Texas: The University of Texas at Austin, Bureau of Economic Geology Report of Investigations No. 217, 52 p.

Hamlin, H. S., 2006, Salt domes in the Gulf Coast aquifer, *in* R. E. Mace, S. C. Davidson, E. S. Angle, and W. F. Mullican (eds.), Aquifers of the gulf coast of Texas: Texas Water Development Board, Report 365, p. 217-230.

Handbook of Texas Online, 2008, Uranium Mining, last updated: January 10, 2008, last accessed February 2009, http://www.tshaonline.org/handbook/online/articles/UU/dku1.html

Harris, H. B., 1965, Ground-water resources of La Salle and McMullen Counties, Texas: Texas Water Commission Bulletin 6520.

Hay, R., 1999, The development and applications of a numerical groundwater flow model of the Gulf Coast aquifer along the South Texas Gulf Coast: Texas A&M University, Corpus Christi, Master's thesis, 47 p.

Hem, J. D., 1985, Study and interpretation of the chemical characteristics of natural water: U.S. Geological Survey Water Supply Paper 2254, 3rd ed., 263 p.

Henry, C. D., W. E. Galloway, and G. E. Smith, 1982b, Considerations in the extraction of uranium from a fresh-water aquifer—Miocene Oakville sandstone, South Texas: The University of Texas at Austin, Bureau of Economic Geology Report of Investigations No. 126, 36 p.

Henry, C. D., W. E. Galloway, G. E. Smith, C. L. Ho, J. P. Morton, and J. K. Gluck, 1982a, Geochemistry of ground water in the Miocene Oakville sandstone—a major aquifer and uranium host of the Texas coastal plain: The University of Texas at Austin, Bureau of Economic Geology Report of Investigations No. 118, 63 p.

Henry, C. D., and R. R. Kapadia, 1980, Trace elements in soils of the south Texas uranium district: concentrations, origin, and environmental significance: The University of Texas at Austin, Bureau of Economic Geology Report of Investigations No. 101, 52 p.

Henry, C. D., and A. W. Walton, 1978, Formation of uranium ores by diagenesis of volcanic sediments: The University of Texas at Austin, Bureau of Economic Geology, report prepared for Bendix Field Engineering Corporation, a prime contractor to U.S. DOE, contract No. 77-067E, variously paginated.

Hershfield, D. M., 1961, Rainfall frequency atlas of the United States for durations from 30 minutes to 24 hours and return periods from 1 to 100 years: Weather Bureau, U.S. Department of Commerce, Technical Paper 40, 61p., http://hdsc.nws.noaa.gov/hdsc/pfds/other/tx_pfds.html, last accessed April 2009.

Hitchon, B., E. H. Perkins, and W. D. Gunter, 1999, Introduction to groundwater geochemistry: Canada, Geoscience Publishing Ltd..

Hobday, D. K., and W. E. Galloway, 1999, Groundwater processes and sedimentary uranium deposits: Hydrogeology Journal, 7, p. 127-138.

Hoel, H. D., 1982, Goliad Formation of the south Texas Gulf Coastal plain: regional genetic stratigraphy and uranium mineralization: The University of Texas at Austin, Department of Geological Sciences, Master's thesis.

Hosman, R. L., 1996, Regional stratigraphy and subsurface geology of Cenozoic deposits, Gulf Coastal Plain, south-central United States: U.S. Geological Paper Professional Paper 1416-G, 35 p., 14 plates in separate case

Hosman, R. L., and Weiss, J. S., 1991, Geohydrologic units of the Mississippi Embayment and Texas Coastal uplands aquifer systems, South-Central United States—regional aquifer system analysis—Gulf Coastal Plain: U.S. Geological Survey Professional Paper 1416-B, 19 p.

Huang, W. H., 1978, Geochemical and sedimentologic problems of uranium deposits of Texas Gulf Coastal plain: AAPG Bulletin, 62(6), p.1049-1062

Ilger, J. D, Ilger, W. A., Zingaro, R. A., and Mohan, M. S., 1987, Modes of occurrence of uranium in carbonaceous uranium deposits: characterization of uranium in a South Texas (U.S.A.) lignite: Chemical Geology, 63(3-4), p.197-216.

Jackson, M. P. A., and Galloway, W. E., 1984, Structural and depositional styles of Gulf Coast Tertiary continental margins—applications to hydrocarbon exploration: American Association of Petroleum Geologists, Continuing Education Course Notes No. 25, 225 p.

Jorgensen, D. G., 1975, Analog-model studies of ground-water hydrology in the Houston district, Texas: Texas Water Development Board Report 190, 84 p.

Kalaswad, S., and J. Arroyo, 2006, Status report on brackish groundwater and desalination in the Gulf Coast aquifer of Texas, *in* R. E. Mace, S. C. Davidson, E. S. Angle, and W. F. Mullican (eds.), Aquifers of the gulf coast of Texas: Texas Water Development Board, Report 365, p. 231-240.

Knox, P. R., V. A. Kelley, A. Vreugdenhil, N. Deeds, and S. Seni, 2007, Structure of the Yegua-Jackson aquifer of the Texas Gulf Coast Plain: Intera, Inc., report prepared for the Texas Water Development Board, variously paginated.

Kosters, E. C., D. G. Bebout, S. J. Seni, C. M. Garrett, Jr., L. F. Brown, Jr., H. S. Hamlin, S. P. Dutton, S. C. Ruppel, R. J. Finley, and N. Tyler, 1989, Atlas of major Texas gas reservoirs: The University of Texas at Austin, Bureau of Economic Geology, 161 p.

Kreitler, C. W., E. Guevera, G. Granata, D. McKalips, 1977, Hydrogeology of Gulf Coast Aquifers, Houston-Galveston Area, Texas, Gulf Coast Association of Geological Societies Transactions, 27, p. 5-16.

Kreitler, C. W., T. J. Jackson, P. W. Dickerson, and J. G. Blount, 1992, Hydrogeology and hydrochemistry of the Falls City uranium mine tailings remedial action project, Karnes County, Texas: The University of Texas at Austin, Bureau of Economic Geology, prepared for the Texas Department of Health under agreement No IAC(92-93)-0389, September, 332 p.

Kyle, J. R., 2008, Industrial minerals of Texas (page-sized map): The University of Texas at Austin, Bureau of Economic Geology.

Lambert, R. B., 2004, Hydrogeology of Webb County, Texas: U.S. Geological Survey Scientific Investigations Report 2004-5022, 7 plates.

Langmuir, D., 1997, Aqueous environmental geochemistry: New Jersey, Prentice Hall, 600 p.

Langmuir, D., and J. R. Chatham, 1980, Groundwater prospecting for sandstone-type uranium deposits: a preliminary comparison of the merits of mineral solution equilibria, and single-element tracer methods, *in* R. H. Carpenter (ed.), Geochemical exploration for uranium: Journal of Geochemical Exploration, 13, p. 201-219.

Lanning-Rush, J., W. H. Asquith, and R. M. Slade, Jr., 1998, Extreme precipitation depths for Texas, excluding the Trans-Pecos region: U.S. Geological Survey Water Resources Investigation Report 98-4099, 38 p.

Larkin, T. J., and G. W. Bomar, 1983, Climatic atlas of Texas: Texas Department of Water Resources LP-192, 151 p.

LBG-Guyton & Associates, 2003, Brackish groundwater manual for Texas Regional Water Planning Groups: Report prepared for the Texas Water Development Board, Austin, Texas, 188 p.

Ledger, E. B., 1981, Evaluation of the Catahoula Formation as a source rock for uranium mineralization, with emphasis on East Texas: Texas A&M University, Ph.D. thesis, 249 p.

Ledger, E. B., T. T. Tieh, and M. W. Rowe, 1984, An evaluation of the Catahoula Formation as a uranium source rock in east Texas: Gulf Coast Association of Geological Societies Transactions, 34, p. 99-108.

Livingston, P. P., and T. W. Bridges, 1936, Ground-water resources of Kleberg County, Texas, *in* U.S. Geological Survey Water Supply Paper 773-D, p. 197-232.

Lonsdale, J. T., 1935, Geology and ground-water resources of Atascosa and Frio Counties, Texas: U.S. Geological Survey Water Supply Paper 676, 90 p.

Lonsdale, J. T., and J. R. Day, 1937, Geology and ground-water resources of Webb County, Texas: U.S. Geological Survey Water Supply Paper 778, 104 p.

Loskot, C. L., W. M. Sandeen, and C. R. Follett, 1982. Ground-water resources of Colorado, Lavaca, and Wharton Counties, Texas: Texas Water Development Board, Report 270.

Ludwig, K. R., R. L. Reynolds, M. B. Goldhaber, and K. R. Simmons, 1982, Uranium-lead isochron age and preliminary sulfur isotope systematics of the Felder uranium deposit, South Texas: Economic Geology and the Bulletin of the Society of Economic Geologists, 787, p. 557-563.

Mace, R. E., S. C. Davidson, E. S. Angle, and W. F. Mullican, III, 2006, Aquifers of the gulf coast of Texas: Texas Water Development Board Report 365, 304 p.

Mason, C. C., 1963, Ground-water resources of Refugio County, Texas: Texas Water Commission Bulletin 6312.

Marvin, R. F., G. H. Shafer, and O.C. Dale, 1962, Ground-water resources of Victoria and Calhoun Counties, Texas: Texas Water Commission Bulletin No. 6202.

Masch, F. D., and K. J. Denny, 1966, Grain-size distribution and its effect on the permeability of unconsolidated sand: Water Resources Research, 2(4), p. 665-677

Maynard, J. B., 1984, Uranium: syngenetic to diagenetic deposits in foreland basins, *in* E. R. Force, J. Eidel, and J. B. Maynard, (eds.) Chapter 15, Sedimentary and diagenetic mineral deposits: a basin analysis approach to exploration: Reviews in Economic Geology, 5, p. 187-197.

McBride, E. F., W. L. Lindemann, and P. S. Freeman, 1968, Lithology and petrology of the Gueydan (Catahoula) Formation in south Texas: The University of Texas at Austin, Bureau of Economic Geology Report of Investigations No. 63, 122 p.

McCoy, T. W., 1990, Evaluation of groundwater resources in the Lower Rio Grande Valley, Texas: Texas Water Development Board, Report 316, 47 p.

McCulloh, R. P., 1982, A preliminary assessment of Louisiana's uranium potential: Gulf Coast Association of Geological Societies Transactions, 32, p. 221-230.

Meyer, W. R., and J. E. Carr, 1979, A digital model for simulation of ground-water hydrology in the Houston area, Texas: Texas Department of Water Resources LP-103, 133 p.

Min, M., H. Xuc, J. Chena, and M. Fayek, 2005, Evidence of uranium biomineralization in sandstone-hosted roll-front uranium deposits, northwestern China: Ore Geology Reviews, 26, p. 198-206.

Mohan, M., J. D. Ilger, and R. A. Zingaro, 1991, Speciation of uranium in a South Texas lignite: additional evidence for a mixed role of evidence: Energy & Fuels, 5, p. 568-573.

Moon, C. J., M. K.G. Whateley, and A. M. Evans (Editors), 2006, Introduction to mineral exploration: Blackwell Publishing, Malden, MA, 2nd Edition, 432 p.

Morton, R. A., L. A. Jirik, and W. E. Galloway, 1988, Middle-upper Miocene depositional sequences of the Texas coastal plain and continental shelf: geologic framework, sedimentary facies, and hydrocarbon plays: The University of Texas at Austin, Bureau of Economic Geology Report of Investigations No. 174, 40 p.

Moxham, 1964, Radioelement dispersion in a sedimentary environment and its effect on uranium exploration: Economic Geology, 59, p. 309-321.

Muller, D. A., and R. D. Price, 1979, Groundwater availability in Texas, estimates and projection through 2030: Texas Department of Water Resources, 238, 77 p.

Myers, B. N., and O. C. Dale, 1966, Ground-water resources of Bee County, Texas: Texas Water Development Board Report 17.

Myers, B. N., and O. C. Dale, 1967, Ground-water resources of Brooks County, Texas: Texas Water Development Board Report 61.

NCDC (National Climatic Data Center, operated by NOAA), 2009, Heavy rainfall frequencies for the U.S., http://www.ncdc.noaa.gov/oa/documentlibrary/rainfall.html, last accessed February 2010.

Nicot, J.-P., 2008, Methodology for bounding calculations of nuclear criticality of fissile material accumulations external to a waste container at Yucca Mountain, Nevada: Applied Geochemistry, 23, p. 2065-2081.

Nordstrom, P. L., and R. Quincy, 1999, Ground-water data system dictionary: Texas Water Development Board, Report UM-50, 104 p.

NURE (National Uranium Resource Evaluation) database available for the State of Texas at http://pubs.usgs.gov/of/1997/ofr-97-0492/state/nure_tx.htm, last accessed February 2010.

Okerman, D. J., and B. L. Petri, 2001, Hydrologic conditions and water quality in an agricultural area in Kleberg and Nueces Counties, Texas, 1996–98: U.S. Geological Survey Water Resources Investigation Report 01-4101, 37 p. + appendices

Osmond, J. K.. and J. B. Cowart, 1981, Uranium-series disequilibrium in ground water and core composite samples from the San Juan Basin and Copper Mountain research sites: Grand

Junction, CO, U.S. Department of Energy, Bendix Field Engineering Corporation, Report GJBX-364-81.

Parker, D. F., J. G. Krystinik, and B. J. Mckee, 1988, Provenance of the Gueydan Formation, south Texas: implications for the late Oligocene-early Miocene tectonic evolution of the Trans-Pecos volcanic field: Geology, 16, p. 1085-1088.

Petersen, M. D., A. D. Frankel, S. C. Harmsen, C. S. Mueller, K.M. Haller, R. L. Wheeler, R. L. Wesson, Y. Zeng, O. S. Boyd, D. M. Perkins, N. Luco, E. H. Field, C. J. Wills, and K. S. Rukstales, 2008a, Documentation for the 2008 update of the United States national seismic hazard maps: USGS Open-File Report 2008–1128, 128 p.

Petersen, M. D., A. D. Frankel, S. C. Harmsen, C. S. Mueller, K. M. Haller, R. L. Wheeler, R. L. Wesson, Y. Zeng, O. S. Boyd, D. M. Perkins, N. Luco, E. H. Field, C. J. Wills, and K. S. Rukstales, 2008b, U.S. national seismic hazard maps: U.S. Geological Survey Fact Sheet FS-2008-3017, 4 p; http://pubs.usgs.gov/fs/2008/3017/pdf/FS08-3017_508.pdf, last accessed February 2010.

Pettijohn, R. A., 1988, Dissolved-solids concentrations and primary water types, Gulf Coast aquifer systems, south-central United States: U.S. Geological Survey Hydrologic Atlas 706, 12 maps on 2 sheets.

Pettijohn, R. A., J. S. Weiss, and A. K. Williamson, 1988, Distribution of dissolved-solids concentrations and temperature in ground water of the Gulf Coast aquifer systems, south-central United States: U.S. Geological Survey Water-Resources Investigations Report 88-4082, 10 maps on 5 sheets.

Pirlo, M. C. and A. M. Giblin, 2004, Application of groundwater–mineral equilibrium calculations to geochemical exploration for sediment-hosted uranium: Observations from the Frome Embayment, South Australia: Geochemistry: Exploration, Environment, Analysis, v.4, p.113–127.

Preston, R. D., 2006, The Yegua-Jackson Aquifer, *in* R. E. Mace, S. C. Davidson, E. S. Angle, and W. F. Mullican (eds.), Aquifers of the gulf coast of Texas: Texas Water Development Board, Report 365, p. 51-59.

Prudic, D. E., 1991, Estimates of hydraulic conductivity from aquifer-test analyses and specific-capacity data: gulf coast regional aquifer systems, south-central United States: U.S. Geological Survey Water-Resources Investigations Report 90-4121, 38 p.

Quarles, M., 1952, Salt-ridge hypothesis of Texas gulf coast type of faulting: American Association of Petroleum Geologists Bulletin, v. 37, p. 489-508.

Reedy, R. C., Nicot, J.-P., Scanlon, B. R., Deeds, N. E., Kelley, V. A., and Mace, R. E., 2009, Chapter 11. Groundwater recharge in the Carrizo-Wilcox aquifer, *in* Aquifers of the upper coastal plains of Texas: Texas Water Development Board Report 374, p. 185-203.

Rein, H., and J. Hopkins, 2008, Explanation of the groundwater database and data entry: Texas Water Development Board, Report UM-50 Revised 2008, 65 p. + appendices.

Reynolds, R. L., and M. B. Goldhaber, 1978, Origin of a South Texas roll-type uranium deposit: I. Alteration of iron-titanium oxide minerals: Economic Geology and the Bulletin of the Society of Economic Geologists, 73, p. 1677-1689.

Reynolds, R. L., and M. B. Goldhaber, 1983, Iron disulfide minerals and the genesis of roll-type uranium deposits: Economic Geology and the Bulletin of the Society of Economic Geologists, 78, p. 105-120.

Reynolds, R. L., M. B. Goldhaber, and Carpenter, 1982, Biogenic and non-biogenic ore-forming processes in the South Texas Uranium District: evidence from the Panna Maria deposit: Economic Geology and the Bulletin of the Society of Economic Geologists, 77, p. 541-556.

Reynolds, R. L., M .B. Goldhaber, R. O. Rye, N. S. Fishman, K. R. Ludwig, and L. T. Grauch, 1980, History of sulfidization of the Felder uranium deposit, South Texas: U.S. Geological Survey Open-File Report 80-1096, 23 p.

Rose, R. W., and R. J. Wright, 1980, Geochemical exploration models for sedimentary uranium deposits, *in* R. H. Carpenter (ed.), Geochemical exploration of uranium: Journal of Geochemical Exploration, 13, p. 153-179

Runnells, D. D., and R. D. Lindberg, 1981, Hydrogeochemical exploration for uranium ore deposits: use of the computer model WATEQFC: Journal of Geochemical Exploration, 15, p. 37-50.

Rukstales, K. S., 2008, Documentation for the 2008 Update of the United States National Seismic Hazard Maps, USGS Open-File Report 2008–1128, 128 p.

RRC, 1994, South Texas uranium district abandoned mine land inventory: Railroad Commission of Texas, Surface Mining and Reclamation Division, variably paginated.

Ryder, P. D., 1988, Hydrogeology and predevelopment flow in the Texas gulf coast aquifer systems: U.S. Geological Survey Water-Resources Investigation Report 87-4248, 109 p.

Ryder, P. D., and A. F. Ardis, 1991, Hydrology of the Texas gulf coast aquifer systems: U.S. Geological Survey Open-File Report 91-64, 147 p.

Ryder, P. D., and A. F. Ardis, 2002, Hydrology of the Texas gulf coast aquifer systems: U.S. Geological Survey Professional Paper 1416-E, 77 p.

San Juan, F. C., Jr., 1982, A study of uranium and thorium isotopes in ground waters and solids of two uranium mines, South Texas: Florida State University, Ph.D. dissertation, 255 p.

Sayre, A. N., 1937, Geology and groundwater resources of Duval County, Texas: U.S. Geological Survey Water Supply Paper 776.

Scanlon, B. R., Nicot, J.-P., Reedy, R. C., Tachovsky, J. A., Nance, H. S., Smyth, R. C., Keese, K., Ashburn, R. E., and Christian, L., 2005, Evaluation of arsenic contamination in Texas: The University of Texas at Austin, Bureau of Economic Geology, final report prepared for Texas Commission on Environmental Quality under umbrella contract no. 582-4-56385 and work order no. UT-08-5-70828, 167 p.

Schumann, R. R. (ed.), 1993, Geologic radon potential of EPA Region 6; Arkansas, Louisiana, New Mexico, Oklahoma, and Texas: U.S. Geological Survey Open-File Report Number 93-292-F, 160 p.

SECO (State Energy Conservation Office), 2008, Texas renewable energy resource assessment: Texas Comptroller Office, Chapter 2, http://www.seco.cpa.state.tx.us/publications/renewenergy, last accessed April 2009.

Seni, S. J., and S.-J. Choh, 1994, Targeted secondary recovery of hydrocarbons from barrier-bar and tidal-channel facies, Jackson Group, Prado field, South Texas: The University of Texas at Austin, Bureau of Economic Geology, Geological Circular 94-2, 47 p.

Sellards E. H., W. S. Adkins, and F. B. Plummer, 1932, The geology of Texas—Volume I, stratigraphy: University of Texas, Austin, Bureau of Economic Geology, 1007 p.

Shacklette, H. T., and J. G. Boerngen, 1984, Element concentrations in soils and other surficial materials of the conterminous United States: U.S. Geological Survey Professional Paper 1270, 104 p.

Shafer, G. H., 1965, Ground-water resources of Gonzales County, Texas: Texas Department of Water Resources, Report No. 04.

Shafer, G. H., 1968, Ground-water resources of Nueces and San Patricio Counties, Texas: Texas Department of Water Resources, Report No. 73, 137 p.

Shafer, G. H., 1970, Ground-water resources of Aransas County, Texas: Texas Department of Water Resources, Report No. 124, 83 p.

Shafer, G. H., 1974, Ground-water resources of Duval County, Texas: Texas Water Development Board Report 181.

Shafer, G. H., and E. T. Baker, 1973, Ground-water resources of Kleberg, Kenedy, and southern Jim Wells Counties, Texas: Texas Department of Water Resources, Report No. 173, 69 p.

Shelby, C. A., S. Pieper, S. Aronow, and V. E. Barnes, 1992, Beaumont sheet: The University of Texas at Austin, Bureau of Economic Geology, Geologic Atlas of Texas, scale 1:250,000..

Smedley, P. L., and D. G. Kinniburgh, 2002, A review of the source, behaviour and distribution of arsenic in natural waters: Applied Geochemistry 17, p. 517-568.

Smith, S. M., 2001, National Geochemical Database: Reformatted data from the National Uranium Resource Evaluation (NURE) Hydrogeochemical and Stream Sediment Reconnaissance (HSSR) Program, Version 1.30. U.S. Geological Survey Open-File Report 97-492, WWW release only, URL: http://greenwood.cr.usgs.gov/pub/open-file-reports/ofr-97-0492/index.html, last accessed February 2010.

Smith, G. E., W. E. Galloway, and C. D. Henry, 1982a, Regional hydrodynamics and hydrochemistry of the uranium-bearing Oakville Aquifer (Miocene) of South Texas: The University of Texas at Austin, Bureau of Economic Geology Report of Investigations No. 124, 31 p.

Smith, D. B., R. A. Zielinski, and W. I Rose, 1982b, Leachability of uranium and other elements from freshly-erupted volcanic ash: Journal of Volcanology and Geothermal Research, v. 13, p.1-30.

Solis, R. F., 1981, Upper Tertiary and Quaternary depositional systems, Central Coastal Plain, Texas—Regional geology of the coastal aquifer and potential for liquid-waste repository: The University of Texas at Austin, Bureau of Economic Geology Report of Investigations No. 108, 89 p.

Stewart C., D. M. Johnston, G. S. Leonard, C. J. Horwell, T. Thordarson, and S. J. Cronin, 2006, Contamination of water supplies by volcanic ashfall: a literature review and simple impact modeling: Journal of Volcanology and Geothermal Research, 158, p. 296-306.

Sundstrom, R. W., and C. R. Follett, 1950, Ground-water resources of Atascosa County, Texas, *in* U.S. Geological Survey Water Supply Paper 1079-C, p. 107-153.

Toth, J., 1963, A theoretical analysis of groundwater flow in small drainage basins: Journal of Geophysical Research, 68(16), p. 4795-4812.

TPWD (Texas Parks and Wildlife Department), Plant guidance by ecoregions: Ecoregion 6, http://www.tpwd.state.tx.us/huntwild/wild/wildscapes/guidance/plants/ecoregions/ecoregion_6.phtml, last accessed February 2010.

Trentham, R. C., 1981, Leaching of uranium from felsic volcanics and volcanoclastics: model, experimental studies and analysis of sites: The University of Texas at El Paso, Ph.D. dissertation, 204 p.

USGS, 2004, The national geochemical survey; database and documentation: U.S. Geological Survey Open-File report 2004-1001, http://tin.er.usgs.gov/geochem/doc/home.htm, last accessed February 2010.

USGS, 2008, The national geochemical survey; database and documentation: U.S. Geological Survey Open-File report 2004-1001, version 5, updated September 30, 2008.

U.S. Landfalling Hurricane Probability Project, 2010, http://www.e-transit.org/hurricane/welcome.html, last accessed February 2010.

Verbeek, E. R., Ratzlaff, K. W., and Clanton, U. S., 1979, Faults in parts of north-central and western Houston metropolitan area, Texas: U.S. Geological Survey Miscellaneous Field Studies Map MF-1136, 1 sheet.

Walton, A. W., Galloway, W. E., and Henry, C. D., 1981, Release of uranium from volcanic glass in sedimentary sequences: an analysis of two systems: Economic Geology, 76, p. 69-88.

Warwick, P. D, S. S. Crowley, L. F. Ruppert, and J. Pontolillo, 1994, Petrography and geochemistry of the San Miguel lignite, Jackson Group (Eocene), south Texas: Organic Geochemistry, 24(2), p. 197-217.

Waterstone, 2003, Groundwater availability of the central Gulf Coast aquifer: numerical simulations to 2050, Central Gulf Coast, Texas: draft report submitted to the Texas Water Development Board, Austin, Texas, variously paginated.

Welch, A. H., D. B. Westjohn, D. R. Helsel, and R. B. Wanty, 2000, Arsenic in ground water of the United States: occurrence and geochemistry: Ground Water, 38, p. 589-604.

Wesselman, J. B., 1983, Structure, temperature, pressure, and salinity of Cenozoic aquifers of South Texas: U.S. Geological Survey Hydrologic Atlas No. 654, 10 figures + text on a 96 × 127 cm sheet.

Williamson, A. K., and Grubb, H. F., 2001, Groundwater flow in the Gulf Coast aquifer systems, Regional aquifer system analysis—Gulf Coastal Plain: U.S. Geological Survey Professional Paper 1416-F, 173 p.

Williamson, A. K., Grubb, H. F., and Weiss, J. S., 1990, Ground-water flow in the Gulf Coast aquifer systems, south central United States—a preliminary analysis: U.S. Geological Survey Water-Resources Investigations Report 89-4071, 124 p.

Zielinski, R. A., Lindsey, D. A., and Rosholt, J. H., 1980, The distribution and mobility of uranium in glassy and zeolitized tuff, Keg Mountain area, Utah, USA: Chemical Geology, 29, p. 139-162.